PRODUCTION OF LITHIUM PEROXIDE AND LITHIUM OXIDE IN AN ALCOHOL MEDIUM

by

Javad Khosravi

Department of Mining, Metals and Materials Engineering

McGill University, Montreal, Canada

March 2007

A thesis submitted to the Office of Graduate and Postdoctoral Studies in fulfillment of the requirements for the degree of Doctor of Philosophy

Your file Votre référence
ISBN: 978-0-494-38597-5
Our file Notre référence
ISBN: 978-0-494-38597-5

"Engineering is the science of economy, of conserving the energy, kinetic and potential, provided and stored up by nature for the use of man. It is the business of engineering to utilize this energy to the best advantage, so that there may be the least possible waste."

William A. Smith, 1908

ABSTRACT

Experiments to measure (i) the reactivity of lithium peroxide and lithium oxide in ambient air as a function of relative humidity and reactant particle size, (ii) the solubility of lithium hydroxide and lithium hydroxide monohydrate in three alcohols, namely methanol, ethanol and 1 and 2-propanol, as a function of time and temperature, (iii) the efficiency of the production of lithium peroxide in alcohol medium as a function of the concentration of $LiOH.H_2O$ in methanol, the concentration of hydrogen peroxide, the kind of alcohol, the kind of feed material, and temperature and the time of mixing, (iv) the analysis of the precipitates, (v) the temperature of the precipitate decomposition in isothermal and non-isothermal conditions in ambient and neutral conditions as function of time, (vi) the activation energy of the precipitate decomposition, (vii) the temperature of the lithium peroxide decomposition in isothermal and non-isothermal conditions as function of time and (viii) the activation energy of lithium peroxide decomposition were performed.

The purpose of the study was to gather the data necessary to evaluate the production of lithium peroxide, Li_2O_2, and subsequently lithium oxide, Li_2O, to be used as a feed for a silicothermic reduction process for the production of metallic lithium. The proposed basis for the production of Li_2O_2 was the conversion of lithium hydroxide or lithium hydroxide monohydrate by hydrogen peroxide in an alcohol medium. Alcohols were chosen because they are members of a class of non-aqueous solvents that can selectively dissolve the anticipated contaminants while precipitating the desired products.

It was found that the addition of hydrogen peroxide to alcohol solutions containing lithium hydroxide monohydrate resulted in the formation of lithium peroxide as lithium hydroperoxidate trihydrate with eight adduct molecules of methanol, i.e., $Li_2O_2 \cdot H_2O_2 \cdot 3H_2O \cdot 8CH_3OH$ and involved the peroxide group transfer. The optimum conditions for the production of lithium peroxide were found to be (i) the least water concentration in the system (ii) the use of the temperature lower than ambient temperature

and (iii) fast separation of the precipitate and raffinate to prevent dissociation of the precipitate or dissolving into the raffinate.

The high solubility of $LiOH.H_2O$ and at the same time the low solubility of Li_2CO_3 and of Li_2O_2 in methanol resulted in selection of methanol as the best alcohol of those studied for the proposed method of Li_2O_2 production. It also yielded high purity lithium peroxide. The production of Li_2O_2 using H_2O_2 (35 %wt) required an excess of hydrogen peroxide equal to 2.6 times the stoichiometric amount.

The thermal decomposition of the lithium hydroperoxidate trihydrate precipitate started with the rejection of the adduct methanol molecules, followed by co-evolution of H_2O and H_2O_2 from the resulting $Li_2O_2 \cdot H_2O_2 \cdot H_2O$. The activation energy of the decomposition reaction of the precipitate was measured as 141 kJ/mol. At temperatures greater than 200 °C, lithium peroxide was found to be very reactive with atmospheric air. However, in an argon atmosphere, it rapidly decomposed losing the majority of the oxygen atoms, followed by the gradual slow diffusion of oxygen gas absorbed on the lithium oxide.

RESUME

Des expériences pour mesurer (i) la réactivité du peroxyde de lithium et de l'oxyde de lithium dans l'air ambiant en fonction de l'humidité relative et de la distribution particulaire des réactants, (ii) la solubilité de l'hydroxyde de lithium et de l'hydroxyde de lithium monohydraté dans trois alcools, à savoir le méthanol, l'éthanol et le 1 et 2-propanol, en fonction du temps et de la température, (iii) l'efficacité de production du peroxyde de lithium en milieu alcoolique en fonction de la concentration de $LiOH.H_2O$ dans le méthanol, la concentration de peroxyde d'hydrogène, le type d'alcool, le type d'alimentation, et la température et la durée de mélange, (iv) l'analyse des précipités, (v) la température de décomposition des précipités en conditions isothermes et non-isothermes en milieux ambiant et neutre en fonction du temps, (vi) l'énergie d'activation de décomposition des précipités, (vii) la température de décomposition du peroxyde de lithium en conditions isothermes et non-isothermes en fonction du temps et (viii) l'énergie d'activation de décomposition du peroxyde de lithium furent effectuées.

Le but de cette étude était de récolter les données nécessaires à l'évaluation de la production de peroxyde de lithium, Li_2O_2, et par la suite d'oxyde de lithium, Li_2O, pour être utilisé comme alimentation pour un procédé de réduction silicothermique pour la production de lithium métallique. La base proposée pour la production de Li_2O_2 était la conversion d'hydroxyde de lithium ou d'hydroxyde de lithium monohydraté par le peroxyde d'hydrogène en milieu alcoolique. Les alcools furent choisis car ils font parti des membres de la famille des solvants non-aqueux qui peuvent dissoudre sélectivement les contaminants engendrés tout en précipitant les produits désirés.

Il fut établi que l'addition de peroxyde d'hydrogène aux solutions alcooliques contenant de l'hydroxyde de lithium monohydraté résultait en la formation de peroxyde de lithium sous la forme d'hydroperoxydes trihydratés avec huit molécules d'alcool liées, i.e. $Li_2O_2 \cdot H_2O_2 \cdot 3H_2O \cdot 8CH_3OH$ et impliquant le transfert du groupe peroxyde. Les conditions optimales pour la production de peroxyde de lithium furent établies comme étant (i)

l'absence d'eau dans le system (ii) l'utilisation de températures inferieures à la température ambiante et (iii) la décantation rapide des précipités.

Le Li_2O_2 dans le méthanol résulta en la sélection du méthanol comme étant le meilleur alcool étudié pour la méthode proposée de production de Li_2O_2. Ceci produisit aussi du peroxyde de lithium de haute pureté. La production de Li_2O utilisant du H_2O_2 (35 %m) demanda un excès de peroxyde d'hydrogène égal à 2.6 fois la quantité stoichiométrique.

La décomposition thermique des précipités d'hydroxyperoxydes trihydratés de lithium débuta avec le rejet du méthanol lié, suivit par la coévolution de H_2O et de H_2O_2 provenant de $Li_2O_2 \cdot H_2O_2 \cdot H_2O$. L'énergie d'activation de la réaction de décomposition des précipités fut mesurée à 141 kJ/mol. A des températures supérieures à 200°C, le peroxyde de lithium apparut comme étant très réactif avec l'air atmosphérique. Cependant, dans une atmosphère d'argon, il se décomposa rapidement perdant la majorité des atomes d'oxygène, suivit par la lente graduelle diffusion de l'oxygène gazeux absorbé sur l'oxyde de lithium.

ACKNOWLEDGMENTS

I would like to express my sincerest appreciation to my supervisor, Professor Ralph Harris for his guidance and support throughout my studies in McGill. His approach to scientific issues encouraged me to broaden my insight beyond mere engineering and technical aspects.

I would like to extend my greatest thanks to Prof. Janusz Koziński, who graciously offered support for my research.

I am grateful to Monique Riendeau for her assistance in the use of analytical instruments of the Department, Guillermo Mendoza-Suarez for performing TGA/DTA analysis. I am also thankful to Vincent Menard for translation of the abstract of my thesis to French. My grateful thanks go to Barbara Hanely, who always assisted me and patiently answered all my questions.

Special thanks to John Roumeliotis for his perpetual assistance and helpful advice throughout the research all along, Graeme Goodall for proofreading the thesis, Sina Kashani-Nejad and Sadegh Firoozi for their friendship and outstanding help.

This would not have been possible without the love, never-ending support and encouragement from my dear family: my dear father and mother, my brother and my sisters.

Dedicated to my dear wife, *Sargol*.

TABLE OF CONTENTS

LIST OF FIGURES

LIST OF TABLES

NOMENCLATURE

Symbol	Designation	Unit
A	exponential factor	unitless
a	activity	unitless
c	cohesive energy density	MPa
δ	solubility parameter	$(MPa)^{1/2}$
E	activation energy	$J\ mol^{-1}$
ε_r	relative permittivity	unitless
F	force	$kg\ m\ s^{-2}$
ΔG^o	standard Gibbs energy of i	J
ΔG^o_{latt}	lattice Gibbs free energy	J
ΔG^o_{soln}	solution Gibbs free energy	J
ΔG^o_{solv}	solvent Gibbs free energy	J
$\Delta G^o_{sv}(i, R)$	solvation energy of a species, i, in a solvent, R	J
$\Delta G^o_{sv}(i, S)$	solvation energy of a species, i, in a solvent, S	J
$\Delta G^o_t(i, R \rightarrow S)$	Gibbs energy of transfer of species i from solvent R	J

γ_i	activity coefficient of component *i*	unitless
H_i^0	standard enthalpy of *i*	J
ΔH^0	standard enthalpy change	J
ΔHv	heat of vaporization	J
K	autoprotolysis constants	mol^2L^{-2}
m	mass	kg
μ	viscosity	cP
P_i	partial pressure of *i*	atm
R	gas constant	$J\ mol^{-1}\ K^{-1}$
S	solubility	g solute/100g solvent
t	time	s
T	temperature	K
V_m	molar volume	$m^3\ mol^{-1}$
X_i	mole fraction of *i*	unitless
ρ	density	$kg\ m^{-3}$

1. INTRODUCTION

A new generation of rechargeable batteries that use metallic lithium for electrode material is expected to increase the demand for high purity metallic lithium in the future. All metallic lithium is currently made by the electrolytic reduction of high purity anhydrous lithium chloride at temperatures of roughly 460 °C. The normal process is energy intensive and has a number of technical, economic and environmental drawbacks associated with the containment and treatment of chlorine based compounds. To avoid these issues, a silicothermic vacuum reduction process has been considered for the production of lithium metal. The best lithium compound to be used as a feed to this reduction process would be lithium oxide, Li_2O, due to its high lithium assay. However, little technical information regarding the production of Li_2O by any means was found in published articles and patents. In addition, there was no suggestion that any of the alcohol-based processes mentioned in the patent literature have been employed on an industrial scale.

In this light, the present study evaluated a new method to produce commercial stocks of lithium peroxide, Li_2O_2, as an intermediate compound in the production of lithium oxide, Li_2O from lithium hydroxide and/or lithium hydroxide monohydrate [1, 2].

The conventional hydrometallurgical method for lithium peroxide production involves the reaction of lithium hydroxide with hydrogen peroxide in a highly alkaline solution to yield lithium hydroperoxidate tri-hydrate, $Li_2O_2 \cdot H_2O_2 \cdot 3H_2O$. This precipitate is then dehydrated under vacuum to produce Li_2O_2 [3]. Such methods have a low efficiency along with a high contamination of the product by lithium hydroxide.

Such contamination is a concern because the purity of the lithium peroxide is crucially important for downstream applications to yield high purity lithium oxide for other applications.

An alternative method that is proposed here is believed to sufficiently solve the contamination problem and yield high purity lithium peroxide. It uses an alcohol-based reaction medium. Alcohols, which have an extensive application as separation reagents,

were used in this work to produce a pure product by selectively dissolving the contaminants and precipitating the products. Previous publications on the general use of alcohols as a reaction medium were used as a guideline in designing the method for producing Li_2O that is proposed in this study.

The research objectives were thus:

1. To study the mechanism of the reaction of lithium peroxide and lithium oxide with carbon dioxide and water in ambient air considering the effects of the particle size of the lithium peroxide, the lithium oxide, and the relative humidity of the air. To determine the mechanisms that govern the kinetics of the carbonation reaction of lithium peroxide and lithium oxide in ambient air.
2. To measure the solubility of lithium hydroxide monohydrate, lithium hydroxide, lithium peroxide and lithium carbonate in the alcohols: methanol, ethanol, 1-propanol and 2-propanol.
3. To select the most suitable alcohol which would have a low solubility for lithium peroxide as the product and a high solubility for lithium hydroxide as the contaminant.
4. To comprehensively study the parameters that were thought to influence the production of lithium peroxide by the proposed method, namely: the concentration $LiOH.H_2O$ in methanol, the concentration of hydrogen peroxide, the kind of alcohol, the kind of feed material, the temperature and the time of mixing.
5. To understand the "alcohol process" in order to advance the separation performance and to produce high purity lithium peroxide and lithium oxide.
6. To analyze (i) the product that is precipitated upon the reaction of lithium hydroxide monohydrate with hydrogen peroxide in an alcohol medium and (ii) the raffinate, which contains alcohol, water, hydrogen peroxide and lithium hydroxide.
7. To study the kinetics of the decomposition of the precipitate to remove the water, hydrogen peroxide and methanol to yield pure lithium peroxide.

8. To study the kinetics of the decomposition of lithium peroxide to yield pure lithium oxide.

Outline of thesis:

The present work is organized into a number of chapters and appendices. Chapter 2 presents a survey of the applications of lithium metal and lithium compounds, the producers of lithium and lithium compounds and the demand for metallic lithium.

Chapter 3 explains the silicothermic reduction of lithium.

Chapter 4 describes a survey of the methods for the production of lithium oxide. It draws conclusions about the nature of the challenge of thermal decomposition of lithium hydroxide and lithium carbonate in order to produce lithium oxide. The chapter continues with the suggestion of producing lithium peroxide, Li_2O_2, as precursor instead of producing lithium oxide directly from lithium hydroxide.

Chapter 5 reviews the properties of lithium peroxide and methods for its production. This chapter describes the hydrometallurgical methods for production of lithium peroxide and related drawbacks. The significance of using an alcohol-medium is discussed. The outline of a proposed method for lithium peroxide production and the technical criteria, which led to the proposed method, are addressed.

Chapter 6 briefly explains the chemical and physical properties of hydrogen peroxide as are relevant to the production of lithium peroxide.

Chapter 7 provides the key chemical and physical properties of alcohols that explain the ability of alcohols to precipitate lithium compounds.

Chapter 8 presents the experimental methodologies preformed in the course of this study. The experiments are presented in four parts: i) the study of the reactivity of lithium peroxide and lithium oxide in ambient air as function of humidity and particle size, ii) the experiments for determining the solubility of different lithium compounds in commercial alcohols, iii) the study of the lithium peroxide formation by hydrogen peroxide in alcohol medium and the prediction of the precipitate using different alcohols and iv) the study of

the conditions leading the formation of lithium oxide from lithium peroxide using TGA and DTA.

Chapter 9 presents the results of the experiments, whereas, the relevant discussion and interpretation are comprehensively discussed in Chapter 10.

Appendix I describes the method for calculation of the 95% confidence interval. The analytical methods for the analysis of lithium, active oxygen and methanol are described in Appendixes II, III and IV, respectively. Appendix V explains the method for determination of kinetic parameters from the TGA data. Appendix VI describes the method of the reduced time plots for validation of carbonation kinetics for lithium peroxide and lithium oxide. Finally, Appendix VII describes the experiment and presents the results of using lithium carbonate instead of lithium hydroxide monohydrate as precursor. Chapter VIII presents the structural data for the compounds and PDF cards were used for XRD analysis in this study.

2. LITHIUM: APPLICATIONS AND PRODUCTION

This chapter presents a brief survey of the current lithium metal applications and includes a list of the current suppliers of lithium and lithium compounds. At the end of the chapter, the likely demand for metallic Li is considered.

2.1 Properties

Lithium, atomic weight 6.94 g/mol, is the lightest of all metals with a density of 0.53 g/cm^3 at 20 °C. It is a member of Group 1 of the periodic table and has a valence of +1 when ionized. Lithium has the highest melting point (180 °C), boiling point (1342 °C), and heat capacity (3.3 J/mol/°K) in the alkali metal Group. Lithium is highly reactive when exposed to air or moisture and therefore never occurs in nature in its metallic state. It remains untarnished in dry air but in moist air, its surface becomes coated with a black deposit comprised of a mixture of LiOH, $LiOH{\cdot}H_2O$, Li_2CO_3, and Li_3N. Unlike the other alkali metals, lithium has properties similar to magnesium, such as the high solubility of its halides in both water and polar organic solvents [2, 4].

Lithium is sold in the form of brines (aqueous salts), compounds, metal, or mineral concentrates depending on the end use. The largest uses of lithium compounds are for applications areas such as the preparation of glass, glass-ceramics, in the preparation of lithium greases, and as polymerization initiators. Lithium compounds are also employed as psychopharmacological agents. Because of the unique physical and chemical properties of lithium metal, it is useful in a wide range of applications. Such uses include the production of organolithium compounds, e.g., butyllithium (LiC_4H_9) and lithium hydride (LiH), and as an alloying addition to aluminum and magnesium. Lithium and its compounds play a number of important roles in the nuclear industry as well. For example, it is used in the production of tritium, as a heat-exchange medium, as a shielding material, and in the form of a molten salt mixture as a solvent for other nuclear fuels[2, 5].

2.2 Lithium application in batteries

Lithium metal is attractive as a battery anode material because of its low density, high voltage, high electrochemical equivalence, and good conductivity. Because of these features, the use of lithium and its compounds has received keen attention in the development of high-performance primary and secondary batteries for the last two decades [6].

Two commercially available technologies for rechargeable Li batteries are lithium-ion and lithium metal-polymer (LMP) batteries. LMP batteries have been found to be more advantageous as they are less hazardous, nonflammable, capable of being constructed in unusual shapes, and have notably higher charge/discharge cycles [6]. Two targeted applications for LMP batteries are power sources in electric vehicles and emergency power supplies for telecommunication systems [7]. The use of lithium batteries in hybrid electric vehicles is expected to increase and is anticipated to increase lithium demand as well as its value [4, 8].

2.3 Lithium supply

Lithium is found in nature, (i) as hard-rock ore associated with pegmatite in the USA, Australia, Zaire and Canada; and (ii) as brine in the USA (Great Salt Lake), and (iii) as brine in Chile (Salar de Atacama). The four main non-brine compound/minerals of lithium currently showing commercial promise are Spodumene ($Li_2O.Al_2O_3.4SiO_2$ or $LiAlSi_2O_4$), Petalite ($Li_2O.Al_2O_3.8SiO_2$ or $LiAlSi_4O_6$), Eucryptite ($Li_2O.Al_2O_3.2SiO_2$), and Lepidolite ($Li(Na,K,Rb)_2O.Al_2O_3.3SiO_2(F,O,H)$). The normal strategy for the extraction of these resources to metal involves the conversion first to carbonate, then to chloride, followed by molten salt electrolysis. The conversion from the mineral to carbonate form involves alkaline fusion and carbonation or, acid roasting, calcination, and carbonation.

One example of a brine resource is the double salt, $KLiSO_4$. Conversion of this double salt to lithium carbonate involves purification (removal of potassium) and precipitation. The lithium carbonate is converted to chloride by the action of a chlorinating agent such as hydrogen chloride.

Chemetall Foote [9] and FMC (Lithium Division) [10] are currently the main world suppliers of lithium metal and lithium compounds. Chemetall Foote produces lithium carbonate and lithium hydroxide from brines at its facilities in the USA and Chile. FMC (Lithium Division) produces a full range of downstream compounds, including lithium metal, lithium chloride and organic lithium compounds at its facilities in the USA and Argentina. The United States is still the leading producer of value-added lithium materials. The extent of recycling of lithium is small, but it has grown through the recycling of lithium batteries [9-11]. Figure 1 depicts a schematic flow sheet of an integrated lithium plant.

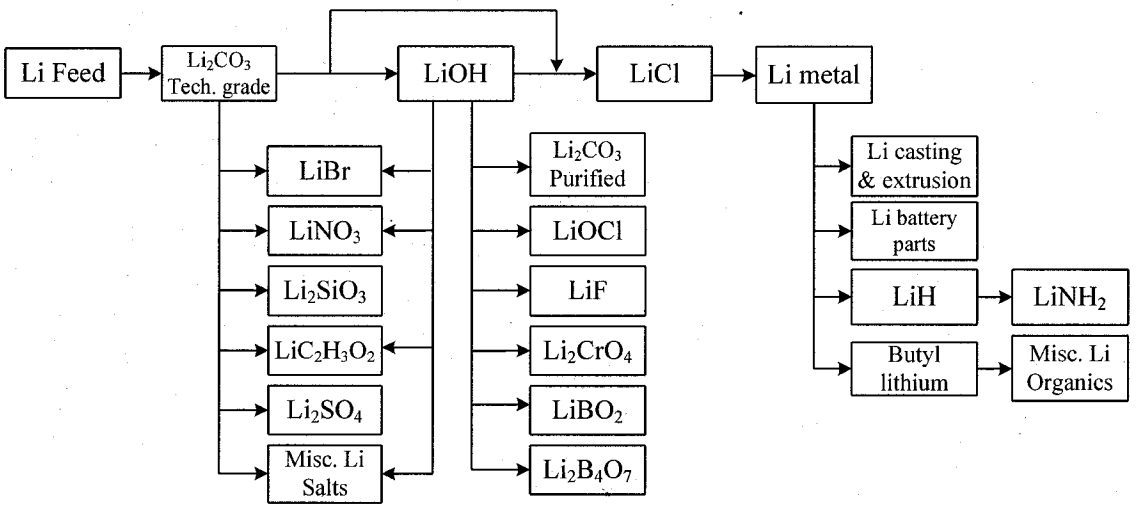

Figure 1: Schematic flow sheet of an integrated lithium plant [12]

Subsurface brines, in particular those found in the Salar de Atacama, Chile, have become the dominant raw material for lithium carbonate production worldwide because of the lower production costs as compared with the mining and processing costs for hard-rock ores and even other brine resources [2, 4, 11].

2.4 Current method for lithium metal production

Currently, all high purity lithium metal is made by the electrolytic reduction of high purity anhydrous lithium chloride from molten salt electrolytes at elevated temperatures in the range of 410 to 460 °C. This electrolysis process is energy intensive. An energy demand of 100-115 MJ/kg of lithium is additionally burdened by a number of technical, economic

and environmental drawbacks associated with the design, containment, and treatment of chlorine-based compounds and chlorine gas [13].

A further disadvantage to electrolytic reduction of high temperature of lithium is the need for a highly pure electrolysis fee. In particular, the need for the removal of impurities associated with lithium metal deposits such as sodium (Na) and potassium (K). Sodium and potassium are found closely associated with most lithium minerals and brines and they exhibit similar physico-chemical behavior to lithium. As a result, if these elements are present in the LiCl electrolysis feed they accompany the product because their electronegativities are such that they are also reduced in part. Lithium battery specifications restrict the content of these impurities to less than 200 ppm, with the result that there is a concomitant constraint on the entire process flow sheet [5, 14, 15].

The potential demand for lithium for battery applications requires that lithium metal producers revise their production capacity and the quality of lithium metal produced. In addition, the challenges of electrolysis necessitate considering other methods to produce high purity lithium metal, in particular by cleaner, sustainable methods [14, 15].

In this regard, the silicothermic reduction method is under examination as an alterative method for lithium metal production. This novel method has been investigated at McGill University's Department of Mining, Metals and Materials Engineering under the supervision of Professor Ralph Harris since 1988 [16].

3. SILICOTHERMIC REDUCTION OF LITHIUM

The silicothermic reduction of lithium as a substitute method for electrolysis is explained in this chapter. In addition, previous studies on the silicothermic reduction of lithium are reviewed and the method that has been developed at McGill University is described.

3.1 Silicothermic reduction of lithium

The idea of producing lithium metal by a pyrometallurgical process can be traced to the works of Morris and Kroll [17, 18]. Inspired by the Pidgeon process, they developed a silicothermic reduction method for lithium production. The silicothermic reduction of lithium oxide uses the same concept that Pidgeon developed for magnesium production in 1940's

In the Pidgeon process, calcined dolime (CaO.MgO) is reduced in the solid state to magnesium metal by silicon in the form of ferrosilicon, at 1150 °C under low pressure (Reaction 1). The magnesium metal is produced as vapor is recovered by condensation.

$$2MgO.CaO_{(s)} + Fe\text{-}Si_{(s)} \rightarrow 2Mg_{(g)} + 2CaO.SiO_{2(s)} + Fe_{(s)} \quad (1)$$

Kroll and Schlechton [18] substituted Li_2O for the dolime to produce lithium metal (Reaction 2).

$$2Li_2O_{(s)} + 2CaO_{(s)} + Fe\text{-}Si_{(s)} \rightarrow 4Li_{(g)} + 2CaO.SiO_{2(s)} + Fe_{(s)} \quad (2)$$

The basic criteria for the selection of lithium oxide as feed material rather than the other potential alternatives, such as lithium hydroxide monohydrate ($LiOH.H_2O$) and lithium carbonate (Li_2CO_3), were its higher lithium assay and melting point. Silicothermic reduction takes place in the solid state; therefore, this process requires a feed that is solid at temperatures of about 1200 to 1300 °C. Both lithium hydroxide monohydrate and lithium carbonate have low melting points of 470 °C and 725 °C, respectively, while the melting point of Li_2O is 1570 °C [19].

The use of spodumene as feed material in the silicothermic production of lithium has also been reported, but resulted in an unpromising amount of extraction [20]. By using spodumene as feed material, the condensed lithium vapor yielded only 45% of the lithium in the feed [21].

Thermodynamically, Li_2O can be reduced by any metal whose oxide is more stable than Li_2O at a given temperature and pressure. Figure 2 demonstrates that Mg and Ca reduce Li_2O at all temperatures, whereas Al and Si can only reduce Li_2O at high temperatures or at a reduced lithium partial pressure. A survey of the literature shows that C, Al, Mg and Si are the reducing agents which have been explored for lithium production [21].

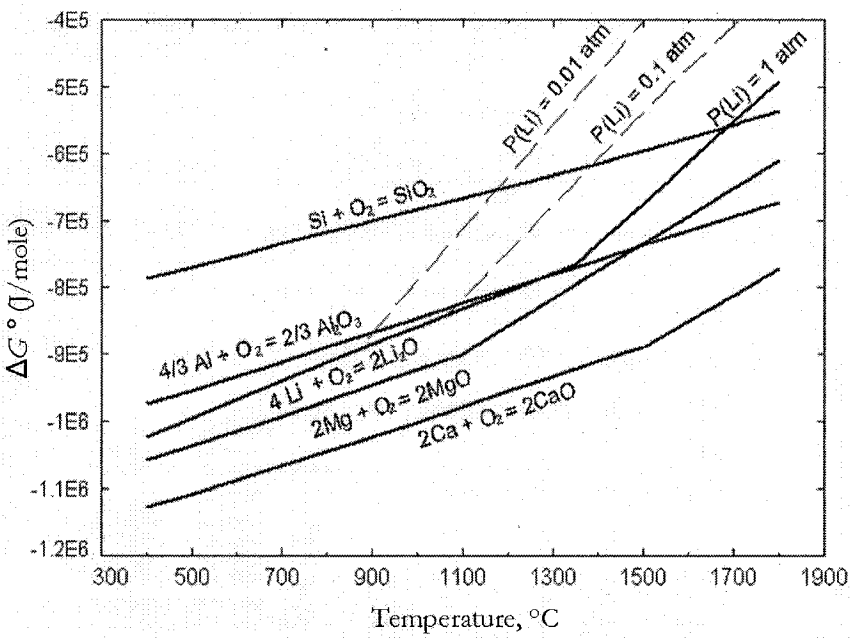

Figure 2: Standard Gibbs Energy of formation of Li_2O and oxides of potential reductants per mole O_2 [22].

The measurement of the vapor pressure of lithium during silicothermic reduction has shown that the Reaction 2 is an oversimplification of the process [17]. Inevitably, stable dual oxides of lithium and silica such as Li_2SiO_4 and/or possibly $CaSiO_4.Li_2SiO_4$ are formed [17]. By adding CaO, not only the co-evolution of SiO gas in addition to the lithium was suppressed, but also the temperature at which lithium vapor formed was reduced [21].

The use of aluminum as a reducing agent has also been reported to reduce the temperature of reaction as compared to silicon. However, the reaction of lithium oxide with aluminum was observed to lead to the formation of mono-aluminate ($LiAlO_2$) and precluded further extraction of lithium [18]. In order to prevent the formation of lithium mono-aluminate the addition of a strong base such as CaO (Reaction 3) was recommended.

$$3\ Li_2O_{(s)} + CaO_{(s)} + 2\ Al_{(l)} \rightarrow 6\ Li_{(g)} + CaO.Al_2O_{3\ (s)} \qquad (3)$$

Thermodynamically, it is favorable to use aluminum as reducing reagent. Unfortunately, Reaction 3 has a slow kinetics [21]. In addition, attention should be paid to the vaibility of using the more costly aluminum versus the cheaper ferrosilicon.

3.2 Recent methods for lithium production

Harris [16] proposed a modified process flow sheet that was based on a Pidgeon-type vacuum thermal reduction process. This process flow not only avoids the drawbacks of electrolysis but is also capable of accepting new and old lithium scrap at various points of the process. By the inclusion of a vacuum refining step, it can also cope with feed material that is contaminated with Na and K.

Figure 3 shows that following its preparation, lithium oxide is mixed with a reducing agent, likely ferro-silicon ($FeSi_6$), and a flux, such as lime (CaO). The mixture is then compacted into briquettes. The briquettes are reacted in a sealed retort at temperatures above 1000 °C and pressures below 100 Pa to produce lithium vapor [16]. The proposed reaction for this method is the same as Reaction 2.

As shown in Figure 3, the initial step in this process is the preparation of the lithium oxide, Li_2O. The preparation of this compound is critical to the proposed flow sheet because lithium oxide has the requisite physic-chemical properties and high concentration of lithium to permit potentially viable extraction of lithium metal via the proposed vacuum silicothermic processing route. In addition, it can be speculated that if the feed material at the reduction step is pure enough, the step for vacuum refining might be eliminated in the absence of contaminated recycle materials [16].

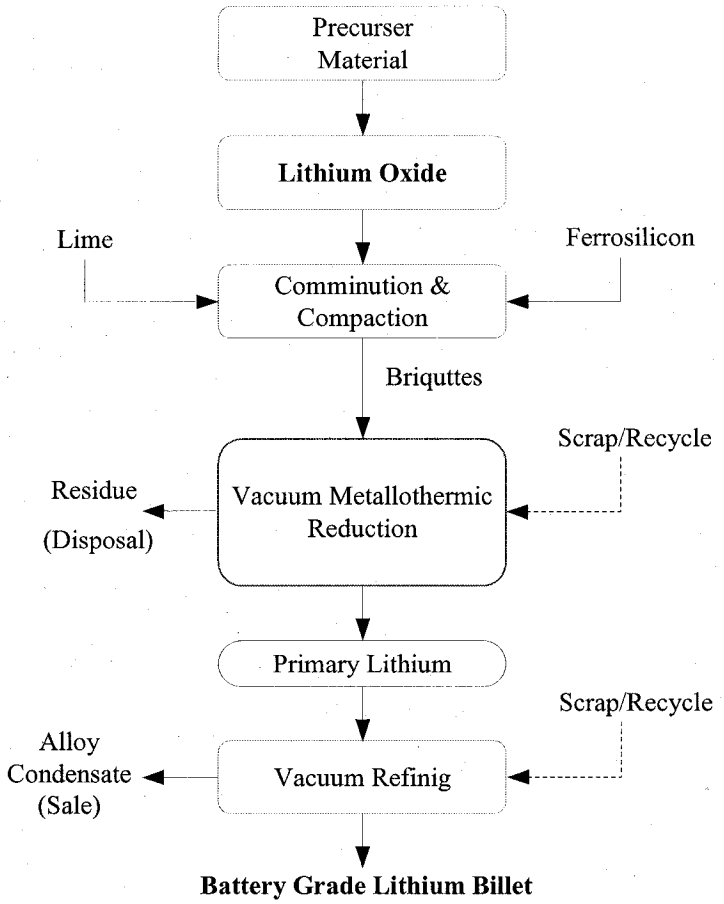

Figure 3: Process for lithium metal production after Harris [16]

4. LITHIUM OXIDE PRODUCTION

The methods for production of lithium oxide are described in this chapter. The challenges inherent in the direct production of lithium oxide from lithium hydroxide monohydrate are also explained. Subsequently, the author proposes the production of lithium peroxide, Li_2O_2, from lithium hydroxide monohydrate as precursor to the production of lithium oxide. Finally, the advantages and disadvantages of this intermediate material product are considered in this section.

4.1 Lithium oxide production

As previously mentioned, lithium oxide is the best candidate to serve as the feed material for the silicothermic vacuum reduction process from among the lithium compounds. Lithium oxide has the highest lithium assay and more importantly, due to its high melting point (1570 °C), Li_2O maintains its physical integrity in the vacuum reduction retort [22].

Currently, lithium oxide is principally used in the making of pharmaceuticals, lithium-ion batteries and in thermonuclear fusion reactors. Lithium oxide and other mixtures of Li_2O-metal oxides are well known as good CO_2-sorbents in various applications, specifically in ventilation industries. However, there are few published articles regarding the preparation of this compound [7].

Several patents [23, 24] outline methods for the preparation of small amounts of lithium oxide via the thermal decomposition of various precursor lithium compounds under inert atmosphere and/or vacuum. For example, lithium oxide has been prepared by the thermal decomposition of either lithium carbonate (Li_2CO_3), lithium hydroxide monohydrate ($LiOH.H_2O$), or lithium peroxide (Li_2O_2). Lithium carbonate was used less, because of the difficulty in achieving complete decomposition [25].

The products of thermal decomposition or conversion are solid lithium oxide and CO_2, H_2O or oxygen O_2 when the precursors are Li_2CO_3, LiOH or Li_2O_2, respectively. Conversion can proceed in the open atmosphere at temperatures where the CO_2 or H_2O

partial pressure over the converted product is higher than the respective partial pressures in normal humid ambient air atmosphere [25].

Cohen [3] reported a process for producing lithium oxide by heating anhydrous lithium hydroxide at approximately 675 °C in a vacuum. The process was accomplished in 16.5 hours in a vacuum close to 150 Pa.

Anno and Bowing [24] disclosed a method for making porous lithium oxide from lithium hydroxide monohydrate having a purity of at least 97 wt%. They heated the $LiOH.H_2O$ to its melting point in a silver container to drive off the water and produce anhydrous lithium hydroxide. Heating continued above the melting point in an inert atmosphere. The molten anhydrous lithium hydroxide was then cooled to a temperature below its melting point (i.e., below 150 °C) while protected by an inert atmosphere. The crucible containing the anhydrous lithium hydroxide was then heated under vacuum.

4.2 The challenge of using $LiOH.H_2O$/LiOH for Li_2O production

A literature review found that lithium hydroxide monohydrate has been used as the precursor compound for the thermal methods of lithium oxide production. The hydrated form of lithium hydroxide, $LiOH.H_2O$, is readily available from commercial suppliers at a lower cost than anhydrous lithium hydroxide [26].

Lithium hydroxide monohydrate can be dehydrated to anhydrous, solid lithium hydroxide under air and at temperatures above 125 °C (Reaction 4). A dehydration study found that no fractional hydrates exist between $LiOH.H_2O$ and LiOH [27].

$$LiOH.H_2O_{(s)} \rightarrow LiOH_{(s)} + H_2O_{(g)} \quad (4)$$

By reducing the pressure, the transformation of LiOH to Li_2O can proceed at temperatures below the melting point of LiOH [28]. Anhydrous lithium hydroxide melts at 471°C at 1 atm. Solid Li_2O can be formed from a LiOH melt at the temperature of 1035 °C (Reaction 5).

$$2LiOH_{(l)} \rightarrow Li_2O_{(s)} + H_2O_{(g)} \quad (5)$$

A notable point regarding liquid lithium hydroxide is that it is highly corrosive and/or reactive towards metallic or ceramic container materials. Research for finding the appropriate container which can resist the hot corrosion of molten LiOH, specifically in the nuclear field, is ongoing [29].

4.2.1 Reactivity of LiOH with CO_2 and water

Storage of solid LiOH under atmosphere conditions is difficult. Anhydrous lithium hydroxide can absorb CO_2 from the atmosphere at water partial pressures above 0.27 kPa [30]. Therefore, at 20 °C where the partial pressure of water is equal 2.33 kPa, absorption of CO_2 by LiOH occurs very readily (Reaction 6) [30].

$$2LiOH + CO_{2\,(g)} \rightarrow Li_2CO_3 + H_2O \qquad \Delta G°_{298} = -96.99\ kJ \qquad (6)$$

In the absence of CO_2, when the water vapor pressure is enough, LiOH can rehydrate to $LiOH.H_2O$ (Reaction 7) [31]. However, during the rehydration of LiOH, a thin layer of $LiOH.H_2O$ forms and deters further reaction between LiOH and water vapor [32].

$$LiOH + H_2O \rightarrow LiOH.H_2O \qquad (7)$$

Lithium hydroxide monohydrate also reacts with CO_2 (Reaction 8). However, due to the crystalline structure of lithium hydroxide monohydrate, the rate of CO_2 absorption is lower than that for LiOH, all other things being equal [30].

$$2LiOH.H_2O + CO_{2\,(g)} \rightarrow Li_2CO_3 + 3H_2O \qquad \Delta G°_{298} = -82.17\ kJ \qquad (8)$$

Figure 4 shows the stability of Li_2CO_3 vs. LiOH and $LiOH.H_2O$ as function of CO_2 and H_2O partial pressures. The shaded rectangle shown in Figure 4 represents typical ambient atmosphere ($P_{CO2} \sim 0.03$ kPa and $P_{H2O} = 2.56$ kPa) and shows that $Li_2CO_{3\,(s)}$ is the stable phase under ambient conditions. Therefore, in addition to the problems associated with Li_2O production, its storage is also difficult. Lithium oxide reacts with atmospheric moisture forming initially LiOH (Reaction 9) that further reacts with moisture to form $LiOH.H_2O$ [32].

$$Li_2O + H_2O_{(g)} \rightarrow 2\ LiOH \qquad \Delta G°_{298} = -93.3\ kJ \qquad (9)$$

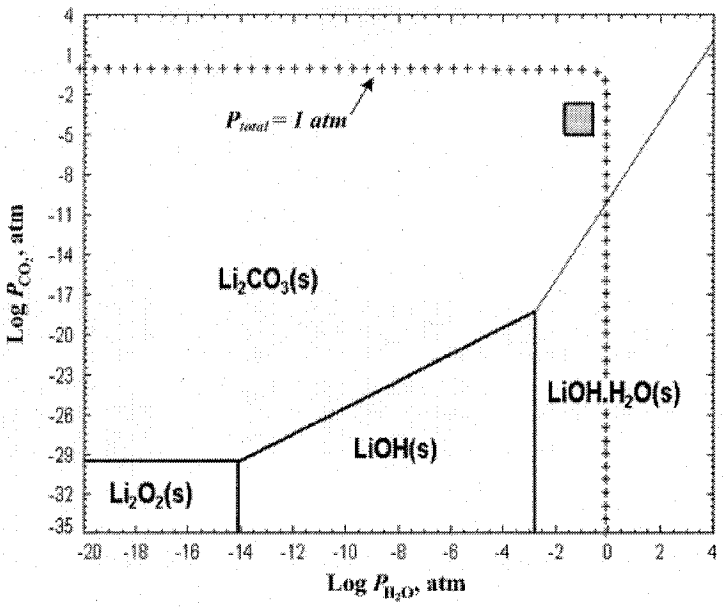

Figure 4: Phase Stability Diagram at P_{O2} = 0.21 atm and 25 °C [22].

Thermodynamically, carbonation of lithium oxide can be favorable (Reaction 10).

$$Li_2O + CO_{2\,(g)} \rightarrow Li_2CO_3 \qquad \Delta G°_{298} = -176.6\ kJ \quad (10)$$

Unlike the extensive studies of the reactivity of lithium oxide at high temperature, conducted primarily by the nuclear sector, information on the reactivity of lithium oxide at ambient temperatures is limited.

The major obstacles to the use of thermal decomposition of LiOH in order to produce Li_2O are i) the slow rates of thermal conversion (Reaction 5) ii) the production of a highly reactive compound, LiOH, and iii) the reactivity of lithium oxide in ambient conditions, (Reaction 10). It can be concluded that the production of lithium oxide via the thermal conversion of LiOH.H_2O is likely unpractical.

4.3 Production of lithium oxide from lithium peroxide

For the purposes of preparing lithium oxide, lithium peroxide, Li_2O_2, is potential precursor. Lithium peroxide loses one oxygen atom when heated to about 300 °C and forms lithium monoxide, Li_2O. Thermodynamic calculations find that lithium peroxide decomposes to Li_2O at the low temperature of about 195 °C (Reaction 11) [19].

$$Li_2O_{2\,(s)} \rightarrow Li_2O_{(s)} + \tfrac{1}{2}\,O_{2\,(g)} \qquad \Delta G^\circ_{195} = -4.1\ \text{kJ} \qquad (11)$$

In this regard, if lithium peroxide could be produced commercially and safely stored, it would be a good "container" for lithium oxide.

5. Lithium Peroxide Properties and Production

The properties and methods of production of lithium peroxide are reviewed in this chapter. First, the physical and chemical properties of lithium peroxide are explained. The hydrometallurgical methods for production of lithium peroxide are then described. Subsequently, the methods involving an alcohol-medium are explored and an outline of a proposed method for lithium peroxide production is presented. Next, the technical criteria, which led the author to the proposed method, are explained. Finally, the parameters involved in the optimum production of lithium peroxide are explained.

5.1 Lithium peroxide properties

Peroxide or peroxo compounds contain at least one pair of oxygen atoms joined by a single covalent bond. The oxygen atoms are present in the comparatively unstable oxidation state of –1. This configuration is symbolically represented as -O-O- and is known as the peroxide group. The prefix peroxo is used for inorganic compounds, and peroxy for organic compounds [33]. The bonds between the peroxide group and other compounds may be different. Figure 5 shows that the peroxide group can be attached to a metal, M, or an inorganic element through one (1) or two oxygen atoms (2), or it can bridge two metals (3).

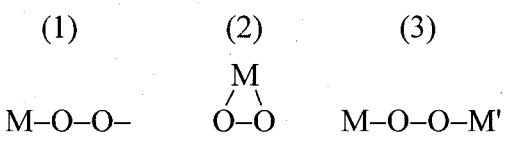

Figure 5: Bonding of peroxide group with metals [34]

The peroxo compounds can be classified into three categories according to their chemical bonding. The category is determined by whether the bond between the peroxo group and the ligands is i) heteropolar, ii) covalent, or iii) dipolar:

i) There are peroxo compounds with heteropolar bonds having a crystalline structure in an ionic lattice and containing O_2^{2-} anions. Typical examples of this class are lithium peroxide, Li-O-O-Li, and sodium peroxide, Na-O-O-Na [1].

ii) Hydrogen peroxide is an example of peroxo compounds with covalent bonds. Elements such as boron, carbon, silicon, phosphorus, and sulfur, also form mainly covalent bonds with the peroxide group [1].

iii) The cations of polyvalent transition metals such as Ti, Cr, Mo, W, and U can form with the peroxo ligands having dipolar bonds, e.g., $2Li_2O_2.V_2O_5$ [35].

Solid lithium peroxide has a hexagonal crystalline structure that contains the O_2^{2-} anion (-O-O-). The distance between the oxygen atoms in this hexagonal structure is 1.55 Å [36]. Lithium peroxide with a density of 2.36 g/cm^3 has an active oxygen content of 34.8%; the highest of all metal peroxides. Lithium peroxide is a pale yellow solid, stable at ambient temperature and not hygroscopic [34].

Unlike the peroxide compounds of sodium, potassium and cesium which form M_2O_2 and M_2O_4 or MO_2, respectively, lithium peroxide only forms the single peroxide compound of Li_2O_2 [37]. Lithium peroxide can form hydrates, $Li_2O_2.nH_2O$, hydroperoxidate[i], $Li_2O_2.H_2O_2$, and hydroperoxidate n-hydrates, $Li_2O_2 \cdot H_2O_2 \cdot nH_2O$.

Lithium peroxide dissolves in water exothermically, forming LiOH and H_2O_2 (Reaction 12).

$$Li_2O_{2\,(s)} + H_2O_{\,(l)} \rightarrow LiOH_{\,(aq)} + H_2O_{2\,(aq)} \qquad (12)$$

Lithium peroxide is a powerful oxidizing agent and can promote combustion when in contact with combustible materials. It is also a powerful irritant to skin, eyes, and mucous membranes. Commercial Li_2O_2 contains about 96% Li_2O_2 [9]. Lithium carbonate and lithium hydroxide monohydrate are the two major impurities in this compound.

---

[i] The hydroperoxidate compounds are also regarded as peroxohydrate. In this thesis, the former terminology, stemming from IUPAC definition, is used.

5.1.1 Reactivity of lithium peroxide in ambient atmosphere

Lithium peroxide is known to be less hygroscopic than Li_2O [38, 39] despite, as Figure 4 shows, the equilibrium P_{CO_2} being equal to 10^{-24} Pa ($P_{CO_2,Air}$ = 30 Pa). However, this reaction does not happen in practice. Lithium peroxide does not react with CO_2 at ambient temperature because it needs a catalyst, water vapor, and elevated temperature typically 20 °C [39].

In other words, the following reaction (Reaction 13) is driven to the right at reasonable rates only at elevated temperatures near 200 °C and in the presence of H_2O vapor.

$$Li_2O_2 + CO_{2\,(g)} \rightarrow Li_2CO_3 + \tfrac{1}{2}\,O_{2\,(g)} \qquad \Delta G^{\circ}_{298} = -166.4 \text{ kJ/mol} \quad (13)$$

Studies found that a multi-component reaction sequence takes place [39]. Lithium peroxide initially absorbs moisture from air turning into LiOH or $LiOH.H_2O$ (Reactions 14 and 15).

$$Li_2O_2 + 2H_2O \rightarrow 2LiOH + H_2O_2 \quad (14)$$

$$LiOH + H_2O \rightarrow LiOH.H_2O \quad (15)$$

Lithium hydroxide or lithium hydroxide monohydrate go on to react with CO_2 to form Li_2CO_3 (Reactions 16 and 17). In other words, Li_2O_2 does not directly react with CO_2.

$$2LiOH + CO_2 \rightarrow Li_2CO_3 + H_2O \quad (16)$$

$$2LiOH.H_2O + CO_2 \rightarrow Li_2CO_3 + 3H_2O \quad (17)$$

In addition, the resulting Li_2CO_3 impedes further CO_2 penetration into the Li_2O_2 core and thus the reaction is self-extinguishing to some extent [25]. No studies were found to give the extent of stability or reactivity of lithium peroxide or lithium oxide at ambient conditions. In this regard, experiments were carried out at McGill to evaluate the reactivity of lithium peroxide versus lithium oxide as a function of its particle size and the humidity content of the reaction atmosphere.

5.1.2 Thermal analysis of lithium peroxide

In sources dealing with the transformation of Li_2O_2 to Li_2O, the only reference indicating the temperature at which Li_2O_2 is decomposed states that this occurs above 300 °C [40]. Few detailed studies have been carried out on the thermal decomposition of lithium peroxide.

Rode [41] studied the thermal decomposition of Li_2O_2 (98%) and reported that the first change occurred at 100 °C due to removal of water (moisture). At 225 °C, an exothermic reaction was observed and was attributed to the α to β transformation. This was followed by endothermic effects at 315 and 342 °C corresponding to the decomposition of Li_2O_2 to Li_2O. At 495-510 °C there was a small exothermic effect that was attributed to the crystallization of lithium oxide (Figure 6) [41].

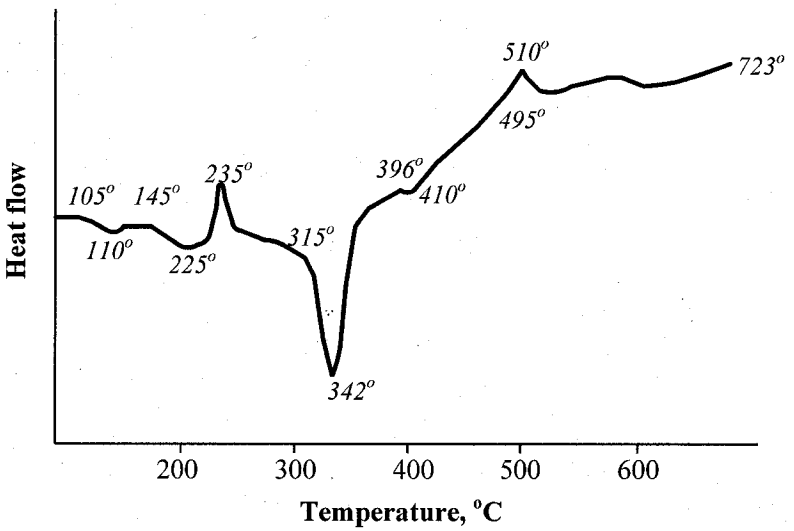

Figure 6: Thermal decomposition of Li_2O_2 as function of time, after Rode [41] (the values on the plot are the sample temperature, °C)

Pavlyuchenko et al. studied the kinetics of thermal decomposition of Li_2O_2 in vacuum. It was reported that at 280 to 300 °C, the thermal decomposition of Li_2O_2 was a zero-order reaction [42]. Tanifuji showed that the thermal decomposition of Li_2O_2 powders in dynamic vacuum proceeded by a first order reaction [43]. Tsentsiper reported that the rate-limiting step in the decomposition of Li_2O_2 is the dissociation of the O-O bond in the peroxide. He also observed the formation of Li_2O_2-Li_2O solid solution at 50% conversion of the peroxide [44].

Some studies have also reported the measurement of the activation energy of Li_2O_2 decomposition. Tsentsiper measured the activation energy of Li_2O_2 (97% with Li_2CO_3 as the contaminant) decomposition as 209.2 kJ/mol [44]. Pavlyuchenko reported the activation energy of Li_2O_2 decomposition in vacuum as 233.9 kJ/mole [42]. Tanifuji's investigation was performed on powdered and compacted Li_2O_2 (98%). In an argon atmosphere, the decomposition of activation energies for the powder and compact samples were reported as 215 and 221 kJ/mol, respectively [43].

From reviewing the study mentioned above, it can be seen that the first challenge of a kinetic study on the thermal decomposition of Li_2O_2 is the purity of the samples. Another significant problem is the high reactivity of Li_2O_2 and Li_2O at temperatures above 200 °C.

5.2 Production of lithium peroxide by aqueous methods

A survey of the literature found the only sources describing methods of production of lithium peroxide were limited to patents. In addition, unlike the other lithium compounds there is no commercial supplier of Li_2O_2. As it was stated by Kamienski: "Lithium peroxide has not attained its industrial importance because of comparatively high cost of lithium and its compounds and high manufacturing costs, among other reasons" [1, 2].

The known method for the production of lithium peroxide is the hydrometallurgical method. Cohen [3] described a method of reaction of lithium hydroxide in a high alkalinity solution with hydrogen peroxide, to yield lithium hydroperoxidate tri-hydrate ($Li_2O_2 \cdot H_2O_2 \cdot 3H_2O$), which is then dehydrated under vacuum to Li_2O_2.

Another method includes the reaction of lithium alkoxides in alcohol solutions with concentrated hydrogen peroxide. For example, a solution of lithium ethoxide, LiC_2H_5O, in ethanol was reacted with 30 % wt hydrogen peroxide to produce a compound that was characterized as lithium hydroperoxidate monohydrate, $LiOOH.H_2O$ [45].

Smith [46] introduced an alternative procedure comprised of mixing lithium hydroxide and hydrogen peroxide and applying heat to the mixture during the endothermic reaction stage. The mixture was heated to at least a temperature of 70 °C. The reported product was pure lithium peroxide.

Bach [47] reported a process by which hydrogen peroxide and saturated aqueous lithium hydroxide solution was sprayed together into a spray dryer. The product was a compound of lithium hydroperoxide and lithium hydroxide, requiring a further step to separate them.

5.2.1 Theory of hydrometallurgical production of Li_2O_2

In aqueous solution, the lithium cation, Li^+, is usually tetrahedrally surrounded by four water molecules, $[Li(H_2O)_4]^+$, or anions [48]. The lithium cation, Li^+, is soluble and stable in aqueous solution over the entire pH range [49]. Therefore, there is no change in the oxidation state of lithium under oxidizing or reducing conditions.

In the system $LiOH\text{-}H_2O_2\text{-}H_2O$, lithium peroxide is formed upon precipitation as a compound that is associated with water and hydrogen peroxide. The direct formation by precipitation of pure lithium peroxide does not happen. The process to form Li_2O_2 takes place in two stages: an exothermic stage (Reaction 18) and an endothermic stage (Reaction 19) [27].

$$LiOH.H_2O_{(s)} + H_2O_2.XH_2O_{(l)} \rightarrow LiOOH + (X+2)H_2O_{(l)} \quad (18)$$

$$LiOH.H_2O_{(s)} + LiOOH_{(aq)} \rightarrow Li_2O_{2\,(s)} + 2H_2O_{(l)} \quad (19)$$

The generally accepted overall reaction equation for forming hydrated lithium peroxide hydroperoxidate may be written as follows (Reaction 20).

$$2LiOH.H_2O_{(s)} + H_2O_2.XH_2O_{(l)} \rightarrow Li_2O_2.H_2O_2.(2+X)H_2O_{(s)} \quad (20)$$

In an aqueous system, the composition of the triple compound, $Li_2O_2{\cdot}H_2O_2{\cdot}nH_2O$, depends on the concentration of hydrogen peroxide in the liquid phase. When the concentration of hydrogen peroxide reaches 40 wt %, a compound with the composition of $Li_2O_2{\cdot}H_2O_2{\cdot}3H_2O$ dominates. By further increasing the concentration of hydrogen peroxide, the compounds $Li_2O_2{\cdot}H_2O_2{\cdot}2H_2O$ and, then, $Li_2O_2{\cdot}2H_2O_2$ are formed (Figure 7) [50]. As previously mentioned, lithium peroxide is not formed directly. However, lithium peroxide can be isolated by thermal decomposition of the triple compound $Li_2O_2{\cdot}H_2O_2{\cdot}2H_2O$.

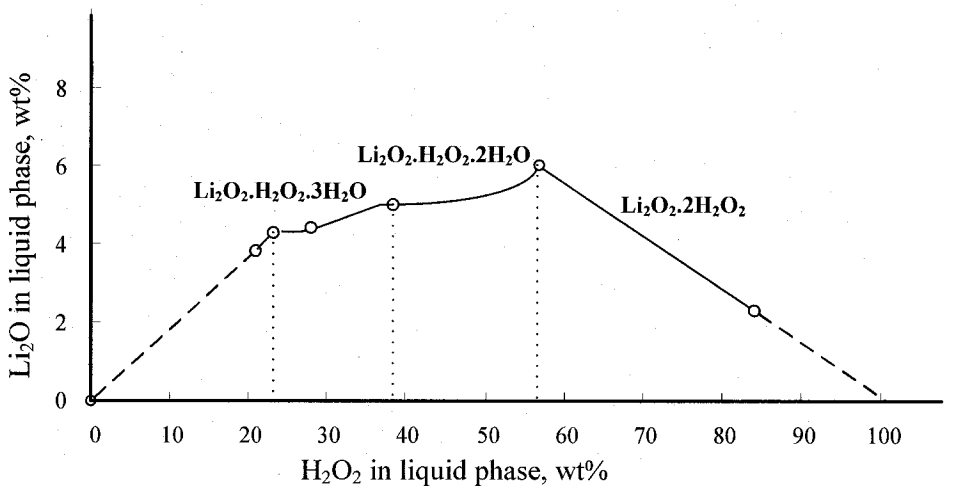

Figure 7: Isotherm of system LiOH-H_2O_2-H_2O at 21°C, after Makarov [37]

By heating the $Li_2O_2 \cdot H_2O_2 \cdot 2H_2O$ under vacuum to 50 °C at which point one molecule of H_2O is lost (Reaction 21) and by continuing to heat it to 75 °C, where dehydration is completed, yields relatively pure $Li_2O_2 \cdot H_2O_2$ (Reaction 22).

$$Li_2O_2.H_2O_2.2H_2O_{(s)} \rightarrow Li_2O_2.H_2O_2 + 2H_2O_{(g)} \quad (21)$$

$$Li_2O_2.H_2O_2.H_2O_{(s)} \rightarrow Li_2O_2.H_2O_2 + H_2O_{(g)} \quad (22)$$

Lithium hydroperoxidate, LiOOH, (or $Li_2O_2.H_2O_2$) is an unstable compound in aqueous systems because the water activity is high. Therefore, lithium hydroperoxidate is completely dissociated to lithium hydroxide and hydrogen peroxide in aqueous systems (Reaction 23).

$$LiOOH_{(aq)} + H_2O_{(l)} \rightarrow LiOH_{(aq)} + H_2O_{2(l)} \quad (23)$$

The other reaction that leads to the dissociation of lithium hydroperoxidate in aqueous systems is its reaction with hydrogen peroxide to form lithium hydroxide, water and oxygen, through the reaction of intermediate radicals (Reactions 24 and 25).

$$LiOOH_{(aq)} + H_2O_{2(l)} \rightarrow HOO\bullet + LiOH + HO\bullet \quad (24)$$

$$HOO\bullet + HO\bullet \rightarrow H_2O_{(l)} + O_{2(g)} \quad (25)$$

Lithium hydroperoxidate (LiOOH) is a reactive compound that absorbs CO_2 from the open atmosphere at ambient temperatures and can then be converted to Li_2CO_3. Therefore, during the drying of LiOOH, a moderate vacuum of about 10^{-2} to 10^{-3} atm is needed to isolate the products from CO_2.

5.3 Production of lithium peroxide using alcohol

In this section, previous methods for the production of lithium peroxide are described and an outline of a proposed method for lithium oxide production is presented.

5.3.1 Review of methods

Strater [51] patented a procedure to use organic solvents such as methanol to dissolve a starting material of anhydrous lithium hydroxide. Lithium hydroxide, which was created in an excess, was then dissolved in methanol. Next, the filtered solution was reacted with hydrogen peroxide. Subsequently, excess lithium peroxide was precipitated from the solution, the lithium hydroxide remained in the solution and the filtered solution was recycled for its methanol content. Strater stated that the reaction for lithium peroxide formation was the oxidation of lithium hydroxide by hydrogen peroxide. He also reported that lithium peroxide and lithium carbonate were insoluble in the organic solvents, but lithium hydroxide was soluble in the solvent.

Bach [47] described a method for the treatment of solid lithium hydroxide with concentrated hydrogen peroxide, followed by washing the precipitate with alcohol and drying in a conveying dryer.

Bach [27] also patented a method of producing lithium oxide containing no lithium hydroxide from lithium peroxide. In Bach's process, lithium hydroxide was reacted with hydrogen peroxide to produce lithium peroxide. The product was scrubbed with methanol to dissolve un-reacted lithium hydroxide and to precipitate the lithium peroxide product. Lithium peroxide was then thermally decomposed to lithium oxide by heating it slowly at 225 to 250 °C in an inert atmosphere; preferably, at a pressure of 100 to 600 Pa. Bach claimed a higher conversion yield of conversion could be obtained from a solution

saturated with respect to lithium hydroxide. It was stated that a higher concentration solution suppressed the active oxygen content as well as the solubility of lithium peroxide in the aqueous solution.

Klebba [52] reported a method whereby the alkali metal hydroxide was treated with H_2O_2 in an alcohol medium. The alcohol could be a primary, secondary, or tertiary aliphatic alcohol. Solid alkali metal peroxide was separated from the liquid alcohol phase. The peroxohydrate, for example $Li_2O_2 \cdot H_2O_2 \cdot 2H_2O$, precipitated and was then filtered from the alcohol solution and transferred to vacuum desiccators, at 30 to 50 mmHg for 24 h. Li_2CO_3 was precipitated and heated to between 90 to 95 °C. Alcohol in the filtrate was returned for reuse in the system.

In another method [53, 54], a mixture of ethanol and lithium hydroxide monohydrate was heated and followed by the addition of H_2O_2 30 %wt. It was stated that the heating of the mixture to the boiling point of ethanol increased the efficiency. The precipitate was dried at 130 °C under vacuum of 0.03 atm for 9 hours. The filtered solution was reused by adding fresh $Li_2O_2.H_2O$ [54].

5.3.2 The proposed alcohol-based process for lithium peroxide production

The available articles and patents on this subject revealed very little technical information. In addition, there was no indication that any of the alcohol-based processes have been employed on an industrial scale. The previous works were used as guidelines in designing the method that is proposed in this study.

The major differences between the previously discussed methods and the present study can be attributed to the precipitation step, in particular the use of different alcohols and/or separation procedures. The reported methods can be divided into two categories according to the sequence of processing steps. The first category includes the reaction of H_2O_2 with $LiOH.H_2O$ (in the form of a solution or solid), followed by heating to remove water and hydrogen peroxide and the use of alcohol for purification of the produced Li_2O_2.

The second category involves preparing a mixture of $LiOH.H_2O$ with alcohol (low or high concentration), then adding H_2O_2, followed by precipitation as described by Strater [51], Klebba [52], Ferapontov [53] and Gladyshev [54].

The first category was eliminated from this study for the following reasons:

1. Lithium carbonate is usually present as a contaminant in both technical and analytical grades of $LiOH.H_2O$. Because the reactivity of Li_2CO_3 with H_2O_2 is remarkably low[ii], upon addition of H_2O_2 only a very small amount of Li_2CO_3 is converted to Li_2O_2. Moreover, Li_2CO_3 has a low solubility in all alcohols and it remains in the precipitate. Hence, in the presence of Li_2CO_3 in $LiOH.H_2O$, the Li_2O_2 produced is contaminated with Li_2CO_3.
2. By the addition of H_2O_2 (generally containing 65 wt% water), the water content in aqueous solution inevitably increases. Because of the presence of a large amount of water in aqueous solution, the $Li_2O_2.H_2O_2$ that is produced is less stable and is easily backreacted to LiOH. Consequently, the efficiency of producing lithium peroxide is decreased.
3. The compound containing lithium peroxide can be precipitated at high pH, i.e., a higher concentration of $LiOH.H_2O$. A solution with a high concentration also results in co-precipitation of LiOH with the lithium peroxide compound. Therefore, the precipitate needs a further purification such as washing with alcohol.

In the light of the problems listed above, it was concluded that the first category of methods was not appropriate for producing of high-purity lithium peroxide. Therefore, it was decided that the second type would be used as the basis for the study of a conversion process for producing Li_2O_2. Consequently, the proposed method for production of lithium peroxide contained many steps.

[ii] In Annex VII, the results of the use of lithium carbonate as a reactant are presented.

First, lithium hydroxide monohydrate (or lithium hydroxide) would be mixed in an alcohol, and the resulting solution would be filtered. Hydrogen peroxide would then be added to the solution, followed by centrifuging. The precipitate would be heated in a vacuum oven to produce high purity lithium peroxide. Figure 8 shows the flow chart of the proposed method.

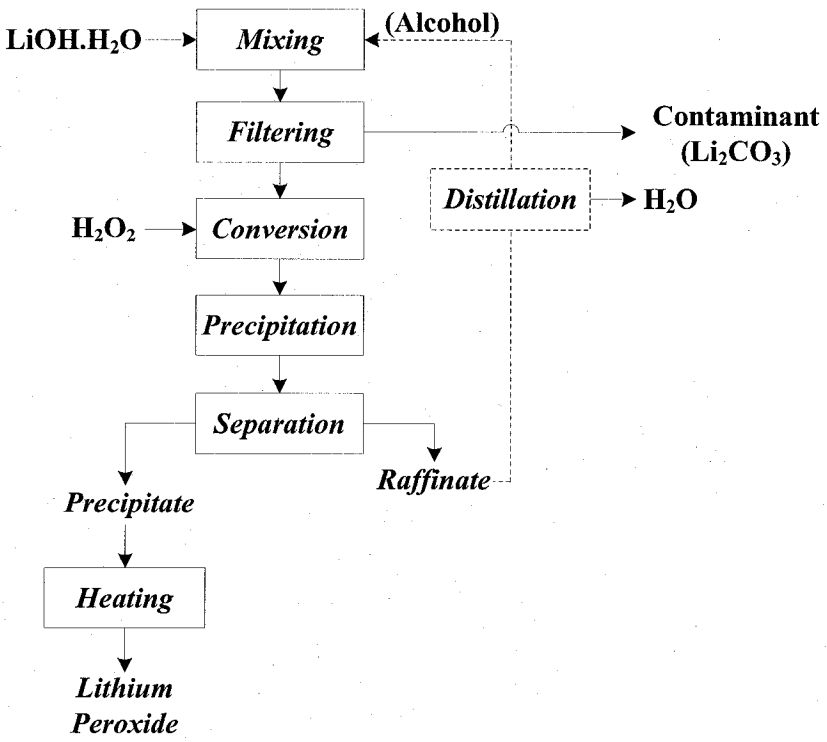

Figure 8: The outline of the process proposed in this study.

This method is believed to have the following advantages:

1. The method takes advantage of the very low solubility of Li_2CO_3 in alcohols. In other words, dissolving the starting material, $LiOH.H_2O$ in alcohols can be referred as the pre-refining step for purifying $LiOH.H_2O$ of Li_2CO_3.
2. The alcohol medium does not react with H_2O_2 and $LiOH.H_2O$; therefore, it can be recovered from the mixture of alcohol and water and recycled.
3. The product can easily be precipitated and filtered. Therefore, the time and energy required to separate the product from the unreacted reagent is low.

6. HYDROGEN PEROXIDE

This chapter explains the chemical and physical properties of hydrogen peroxide as they are relevant to the production of lithium peroxide.

6.1 Hydrogen peroxide

Almost all of the published processes for the production of lithium peroxide from lithium hydroxide or lithium hydroxide monohydrate use hydrogen peroxide as the reagent [3, 23, 24]. Some methods involve techniques that result in less hydrogen peroxide consumption than others but the major differences between among them are the separation techniques. Therefore, a review of the physical and chemical properties of hydrogen peroxide can lead to better insight regarding the reactions of hydrogen peroxide with lithium hydroxide which lead to the formation of lithium peroxide.

Hydrogen peroxide is a clear, colorless liquid and like other inorganic peroxo compounds, it contains dioxide pair atoms, O_2^{2-}, in which oxygen is present in the unstable oxidation state of –1 [55]. Two hydrogen atoms are linked to the O_2 moiety to form a non-planar structure. Either one or both hydrogen atoms of hydrogen peroxide can be substituted.

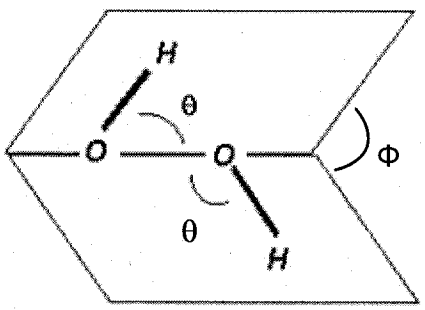

Figure 9: Hydrogen molecule θ (H-O-O angle) = 95° , Φ (Dihedral angle) = 120° [56]

In hydrogen peroxide, the bond strength between oxygen–oxygen (HO–OH) is 209 kJ/mol, which is approximately half of the normal bond strength for a single covalent oxygen bond. The oxidizing power of the peroxides results from this low bond energy as

well as the high energies of O–M, O–C, and O–H bonds. For example, the bond strength in HOOH between O-H is 377 kJ/mol [57].

Hydrogen peroxide is miscible with water at all proportions. The mixture of hydrogen peroxide and water does not form an azeotrope, thus, they can theoretically be separated by distillation. The attractive forces in a mixture of hydrogen peroxide and water come from hydrogen bonding between H_2O_2-H_2O_2 and H_2O_2-H_2O. Pure hydrogen peroxide is of scientific interest only and is not produced on an industrial scale [56].

Hydrogen peroxide is a weak acid in aqueous solution with a dissociation constant of 1.78×10^{-12} (pK_H = 11.75) at 20 °C. Hydrogen peroxide is dissociated to hydroxonium, H_3O^+, and hydroperoxide anion, HO_2^-, as shown in Reaction 26.

$$H_2O_2 + 3H_2O \rightarrow H_3O^+ + HO_2^- \quad (26)$$

Moreover, hydrogen peroxide can form free radicals by homolysis cleavage[iii] of the O–H (Reaction 27) or the O–O bond (Reaction 28). The formation of the radicals can be initiated by either thermal dissociation or the presence of catalysts, e.g., metal ions [5].

$$HOOH \rightarrow H\bullet + OOH\bullet \quad (27)$$

$$HOOH \rightarrow 2OH\bullet \quad (28)$$

The mechanism of radical formation is relatively complex and depends primarily on the presence of catalysis in solution. Therefore, the nature of the reactants determines which of above reactions is predominant. The hydroxyl radical, OH•, in comparison to OOH• is a very strong oxidant [58].

Hydrogen peroxide can react directly or after it has ionized or dissociated into free radicals. These reactions may be organized into four categories: I) oxidation or reduction

---

[iii] The cleavage of a bond so that each of the molecular fragments between which the bond is broken retains one of the bonding electrons. A uni-molecular reaction involving homolysis of a bond in a molecular entity containing an even number of (paired) electrons results in the formation of two radicals: A–B → A• + B•[33].

reactions, II) decomposition processes, III) addition-compound formation and IV) peroxide group transfer [55].

I) Oxidation or reduction reactions

Hydrogen peroxide can behave either as an oxidizing or as a reducing agent. In these reactions, both reactants and the oxygen undergo a change in valence. Hydrogen peroxide is a strong oxidant that undergoes two-electron reduction in an acidic solution to give water, (Reaction 29). In a basic solution, hydrogen peroxide is reduced to OH^-, (Reaction 30). Most of the uses for hydrogen peroxide and its derivatives depend on these oxidation or reduction reactions.

$$H_2O_2 + 2H^+ + 2e^- \rightarrow 2H_2O \qquad E_{\circ\,(pH=0)} = +1.77\ V \quad (29)$$

$$H_2O_2 + 2e^- \rightarrow 2OH^- \qquad E_{\circ\,(pH=14)} = +0.87\ V \quad (30)$$

Iron oxidation in an acidic solution is an example of a net oxidation by hydrogen peroxide, (Reaction 31).

$$H_2O_2 + 2Fe^{2+} + 2H^+ \rightarrow 2Fe^{3+} + 2H_2O \quad (31)$$

With some strong oxidizing substances, such as $KMnO_4$, the ionic peroxides can act as reducing agents, (Reactions 32 and 33).

$$H_2O_2 \rightarrow 2H^+ + O_2 + 2e^- \qquad E_{\circ\,(pH=0)} = -0.66\ V \quad (32)$$

$$H_2O_2 + 2OH^- \rightarrow 2H_2O + O_2 + 2e^- \qquad E_{\circ\,(pH=14)} = +0.08\ V \quad (33)$$

Hydrogen peroxide can reduce the strong oxidizing agent of potassium permanganate, (Reaction 34).

$$2KMnO_4 + 5H_2O_2 + 3H_2SO_4 \rightarrow 2MnSO_4 + K_2SO_4 + 8H_2O + 5O_2 \quad (34)$$

II) Decomposition processes

Another typical reaction for hydrogen peroxide is exothermic redox disproportionation[iv]. Hydrogen peroxide decomposes to water and oxygen in the presence of alkali metal ions (Reaction 35) [55].

$$H_2O_{2\,(aq)} \rightarrow H_2O_{(l)} + \tfrac{1}{2}O_{2\,(g)} \qquad \Delta G^{\circ}_{298} = -117\ \text{J/mol} \quad (35)$$

The mechanism and rate of hydrogen peroxide decomposition depends on many factors, including temperature, pH, and the presence or absence of a catalyst. The decomposition is slow in pure solutions and can be suppressed or considerably reduced by adding small quantities of stabilizers such as magnesium sulfate or sodium silicate [55].

III) Addition-compound formation

The hydrogen peroxide molecule as a whole may be attached to another molecule to form addition compound or hydroperoxidate, which are analogues to hydrates. Hydrogen peroxide, like water, may be present in the crystal structure and forms crystalline adducts, e.g., $Li_2O_2.H_2O_2$ or $Na_2CO_3.H_2O_2$, (Reaction 36).

$$3H_2O_2 + 2Na_2CO_3 \rightarrow 2Na_2CO_3.H_2O_2 \qquad (36)$$

IV) Peroxide group transfer

A variety of peroxo compounds can be formed through the transfer of the intact peroxide group from molecule to molecule. There is no change in valance of either the oxygen in hydrogen peroxide or the elements of ligands. These kinds of reactions are generally referred as to metathetical[v].

Barium peroxide is formed through the reaction of barium hydroxide with hydrogen peroxide, in such a way that a hydrogen atom from hydrogen peroxide is substituted by a

---

[iv] A reversible or irreversible transition in which species with the same oxidation state combine to yield one of the higher oxidation state and one of the lower oxidation state, e.g., $3Au^{+} \rightarrow Au^{3+} + 2Au$ [33].

[v] A metathetical reaction is a reaction in which two or more compounds exchange parts [33].

barium cation, (Reaction 37). Substitution of Ba^+ is an example of a peroxide group transfer.

$$H_2O_2 + Ba(OH)_2 \rightarrow BaO_2 + 2H_2O \quad (37)$$

Peroxy compounds such as alkyl hydroperoxide (H–O–O–R) and dialkyl hydroperoxide (R–O–O–R) can be prepared through substitution of one or two hydrogen atoms of hydrogen peroxide by alkyl groups. The formation of the strong inorganic oxidant, monoperoxosulfuric acid (H_2SO_5 or Caro acid), is also an example for peroxide group transfer, (Reaction 38) [34].

$$H_2SO_4 + H_2O_2 \rightarrow H_2SO_5 + H_2O \quad (38)$$

Similarly, in the formation of lithium hydroperoxidate, one atom of hydrogen from hydrogen peroxide is substituted by a lithium cation, Li^+, (Reaction 39). Therefore, the ions making up the lithium hydroperoxidate (LiOOH) are Li^+ and HO_2^-.

$$LiOH + H_2O_2 \rightarrow Li^+{}^-OOH + H_2O \quad (39)$$

7. Theory of Alcohol Solutions in the Production of Lithium Peroxide

Non-aqueous solvents have been extensively used as separation and precipitation reagents. Alcohols, as a member of the class of non-aqueous solvents, have also shown interesting characteristics in the purification of chemical products. For example, alcohols can selectively dissolve the products or precipitate contaminants. When an alcohol is to be used for a given purpose a suitable one must be selected from the variety available. The following text borrows heavily from Reichardt [59] and Izutsu [60] and describes the alcohol properties that were thought to be involved in the processes examined in this study.

7.1 Primary alcohols

Alcohols are compounds in which a hydroxyl group, –OH, is attached to a saturated carbon atom, such as R_3COH. The term 'hydroxyl' refers to the radical, HO•. Methanol (CH_3OH), ethanol (CH_3CH_2OH), and 1-propanol ($CH_3CH_2CH_2OH$) are considered primary alcohols[vi]. The chemical properties of primary alcohols are related to the occurrence of the hydroxyl groups (-OH) and their position in the molecule. The first two members of the monohydric series resemble water to a large extent. Methanol, ethanol, and the propanols are completely miscible with water and are partially ionized in water [61, 62].

Methanol is the simplest alcohol and its reactivity is determined by the functional hydroxyl group. Reactions of methanol take place via cleavage of the C–O or O–H bond and are characterized by the substitution of the –H or –OH group. Methanol is clear, colorless and flammable liquid with a characteristic odor. It is hygroscopic and miscible in all proportions with water as well as with many organic solvents. Methanol is toxic

[vi] Primary alcohols are characterized by following structure: $-CH_2-OH$ [33].

although cases of poisoning are extremely rare if it is used correctly. Methanol does not form an azeotropic mixture[vii] with water [62, 63].

Ethanol is commonly available as an ethanol–water azeotrope and in anhydrous form. Ethanol is miscible in all proportions with water and is also readily miscible with many organic solvents [64].

The propanols comprise two isomers, 1-propanol and 2-propanol. The later is also called isopropyl alcohol. Both are clear, colorless, flammable liquids with a slight odor resembling that of ethanol. 2-propanol is industrially more important than 1-propanol. It is used mainly as a solvent for coatings, in antifreeze and as a chemical intermediary for the production of organic derivatives [65].

The properties and classification of alcohols have been dealt in the literature. The properties of solvents that are important in characterizing solvents and solutes are listed Table 1 [60, 61]. It is common to classify alcohols according to their properties.

Table 1: Physical and chemical properties of solvents [60]

Physical properties	Boiling point, melting (or freezing) point, molar mass, density, viscosity, vapor pressure, heat capacity, heat of vaporization, relative permittivity[viii], electric conductivity; polarizability
Chemical properties	Acidity (including the abilities to act as proton donor, hydrogen-bond donor, electron pair acceptor, and electron acceptor), Basicity (including the abilities to act as a proton acceptor, hydrogen-bond acceptor, electron pair donor, and electron donor)

7.2 Solvent miscibility and solubility parameter

The heat of vaporization, ΔHv, determines the cohesive energy density (cohesive pressure) of a liquid. The cohesive energy density is a measure of the "stickiness" of a solvent and is

[vii] Molecular associations between the components of a mixture can result in systems that have a constant boiling point at a given concentration. The composition of the liquid phase of the azeotrope is the same as that of the vapor phase with which it is in equilibrium. This means that the composition of liquid cannot be changed at its azeotropic composition by simple boiling [33].

[viii] Dielectric constant

related to the work necessary to create "cavities" to accommodate solute particles in the solvent. The cohesive energy density, c, is defined by Equation 40, where V_m, R and T are the molar volume, the gas constant and temperature, respectively.

$$c = (\Delta H_v - RT)/V_m \tag{40}$$

Hilebrand defined the solubility parameter, δ, as a square root of the cohesive energy density. He showed that liquids with similar solubility parameters are miscible. The concept has been very useful and successful in predicting solubilities of non-electrolyte solutes in low polarity solvents. The solubility parameter, δ, is defined by Equation 41 [59, 66].

$$\delta = c^{1/2} = [(\Delta Hv - RT)/V_m]^{1/2} \tag{41}$$

In many cases, two liquid substances with similar δ-values are miscible, while those with dissimilar δ-values are immiscible. While solubility parameters are tabulated for many solvents, data for solid solutes are very restricted, in particular for low volatility solutes.

Table 2: Physical properties of organic solvents and some inorganic solvents of electrochemical importance [60, 66].

Solvent	**Boiling Point**	**Vapor Pressure***	**Density**	**Viscosity***	**Solubility Parameter**	**Relative permittivity**
Unit	(°C)	(mmHg)	(g/cm^3)	(cP)	$(MPa)^{1/2}$	
Water	100	23.8	0.997	0.89	47.9	78.4
Methanol	64.5	127	0.786	0.55	29.6	32.7
Ethanol	78.3	59	0.785	1.08	26.4	24.6
1-Propanol	97.2	21	0.799	1.94	24.4	20.5
2-Propanol	82.2	43.3	0.781	2.04	23.5	19.9

* at 20 °C

As with miscibility, it has been found that a good solvent for a certain non-electrolyte compound has a solubility parameter value close to that of the solute. For example, polar

solutes with $\delta = 18$ $(MPa)^{1/2}$ will not dissolve in solvents with $\delta = 14$ or $\delta = 26$ $(MPa)^{1/2}$ [66]. These are important data because they help to narrow the group of solvents that would be potentially suitable for a given solute.

7.3 Polarity and relative permittivity

There is an old principle 'like dissolves like'. According to this rule of thumb, polar solvents can dissolve polar substances, while nonpolar solvents can dissolve nonpolar substances. Polarity is the ability to form opposite and asymmetrical distribution, specifically electrical charge in a molecule. A similarity in chemical structure or the presence of like functional groups in molecules predicts the possibility of solute solvation in a solvent. Solvents whose molecules possess a permanent dipole moment are designated dipolar as opposed to apolar or nonpolar, for those lacking a dipole moment, (Figure 10) [67].

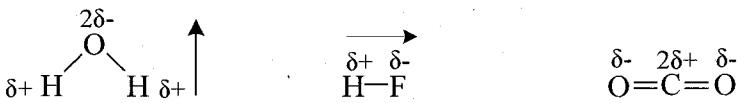

Figure 10:Dipoles and charges in polar water and hydrogen fluoride molecules, and nonpolar CO_2 [67].

The dipole moment has the greatest influence on the polar properties of solvents. The concept of polarity is used in solvents to describe their dissolving capabilities or the interactive forces between solvent and solute. Alcohols are examples of compounds having dipole moments as these are dipolar liquids. Table 3 shows the relationship between the polarities of solvents and solutes as well as their mutual solubilities.

Table 3: Solubility and polarity [59]

Solvent A	Solute B	Interaction			Mutual
		A···A	B···B	A···B	Solubility
Nonpolar	Nonpolar	Weak	Weak	Weak	Can be high
Nonpolar	polar	Weak	Strong	Weak	Probably low
polar	Nonpolar	Strong	Weak	Weak	Probably low
polar	polar	Strong	Strong	Strong	Can be high

Polarity depends on the action of all possible intermolecular interactions between solute ions or molecules and solvent molecules. The relative permittivity (or dielectric constant) of a solvent represents i) the extent of polarity of a solvent and ii) ability of the solvent to separate its charges and orient its dipoles [60].

The relative permittivity, ε_r, of a solvent is measured by placing it between the plates of a capacitor. If the electric field strength between the capacitor plates in a vacuum is E_o, this is lowered to E when a solvent is introduced. The relative permittivity, ε_r , is defined by Equation 42 [67].

$$\varepsilon_r = \frac{E_o}{E} \tag{42}$$

The relative permittivity influences the electrostatic interactions between electric charges. If two charge particles are placed in a solvent with relative permittivity with a distance of r between them, the electrostatic force, F_{solv}, between them is expressed by Equation 43:

$$F_{\text{solv}} = \frac{q_1 q_2}{4\pi\varepsilon_o\varepsilon_r r^2} = \frac{F_{vac}}{\varepsilon_r} \tag{43}$$

In Equation 46, ε_o is the permittivity in a vacuum and is equal to 8.854×10^{-12} C^2/J.m. The relative permittivity of a solvent has a major influence on the electrostatic solute-solute and solute–solvent interactions as well as on the dissolution and dissociation of electrolytes. Thus, relative permittivity is used in classifying solvent polarity or solvating capability. Solvents with high relative permittivity ($\varepsilon_r \geq 15$ or 20) are called polar solvents, while those with low relative permittivity are called nonpolar solvents [60, 67].

The Columbic force of attraction between two oppositely charged ions is inversely proportional to the relative permittivity of the solvent, according to Equation 46. Therefore, only solvents with sufficiently high relative permittivity will be capable of reducing the strong electrostatic attraction between oppositely charged ions to an extent that ion pairs can dissociate into free solvated ions. These solvents are usually called dissociating solvents [59].

Figure 11 shows the schematic steps of solvation. First, immediately after ionization, contact ion pairs are formed. Here no solvent molecules intervene between the two ions that are in close contact. The contact ion pair constitutes an electric dipole having only one common primary solvation shell, (a). Where the components of an ion pair are separated by the thickness of only one solvent molecule it is called a solvent-shared ion pair[ix], (b). In solvent-shared ion pairs, the two ions already have their own primary solvation shells, (c). Further dissociation leads to solvent-separated ion pairs, (d). An increase in ion-solvating power and relative permittivity of the solvent favors solvent-shared and solvent-separated ion pairs [59, 60].

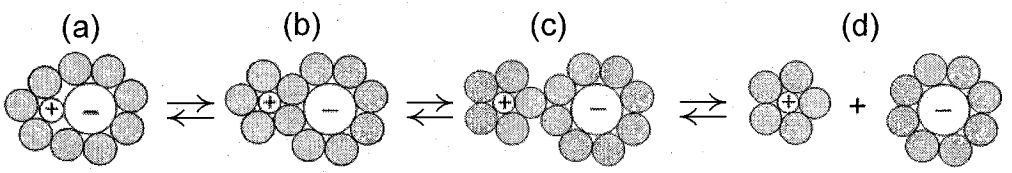

Figure 11: The schematic equilibrium between (a) a solvated contact ion pair, (b) a solvent-shared ion pair, (c) a solvent separated ion pair, and (d) unpaired solvated ions in solution [67].

Ion association, (a and b), is only noticeable in aqueous solutions at very high concentrations because of the exceptionally high relative permittivity of water (ε_r = 78.4). Ion association is found at much lower concentrations in alcohols. With a decrease in relative permittivity, complete dissociation becomes difficult. Some part of the dissolved electrolyte[x] remains undissociated. In solvents of relative permittivities less than 10 to 15, practically no free ions are found. On the other hand, when the relative permittivity exceeds 40 such as water, ion associates barely exist.

In solvents with intermediate relative permittivity such as ethanol, with ε_r = 15~20 the ratio between free and associated ions depends on the structure of the solvent as well as on the solute (e.g., ion size, charge distribution, hydrogen-bonded ion pairs.). The relative

---

ix Ion pairs are defined as pairs of oppositely charged ions with a common solvation shell [33].

x An electrolyte is a substance that dissociates into free ions when dissolved (or molten), to produce an electrically conductive medium. Because they generally consist of ions in solution, electrolytes are also known as ionic solutions. Electrolytes generally exist as acids, bases or salts [33].

permittivity values for water and primary alcohols are shown in Table 2. It can be seen that primary alcohols have approximately the same low relative permittivity in comparison to water. Therefore, free and dissociated ions are much less common in these primary alcohols. The solubility of alkali salts such as alkali chloride and alkali picrate[xi], is correlated to the solubility parameter and relative permittivity of alcohol [68]. The logarithmic solubility of alkali chlorides in alcohols is linearly proportional to solubility parameters of alcohols. On the other hands, the logarithmic solubility of alkali salts in alcohol is proportional to the reciprocal of the relative permittivity of alcohols (Figure 12).

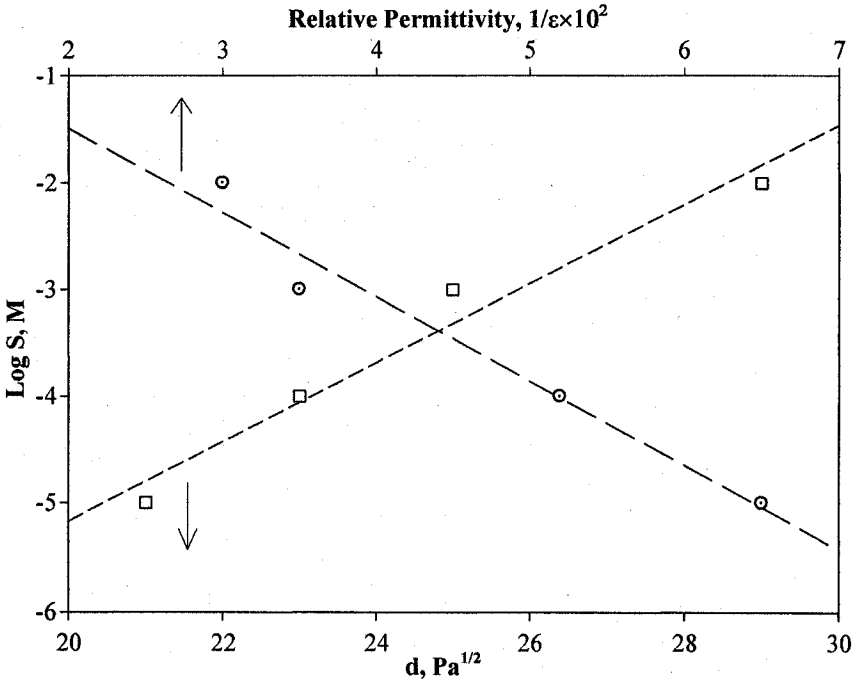

Figure 12: The relation between log S of potassium picrate in alcohols with solubility parameters and relative permittivity of alcohols, after Takamatsu [68].

The behavior of the relative permittivity of water in the presence of alcohols has been reported for a large variety of mixtures [69]. The influence of temperature for H_2O-CH_3OH mixtures is shown in Figure 13. Elevated temperature caused a decrease in relative permittivity of the mixture of water-methanol by reducing the strength of the hydrogen-hydrogen bonds.

[xi] For example, potassium picrate ($KC_6H_2N_3O_7$)

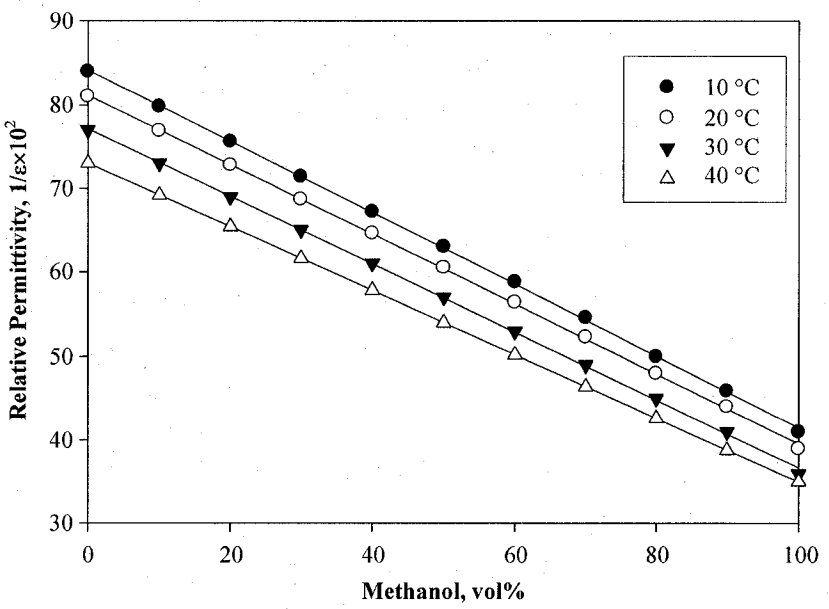

Figure 13: Relative permittivity for water-methanol mixtures, after Bates [69].

7.4 Solvation

"Solvation is a process in which solutes (molecules or ions) in a solution interact with the solvent molecules surrounding them" [60]. The solvation energy is defined as the standard chemical potential of a solute in the solution referred to that in the gaseous state, (Figure 14). Solvation of a solute has a significant influence on its dissolution and on the chemical reactions in which it participates. Conversely, the solvent effect on dissolution or on a chemical reaction can be predicted quantitatively from knowledge of the solvation energies of the relevant solutes. Ion solvation is of vital importance in the dissolution of an electrolyte [60, 70].

The necessary condition for dissolution of a substance is that energetic stabilization is obtained by dissolution, i.e., the Gibbs energy is decreased. The energetic stabilization depends on the energies of three interactions, i) solute-solvent, ii) solute-solute, and iii) solvent-solvent interactions. For the dissolution of a crystalline solute, AB, the lattice Gibbs energy of crystal AB is denoted by $\Delta G^{o}_{\text{latt}}$. If AB is completely dissociated into free

ions in the solution, the sum of the solvation energies of A^+ and B^- is equal to the solvation energy, ΔG^o_{solv} [59].

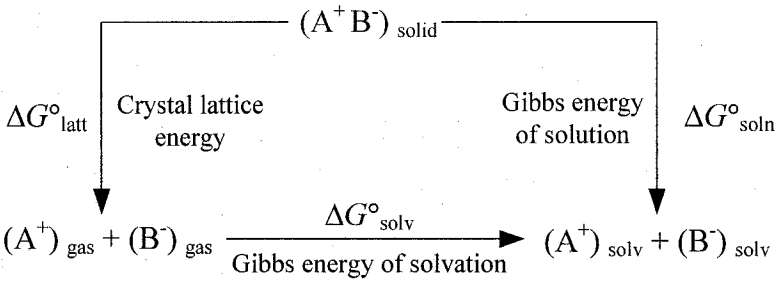

Figure 14: The relationship between standard Gibbs energies of solvation, solution, and crystal lattice energy [59]

The Gibbs energy of solvation of the solute AB is expressed by Equation 44.

$$\Delta G^o_{solv} = \Delta G^o_{soln} - \Delta G^o_{latt} \tag{44}$$

"Solubility is commonly defined as the concentration of the dissolved solute in a solvent in equilibrium with the undissolved solute at a specified temperature and pressure" [67]. If the solubility product of an electrolyte AB is expressed as K_{sp} (AB), Equation 45 is obtained as the relation between ΔG^o_{soln} and K_{sp} (AB):

$$\Delta G^o_{soln} = -RT \ln K_{sp}\,(AB) \tag{45}$$

The Born equation, Equation 46, attempts to calculate the free energies of ion solvation from the solvent relative permittivity and the size of the ion [67]. It is only a rough approximation, which is satisfactory if used to obtain the order of magnitude of ΔG^o_{solv}.

$$\Delta G^o_{solv} = -\frac{N_A z^2 e^2}{8\pi\varepsilon_o r}\left(1-\frac{1}{\varepsilon_r}\right) \tag{46}$$

The Born approximation indicates that with a decrease in the relative permittivity, ε_r, the solvation Gibbs energies will decrease. Thus, the Gibbs energy of solvation, ΔG^o_{solv}, will be less negative, or, in the other words, the Gibbs energy of solution, ΔG^o_{soln}, will be more

positive. Therefore, an ionic compound will dissolve less in a solvent that has less polarity than water. In general, ionic compounds are most soluble in dipolar solvents with high ε_r.

If the solvation energy of a species, i, in a solvent, R, (the reference solvent) is expressed as $\Delta G^o_{sv}(\mathrm{i, R})$ and is expressed in a solvent, S, (the solvent under study) as $\Delta G^o_{sv}(\mathrm{i, S})$, the difference between the two is expressed as $\Delta G^o_t(\mathrm{i, R \rightarrow S})$ and is called the Gibbs energy of transfer of species i from solvent R to S, Equation 47 [60]:

$$\Delta G^o_t(\mathrm{i, R \rightarrow S}) = \Delta G^o_{sv}(\mathrm{i, S}) - \Delta G^o_{sv}(\mathrm{i, R}) \qquad (47)$$

If the species i is electrically neutral, the value of $\Delta G^o_t(\mathrm{i, R \rightarrow S})$ can be obtained by a thermodynamic method. For example, if the solubilities of i in solvents R and S are S_R and S_S, respectively; $\Delta G^o_t(\mathrm{i, R \rightarrow S})$ can be obtained from Equation 48:

$$\Delta G^o_t(\mathrm{i, R \rightarrow S}) = RT \ln (S_R / S_S) \qquad (48)$$

If the species i is an electrolyte, MX, which is electrically neutral, it is also possible to obtain the value of $\Delta G^o_t(\mathrm{i, R \rightarrow S})$ from the solubilities of MX in the two solvents.

Standard molar energies of the transfer of Li^+, at 25 °C, from water to methanol, ethanol and 1-propanol are 4.4, 11 and 11.2 kJ/mol, respectively. A more positive value of $\Delta G^o_t(\mathrm{i, R \rightarrow S})$ for propanol as compared to methanol, means that the lithium cation is better solvated in methanol than in propanol or ethanol [60].

7.5 Chemical Properties of Solvents

The chemical properties of solvents are referred to as the acidity or the basicity of the solvents. "Conventionally, acidity and basicity are defined by the proton donating and accepting capabilities in term of the Brønsted acid-base concept and the electron pair accepting and donating capabilities by the Lewis acid-base concept" [60].

According to these theories, an acidic solvent has a strong proton-donating ability, and usually has strong hydrogen bond-donating, electron pair-accepting and electron-accepting

abilities. Moreover, a basic solvent has a strong proton-accepting ability and usually has strong hydrogen bond-accepting, electron pair-donating and electron-donating abilities.

In order to discuss the effect of solvents on chemical reactions, it is convenient to use the relative permittivity and acid-base properties as the parameters. The classification of solvents is roughly divided into two groups: 'amphiprotic solvents' and 'aprotic solvents'.

"Amphiprotic solvents have both acidic and basic properties in terms of the Brønsted acid-base concept" [59]. Using water as a reference, an amphiprotic solvent with an acidity and a basicity comparable to those of water is called a 'neutral solvent', whereas one with a stronger acidity and a weaker basicity than water is called a 'protogenic' solvent, and one with a weaker acidity and a stronger basicity than water is called a 'protophilic' solvent [59, 60].

Aprotic solvents (also commonly called inert) have very little affinity for protons and are incapable of dissociating to give protons. Aprotic solvents are also called indifferent, non-dissociating, or non-ionizing [60]. Primary alcohols, specifically methanol and ethanol, are considered as 'amphiprotic' solvents. Like water, alcohols are hydrogen-bond donors and proton donors. Thus, the electron pair is not involved in hydrogen bonding.

If SH is an amphiprotic solvent, it can donate a proton by Reaction 49 and accept a proton by Reaction 50.

$$SH \rightarrow S^- + H^+ \tag{49}$$

$$SH + H^+ \rightarrow SH_2^+ \tag{50}$$

Reaction 51 is the overall reaction or the autoprotolysis (autoionization) of the solvent SH:

$$2SH \rightarrow SH_2^+ + H^- \tag{51}$$

The extent of autoprotolysis is expressed by the autoprotolysis constant, K_{MX}, Equation 52.

$$K_{SH} = a_{SH_2^+} . a_{H^-} \tag{52}$$

Self-ionizing solvents possessing both acid and base characteristics such as water are designated amphiprotic solvents, in contrast to aprotic solvents, which do not self-ionize to a measurable extent.

For water the autoprotolysis constant (K_W) at 25 °C is given by Equation 53:

$$K_W = [H^+][OH^-] = 10^{-14} \quad (53)$$

The state at which H^+ equals OH^- is defined as neutral and occurs when H is 10^{-7} or at a pH of 7. For methanol, the autoprotolysis constant is given by Equation 54 [71].

$$K_{methanol} = [H^+][CH_3OH^-] = 10^{-16.6} \quad (54)$$

In methanol, when H^+ equals CH_3O^-, it is neutral. This occurs when H^+ is $10^{-8.3}$ mol/L or at a pH of 8.3 [71]. Autoprotolysis constants of primary alcohols are listed in Table 4.

Table 4: Autoprotolysis constants of water and primary alcohols (mol^2/L^2) (pK = -log [K) [60]

Water	Methanol	Ethanol	1-Propanol	2-Propanol
14.0	16.6	18.5	19.4	21.1

It can be seen that the higher autoprotolysis constant of ethanol, in comparison to water, means that ethanol is less self-dissociated than water. The K_{SH} is the measure of an acid's strength. A stronger acid has a smaller pK_{SH}. In other words, water more readily accepts a proton than methanol, therefore, water is a stronger base than methanol.

7.6 Structure of solvent and solute

The stoichiometry of the solvate complex is important in solvation. Coordination and solvation numbers reflect the idea that the solvation of ions or molecules consists of a coordination of solute and solvent molecules. The coordination number is defined as the number of solvent molecules in the first coordination sphere of an ion in solution [59]. The first coordination sphere is composed only of solvent molecules in contact with or within bonding distance of the ion (Figure 13).

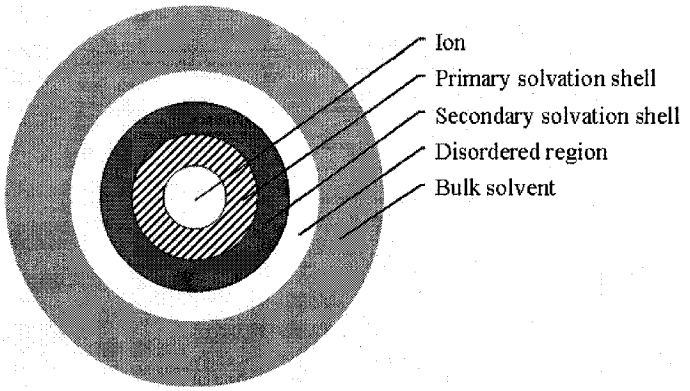

Figure 15: Typical model of solvated ions in structured solvents such as water and alcohols[60]

The solvation number is defined as the number of solvent molecules per ion that remain attached to a given ion long enough to experience its translational movement. The solvation numbers of the lithium cation in methanol, ethanol and 1-propanol are 8, 6 and 8, respectively [72].

7.7 Reaction of alcohol with alkali metals and their oxides

Alcohols can self-ionize to a minor extent when they react with strong alkali metals. The products of the reaction of alcohols with strong alkali metals are an alcoxyl group RO^- and H^+. Therefore, their behavior is characterized as being like acid. Similarly, when alcohols react with strong acids, they show basic behavior. These reactions are not ionic and take appreciably longer than the usual acid-base neutralization, which forms a salt.

Alkali metals such as sodium, potassium and lithium replace the hydrogen atom on the hydroxyl group of the alcohol to form a metal alkoxide, ROM, and hydrogen gas, (Reaction 55) [61, 73].

$$2\ ROH + 2M \rightarrow 2\ ROM + H_2 \qquad (55)$$

Aluminum and magnesium, in reaction with alcohols, may also form alkoxides and/or ROM, but require a catalyst [61]. Dissolving sodium or potassium hydroxide in alcohol forms an alkoxide, but an excess of water will reverse the reaction, Reaction 56 [61, 74].

$$ROH + NaOH = RONa + H_2O \qquad (56)$$

Sodium peroxide reacts with alcohol to form an alkoxide and sodium hydroperoxide, (Reaction 57) [61].

$$ROH + Na_2O_2 \rightarrow RONa + NaOOH \qquad (57)$$

Monohydric alcohols or primary alcohols, which most resemble water, form intramolecular adducts. Water can directly combine with a molecular entity, M, to form the hydrated compound, $M.nH_2O$, or water adduct.

Similarly, alcohols can form alcohol adducts in combination with other molecules to form intramolecular adducts. The new chemical species is formed by the direct combination of two separate molecular entities, M and alcohol, in such a way that there is no loss of atoms within the molecule M or the alcohol [61].

Both methanol and ethanol combine with magnesium chloride to form an alcohol adduct, $MgCl_2.6CH_3OH$. Another example of salt which can react in this manner and form the alcohol adduct is $BaO.2CH_3OH$ [61].

8. EXPERIMENTAL METHODOLOGY

Experimental activities carried out in the course of the present study are described here. The reactivity of lithium peroxide and lithium oxide in ambient air as function of humidity, particle size and the solubility of different lithium compounds in commercial alcohols was measured. The conversion of lithium peroxide was also studied via under vacuum and varying ambient conditions. The conditions leading the formation of lithium oxide from lithium peroxide were determined by TGA and DTA. The activation energy for thermal decomposition of lithium peroxide was measured. The analytical methods are described in the Appendices.

8.1 Experimental objectives

The primary goal of this study was to determine the efficiency of the process in relation to the principal experimental parameters affecting the conversion for production of high purity lithium peroxide. The parameters studied included changes in the reactants, contents of starting materials, and temperature.

8.1.1 Choice of alcohol

In order to effectively separate the products from the reactants, the reaction medium must have a low solubility for the products (oxides). So, they can properly precipitate, while other by-products (hydroxides) remain in various solutions. Alcohols to certain extent exhibit this preferential behavior toward oxides and hydroxides. The following are the main requirements for the alcohol medium:

1. A high solubility for $LiOH.H_2O$: For complete conversion of $LiOH.H_2O$ to Li_2O_2, it is preferred that the conversion reaction takes places in a fluid medium instead of in a slurry. Therefore, an alcohol with a high solubility for $LiOH.H_2O$ is vitally necessary. An alcohol with high solubility leads to a lower consumption of alcohol and H_2O_2.

2. Insolubility for Li_2O_2: The insolubility for lithium peroxide was the key factor for selection of alcohol because the main purpose of using alcohol is to precipitate the produced Li_2O_2. In addition, the stability of Li_2O_2 in the alcohol, is important because decomposition of Li_2O_2 in alcohol results in lower productivity.
3. The alcohol remains stable during the conversion reaction. According to the literature, primary alcohols are not dissociated upon addition of H_2O_2 or by reaction with active oxygen[61].
4. The alcohol is recyclable for further usage. In this regard, the formation of an azeotropic mixture with water must be avoided.
5. The alcohol is commercially available at reasonable cost.
6. The alcohol is safe to use and handle: Although working with alcohols requires careful attention, in case of direct contact with skin, they are not categorized as poisonous materials.

The three primary alcohols of methanol, ethanol and propanol (1 and 2-propanol) were the main candidates. Before performing the conversion tests, solubility tests were performed to select the alcohol.

8.1.2 Choice of starting material

Lithium bearing materials that are commercially available include lithium hydroxide monohydrate ($LiOH.H_2O$), anhydrous lithium hydroxide (LiOH) and lithium carbonate, (Li_2CO_3). Lithium carbonate was discarded early on as a starting material because of remarkably low conversion to Li_2O_2 during preliminary test work. The experiment with Li_2CO_3 and the relevant results are explained separately in Appendix VII. Thus, the starting materials were limited to $LiOH.H_2O$ and LiOH. It was speculated that using LiOH instead of $LiOH.H_2O$, the consumption of H_2O_2 might be decreased and/or the efficiency of the process might be increased.

8.1.3 Choice of hydrogen peroxide concentration

The amount of H_2O_2 for conversion of lithium in the form of hydroxide in solution needed to be determined. Equations of 58 and 59 represent the activity coefficients of water and hydrogen peroxide as function of temperature and mole faction of water in solution of hydrogen peroxide and water, respectivily.

$$\gamma_{water} = \exp\left(\frac{(1-x_w)^2}{RT}\left[(-1017+0.97\times T)+85(1-4x_w)+13(1-2x_w)(1-6x_w\right]\right) \quad (58)$$

$$\gamma_{H_2O_2} = \exp\left(\frac{x_w^2}{RT}\left[(-1017+0.97\times T)+85(3-4x_w)+13(1-2x_w)(5-6x_w\right]\right) \quad (59)$$

As shown in Figure 16, due to the water in the H_2O_2 solution (concentration of H_2O_2 is typically about 35-50 wt %), the activity coefficient of H_2O_2 is reduced. Because of the presence of water, from two sources of H_2O_2 (65 wt% H_2O) and $LiOH.H_2O$ (42.8 wt% H_2O) in the present work , it was anticipated that H_2O_2 consumption might be increased.

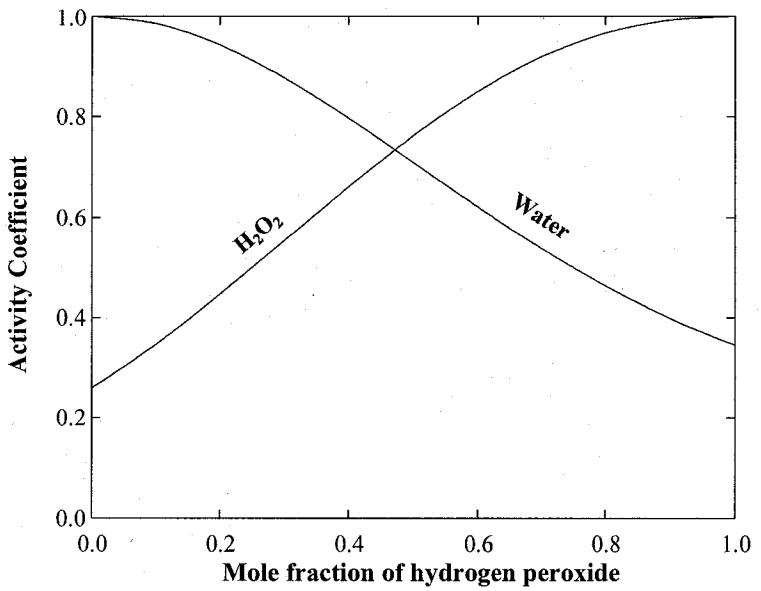

Figure 16: Activity coefficients at 25 °C for aqueous solutions of hydrogen peroxide (after Schumb) [56].

Hydrogen peroxide is not a stable compound, but fortunately, it does not react readily with alcohols, unless a catalyst is present [56]. However, care and precautions are necessary when mixing together hydrogen peroxide and alcohol.

8.1.4 Safety measures for mixing alcohol and hydrogen peroxide

Dangers exist with the use of mixtures of hydrogen peroxide and organic chemicals. Figure 17 shows the ternary hydrogen peroxide–acetone–water system, where the hatched area represents explosive combination of these compounds. Many other organic compounds give similar results. The size of the explosive region depends on the organic compound and the test conditions [75]. When working with active oxygen compounds, steps should be taken to ensure the mixtures do not occur in the explosive area during the reaction or processing phases.

It should be noted that when using 35 % wt or less hydrogen peroxide, it is unlikely that explosive compositions will be formed. Therefore, the use of 35 %wt or less hydrogen peroxide should be employed wherever possible and the use of higher strengths avoided [76].

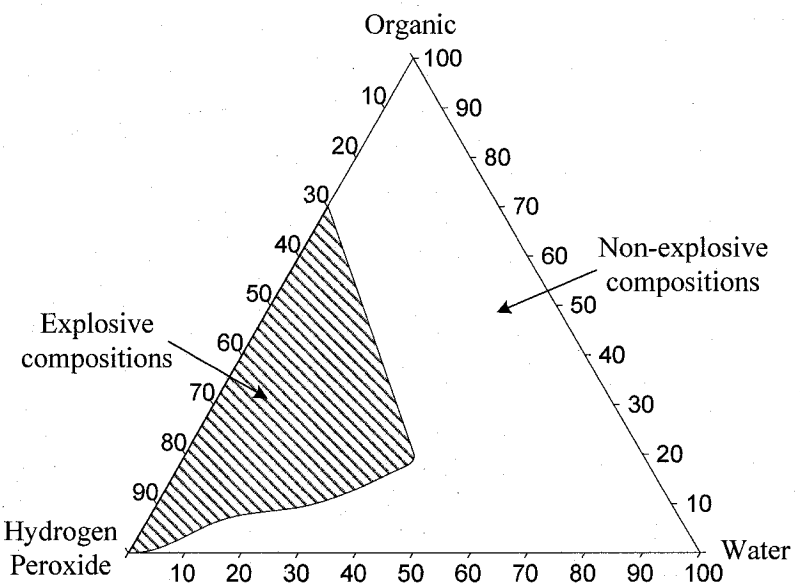

Figure 17: Explosive range (hatched area) of hydrogen peroxide–organic–water mixtures, in wt% at 25 °C [76].

The order of addition of hydrogen peroxide to alcohol is another issue that should be considered. As can be seen from Figure 17, the gradual addition of hydrogen peroxide to a mixture containing alcohol, makes it possible to avoid of formation of an explosive mixture.

8.1.5 Production of Li_2O_2 from precipitate

The addition of H_2O_2 to a mixture of $LiOH.H_2O$ and alcohol does not lead to the direct formation or precipitation of lithium peroxide. Upon completion of the conversion reaction, a compound containing Li_2O_2, H_2O_2, and H_2O is formed. Therefore, heat is required to remove H_2O_2, H_2O and alcohol molecules to yield Li_2O_2. The common device for decomposition of the precipitate, which also has been reported in literature, is the vacuum oven.

Study of the decomposition of the precipitate required the knowledge of the precipitate composition. Hence, it was necessary to determine the composition of the precipitate. In addition, it was speculated that by changing the concentration of reagents, i.e., H_2O_2, or change of alcohol, the composition of the precipitate varied.

In order to characterize precisely the changes of the precipitate during its decomposition, experiments were performed with the precipitate at different ambient and isothermal conditions in a glovebox in addition to using the vacuum oven.

8.2 Reactivity of Li_2O_2 and Li_2O in air

These tests were performed to determine the kinetics of the carbonation of Li_2O_2 and Li_2O. The reaction of Li_2O_2 and Li_2O was studied during exposure to air as a function of time. Different particle sizes of Li_2O_2 and Li_2O and various air humidities were considered in the test conditions. The CO_2 content of air was in the range from 320 to 400 ppm according to the product specification of the supplier.

Lithium oxide was supplied by Zigma-Aldrich with a purity of about 99%. The maximum grade of the lithium peroxide that was commercially available had a maximum Li_2O_2 content of 90 % (Zigma-Aldrich and Alfa-Aesar). There was no choice of particle size.

Therefore, it was decided to use lithium peroxide produced in-house by the method explained in Section 8.4.1. To ensure the lithium peroxide was pure and free of lithium hydroxide; it was washed twice with methanol and then dried in a vacuum oven at a pressure of 0.01 atm at 90 °C for 6 hr. The resulting powdered lithium peroxide was screened with a mechanical shaker on screens of 53, 106 and 212 μm mesh opening to separate the Li_2O and Li_2O_2 into size classifications to test the effect particle size. The resulting particle sizes were measured in propanol by a laser particle-size analyzer, HORIBA LA-920.

All reactivity experiments were performed in a glove box in order to provide a constant atmosphere and temperature. Before starting each test, the glovebox was flushed with commercial air of known composition. The commercial air was then circulated during the test at a rate of 5 mL/min. Table 5 shows air composition provided by commercial suppliers.

Table 5: Specification of commercial air used in the present study

Supplier	Product Code	Relative Humidity (%)[xii]	CO_2 (ppm)
Matheson-Mex	G2001201	5 ± 1	350 - 400
Praxair	AI 0.0Z	21 + 1	320 - 385
Matheson-Mex	G1105818	57 ± 1	350 - 400

The temperature and humidity of at atmosphere inside the glove box were continuously measured by a Thermo-Hygrometer OMEGA RH-31. At the end of each test, the samples were stored in glass vials. The weight of containers was measured before starting the experiment. The changes in the mass of the samples were measured with a balance inside the glove box with a precision of ± 0.1 mg.

Table 6 presents the conditions of the experiments. In the first experiment, the reaction of either Li_2O_2 or Li_2O during exposure to air was measured as function of time. Except for the relative humidity of the atmosphere, the other parameters were held constant. The

[xii] At temperature of 20 °C, the relative humidities of 5, 21 and 57 % are equal to 0.94, 4.14 and 10.7 mg H_2O/Nm^3, respectively.

samples were then weighed inside the glovebox at intervals of about 12 hours. Afterwards, they were placed in their vials and sealed for further testing later.

In the second experiment, the effect of the particle size of Li_2O_2 on the reaction with air atmosphere was studied. As stated, the particle sizes of +53, +106 and +212 μm were prepared for this experiment. The samples were placed inside of the glovebox having a fixed air composition. The temperature inside the glovebox (and also in the laboratory) had a constant temperature of 20 ± 1°C. The change of weight was measured by the balance inside the glovebox.

Table 6: Experimental conditions for reactivity tests

Test 1: Comparing Li_2O_2 and Li_2O	
Material:	Li_2O_2 or Li_2O
Size:	+53 μm
CO_2:	320 - 400 ppm
H_2O_{Air}:	5, 21 and 57 ± 1 RH[xiii]
Temperature:	20 ± 1°C
Test 2: Particle size	
Material:	Li_2O_2
Size:	+53, +106 and +212 μm
CO_2:	320 - 400 ppm
H_2O_{Air}:	57 ± 1 % RH
Temperature:	20 ± 1°C

X-ray diffractometery was used to detect the formation of Li_2CO_3, $LiOH.H_2O$ and LiOH. Pure lithium peroxide and lithium oxide were used as standards to characterize any change in peak intensity of the main peaks of the samples as a function of time. In addition, to detect changes in the lithium peroxide content, the active oxygen content of samples was analyzed by a titration method[xiv]. For quantitative analyses of Li_2CO_3 and LiOH, the

[xiii] Relative humidity

[xiv] This technique is explained in detail in Appendix III.

residue technique was used by dissolving LiOH and Li_2O_2 in methanol. Scanning electron microscopy was also used to take high-resolution pictures to determine the changes of the morphology of Li_2O and Li_2O_2 during exposure to the atmosphere.

8.3 Solubility of lithium compounds in alcohols

Solubility tests were performed in order to investigate the solubilities $LiOH.H_2O$, LiOH, Li_2O_2, Li_2O and Li_2CO_3 in methanol, ethanol, 1-propanol and 2-propanol. Table 7 shows the values of the parameters that were set for these experiments. ASTM standard method, E1148-02, was used for measurement of the solubility of lithium compounds in different alcohols [77, 78].

Table 7: Experimental conditions for solubility tests

Material:	$LiOH.H_2O$, LiOH, Li_2O_2, Li_2O or Li_2CO_3
Size:	from +212 to +300 μm
Alcohol:	methanol, ethanol, 1-propanol or 2-propanol
Stirring time:	1 and 48 h
Stirring speed:	100 rpm
Temperature:	20 ± 0.2°C

The lithium compounds and the alcohols were supplied by Sigma-Aldrich. All reagents were used as received. A thermostatically controlled water bath was used to establish and maintain the temperature during solubility measurements. It held four 250 mL, suitably sealed, glass flasks. The system was operated at 20 ± 0.2 °C. The solution in the beaker was stirred by a plastic-coated magnet loaded impeller at a stirring speed of 100 rpm. Known masses of alcohols and lithium compounds were measured on a Mettler Toledo Co. model AX204 analytical balance with a precision of 0.1 mg.

Based on experience, an excess amount of the lithium compounds was added to the alcohols to ensure the saturation of the solutions. The samples were mixed for the times of 1 hr or 48 hrs. Following the mixing, the samples were allowed to stand for an additional 24 hr. A clear liquid was collected using Versapore® Membrane filters having a nominal

pore size of 0.2 μm. Lithium compound concentrations were determined by an acidimetric titration analysis and residue technique that is described below.

Residue technique: The residue technique involved taking a sample of the solution of known mass by syringe, placing it an open vial and heating it in a vacuum oven at a temperature of 90 °C for 6 hours. The amount of dissolved lithium compound in the alcohols was calculated from the weight difference between the vial after heating and the empty vial and the volume of the sample. In all cases, the analysis of the solubility was done in triplicate. To investigate if there was any change in the composition of lithium compounds during the dissolution process, the dried lithium compounds were analyzed by XRD.

8.3.1 Effect of mixing time on the solubility of $LiOH.H_2O$ in methanol

The first objective of these tests was to measure the time required for mixing of $LiOH.H_2O$ in methanol to reach its solubility limit. This time was then used as the time of mixing for the later tests. These tests also measured the solubility of $LiOH.H_2O$ in methanol as a function of temperature. Two sets of tests were performed (Table 8). The same setup as described in Section 8.3 was used.

Table 8: Experimental conditions for solubility tests of $LiOH.H_2O$ as a function of time

Material:	$LiOH.H_2O$
Size:	+212 μm
Alcohol:	methanol
Time:	20, 40, 60, 80, 100 and 120 min
Temperature:	20 °C
Stirring speed:	100 rpm

For the first experiment, 16.5 g $LiOH.H_2O$ was added to 100 g CH_3OH in a 250 mL beaker. The beaker was completely sealed and placed in the water bath[xv] at a fixed

[xv] Lindberg/Blue M WB1120A

temperature of 20 ± 0.2 °C. Before starting each test, the water bath was maintained at 20 °C for 1 hour to establish a steady temperature. The solution in the beaker was stirred with a magnetic impeller at a stirring speed of 100 rpm for times of 20, 40, 60, 90 and 120 min. Since filtration might not separate unsolved particles and as instructed [77] following the mixing, the samples were allowed to stand for an additional 24 h. The clear liquid was filtered from the flasks using Versapore® membrane filters (0.2 pore size).

Three samples of solution were taken by a glass syringe from each beaker. The difference between the mass of the syringe with solution and after pouring into a glass vial was measured. The vials were heated in a vacuum oven at a pressure of 0.1 atm and temperature of 90 °C for 6 h. The amount of $LiOH.H_2O$ compound dissolved into the alcohols was calculated from the mass difference from empty vial with after drying. To cross check the results, the lithium content of the clear solutions was also analyzed by titration.

8.3.1.1 Measurement of pH and ORP of solution

The changes of pH and oxidation/reduction potential of the solution during the dissolving of $LiOH.H_2O$ in methanol, was measured as a function of time. The pH and ORP of solution were determined by a double-junction ORP electrode[xvi] (Ag/AgCl electrode) along with a pH electrode. In order to read the pH and potential of solution concurrently, a potentiometer[xvii] having a multi-channel recording port was used. The standard potential of the electrode reference, the Ag/AgCl electrode (KCl 4 *M*), was calculated from Equation 60.

$$E = 205 - 0.73 \times (T - 25\ °C) \qquad (60)$$

At a temperature of 20 °C, the potential of the electrode reference was measured to be 207.92 mV.

[xvi] Provided by Cole-Palmer Instrument Co, manufactured by Phoenix Electrode Co.

[xvii] Thermo-ORION Model 720A.

8.3.2 Effect of temperature on the solubility of $LiOH.H_2O$ in methanol

In a second set of experiments, the effect of temperature on the solubility limit of $LiOH.H_2O$ in methanol was measured. A similar procedure to that described in Section 8.3.1 was performed using a water bath at temperatures of 30, 40, 50, and 60 °C[xviii] for fixed mixing times of 60 min. Table 9 shows the experimental conditions for solubility tests of $LiOH.H_2O$ as a function of temperature.

Table 9: Experimental conditions for solubility tests of $LiOH.H_2O$ as a function of temperature

Material:	$LiOH.H_2O$
Size:	+212 μm
Alcohol:	methanol
Time:	60 min
Temperature:	20, 30, 40, 50, 60 °C
Stirring speed:	100 rpm

8.4 Study of conversion to lithium peroxide

The conversion experiments were the major part of this study. The main objective of this set of experiments was to produce high purity lithium peroxide. Finding the conditions that led to an optimum process was also an objective. The optimum was defined as the minimum consumption of the reactants: hydrogen peroxide and methanol for the maximum conversion of raw material to lithium peroxide. In the following sections, the term "efficiency" is extensively used. In this study, the efficiency in percentage terms is defined as moles of lithium peroxide produced per mole of reacted lithium hydroxide monohydrate.

8.4.1 Hydrogen peroxide consumption

The aim of this study was to determine the amount of H_2O_2 required for conversion of $LiOH.H_2O$ to Li_2O_2. Table 10 shows the experimental conditions for the H_2O_2

[xviii] All lower than methanol's boiling point (64 °C).

consumption tests. First, 13 g of $LiOH.H_2O$ were added to 100 g of methanol, and mixed for 1 hour at a stirring speed of 100 rpm at 20 °C.

Then, an amount of either 20, 22, 24, 26, 28, 30, 32 or 34 g of H_2O_2 (35 wt%) was added to the solution and followed by shaking for 15 min. The precipitated solid was settled by centrifuging and separated by decantation of the solution from the solid/slurry. Then, the containers were heated for 6 hours under vacuum of 0.01 atm at 90°C. In all experiments in order to prevent material splash during heating in the vacuum oven, the vacuum pump was run intermittently with a controller.

Table 10: Experimental conditions for H_2O_2 consumption tests

Dissolution:	
$LiOH.H_2O$:	13 g
Methanol:	100 g
Stirring time:	60 min
Temperature:	20 °C
Stirring speed:	100 rpm
Conversion:	
H_2O_2 (35 wt %):	20, 22, 24, 26, 28, 30, 32 and 34 g
Stirring time:	15 min
Temperature:	20 °C
Stirring speed:	100 rpm
Drying:	
Temperature:	90 °C
Vacuum:	0.01 atm
Time:	6 hr

The amount of Li_2O_2 produced was calculated by measuring active oxygen of the solid by a titration method (Appendix III) and the residue technique (Section 8.3). All the precipitated solids were analyzed by XRD. The lithium content in the raffinate was measured by acidimetric titration (Appendix II).

8.4.2 Measurement of pH and ORP of solution

To determine the change in pH and ORP of the solution due to the addition of H_2O_2, the same procedure as in hydrogen peroxide consumption experiments described in 8.3.1.1 was repeated with the respective electrodes in place. Hydrogen peroxide (35 wt%) was added in increments of 2 g to a solution with the concentration of 13 g $LiOH.H_2O$ per 100 g CH_3OH.

8.4.3 Effect of Hydrogen peroxide concentration

To determine the effect of H_2O_2 concentration on the efficiency of Li_2O_2 production, a higher concentration of H_2O_2 (50 wt%) was also examined. In this regard, equal moles of H_2O_2 (in either 35 or 50 wt% solutions) were weighed to convert the same mass of $LiOH.H_2O$, Table 5. A procedure similar to that described in Section 8.4.1 was followed.

Table 11: Experimental conditions for H_2O_2 50 wt % consumption tests

Dissolution:	
$LiOH.H_2O$:	13 g
Methanol:	100 g
Stirring time:	60 min
Temperature:	20 °C
Stirring speed:	100 rpm
Conversion:	
H_2O_2 (50 wt %):	14, 15.4, 16.8, 18.2, 19.6, 21, 22.4 and 23.8 g
Stirring time:	15 min
Temperature:	20 °C
Stirring speed:	100 rpm
Drying:	
Temperature:	90 °C
Vacuum:	0.01 atm
Time:	6 h

8.4.4 Effect of the kind of alcohol on conversion

This set of experiments was performed to determine the effect of changing the kind of alcohol on H_2O_2 consumption and on the efficiency of Li_2O_2 production. In this regard, ethanol and 1-propanol were compared with methanol.

The method described in Section 8.4.1 was used to perform the experiments. For all alcohols, equal masses of $LiOH.H_2O$ and H_2O_2 (35 wt%) were used. Table 12 shows the values that were selected for testing.

Table 12: Experimental conditions for measuring the effect of the kind of alcohol on conversion

Dissolution:	
Ethanol	100 g
1-propanol	100 g
$LiOH.H_2O$:	13.5 g
Stirring time:	60 min
Temperature:	20 °C
Stirring speed:	100 rpm
Conversion:	
H_2O_2 (35 wt %):	21, 24, 27, 30, 33 and 36 g
Stirring time:	15 min
Temperature:	20 °C
Stirring speed:	100 rpm
Drying:	
Temperature:	90 °C
Vacuum:	0.01 atm
Time:	6 h

Each test was performed three times. The lithium peroxide content of each sample was calculated from the measured active oxygen content (Appendix III) and the residue technique (Section 8.3). In order to compare the changes in the composition of the precipitate due to a change of alcohol, solutions with concentrations close the solubility limit of $LiOH.H_2O$ in the ethanol and 1-propanol were prepared. The concentrations of the

solutions, g $LiOH.H_2O$ per 100 g alcohol, were selected according to the solubility limits of $LiOH.H_2O$ in the respective alcohols. From the solubility tests (in Section 8.3), the solubility limit of $LiOH.H_2O$ in methanol, ethanol and 1-propanol were measured as 13.5, 2.0 and 0.9 g in 100 g alcohol, respectively. The alcohol content of the precipitates was measured by Raman spectroscopy according to the method described in Appendix IV. All the precipitated and dried solids were also analyzed by XRD.

8.4.5 Using LiOH in place of $LiOH.H_2O$

These experiments were performed to determine the effect of using lithium hydroxide, instead of lithium hydroxide monohydrate, on hydrogen peroxide consumption. The procedure was the same as that described in Section 8.4.1. Equal moles of $LiOH.H_2O$ and LiOH were weighed to normalize the lithium content in the starting material, Table 13.

Table 13: Experimental conditions for H_2O_2 consumption using LiOH

Dissolution:	
LiOH:	7.7 g
Methanol:	100 g
Stirring time:	60 min
Temperature:	20 °C
Stirring speed:	100 rpm
Conversion:	
H_2O_2 (50 wt %):	21, 24, 27, 30, 33 g
Stirring time:	15 min
Temperature:	20 °C
Stirring speed:	100 rpm
Drying:	
Temperature:	90 °C
Vacuum:	0.01 atm
Time:	6 h

The hydrogen peroxide was added to each flask, followed by stirring for 15 min. The flasks were then centrifuged, followed by decanting the raffinate from the solid/slurry

phase. After this, the flasks were heated for 6 hours under a vacuum of 0.01 atm at 90°C. The lithium peroxide content of each sample was calculated from the measured active oxygen content (Appendix III) and by the residue technique (Section 8.3). All the precipitated solids were also analyzed by XRD.

8.4.6 Effect of temperature on conversion

It was speculated that carrying out the conversion at higher temperatures, could result in lower hydrogen peroxide consumption. To determine the effect of temperature on the conversion reaction, two series of experiments were performed. In this regard, solutions with different concentrations of hydrogen peroxide were used. First, solutions with a concentration near the solubility limit (12.5 g $LiOH.H_2O$ per 100 g CH_3OH) were prepared, followed by addition of H_2O_2 (35 wt%) corresponding to ratios of 0.73, 0.98 and 1.22 H_2O_2:$LiOH.H_2O$. Then, the flasks were placed in a water bath at set temperatures of 10, 20, 30, 40, 50 and 60 °C. The flasks were sealed with a stopper. Each test was repeated three times.

To measure the change in the efficiency of the Li_2O_2 production, the mass of dried slurry was calculated by difference from the empty container. The lithium peroxide content of each sample was calculated from the measured active oxygen content (Appendix III) and by the residue technique (Section 8.3). All the precipitated solids were also analyzed by XRD.

8.4.7 Effect of time on conversion

One of the initial measurements was to determine the time required for the reaction of H_2O_2 with $LiOH.H_2O$. In this regard, 13 g $LiOH.H_2O$ were mixed with 100 g methanol for 1 hour. Then 28 g H_2O_2 (35 wt%) was added, followed by mixing for 5, 10, 15, 20, 25, 30, 35, 40, 45 min. In all tests, the solutions were held at 20 °C and stirred at 100 rpm. At the end of each mixing time, the flasks were centrifuged and raffinate was decanted.

The flasks with the residue were then heated for 6 hours under a vacuum of 0.01 atm at 90 °C. The lithium peroxide content of each sample was calculated from the measured active

oxygen content (Appendix III) and by the residue technique (Section 8.3). All the precipitated solids were also analyzed by XRD. Three repeats were performed for each set of conditions.

8.4.8 Using solutions with additions higher than the solubility limit

This experiment was similar to that described in Section 8.4.1. It used a fixed mass of methanol with increasing amounts of $LiOH.H_2O$ and H_2O_2 at a fixed ratio. The incremental masses of $LiOH.H_2O$ and H_2O_2 were added to 100 g of CH_3OH according to Table 14. The solution was stirred for 1 hr. Hydrogen peroxide (35 wt %) was added at a molar ratio of 2.2 with respect to $LiOH.H_2O$. This molar ratio was obtained from the optimum result of experiments in Section 8.4.1.

Table 14: Masses of reagents

CH_3OH (g)	$LiOH.H_2O$ (g)	H_2O_2 (g)	$H_2O_2/LiOH.H_2O$ (g/g)
100	13	28.3	2.2
100	14	30.5	2.2
100	15	32.8	2.2
100	16	35.1	2.2
100	17	37.3	2.2
100	18	39.6	2.2
100	19	41.9	2.2
100	20	44.1	2.2
100	21	46.4	2.2
100	22	48.6	2.2

The same procedure to decant and dry the precipitated product as per previous tests was used. The concentration of Li_2O_2 produced was calculated by measuring the active oxygen content of solid by the titration method (Appendix III) and the residue technique. All the precipitated solids were analyzed by XRD. For each set of conditions, three repeats were performed.

8.5 Study of decomposition of the precipitate

After precipitation of the compound containing lithium peroxide, a decomposition study was performed. As stated in Section 8.4, lithium peroxide was not formed directly during conversion. Rather, the product of conversion reaction was a precipitate comprising a compound of comprising Li_2O_2, H_2O_2, H_2O and CH_3OH. To yield Li_2O_2, the precipitate was heated to drive off the water and alcohol adducts. In this regard, three sets of experiments were performed including drying in a vacuum oven, in a glovebox at ambient temperature and by TGA/DTA in an inert atmosphere.

8.5.1 Drying at ambient temperature

This experiment was performed to examine the following two speculations.

First, during heating of the precipitate, two or three compounds including H_2O_2, H_2O_2 and CH_3OH might be concurrently evolved. It was speculated that by slowly drying the precipitate at an ambient temperature, it would be possible to distinguish the sequence of adducts evolved from Li_2O_2.

Second, it was believed that at ambient temperature, Li_2O_2 might be less reactive with CO_2 in comparison to higher temperatures. Thus, Li_2O_2 could be dried at low temperature without requiring vacuum. Therefore, it was decided to examine the drying of the precipitate in a glovebox at the ambient temperature.

Thirteen grams of $LiOH.H_2O$ were added to 100 g of CH_3OH, followed by mixing for 1 h. Then 28 g H_2O_2 (35 wt%) were added to the solution and mixed for 15 min. The precipitate was separated from the solution by centrifuging. The initial composition of precipitate was determined by analyzing the contents of lithium, active oxygen and methanol (Appendices II and III). The precipitate was stored in a vial inside the glovebox. Air with two relative humidities namely, 5 ± 1 and 57 ± 1, was used for drying. The specifications of the air are shown in Table 5. Every 12 hrs, the samples were weighed inside the glovebox. The contents of lithium and active oxygen were analyzed by titration

(Appendix II and III). Prior to analysis by XRD, the samples were dried in a microwave oven immediately after removal from the glovebox.

8.5.2 Thermal analysis by TGA and DTA

In order to determine the changes in the composition of the precipitate during drying, the following set of experiments were performed. A SETARAM[xix] Labsys, simultaneous TGA-DTA instrument in the Department of Mining, Metals and Materials Engineering of McGill University was used for thermal analysis experiments.

The precipitate was prepared as described in Section 8.5.1. The composition of the initial precipitate was determined by analyzing the contents of lithium, active oxygen and methanol (Appendix II and III). About 200-300 mg of the precipitate was placed in a 100 μL alumina crucible and positioned very close to a reference sample, which was an identical, but empty, alumina crucible. The sample and the reference were subjected to the same heating at rates of 10 °C/min up to 300 °C under an argon atmosphere.

Two thermocouples attached to the bottom of the crucibles measured the temperatures of the sample and the reference sample. The measured temperature was automatically transferred to a computer that recorded the temperatures and calculated the difference between the two thermocouples.

When exothermic or endothermic events occurred in the sample, the temperature of the sample increased faster or slower than the reference sample. Accordingly, a change in the temperature difference curve would be observed. In order to determine the event initiation temperature, the first derivative of the temperature difference curve was calculated and the temperature of the phase transformation was taken as the point of information in the first derivative curve.

[xix] SETARAM is a trademark of SETARAM Instrument Ltd, France

8.5.3 Thermal decomposition in vacuum

In order to determine the changes in the composition of the precipitate during drying in a vacuum oven as a function of time, the following set of experiments was performed. The precipitate was prepared as described in Section 8.5.1. The precipitate was placed in a vial, which was weighed previously.

The vacuum oven was set at a pressure of 0.01 atm and a temperature of 90 ± 1 °C. This temperature, the temperature before initiation of the precipitate decomposition, was obtained from the results of TGA experiments described in Section 8.5.2. The gas evolved from the precipitate was collected by a vapor trap[xx] that was installed between the vacuum oven and the vacuum pump. The samples were taken every 10 min and were weighed without significant delay. Then, their compositions were determined by analyzing of the contents of lithium, active oxygen and methanol (Appendix II and III). For each set of tests, three samples were used and the all experiment was repeated five times.

8.6 Study of lithium oxide formation

The objective of the following set of experiments was to study the formation of lithium oxide from lithium peroxide or in other words, the decomposition of the lithium peroxide. The lithium peroxide was prepared as described in Section 8.5.1. To be certain of the purity of lithium peroxide, it was washed with methanol and dried in a vacuum oven at a pressure of 0.01 atm at 90 °C for 6 h. Then, the powdered lithium peroxide was screened by a mechanical shaker. The screens of 37, 53, and 212 μm were selected for the experiment described in Sections 8.6.1 and 8.6.2.

8.6.1 Decomposition of lithium peroxide in different atmospheres

In order to determine the effect of the kind of atmosphere on lithium oxide decomposition, the following sets of experiments were performed. Lithium peroxide with a particle size of 37 μm was placed in an alumina crucible in the cylindrical furnace. The furnace was set at

---

[xx] Kontes™ Brand

a temperature of 400 °C. For the first set of experiments, nitrogen was purged through the furnace at a rate of 5 mL/min. In another set of experiments, the tests were run without purging any gas into the furnace. The final set was run with Ar purging through the furnace at a rate of the 5 mL/min and the temperature was increased from 25 °C to 400 °C at a rate of 10 °C/min.

Samples were taken from the furnace every 10 min to analyze the change in their weight and chemical composition. The weight change in samples was measured by a balance with a precision of ± 0.1 mg. The Li_2O_2 content of samples was measured by titration. The other compounds that were formed were analyzed by XRD.

8.6.2 Thermal study by TGA-DTA

A SETARAM Labsys simultaneous TGA-DTA instrument in the Department of Mining, Metals and Materials Engineering of McGill University was used for thermal analysis experiments.

The activation energy of lithium oxide formation was measured according to the method described in Appendix V. The use of thermogravimetric data to evaluate the kinetic parameters of solid-state reactions involving weight loss has been explained by Coats [79]. This method allows the determination of both activation energy and the order of reaction. The most important advantage this method over conventional isothermal studies is using one single sample for the investigation. In addition, using a small sample in the crucible ensures an accurate temperature measurement and precise detection of any departure from a linear heating rate due to endothermic or exothermic reactions. The use of a small sample also reduces the effects of crucible geometry, heating rate, sample pre-history and particle size.

For DTA/TGA experiments, about 200-300 mg of the lithium peroxide powder with a size of 37 μm was placed in a 100 μL alumina crucible. The sample was heated at rate of 10 °C/min up to 650 °C under an argon atmosphere.

For determination of the effect of particle size on the activation energy and for determining of the order of reaction, only the TGA setup was used. In this regard, two particle sizes of 53 and 212 μm were used.

9. RESULTS

The results of experiments described in Chapter 8 are presented in this chapter. First, the results of the reactivity of Li_2O_2 and Li_2O in air are presented. It continues with the solubility tests of lithium compounds in various alcohols. The results of the conversion tests of $LiOH.H_2O$ to Li_2O_2 are next. Finally, the results of the experiments performed on formation the Li_2O form Li_2O_2 are presented.

9.1 Reactivity of Li_2O_2 and Li_2O in air

The results of experiments measuring the reaction of lithium peroxide exposed to air with a relative humidity of 57 % at 21 °C are shown in Table 15 and Figure 18. XRD analysis showed that the products of the conversion reaction of Li_2O_2 were LiOH and Li_2CO_3, Figure 19. There was no evidence of $LiOH.H_2O$. As a result, the values are presented as mole fraction of the species of interest, Li_2O_2 remaining, and Li_2CO_3 and LiOH formed. Table 15 presents values with respect to the oxygen released by Li_2O_2 decomposition.

Table 15: Amount of Li_2O_2, Li_2CO_3 and LiOH present after exposure to air with a humidity of 57% as a function of time at 20°C (mole fraction).

Time(hr)	Li_2O_2	Li_2CO_3	LiOH
0	1	0	0
30	0.507	0.131	0.186
47	0.360	0.224	0.291
72	0.290	0.290	0.310
97	0.258	0.348	0.304
120	0.220	0.380	0.300
144	0.200	0.420	0.290
168	0.190	0.450	0.285
216	0.187	0.470	0.275
264	0.181	0.491	0.265

Figure 18 shows that lithium peroxide decomposed to about 50% of its initial mole fraction after 30 hr. The first derivative graph of the changes of lithium peroxide[xxi] showed two break points at 72 h and 144 h. It can be seen that the rate of decomposition of Li_2O_2 decreased after 72 h. The total mass reached a plateau at 144 h. However, the conversion of lithium peroxide continued albeit after this at a slower rate.

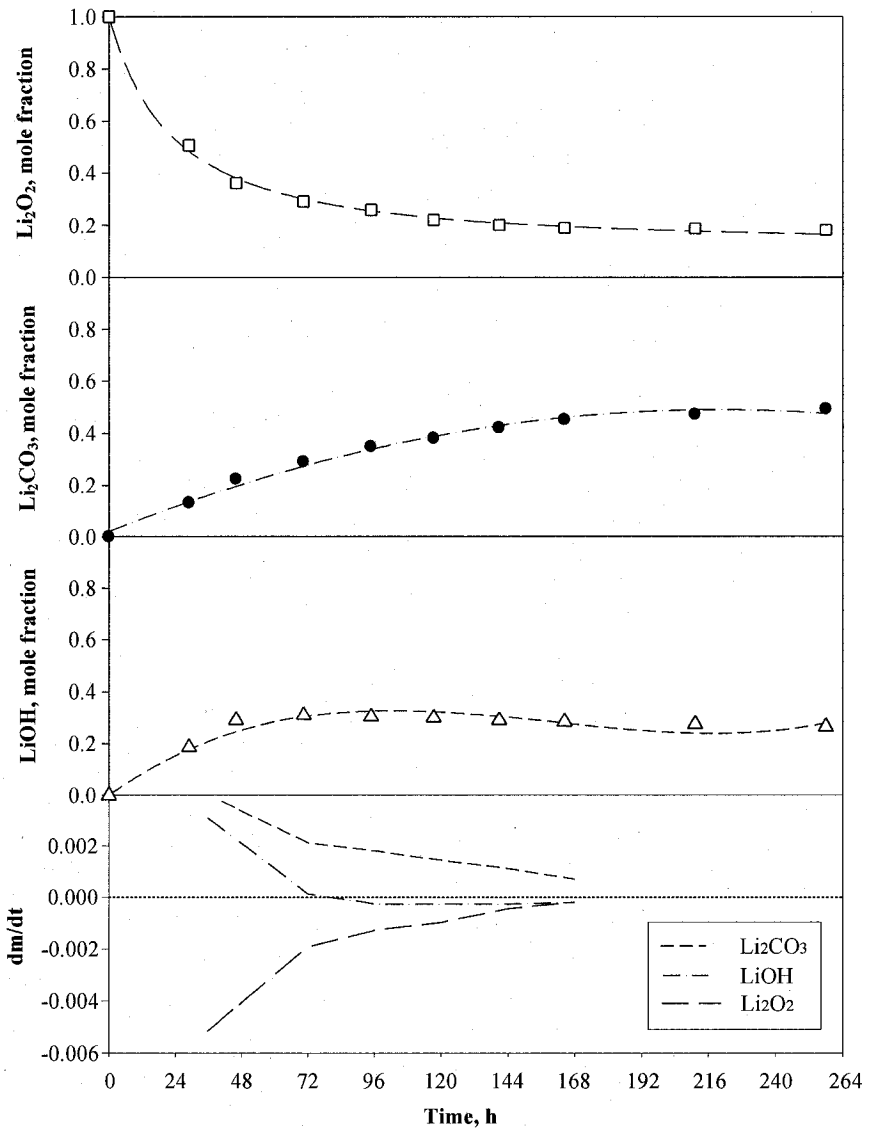

Figure 18: Mole fraction of Li_2O_2, Li_2CO_3 and LiOH as a function of a time. Conditions: 53 μm, 57% relative humidity and 20 °C.

[xxi] First derivative was calculated from the experimental data as follows: $dm/dt = (m_{t+\delta t}-m_t)/\delta_t$ where δt is the time interval between data points.

It can also be seen from Figure 18 that the rate of LiOH formation was approximately equal to the negative of the rate of Li_2O_2 decomposition. The lithium hydroxide assay reached its maximum mole fraction of 0.31 at 72 h. After this time, the rate of LiOH formation decreased. The rate of LiOH formation was constant after 96 h. This was confirmed by XRD analysis that showed that after 96 h, the LiOH content in the samples remained unchanged.

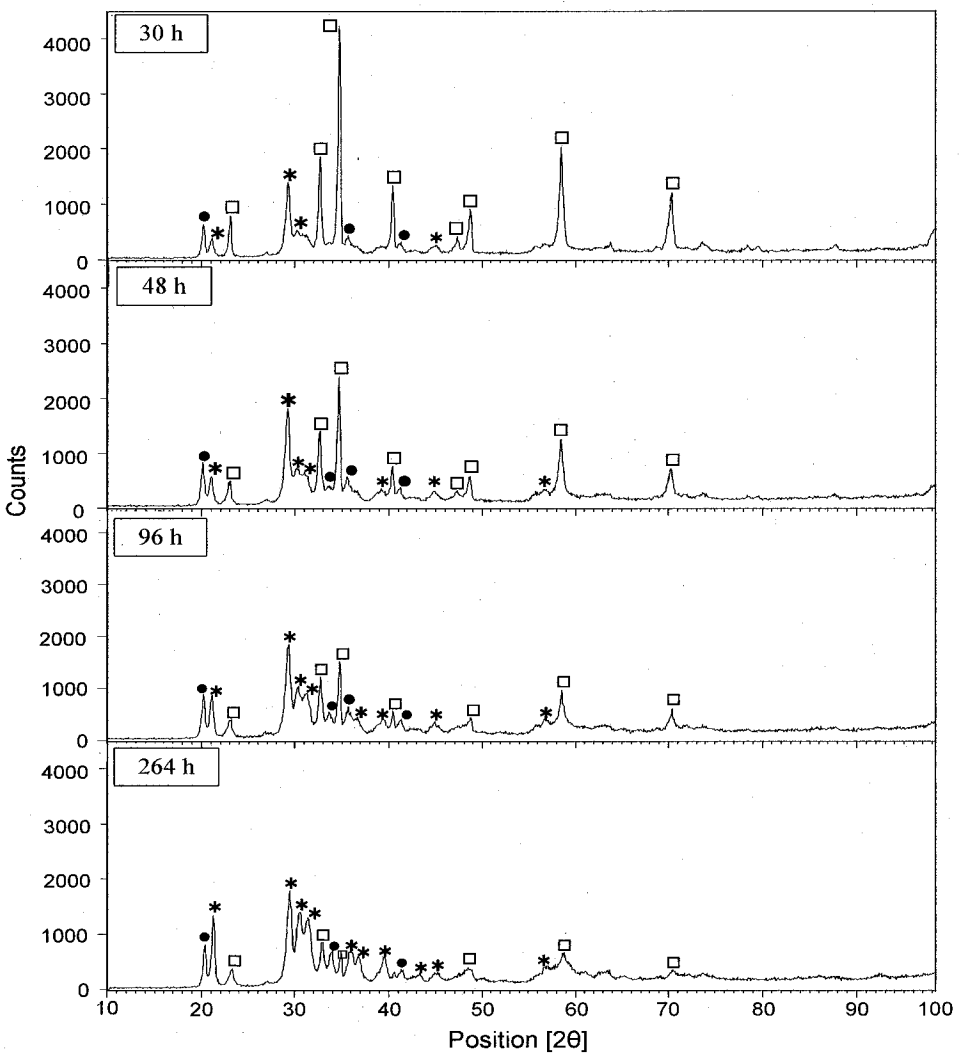

Figure 19: XRD spectra of Li_2O_2 reaction products after exposure to air as function of a time, Li_2O_2 □, LiOH ●, Li_2CO_3 ✱ [53 μm and 57% relative humidity]

Figure 18 also shows that the formation of Li_2CO_3 increased linearly up to 72 h. After this time, the formation of Li_2CO_3 continued at a lower rate. The XRD analysis confirmed that the formation of Li_2CO_3 occurred from the beginning.

Effect of humidity on the reactivity of lithium peroxide

Figure 20 presents the results of the experiments for exposure of the lithium peroxide to air with different relative humidities. It can be seen from Figure 20 that the reactivity of lithium peroxide was dramatically decreased by lowering the humidity of the air.

At a relative humidity of 5%, the rate of Li_2O_2 conversion was low and it continued at the lower rate. That is after 264 h, the conversion fraction of lithium peroxide was 0.035. Here, the term of conversion fraction is defined as the ratio of moles of lithium peroxide was converted to LiOH and Li_2CO_3 to initial value of lithium peroxide in samples. The XRD analysis of samples reacted at a relative humidity of 5 % showed that lithium peroxide was only slightly converted to LiOH and the formation of Li_2CO_3 was not observed (Figure 21).

At 21 % relative humidity, lithium peroxide converted at a higher rate. However, it was less than the rate of conversion at 57 % relative humidity. That is, at 30 h, conversion was 0.12 vs. 0.51. After 264 h at a relative humidity of 21 %, the converted mole fraction of lithium peroxide was 0.32.

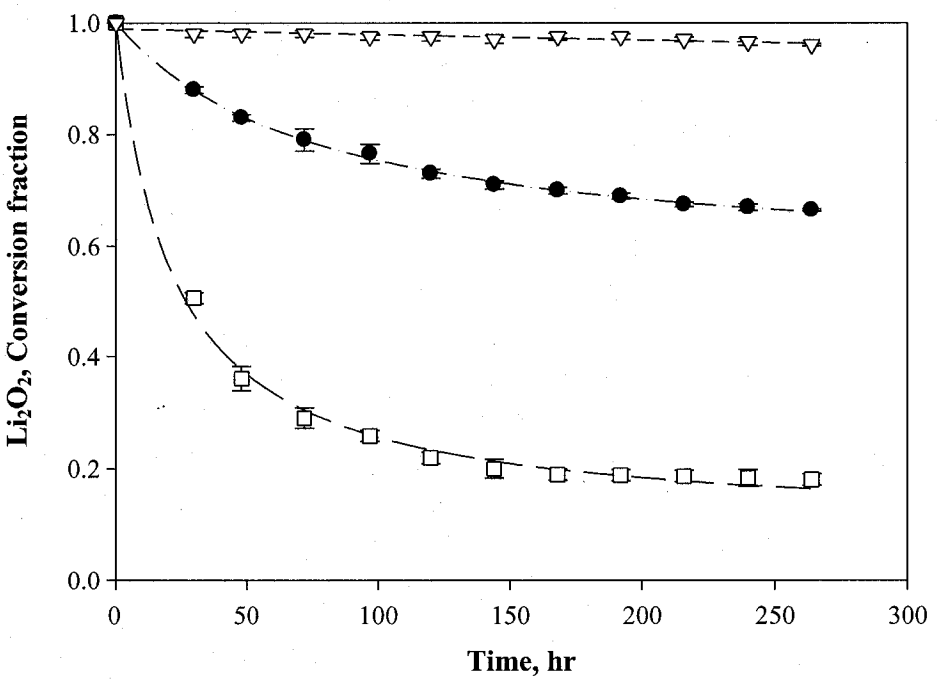

Figure 20: Effect of humidity on reaction of Li_2O_2 as a function of time, at relative humidities of 5 % —▽—, 21 % —●— and 57 % —□—.

The decomposition of lithium peroxide at a relative humidity of 21 % involved the formation of LiOH and Li_2CO_3.

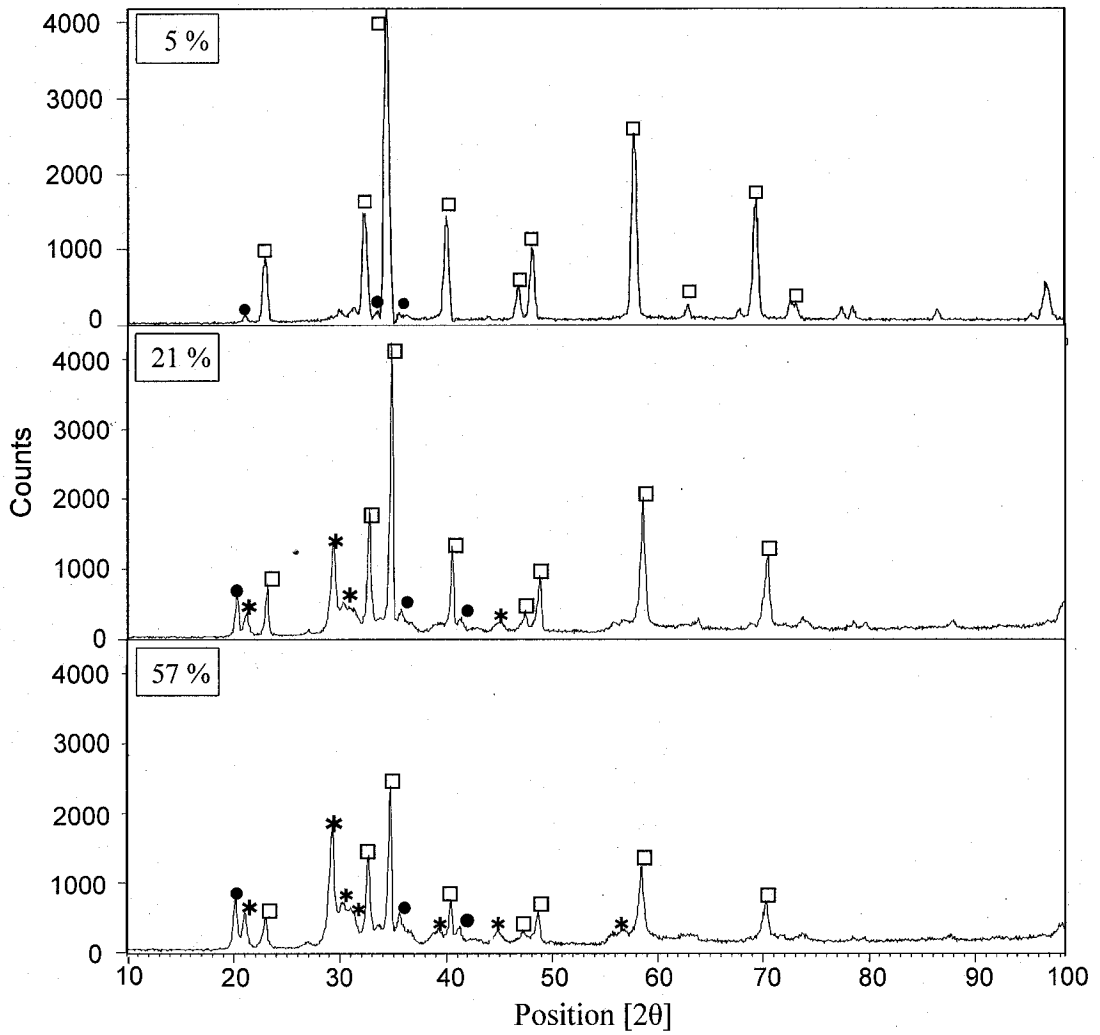

Figure 21: XRD spectra of lithium peroxide exposed to the air atmosphere after 144 h, at 21 °C in different relative humidity Li_2O_2 □, LiOH ●, Li_2CO_3 ✱.

Effect of particle size

Figure 22 shows the influence of particle size on the reactivity of lithium peroxide as a function of time. As was expected, the sample with the smaller particle size was more reactive than the sample having the larger particle size. At early reaction times, the extent of difference between the reactivity of the samples with different particle sizes was more prominent.

Figure 22 shows that after 40 h the mole fraction of the unreacted lithium peroxide for the sizes of 53, 106 and 212 μm were 0.46, 0.54 and 0.60, respectively. The differences were maintained even as time progressed. The XRD analysis of the samples with different particle sizes showed a similar composition of products, which were LiOH and Li_2CO_3.

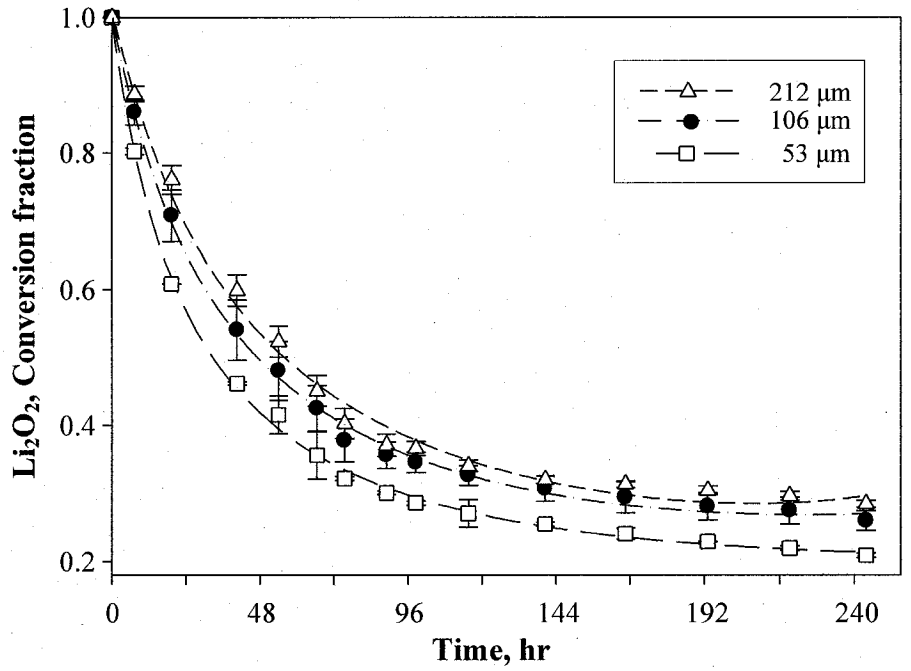

Figure 22: Effect of particle size on the reactivity of Li_2O_2 in air with a relative humidity of 57 % as a function of time.

Reactivity of lithium oxide

The results of the experiments for the reactivity of Li_2O are presented in this part. Figure 23 shows the changes of Li_2O, Li_2CO_3 and LiOH mole fraction as a function of time. The start of exposure to air with a relative humidity of 57 ± 1 %, Li_2O showed a fast conversion up to 76 h. After this time, the rate of conversion decreased.

Conversion continued after 120 hr. The XRD analysis showed that the decomposition of lithium oxide involved the formation of Li_2CO_3 and LiOH. As shown in Figure 24, Li_2CO_3 was formed from the beginning of the exposure to the air atmosphere. As the time progressed, the contents of both Li_2O_2 and LiOH decreased.

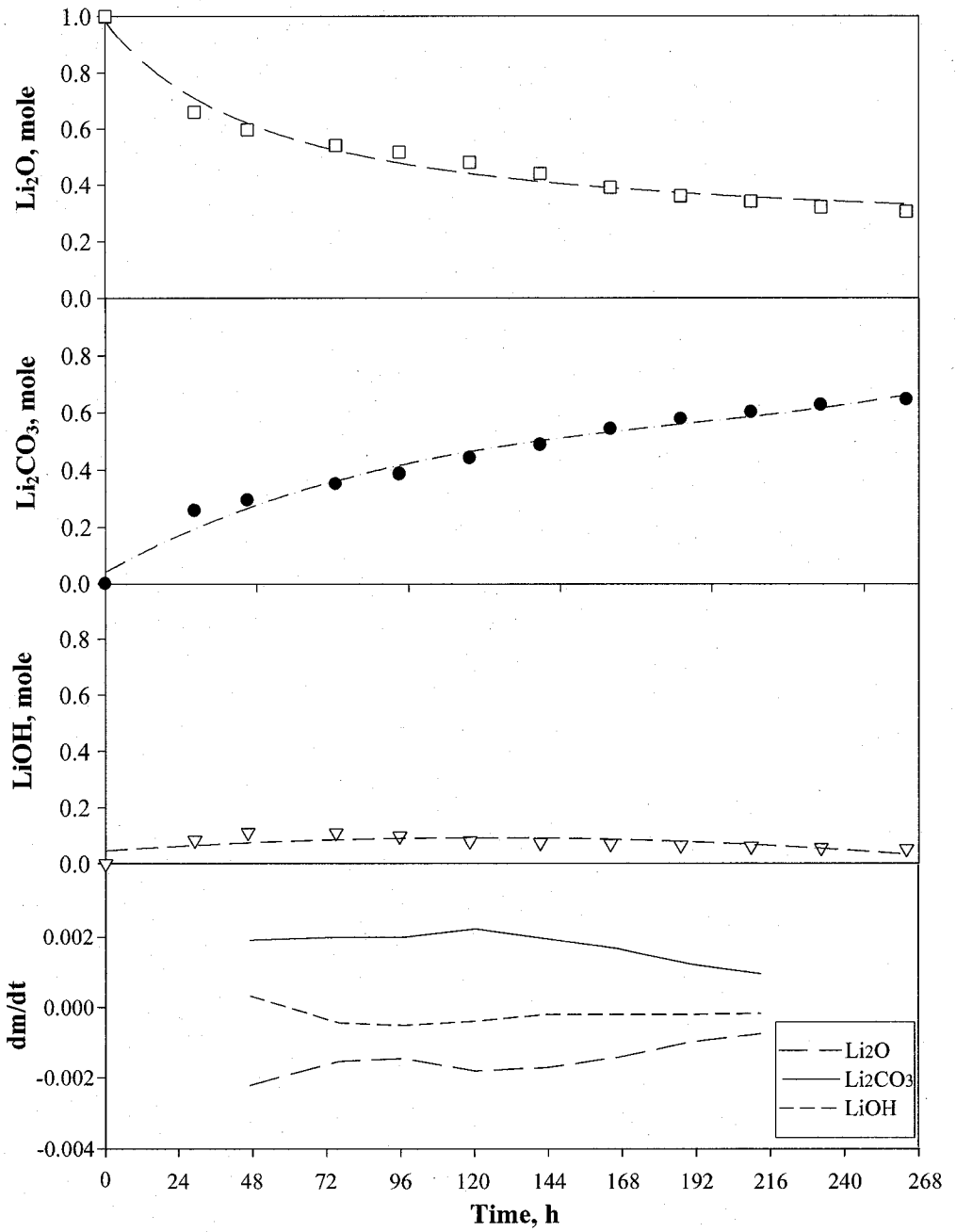

Figure 23: Changes of Li_2O, Li_2CO_3 and LiOH in mole fraction as a function of time, at the condition of 53 μm, 57 RH % and 20 °C.

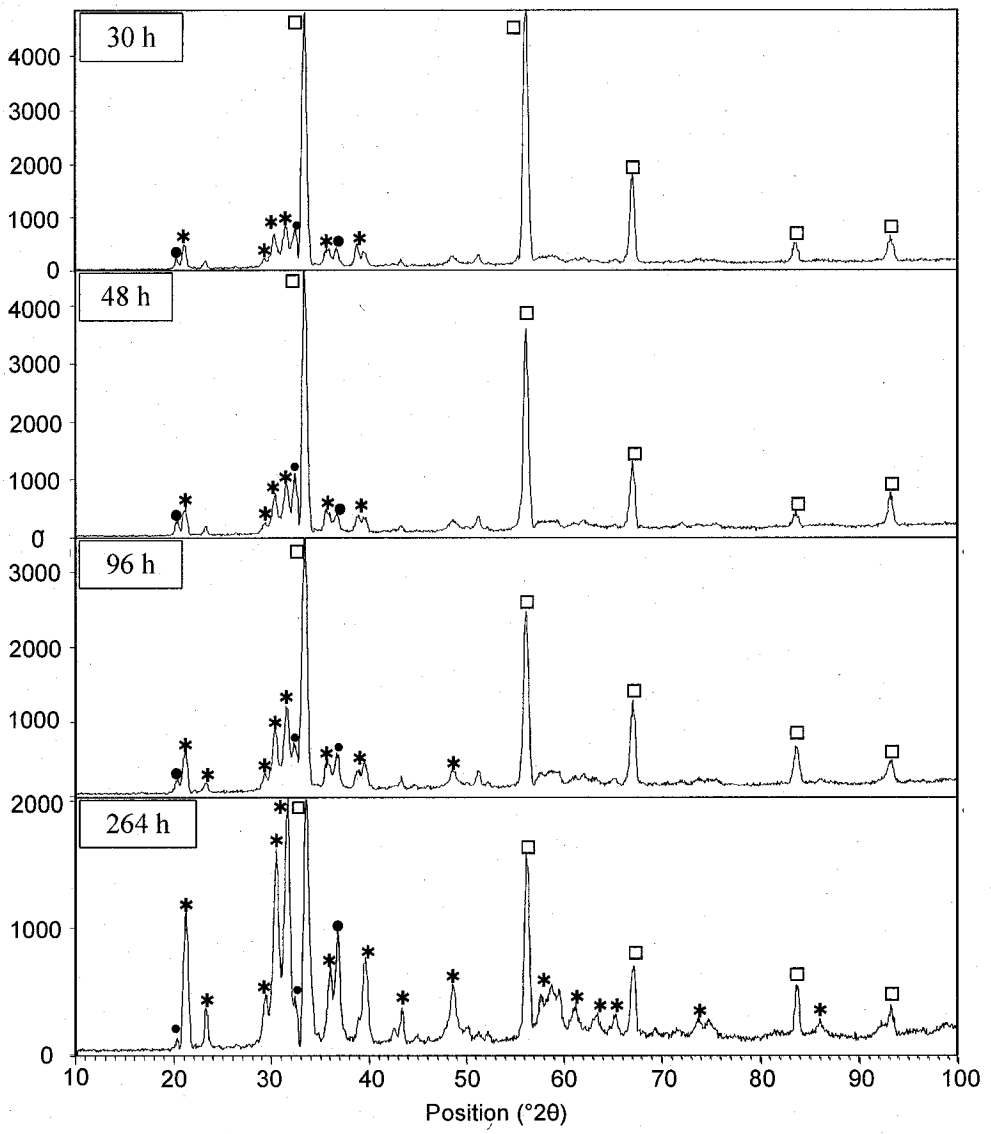

Figure 24: XRD spectra of Li_2O after exposure to air as function of a time Li_2O □ LiOH ●, Li_2CO_3 ✱ at the condition of 53 μm and 57 RH %.

Effect of humidity on lithium oxide reactivity

Figure 25 shows the results of the experiments of exposing lithium oxide to air atmosphere with different relative humidities. It can be seen from Figure 25 that the reactivity of lithium oxide was decreased by lowering the humidity of air.

Figure 25 shows that at a relative humidity of 5 %, the conversion of Li_2O showed little change. After 264 hrs, the lithium oxide was converted by only to 0.04 mole fraction of its initial molar value. The XRD analysis of samples showed that lithium oxide at a relative

humidity of 5% was only slightly converted to LiOH and the formation of Li_2CO_3 was not observed (Figure 25).

Figure 25 shows that at a relative humidity of 21%, the conversion of lithium oxide proceeded linearly. At a relative humidity of 21%, lithium oxide showed a higher conversion in comparison to the relative humidity of 5%. However, it was less than the rate of conversion at 57% relative humidity, i.e., at 30 hr, only 0.07 mole fraction of lithium oxide was converted but at the same time at 57% relative humidity, it was 0.49 mole fraction.

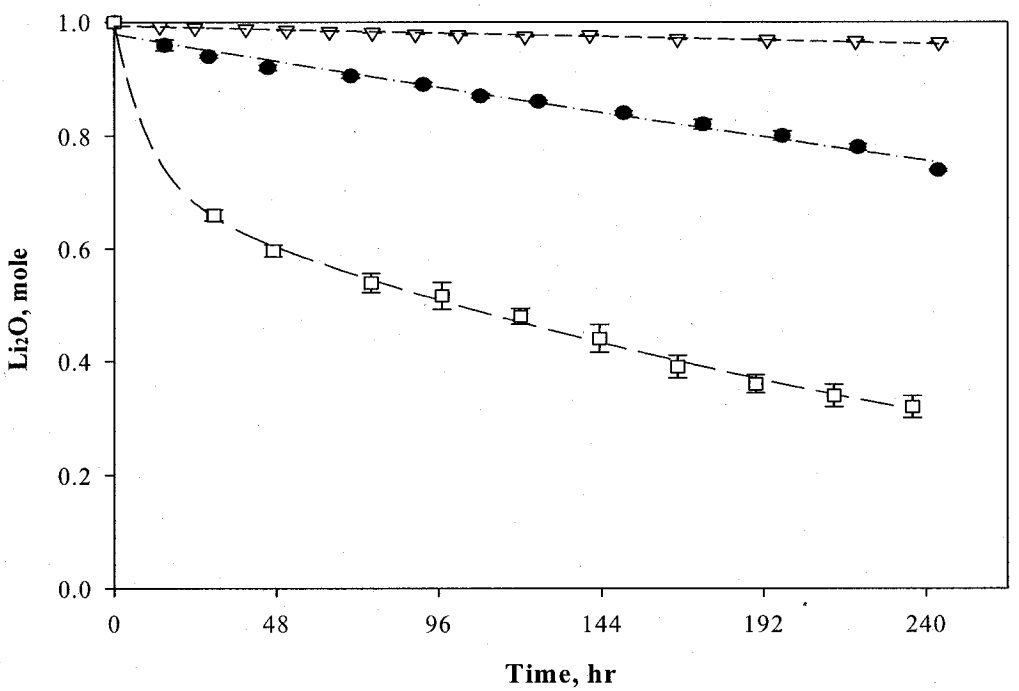

Figure 25: Effect of humidity on reactivity of Li_2O as a function of time at a relative humidity of 5% -▽- 21% -●- and 57%-□-.

Comparison between reactivity of lithium peroxide and lithium oxide

Figure 26 shows a comparison between the reactivity of lithium peroxide and lithium oxide. Despite the previous assumption regarding lithium peroxide being less reactive than lithium oxide in ambient conditions, it can be seen from Figure 26 that under the selected test conditions, lithium peroxide is more reactive.

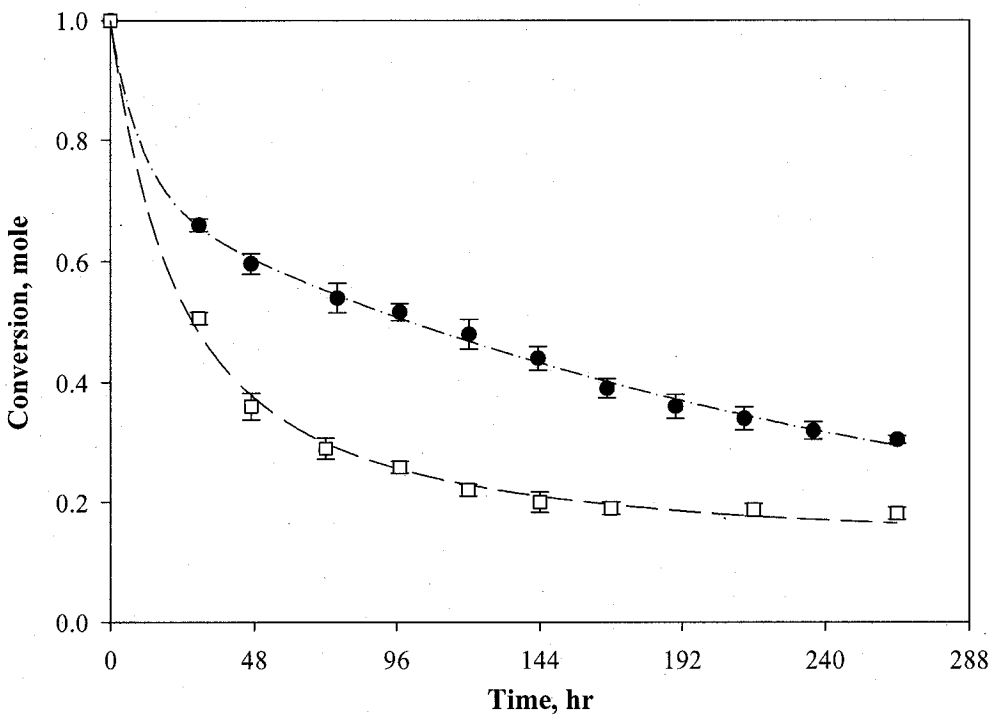

Figure 26: Comparing the reactivity of Li_2O_2 —□—and Li_2O —●—as function of a time, at a similar particle size of +53 μm, 57% relative humidity at a temperature of 21°C.

The decomposition of lithium peroxide and lithium oxide at 48 h were 0.64 and 0.4 mole fraction of their initial values, respectively. The rate of lithium peroxide conversion after 144 hrs decreased, whereas lithium oxide continued to convert at an almost constant rate.

SEM analysis of lithium peroxide and lithium oxide

SEM micrographs of Li_2O_2 and Li_2O are shown in Figure 27. The structure of pure lithium peroxide appeared as porous particles containing clusters of the fine and crossing-blade plates (Figure 27-b). The structure of the pure lithium oxide, that was used for the SEM analysis, showed that it had a dense particle structure with very fine flakes on its surface (Figure 27-a). As explained in Section 8.2, the particle size of both samples was 53 μm. After 320 hrs exposure to air, both lithium peroxide and lithium oxide formed a thin layer of attached particles.

Figure 27-c shows the structure of lithium oxide that was exposed to air with a relative humidity of 57% at 21 °C for 320 h. It can be seen that the crossing-blade plates grew in random directions. Figure 27-d shows the structure of lithium peroxide exposed to air with

a relative humidity of 57% at 21 °C for 320 h. It can be seen that the surface of particles was dense. Even at a higher magnification of 12000X, no formation of the crystalline structure was observed.

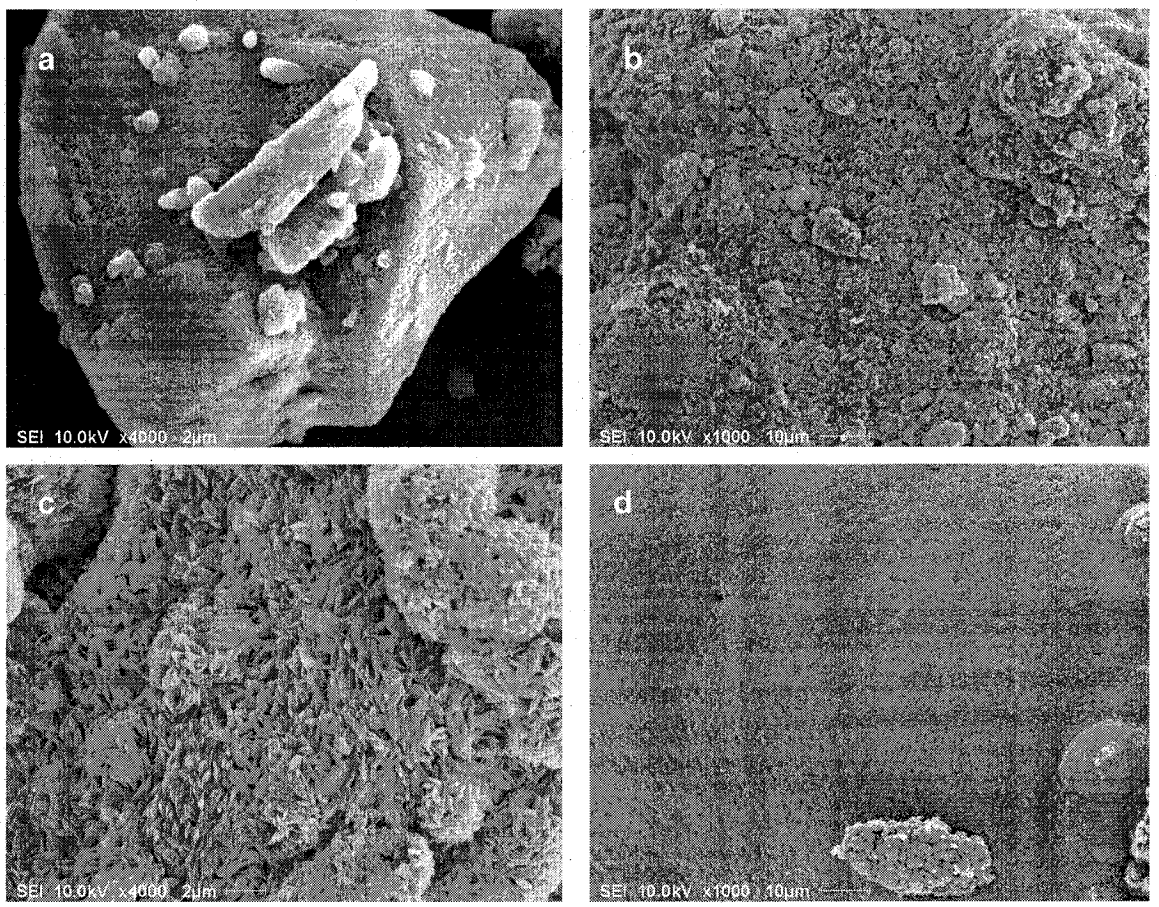

Figure 27: SEM pictures of a) pure Li_2O, b) pure Li_2O_2, c) Li_2O after 320 h in exposure to air and d) Li_2O_2 after 320 h in exposure to air, at a temperature 20 °C, 53 μm and 57% relative humidity.

9.2 Solubility of lithium compounds in alcohols

The results of the solubility tests are presented for 48 hr and for 1 hr mixing times in Table 16 and Table 17, respectively. The 48 h mixing time was assumed to represent "equilibrium" for the present system. The solubility tests showed that all of lithium compounds that were considered had their highest solubility in methanol. Ethanol had the second highest solubility for the lithium compounds of interest. Table 17 shows that for

the 1 hr mixing time, methanol also had the highest solubility for $LiOH.H_2O$, LiOH and Li_2O_2; and no solubility for Li_2CO_3.

Table 16: Solubility of lithium compounds in different alcohols for 48 h mixing times (g /100 g alcohol) at 20 °C.

	Methanol	**Ethanol**	**1-Propanol**	**2-Propanol**
$LiOH.H_2O$	13.69	2.18	0.87	0.11
LiOH	9.76	2.36	0.77	0
Li_2O_2	2.69	0.70	0.53	0.06
Li_2CO_3	0.10	0	0	0

Table 17: Concentration of lithium compounds in different alcohols for 1 h mixing times (g /100 g alcohol) at 20 °C

	Methanol	**Ethanol**	**1-Propanol**	**2-Propanol**
$LiOH.H_2O$	13.47	1.96	0.82	0
LiOH	8.64	1.17	0.54	0
Li_2O_2	1.52	0.44	0.21	0
Li_2CO_3	0	0	0	0

Table 18 presents the ratio of the concentration of Li_2O_2 to $LiOH.H_2O$ in methanol, ethanol and 1-propanol with respect to their capability for Li_2O_2 precipitation. The separation coefficient values in Table 18 were derived from the results of concentrations in Table 17.

Table 18: Separation coefficient of alcohols in respect to Li_2O_2 and $LiOH.H_2O$

Ratio	**Methanol**	**Ethanol**	**1-Propanol**
$Li_2O_2/LiOH.H_2O$	0.11	0.22	0.26

9.2.1 Effect of time on the solubility of $LiOH.H_2O$ in methanol

Table 19 presents the concentration of $LiOH.H_2O$ in methanol as a function of mixing time at 20 °C.

Table 19: Concentration of $LiOH.H_2O$ in methanol as a function of mixing time at 20 °C.

Time	Concentration	95% conf. intrval
min	g $LiOH.H_2O$/100 g CH_3OH	%
0	0.00	0
20	11.98	0.30
40	13.56	0.11
60	13.46	0.03
80	13.49	0.18
100	13.52	0.23
120	13.65	0.23

Figure 28 shows the concentration of $LiOH.H_2O$ in methanol as a function of time at 20 °C. It can be seen that the concentration initially increased with mixing time. After 40 min, the increase in the concentration of $LiOH.H_2O$ in methanol was insignificant and led to the conclusion that 60 minutes of mixing was sufficient to ensure saturation for $LiOH.H_2O$.

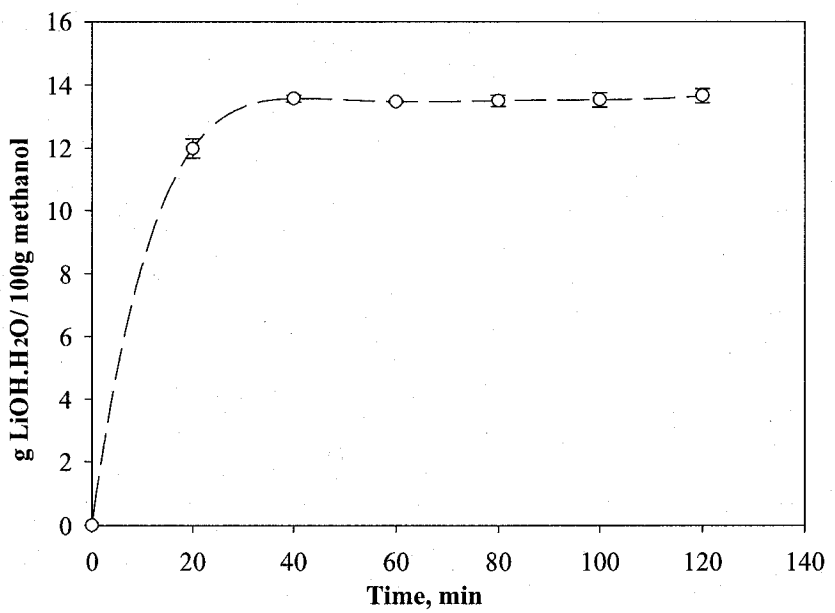

Figure 28: Concentration of $LiOH.H_2O$ in methanol as a function of mixing time.

9.2.1.1 Measurement of ORP and pH of solution

Error! Reference source not found. shows the changes in the oxidation and reduction potential of a mixture of $LiOH.H_2O$ and methanol along with the changes in pH as a function of mixing time for two tests having the additions of 12.5 and 25 g $LiOH.H_2O$/100 g CH_3OH. Less change was observed in pH for the test with addition closer to the measured solubility at 20 °C, 12.5 g $LiOH.H_2O$/100 g CH_3OH. On the other hand, the solution with an addition of 25 g $LiOH.H_2O$/100 g CH_3OH had a higher change in ORP. After 60 min, the changes of ORP and pH for both tests ceased.

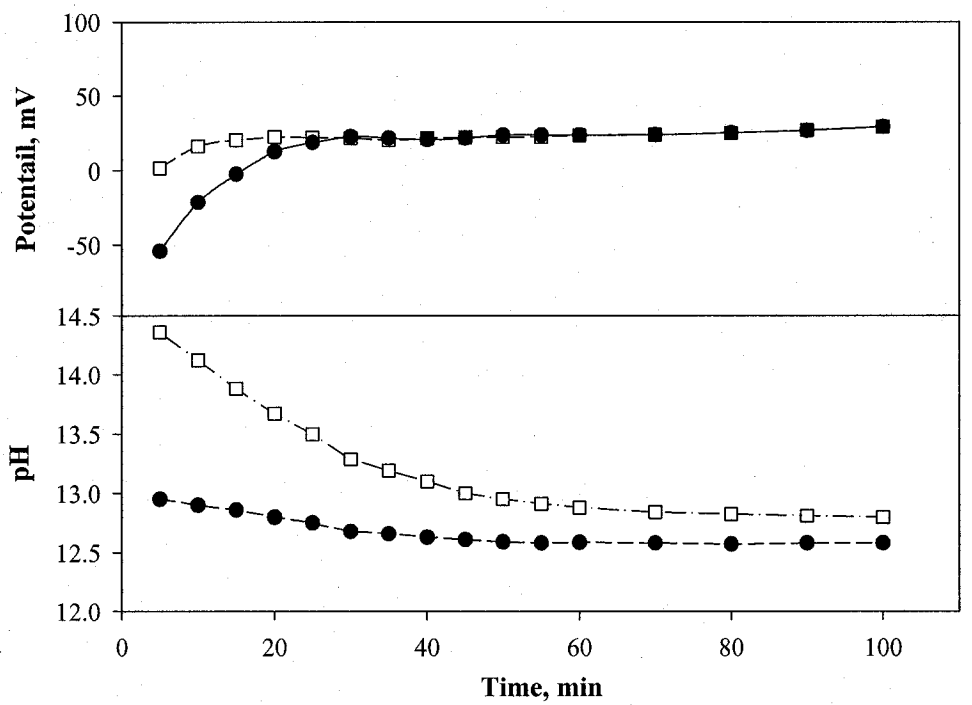

Figure 29: Oxidation-reduction potential and pH of solution of $LiOH.H_2O$ in CH_3OH during mixing at two concentrations of 12.5 g —●— and 25 g —□— $LiOH.H_2O$/100 g CH_3OH.

9.2.2 Effect of temperature on the solubility of $LiOH.H_2O$ in methanol

Figure 30 presents the changes in the solubility of $LiOH.H_2O$ in methanol as a function of temperature. As shown in Figure 30, increasing the temperature decreased the solubility.

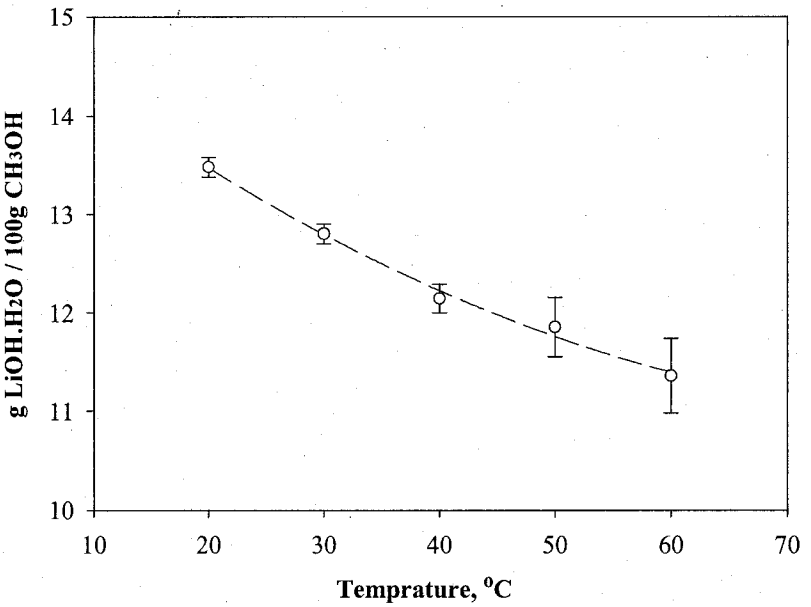

Figure 30: Effect of temperature on the solubility of $LiOH.H_2O$ in methanol.

On contrary to usual experiences that the solubility if solute in solvent increases with increase in temperature, the solubility of lithium hydroxide monohydrate in methanol was decreased as the temperature increased. At temperatures higher than 40 °C, the error in the measurement was increased due to methanol evaporation.

9.3 Study of conversion to lithium peroxide

The following sections present the results of the conversion experiments. The term "efficiency" is defined as moles of lithium peroxide produced per mole of reacted lithium hydroxide monohydrate expressed as percentage.

9.3.1 Hydrogen peroxide consumption

Table 20 presents the results of the experiment for finding the optimum amount of H_2O_2 (35 wt %) required for the conversion of $LiOH.H_2O$ to Li_2O_2. It can be seen from Figure 31 that the highest efficiency for production of lithium peroxide, 96.9 %, was obtained for a molar ratio of $H_2O_2/LiOH.H_2O$ of 1.3. At this ratio, the amount of H_2O_2 (35 wt%) that was added was about 2.8 times the stoichiometric amount by mole. As shown in Figure

31, increased additions were not useful to obtain higher efficiencies because an excess H_2O_2 caused an increase of the methanol solubility for product.

Table 20: The results of using H_2O_2 (35 wt %) for production of Li_2O_2

mole H_2O_2/ mole	mole H_2O_2/mole	Efficiency, %	95 % conf.
0.7	1.5	87.6	0.5
0.9	1.7	90.6	1.8
1.0	2.0	93.6	2.5
1.1	2.2	95.2	1.5
1.2	2.4	96.2	0.5
1.3	2.7	96.9	0.6
1.5	2.9	96.3	1.8
1.6	3.2	95.7	0.3
1.7	3.4	94.8	0.7

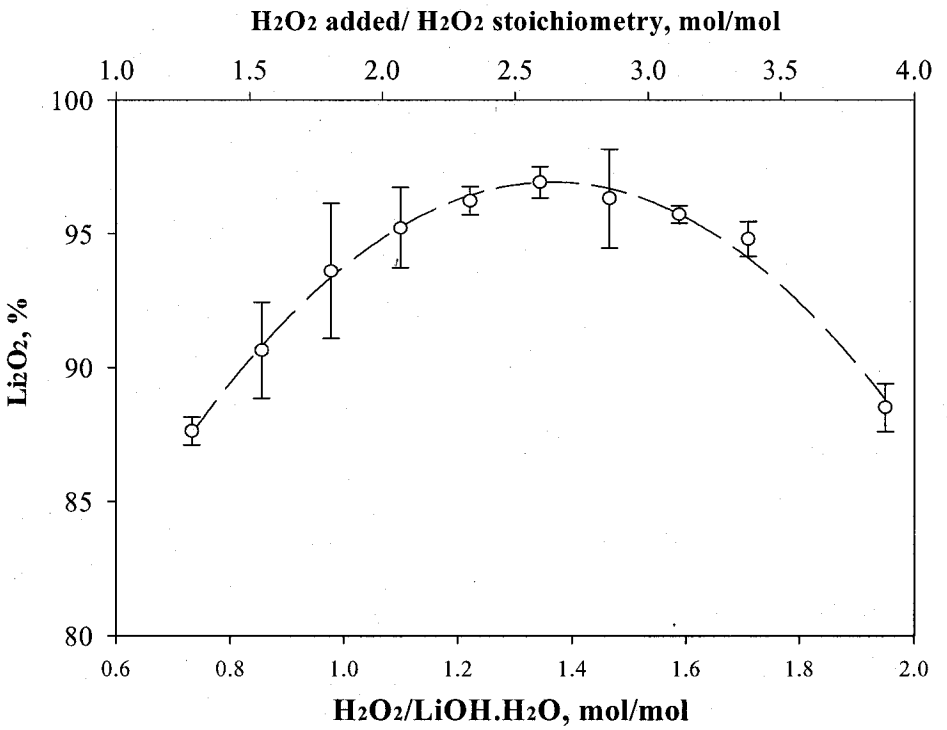

Figure 31: Required hydrogen peroxide (35 wt%) for producing Li_2O_2 from $LiOH.H_2O$ in methanol.

Upon addition of hydrogen peroxide, the conversion reaction occurred rapidly resulting in a milky and somewhat suspended product. The XRD spectra of products are shown in Figure 32 as a function of molar ratios of H_2O_2:LiOH.H_2O equal 1.35, 1.7 and 2.0. At the ratio of 2.0, the lithium compound produced was contaminated by LiOH.

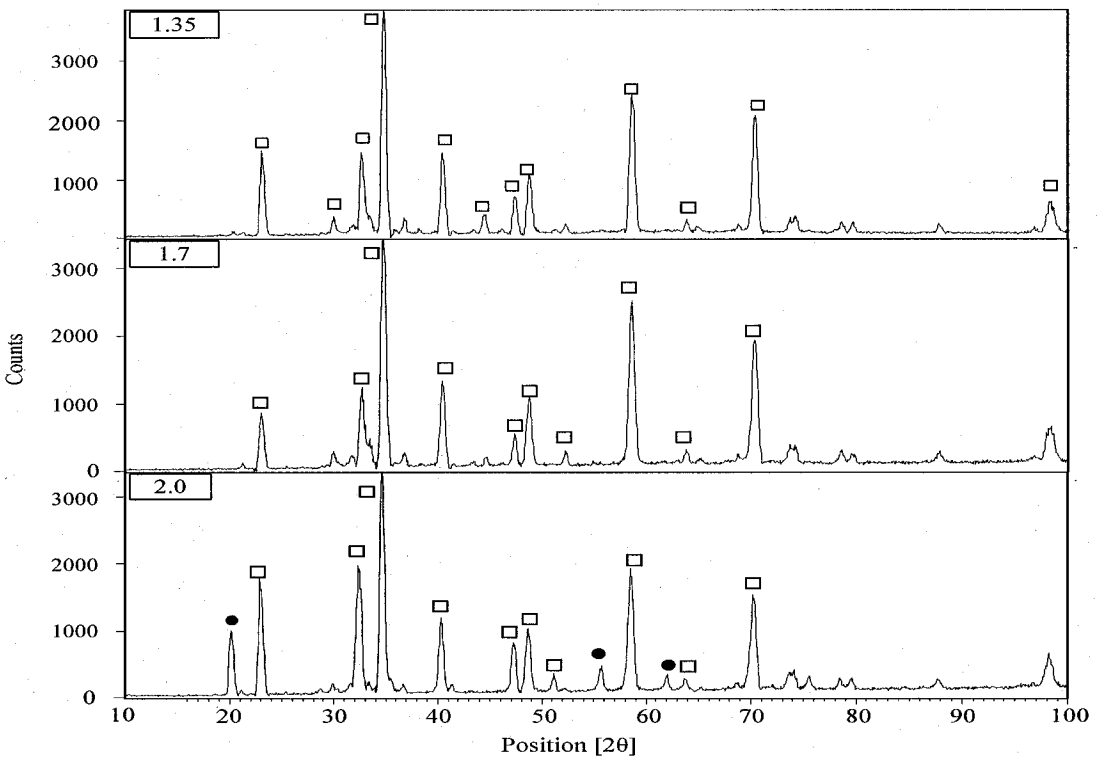

Figure 32: XRD spectra of product at molar ratios (H_2O_2:LiOH.H_2O) of 1.35, 1.7 and 2.0, Li_2O_2 □ and LiOH ●.

9.3.2 Measurement of pH and ORP of solution

Figure 33 shows the oxidation and reduction potential of the solution along with its pH as a function of hydrogen peroxide addition. It can be seen from Figure 33, as hydrogen peroxide was added to the mixture of LiOH.H_2O and methanol, the pH decreased rapidly from 12.4 to 7.8. Beyond this point, the pH remained constant with any further addition of H_2O_2.

Figure 33 shows that the variations in both ORP and pH were small. The error in the measurement of potential of solution was due to the use of a potentiometer having an accuracy of about 0.1 mV and instability in the potential of methanol.

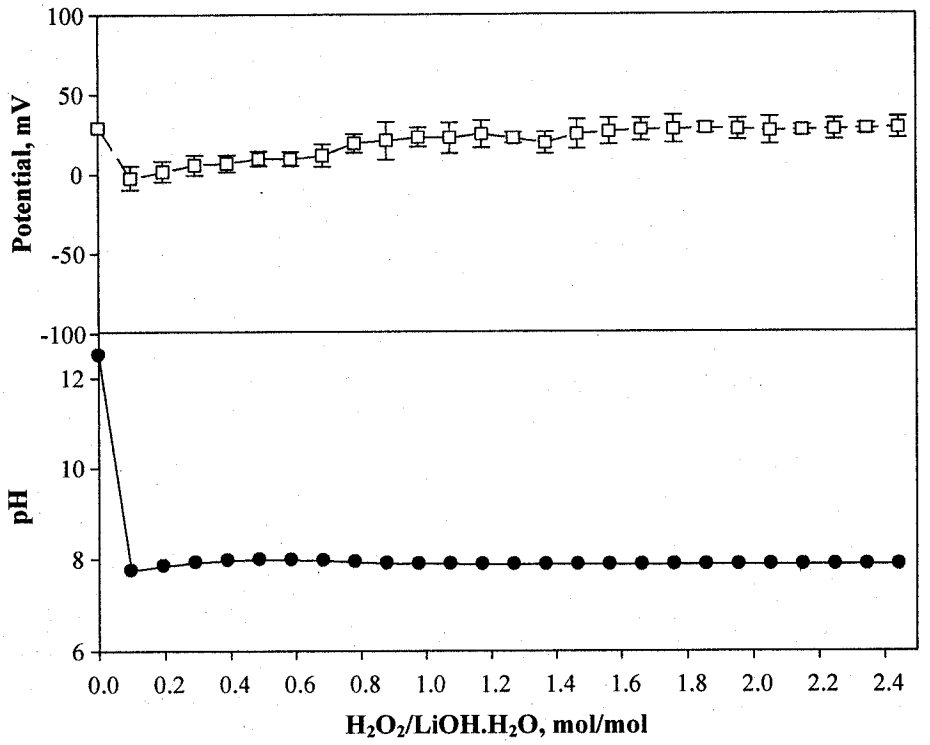

Figure 33: Potential and pH of solution as a function of H_2O_2 addition to a solution with the concentration of 12.8 g $LiOH.H_2O$/100 CH_3OH.

9.3.3 Hydrogen peroxide concentration

The result of experiments using H_2O_2 50 wt% for precipitating Li_2O_2 are presented in Table 21. It can be seen from Figure 34 that the highest efficiency for production of pure lithium peroxide, 96.9 %, was obtained for a ratio (H_2O_2/$LiOH.H_2O$) of 1.25. At this ratio the amount of H_2O_2 (50 wt%) added was about 2.1 times the molar stoichiometric amount.

Table 21: The result of using H_2O_2 50 wt % for Li_2O_2 production.

mole H_2O_2/ mole	Mole H_2O_2/mole	Efficiency, %	95 % conf.
0.66	1.08	85.7	0.6
0.81	1.31	89.6	0.1
0.96	1.55	95.9	0.4
1.11	1.79	98.4	0.6
1.25	2.03	98.7	0.1
1.40	2.27	98.0	0.7
1.55	2.51	97.0	0.9

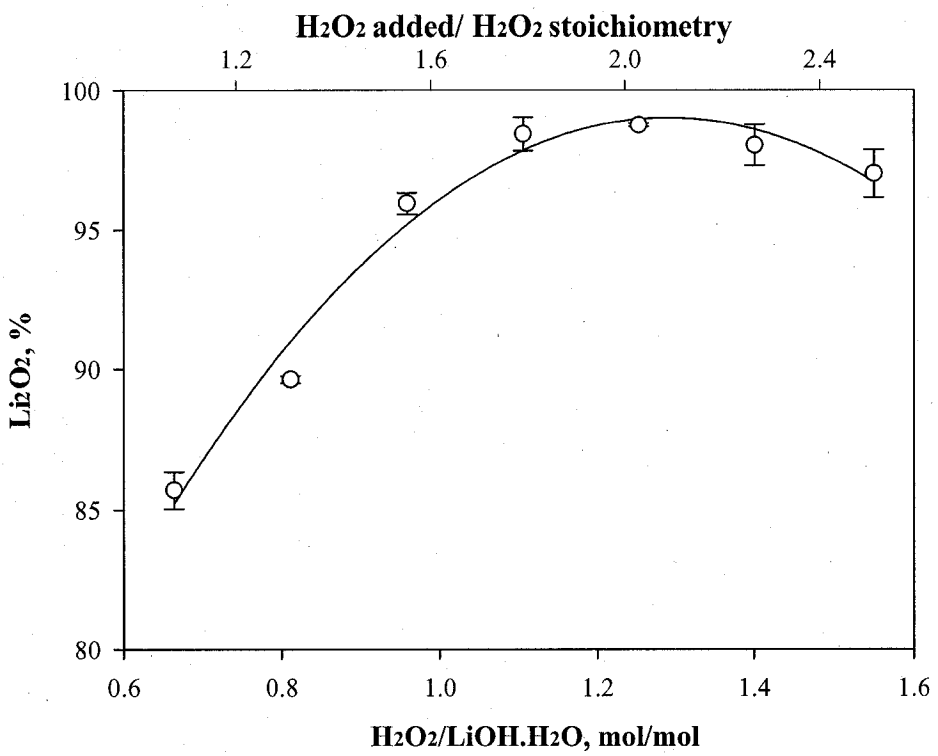

Figure 34: Required hydrogen peroxide 50 wt% for producing Li_2O_2 from $LiOH.H_2O$ in methanol.

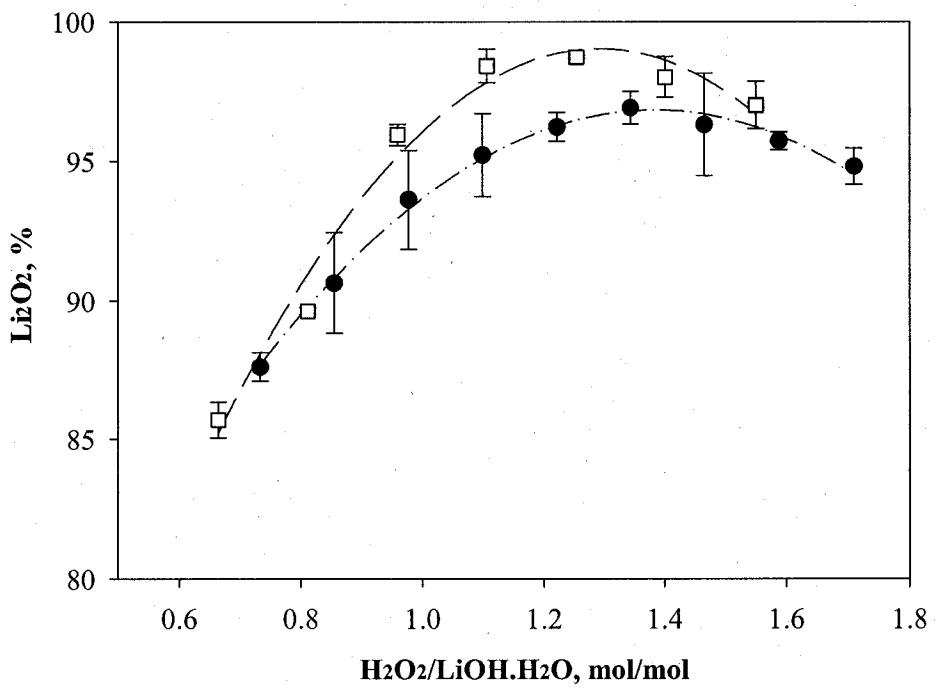

Figure 35: Comparison between H_2O_2 50 wt % —□— and H_2O_2 35 wt % —●— on the efficiency of Li_2O_2 produced in methanol.

As shown in Figure 34, further H_2O_2 addition did not result in higher conversions because an excess H_2O_2 caused an increase of the methanol solubility for the product. Figure 35 shows the influence of using H_2O_2 50 wt% as compared with H_2O_2 35 wt%.

The analysis of the precipitate showed that its composition comprised the compound, $Li_2O_2 \cdot H_2O_2 \cdot 2H_2O \cdot 8CH_3OH$, showing that as the concentration of hydrogen peroxide in solution increased, the water content of the precipitated decreased.

9.3.4 Effect of the kind of alcohol on conversion

The results of experiments using ethanol and 1-propanol as the medium for production of Li_2O_2 using H_2O_2 (35%) are presented in Table 22.

Table 22: Efficiency of Li_2O_2 production using ethanol and 1-propanol as the medium.

	mole H_2O_2/ mole	Efficiency, %	95 % conf.
Ethanol	0.49	43.9	2.2
	0.73	57.0	1.7
	0.98	62.8	1.5
	1.22	64.1	1.4
	1.47	55.2	1.5
1-propanol	0.49	18.4	1.9
	0.73	37.6	2.3
	0.98	54.9	1.5
	1.22	66.8	2.3
	1.47	81.5	3.1
	1.71	76.3	2.1

Figure 36 shows the results of the experiments using ethanol and 1-propanol. For both alcohols, the efficiency of Li_2O_2 production was lower than that for methanol. The maximum efficiency obtained for ethanol was 64.1% at a ratio of 1.2, whereas with 1-propanol, it was 81.5 at a ratio of 1.47.

The analysis of the precipitates showed that when ethanol and 1- propanol were used (a solution with concentrations near the solubility limit and without contaminant), compounds with the composition of $Li_2O_2.H_2O_2.3H_2O.6CH_3CH_2OH$ and $Li_2O_2 \cdot H_2O_2 \cdot 3H_2O \cdot 11C_3H_7OH$ were formed, respectively.

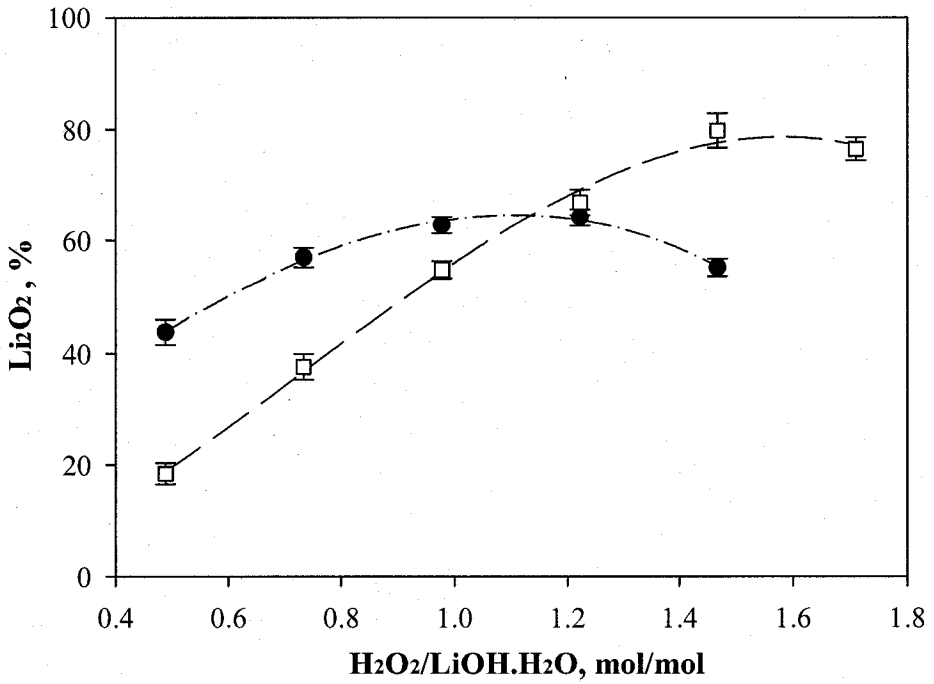

Figure 36: Efficiency of conversion using ethanol —●— and 1-propanol—□—.

9.3.5 Using LiOH

Figure 37 shows the results of using LiOH instead of $LiOH.H_2O$ on the efficiency of Li_2O_2 production using H_2O_2 35 wt%. As a result of using LiOH, the maximum efficiency obtained was 95.9 %.

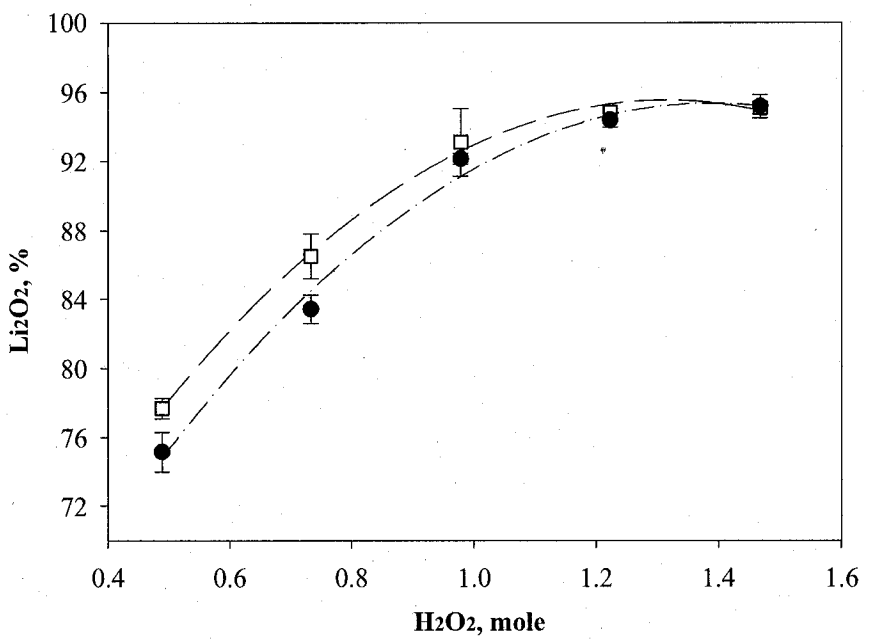

Figure 37: Effect of using LiOH —□— on the efficiency in comparison to using $LiOH.H_2O$ —●— [35 %wt H_2O_2].

9.3.6 Effect of temperature on conversion

Table 23 presents the result of experiments on the effect of temperature on the efficiency of Li_2O_2 produced for two conditions. The mixture contained 20 g $LiOH.H_2O$ per 100 g CH_3OH. H_2O_2 (35 wt%) at a molar addition ratio of H_2O_2:$LiOH.H_2O$ of 1.2. Figure 38 shows that for both mixtures, as the temperature increased, the efficiency of Li_2O_2 production was decreased. Due to the evaporation of methanol at temperatures higher than 50 °C in particular, the confidence interval of the results increased.

Table 23: Effect of temperature on the efficiency of Li_2O_2 production, 20.0 g $LiOH.H_2O$/100 g CH_3OH and molar ratio 1.2 H_2O_2:$LiOH.H_2O$

Temperature, °C	Efficiency, %	95 % conf.
10	96.0	0.3
20	92.5	0.5
30	88.9	0.3
40	85.4	1.0
50	80.0	1.9
60	76.5	1.8

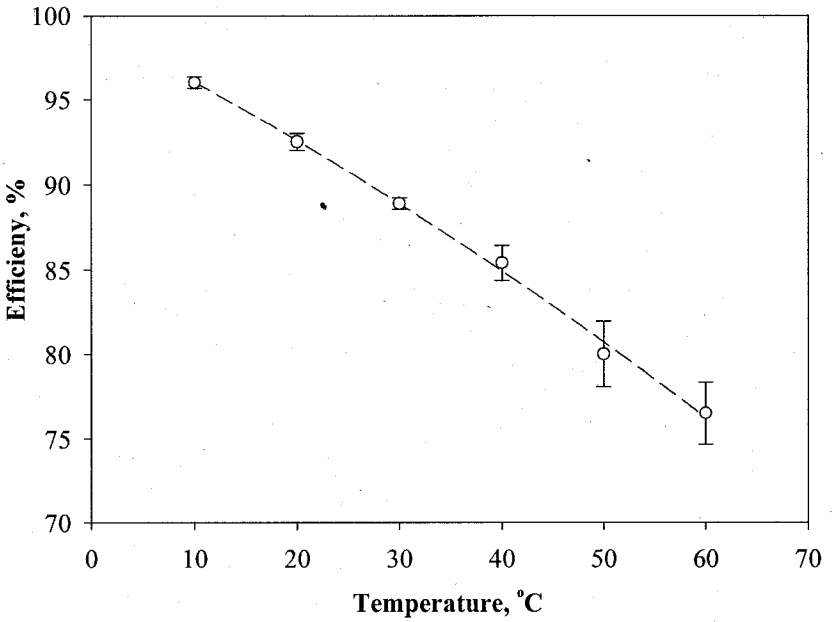

Figure 38: Effect of temperature on the efficiency of Li_2O_2 produced in ratios of 1.22 H_2O_2:$LiOH.H_2O$

9.3.7 Effect of time on conversion

Figure 39 shows the effect of time on conversion. A mixture containing 13.0 g $LiOH.H_2O$ per 100 g CH_3OH and H_2O_2 (35 wt%) at a ratio of H_2O_2:$LiOH.H_2O$ equal to 1:1 was used. The efficiency of production was not improved as the time of mixing was extended, indeed, the efficiency of production showed a decreasing trend with time mixing.

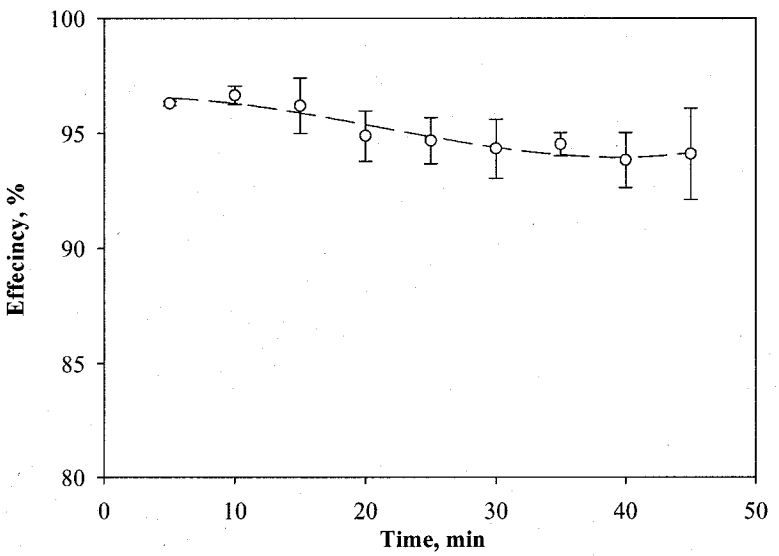

Figure 39: Effect of time of mixing on the efficiency of Li_2O_2 produced.

The results of the conversion of $LiOH.H_2O$ to Li_2O_2 using H_2O_2 (35 %wt) indicated that the reaction occurred quickly (Figure 39). As the time of mixing was extended, no increase in the efficiency was observed. On the contrary, at longer mixing times, the efficiency decreased indicating that the product dissociated to LiOH. As mentioned in Section 9.2.1, the dissolution of $LiOH.H_2O$ in methanol was completed after about 40 min. Therefore, the longer mixing time provided the time for dissolving the precipitate, $Li_2O_2{\cdot}H_2O_2{\cdot}3H_2O{\cdot}8CH_3OH$, in methanol and resulted in the decline in efficiency.

9.3.8 Using solutions with additions higher than the solubility limit

Figure 40 shows the results of the experiments using additions higher than the solubility limit. The optimal H_2O:$LiOH.H_2O$ was not used but rather a ratio of 1:1. As shown in Figure 40, by increasing the amount of $LiOH.H_2O$ added at a fixed ratio of H_2O:$LiOH.H_2O$, the efficiency of Li_2O_2 production decreased.

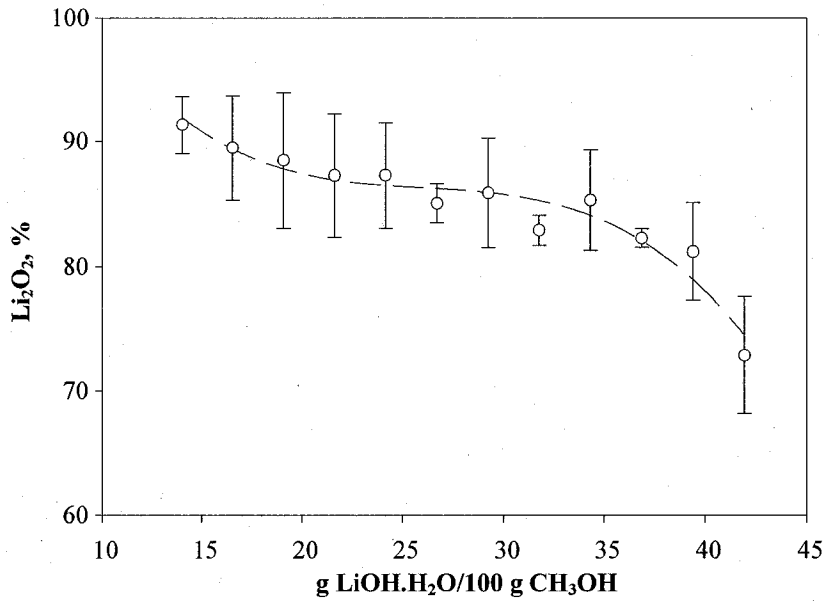

Figure 40: Effect of using a solution with additions higher than the solubility limit at a molar ratio of H_2O_2:$LiOH.H_2O$ = 1.

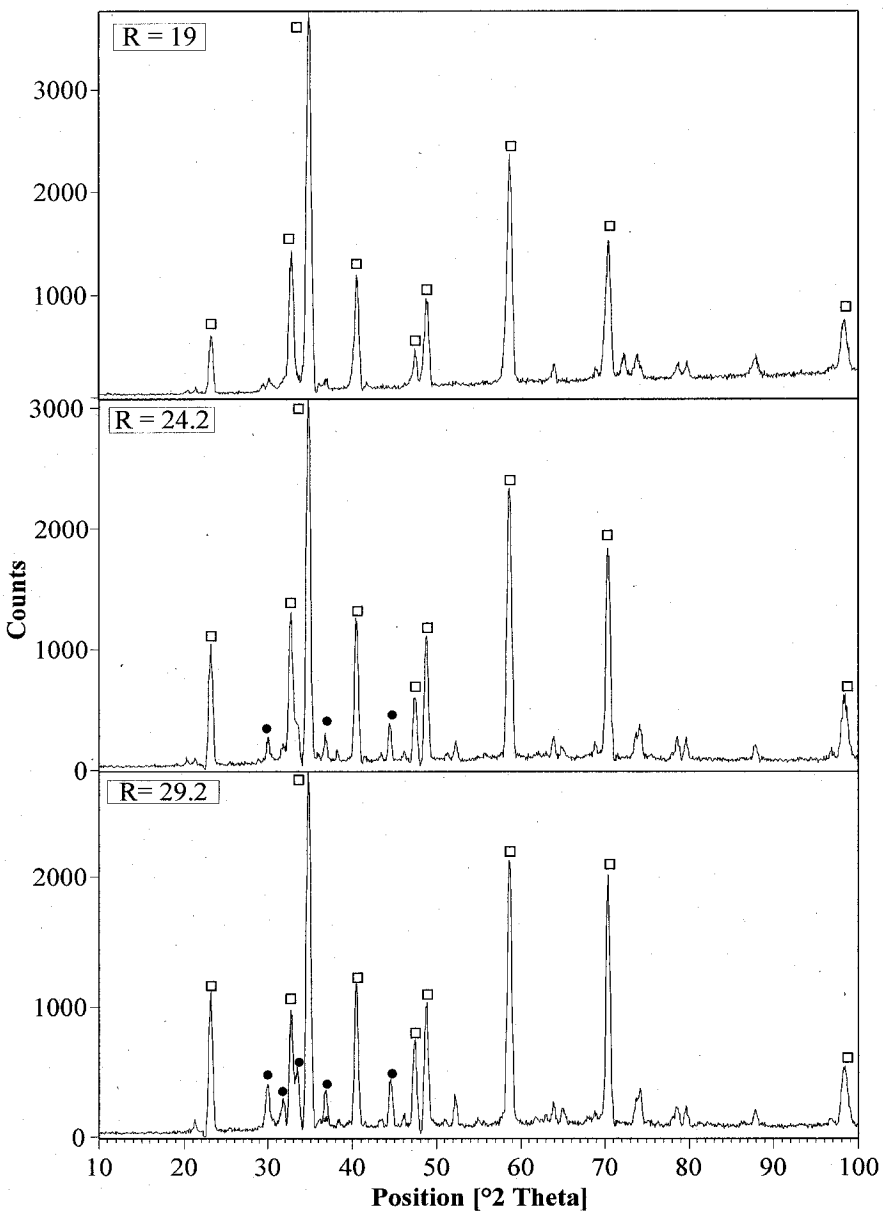

Figure 41: XRD spectra for effect of using solutions with additions higher than the solubility limit at ratios of 19, 24.2 and 29.2 g $LiOH.H_2O$/100 g CH_3OH, Li_2O_2 □ and $LiOH.H_2O$ ●.

Figure 41 shows the XRD spectra of products as a function of the concentrations of $LiOH.H_2O$ in methanol. At concentrations higher than 19.2 g $LiOH.H_2O$/100 g CH_3OH, the lithium produced was contaminated by $LiOH.H_2O$.

9.4 Study of the decomposition of the precipitate

The results of the analysis of the precipitate as a function of H_2O_2 (35 wt%) addition at 20 °C are presented in Table 24. It was found that the precipitate was comprised of Li_2O_2, H_2O_2, H_2O and CH_3OH. Across the range of ratios of H_2O_2:$LiOH.H_2O$ from 1 to 1.5, the composition of the precipitate was the same and contained $Li_2O_2 \cdot H_2O_2 \cdot 3H_2O \cdot 8CH_3OH$.

Table 24: The analysis of the precipitate as a function of H_2O_2 addition.

$H_2O_2/LiOH.H_2O$	Li	O	CH_3OH
mol/mol	wt%	wt%	wt%
1.0	3.2	7.9	65.7
1.1	3.2	8.1	64.7
1.2	3.4	8.2	64.2
1.3	3.2	8.2	64.9
1.5	3.3	8.1	65.1

9.4.1 Drying at ambient temperature

Figure 42 shows the results of drying the precipitate from the tests explained in Section 8.5.1 at an ambient temperature of 20 °C in a controlled air atmosphere.

It can be seen that, up to 60 hr, the precipitate lost weight linearly, which corresponded to 42 % mass loss. Thereafter, it continued to lose weight at a lower rate and reached a plateau after 160 hr. At 312 hr the weight loss was 73.5%. The analysis of the precipitate after drying showed that for drying times less than 60 hrs, the compounds of Li_2CO_3 and LiOH were not formed. After 60 hrs of drying, lithium hydroxide started forming and reaching its maximum value at 130 hr. After this time, the content of lithium hydroxide in the samples decreased. After 215 hrs of drying, lithium hydroxide was no longer detected. The Li_2CO_3 appeared after 185 hr and its formation increased with time. After 312 hrs drying, the amounts of Li_2O_2 and Li_2CO_3 were 0.73 and 0.27 moles, respectively.

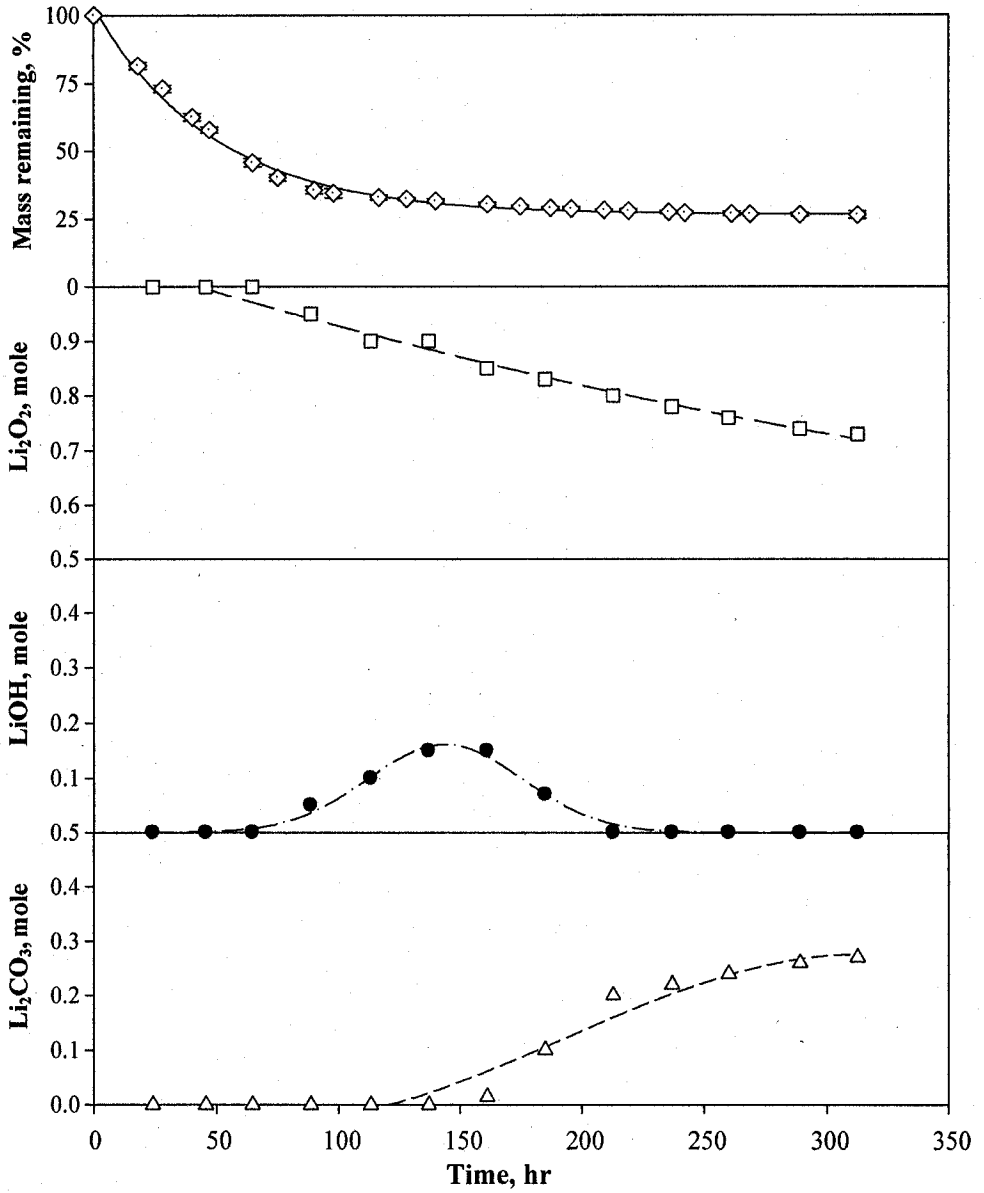

Figure 42: Drying of the precipitate at ambient conditions.

9.4.2 Thermal analysis by TGA and DTA

The thermogravimetric analysis of the precipitate from the tests described in Section 8.5.1 are given in Figure 43 and shows the mass loss of the precipitate with temperature. The mass loss of the precipitate started from the beginning of test at about 40 °C. The initial fast loss ended at 184 °C. Up to 190 °C, the total mass loss was 19 %. The DTG graph shows that the thermogravimetric trace of the precipitate had multiple mass losses. Two

multiple mass losses. Two rapid changes in mass loss were observed at 95 °C and 132 °C. The DTA measurement showed that an endothermic reaction occurred upon heating of the precipitate at an onset temperature of 103 °C.

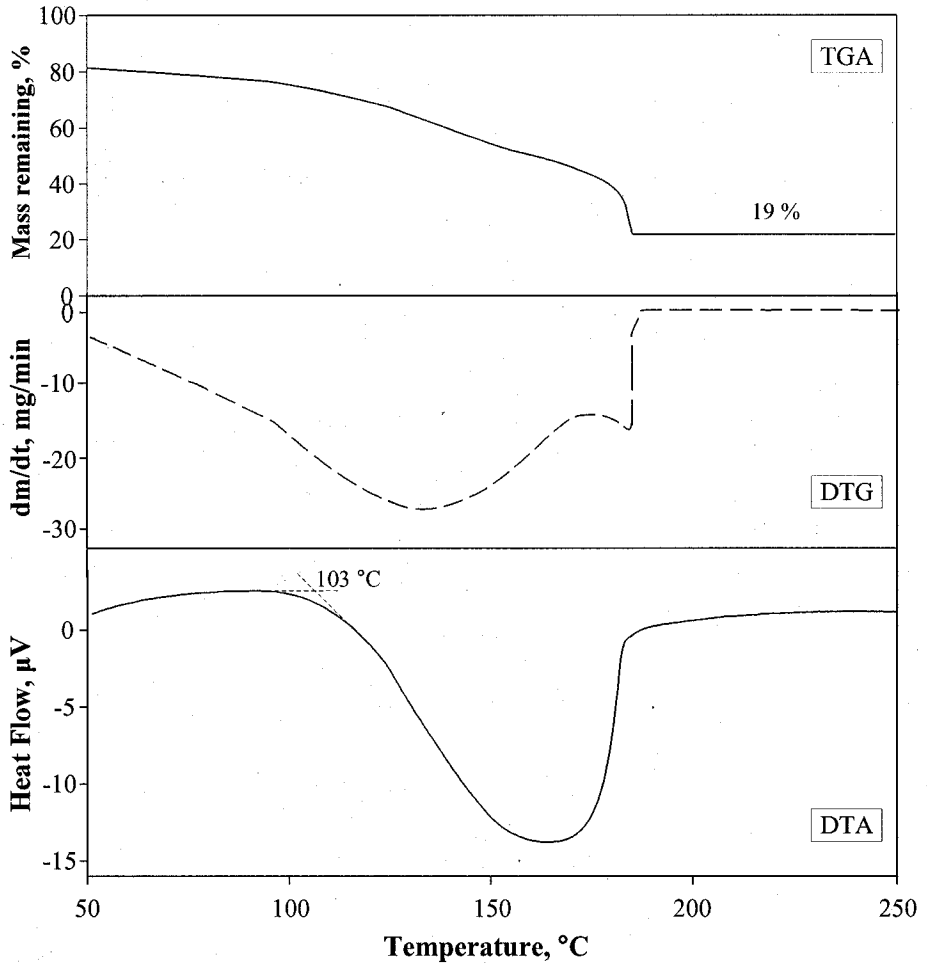

Figure 43: TGA, DTG and DTA results of the precipitate heated in argon.

9.4.3 Thermal analysis in vacuum oven

The decomposition of the precipitate was examined as a function of time at low temperature, 90 °C and at low vacuum 1 kPa (0.1 atm). Figure 44 shows the results of the decomposition at 90 °C as a function of time. The initial mass of the precipitate showed a linear decrease up to 100 min corresponding to 68.8 % mass loss, followed by a lower rate up to 135 min, culminating with 77.2 % loss. After this time, the mass loss continued at a very slow rate. Figure 45 shows the change of active oxygen in the precipitate as function

of time. It can be seen that by decreasing the methanol and water content of the precipitate, the active oxygen increased. The higher variance in the early part of experiment was due to the unsteady evaporation of methanol and water.

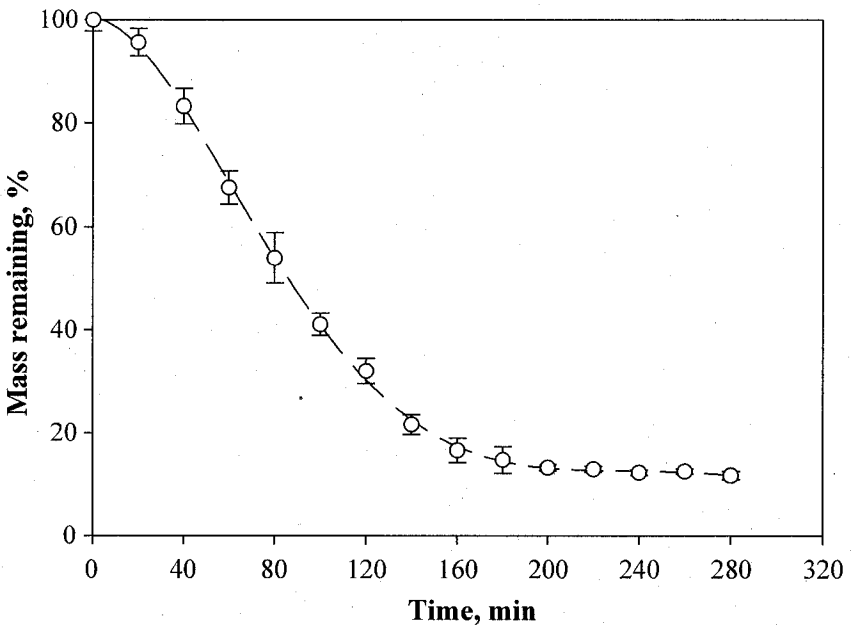

Figure 44: Decomposition of the precipitate as a function of a time at 90 °C at 0.01 atm.

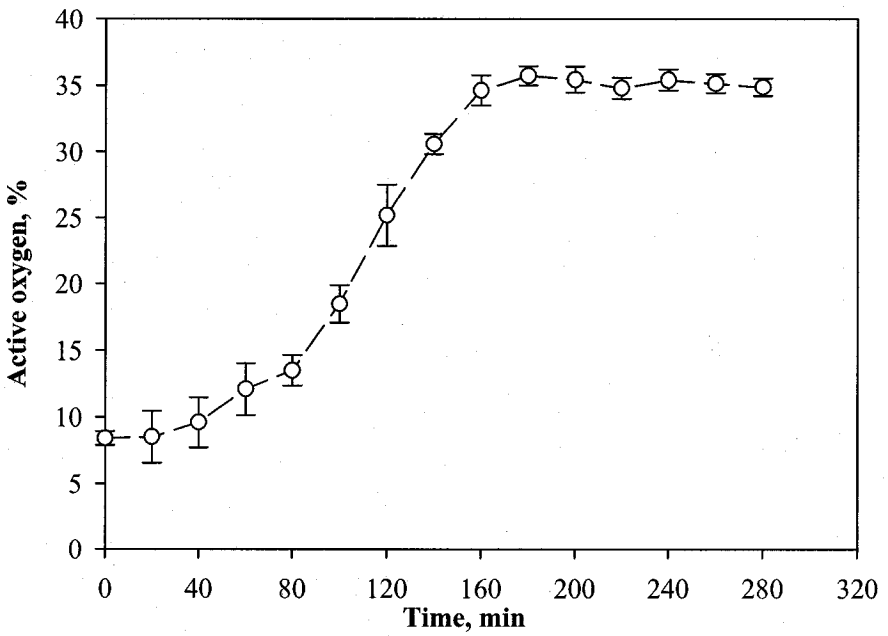

Figure 45: Change of active oxygen of the precipitate as a function of a time at 90°C and 0.01 atm

Table 25: The components measured and the composition of the precipitate as function of a time at 90°C and 0.01 atm

Time	**Li**	**O**	**CH_3OH**	**Composition**
min	%wt	%wt	%wt	
0	3.3	8.4	61.7	Li_2O_2-H_2O_2-3H_2O-8CH_3OH
20	3.5	8.5	60.5	Li_2O_2-H_2O_2-3H_2O-7CH_3OH
40	4.0	9.6	55.7	Li_2O_2-H_2O_2-3H_2O-6CH_3OH
60	5.1	12.1	46.4	Li_2O_2-H_2O_2-3H_2O-4CH_3OH
80	5.9	13.5	39.6	Li_2O_2-H_2O_2-3H_2O-3CH_3OH
100	8.1	18.5	18.0	Li_2O_2-H_2O_2-3H_2O-1CH_3OH
120	13.7	25.2	0	Li_2O_2-H_2O_2-3H_2O
140	14.9	30.6	0	Li_2O_2-H_2O_2-0.6H_2O
160	20.9	34.6	0	Li_2O_2-0.4H_2O_2-0.2H_2O
180	23.4	35.7	0	Li_2O_2-0.3H_2O_2-0.1H_2O
200	24.8	35.4	0	Li_2O_2-0.2H_2O_2
220	27.2	34.8	0	Li_2O_2-0.1H_2O_2
240	28.2	35.4	0	Li_2O_2-0.06H_2O_2
260	28.8	35.1	0	Li_2O_2-0.03H_2O_2
280	29.5	34.9	0	Li_2O_2

As previously explained, in order to track the trend of the decomposition of the precipitate, $Li_2O_2 \cdot H_2O_2 \cdot 3H_2O \cdot 8CH_3OH$, analytical measurements were performed on the changes of mass, lithium content (Appendix II), content of active oxygen (Appendix III) and methanol content (Appendix IV). Table 25 shows the results of the measurements as a function of time at 90 °C and 0.01 atm.

It can be seen from Table 25 that there was a gradual removal of methanol with time that was completed at about 120 min. The resulting composition of the precipitate was $Li_2O_2 \cdot H_2O_2 \cdot 3H_2O$. During the removal of methanol, there was no coevolution of water. The removal of water molecules from $Li_2O_2 \cdot H_2O_2 \cdot 3H_2O$, gradually occurred at a lower rate following methanol evolution. At 140 min, the compound of $Li_2O_2 \cdot H_2O_2$.0.6H_2O was identified, showing that the H_2O_2 was still intact. The decomposition slowly continued with co-evolution of H_2O_2 and H_2O up to 200 min, at which time the water molecules were

completely removed. The decomposition reaction approached its completion to yield pure Li_2O_2, at about 280 min.

Effect of temperature

Figure 46 shows the isothermal decomposition of the precipitate, as per the tests described in Section 8.5.1, as a function of time at the temperatures of 125, 150 and 175 °C. At a temperature of 125 °C, the reaction required a longer time to reach completion in comparison to the tested temperatures of 150 and 175 °C.

The isothermal curves shown in Figure 46 were converted to α vs. time curves (where the fractional decomposition, $\alpha = (m_{in} - m_t)/(m_{in} - m_f)$ where m_{in}, and m_f, are the initial and final sample masses, respectively. The value of m_f, used was that calculated for complete decomposition to the oxide.

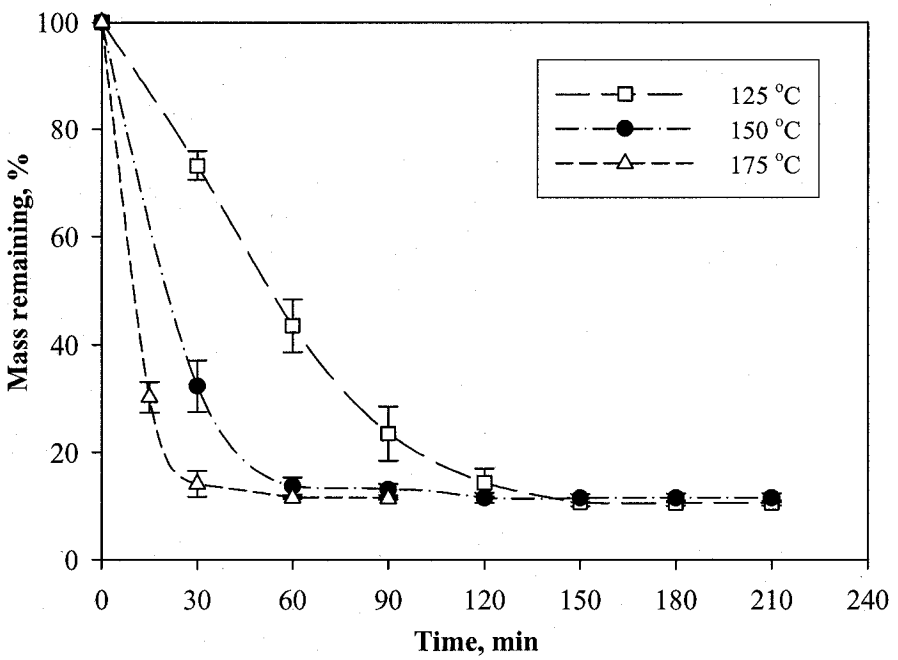

Figure 46: Isothermal decomposition of the precipitate as a function of time at the temperatures of 125, 150 and 175 °C.

It can be seen from Figure 47 that the decomposition occurred in two-stages; there was first a fast and approximately linear change followed by a slower rate. It was found from the experiments of drying the precipitate at ambient temperature and drying and decomposition at 90 °C that, after removal of alcohol and water, the decomposition of

$Li_2O_2 \cdot H_2O_2 \cdot 3H_2O$ was the slowest step of decomposition reaction. Therefore, the kinetics of decomposition of precipitate was analyzed over two ranges of $0 < \alpha < 0.8$ and $0.8 < \alpha < 1$.

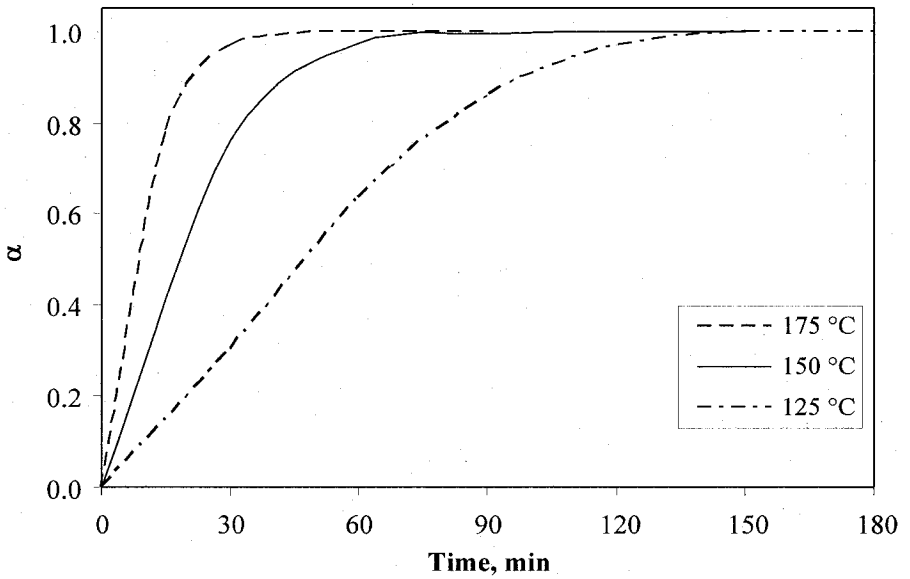

Figure 47: α-graphs for isothermal decomposition of precipitate at the temperatures of 125, 150 and 175 °C.

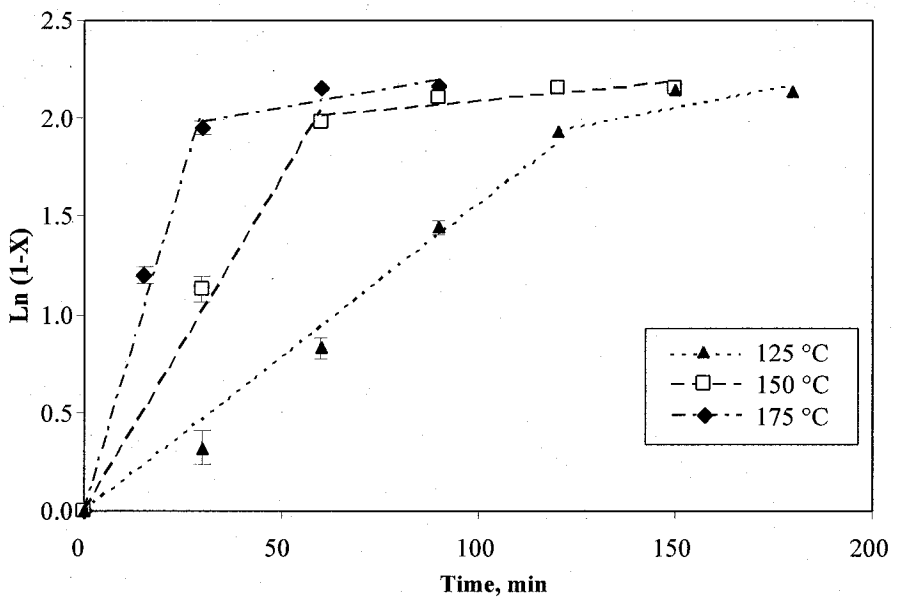

Figure 48: Ln ($1-X_{prec.}$) vs. time.

In order to estimate the kinetics of the decomposition reactions, it was initially assumed that the decomposition of precipitate occurred as a first-order reaction. Then, the initial

slopes of the Ln ($1-X_{prec.}$) vs. time curves were calculated (Figure 48). Table 26 shows the regression equations of the graphs of Ln ($1-X_{prec.}$) against time for the three temperatures 125, 150 and 175 °C. By measuring the slopes of curves in Figure 48, the graph of Ln K was plotted against 1/T (Figure 49).

Table 26: The regression equations for the graphs of Ln K vs.1/T plotted in Figure 48.

Temperature, °C	α	Regression equation	R^2
125	0 - 0.8	006x + 2.0594	0.974
125	0.8 - 1	038x + 1.5151	0.807
150	0 - 0.8	339x	0.992
150	0.8 - 1	019x + 1.9004	0.799
175	0 - 0.8	68x + 0.0725	0.980
175	0.8 - 1	035x + 1.8776	0.785

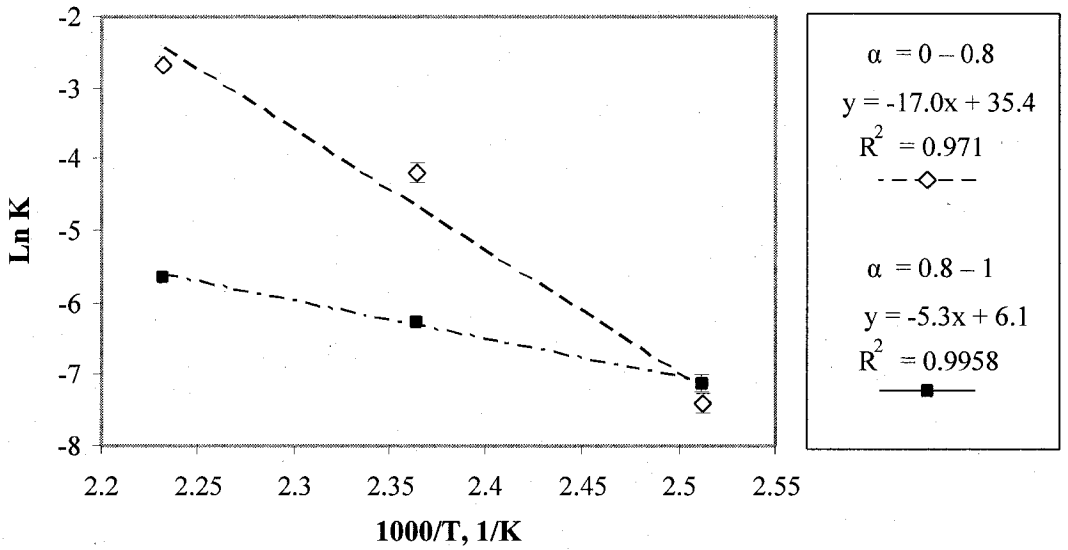

Figure 49: Arrhenius plot for the precipitate decomposition.

The slope of the plots in Figure 49 was calculated as –16.969 and – 5.275 for the α ranges: 0 – 0.8 and 0.8 – 1. The activation energies were therefore calculated as 141.08 kJ/mol (-E/R = -16.969, E = 16.969×8.314 kJ/mol). The activation energy for the removal of alcohol and water from the precipitate, $Li_2O_2{\cdot}H_2O_2{\cdot}3H_2O{\cdot}8CH_3OH$, was calculated as 141 ± 5 kJ/mol. Similarly, the activation energy for the decomposition of $Li_2O_2{\cdot}H_2O_2{\cdot}3H_2O$ was calculated as 48 ± 1 kJ/mol.

9.5 Study of lithium oxide formation

In this section, the results of the experiments on the formation of lithium oxide from lithium peroxide are presented.

9.5.1 Thermal analysis of lithium peroxide in different atmosphere

Figure 50 shows the results of the decomposition of Li_2O_2 in a nitrogen atmosphere. It can be seen that at 400 °C, Li_2O_2 was rapidly decomposed. The formation of LiOH during the decomposition was observed. After 20 min, the sample assayed 0.86 and 0.14 mol fraction of Li_2O and LiOH, respectively. Very little change in the mass and composition of the samples was observed after 20 min.

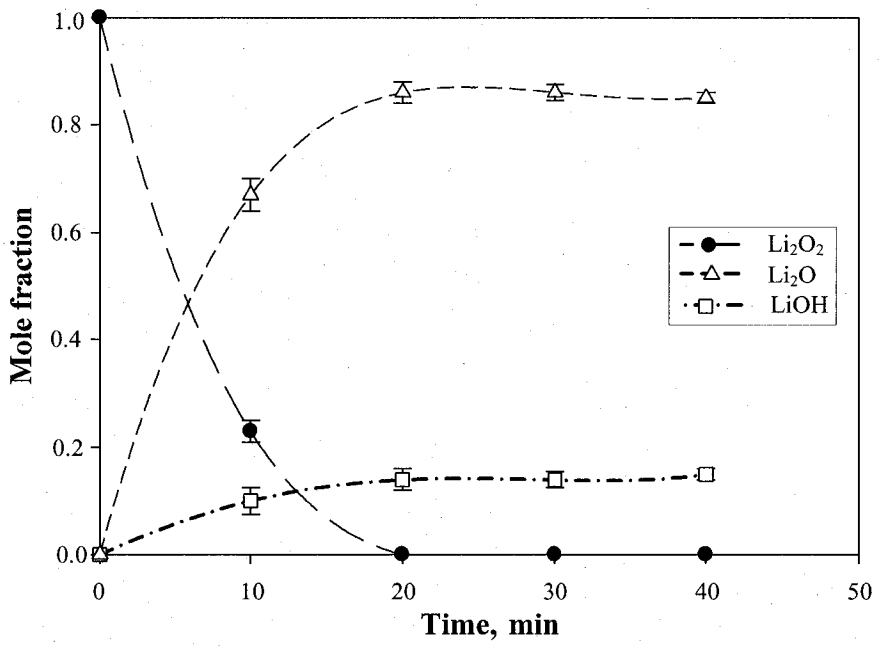

Figure 50: Decomposition of Li_2O_2 in N_2 at 400 °C.

Figure 51 shows the XRD results of products of Li_2O_2 decomposition after 20 min in N_2 at 400 °C. Figure 52 shows the results of the decomposition of Li_2O_2 in an ambient atmosphere at 400 °C. It can be seen that during the decomposition of Li_2O_2, LiOH was formed. After 20 min, the sample assayed 0.59 and 0.41 mol fraction of Li_2O and LiOH, receptively. Figure 53 shows the XRD results of the products of Li_2O_2 decomposition after 20 min in N_2 at 400 °C.

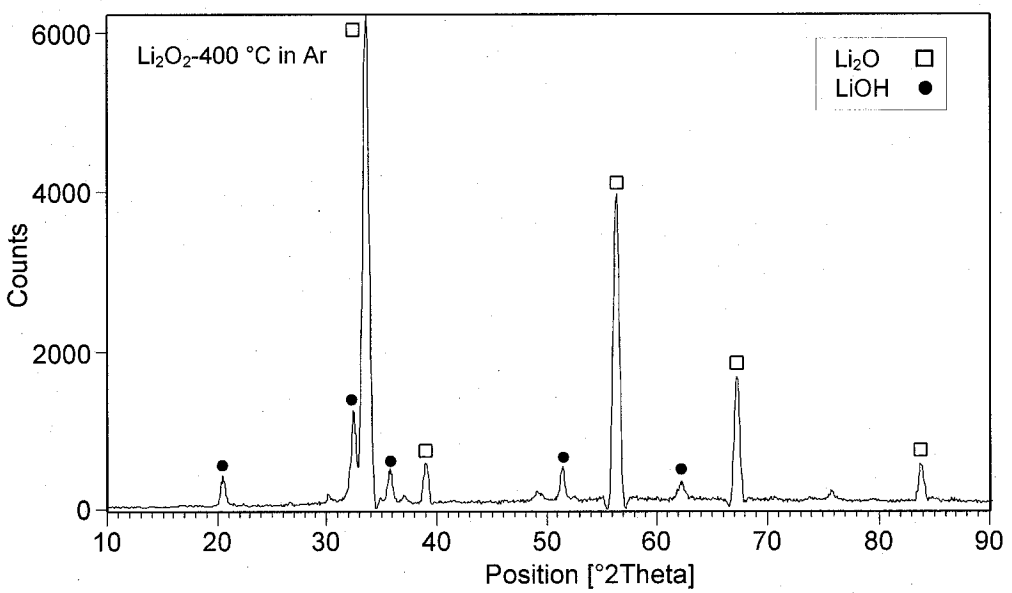

Figure 51: XRD spectra of products of Li_2O_2 decomposition after 20 min in N_2 at 350 °C.

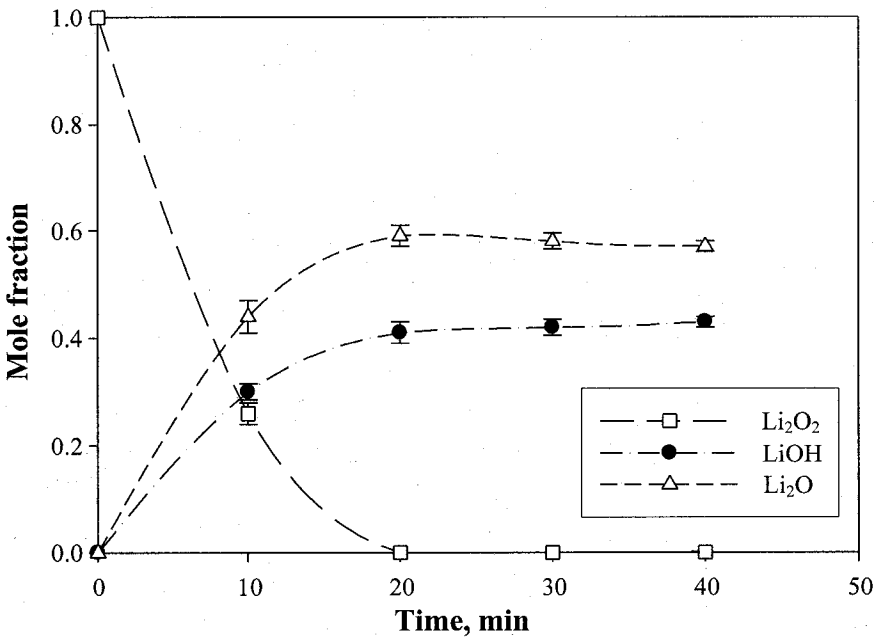

Figure 52: Decomposition of Li_2O_2 in ambient atmosphere, i.e., without atmosphere protection at 400 °C.

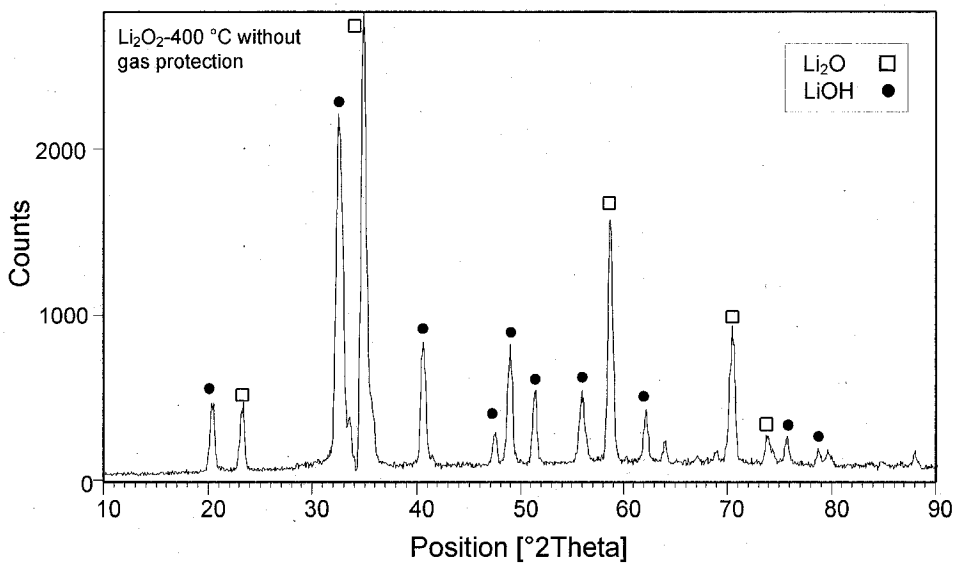

Figure 53: XRD spectra of the products of Li_2O_2 decomposition after 20 min in ambient atmosphere at 400 °C.

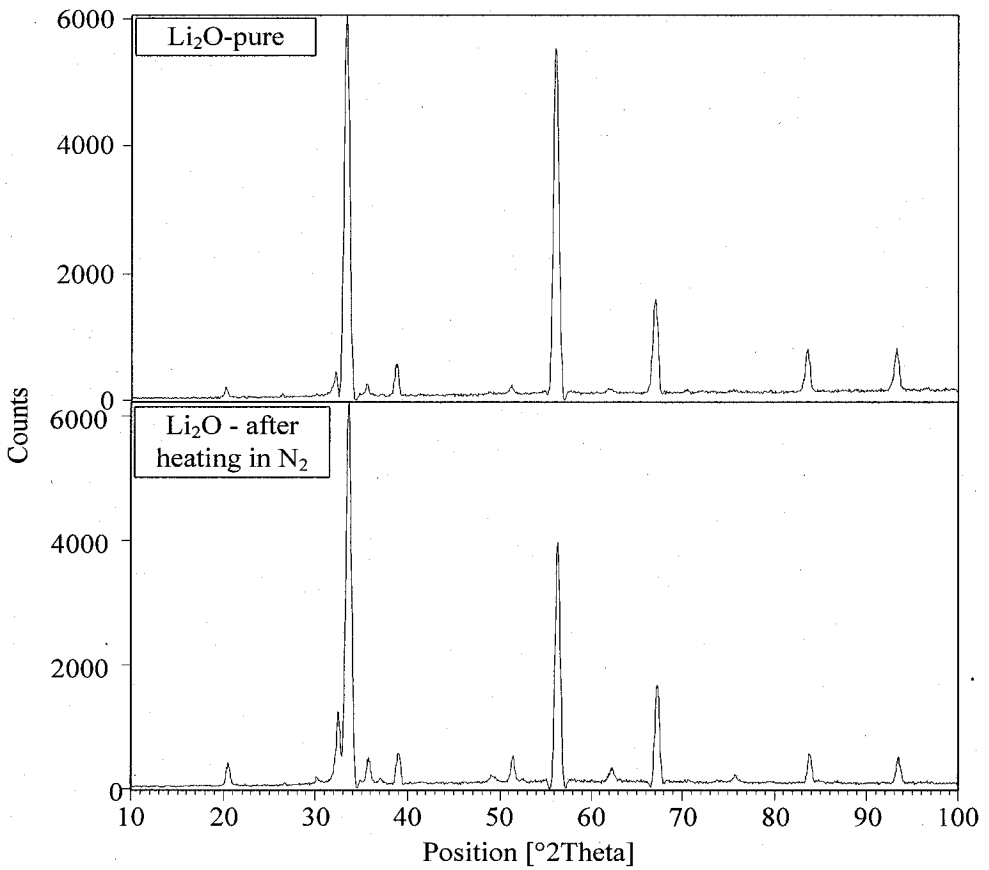

Figure 54: XRD spectra of pure Li_2O after 20 min in 20 min in N_2 at 400 °C.

Figure 54 shows the XRD results of pure Li_2O after its heating in N_2 for 20 min at 350 °C. It can be seen that the lithium oxide was stable in N_2 at 350 °C and did not covert to LiOH.

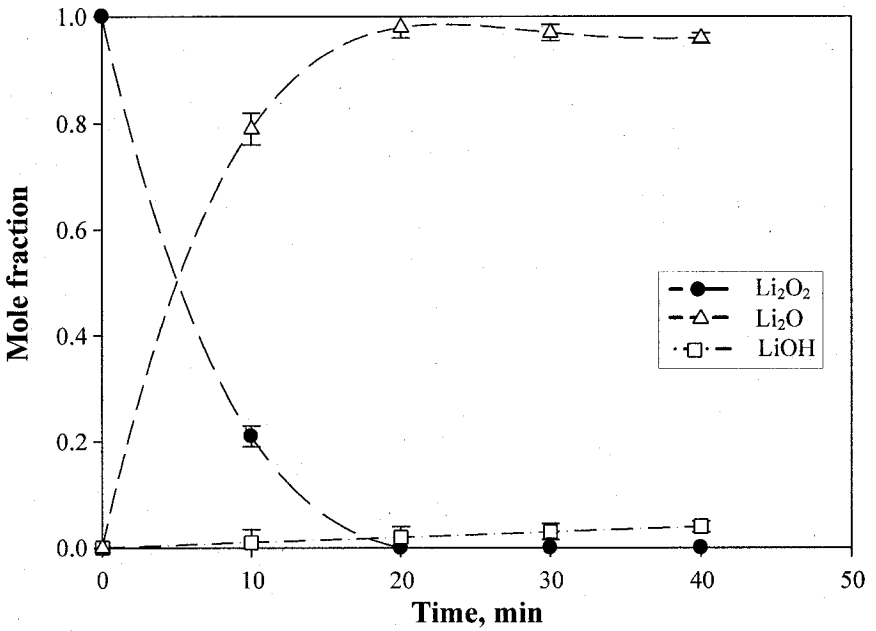

Figure 55: Decomposition of Li_2O_2 in the Ar atmosphere at 400 °C

Figure 55 shows the results of the decomposition of Li_2O_2 in an Ar atmosphere at 400 °C. It can be seen that during decomposition of Li_2O_2, a very small amount LiOH was formed. After 20 min, the sample assayed 0.98 and 0.02 mol fraction of Li_2O and LiOH, respectively. The presence of LiOH in the samples might be due to the hydration of the Li_2O sample before the experiment or the leakage of air into the furnace.

9.5.2 Thermal decomposition by TGA-DTA

The TGA curves for the decomposition of lithium peroxide for four samples with the same condition and particle size, + 37 μm in argon are shown in Figure 56 . It shows that the decomposition of Li_2O_2 was complex. It can be seen that after the initial mass loss, decomposition did not continue at the same rate. However, the onset temperature and the final mass losses were similar in all the samples.

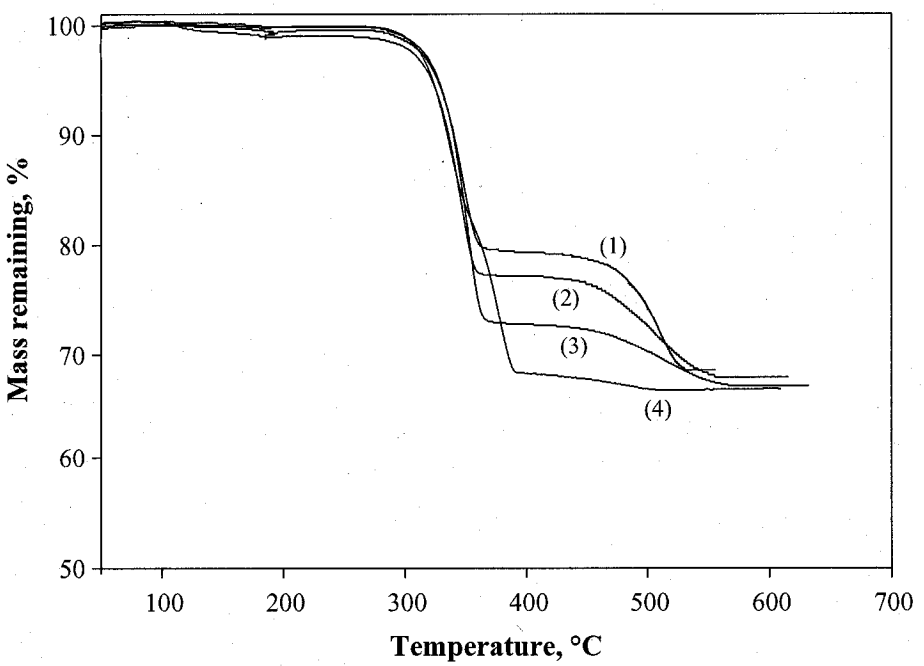

Figure 56: TGA curves for lithium peroxide powder heated at 10 °C/min in argon. Numbers represent No sample.

The TGA analysis showed that the decomposition of lithium peroxide occurred in two steps. Table 27 shows the results of mass losses and onsets temperatures extracted from TGA data and DTG curves (Figure 56). It can be seen from Table 27 that for all samples, the onsets were similar. Except for the removal of small amounts of moisture, about 0.2%, at 130°C, the samples were stable up to about 270 °C. For all the samples, the initial loss was fast followed by a further loss of from 2.5 to 12 %. The decomposition reaction approached completion at a mean 33.3% loss.

Table 27: Mass losses and onsets of TGA

Run	first onset	first mass loss	second onset	Second mass loss*
	°C	%	°C	%
1	284	20.9	410	32.8
2	283	23.1	410	33.0
3	282	27.0	408	33.8
4	284	31.5	410	34.0

* total loss

The stoichiometry of Li_2O_2 decomposition to Li_2O suggests that the loss should be 34.9 %. Therefore, the loss was observed in good agreement with the calculated theoretical value. Among the four experiments, Sample No 4 was the only sample that showed a break in its weight loss curve at 384 °C (Figure 56). This peculiar change, in comparison to other samples tested under the same conditions, is more obvious when plotting the derivatives of mass loss as a function of temperature (Figure 57).

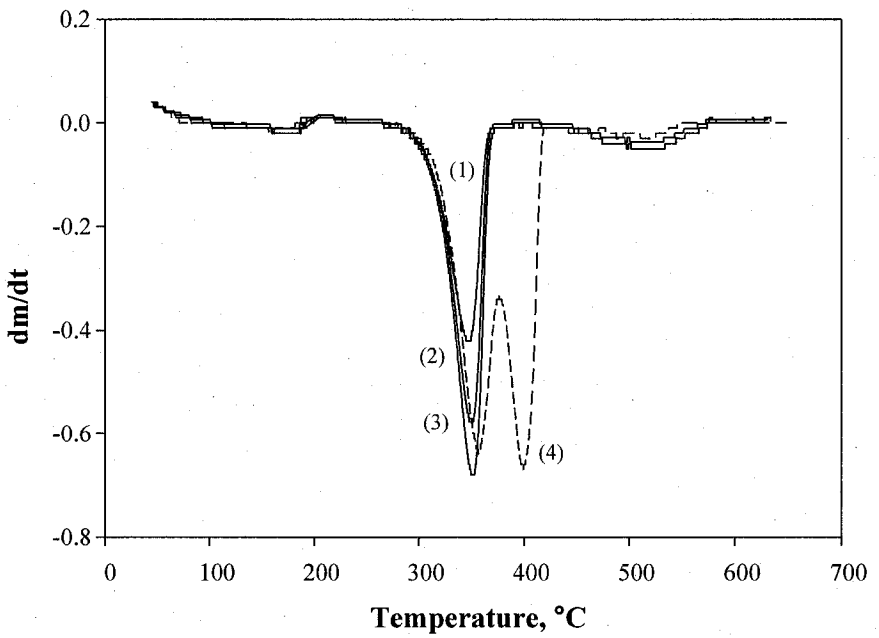

Figure 57: DTG curves for lithium peroxide powder heated at 10 °C/min in argon.

DTA analysis

Differential thermal analysis results for lithium peroxide decomposition are presented in Figure 58. In Figure 58, the range of temperature was selected due to the linear change of the temperature versus time. Two endothermic reactions were observed in onsets of 258 °C and 324 °C. A small exothermic reaction was observed at 410 °C.

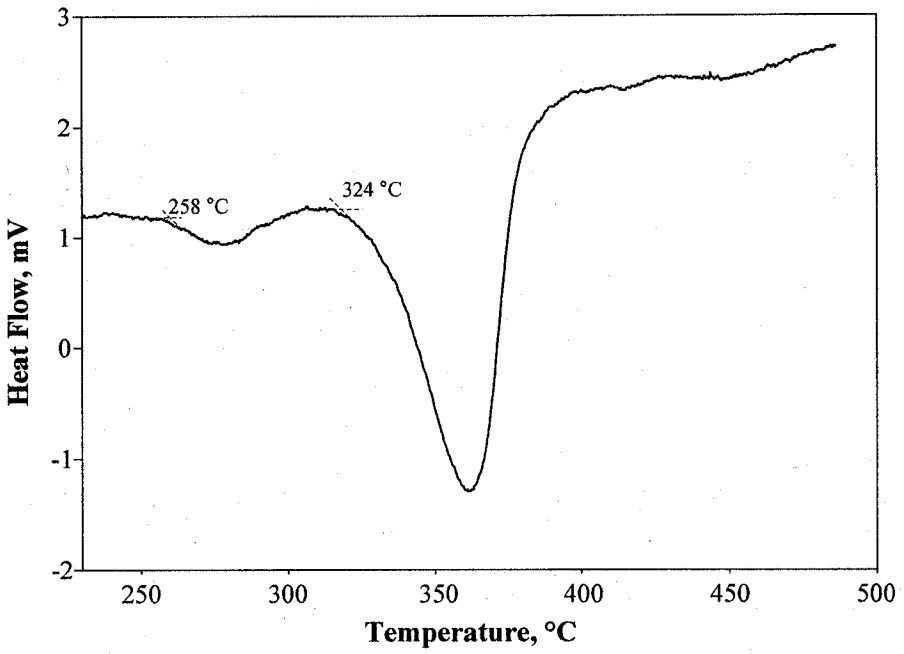

Figure 58: DTA analysis for lithium peroxide powder heated at 10 °C/min in argon.

Kinetic analysis of lithium peroxide decomposition

The procedure for using TGA for the determination of non-isothermal kinetic parameters has been explained in detail in Appendix V. The first step is the calculation of the reacted fraction, α (Figure 59).

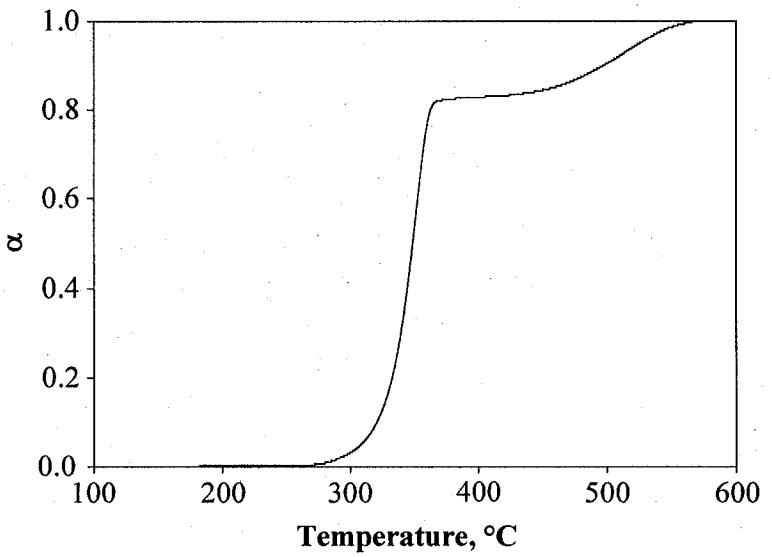

Figure 59: The α vs. T curve for non-isothermal decomposition of lithium peroxide (Sample 3) heated at 10 °C/min in argon.

Then, the curve of either Y = $\log_{10}\left[\frac{1-(1-\alpha)^{1-n}}{T^2(1-n)}\right]$ against $\frac{1}{T}$ or, when n = 1, Y= $\log_{10}\left[-\log_{10}\frac{(1-\alpha)}{T^2}\right]$ against $\frac{1}{T}$, is plotted.

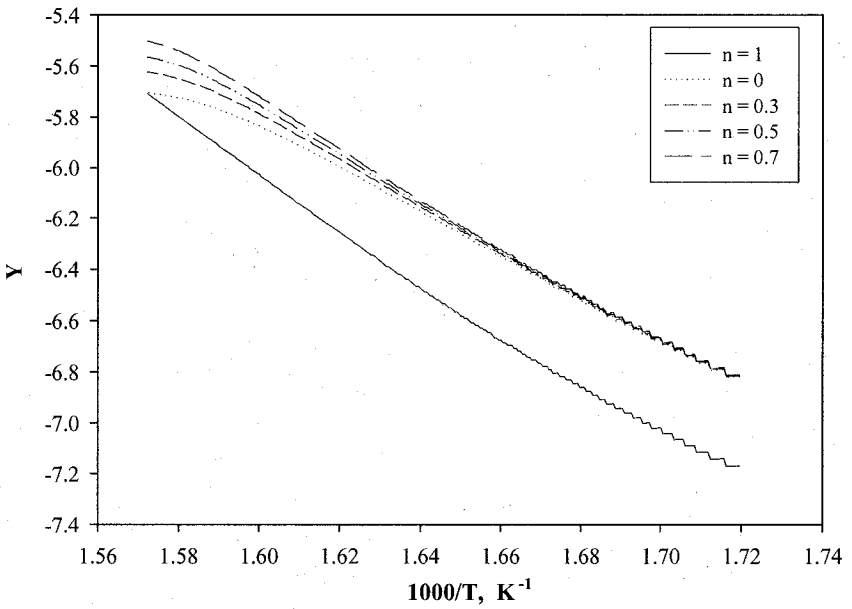

Figure 60: Plots of Y vs. 1/T using different orders of reaction for 0 < α < 0.8.

Figure 60 shows the plots of Y versus 1/T for Sample 3 using different orders of reaction (n = 0, 0.3, 0.5, 0.7 and 1). Figure 61 shows the plot of Y vs. 1/T for Sample 3 over the range: 0 < α < 0.8 for n = 1. It can be seen that the order of 1 was the best fit for the decomposition of Li_2O_2 in the range: 0 < α < 0.8.

The slope of this plot was calculated as – 11.108 and the activation energy was therefore calculated as 212.4 kJ/mol (-*E*/2.3R = -11.108, *E* = 11.108× 2.3 ×8.314 kJ/mol).

Figure 62 shows the plot of Y vs. 1/T for Sample 3 over the range of 0.8 < α < 1. The values of activation energy of Li_2O_2 did not depend strongly on the value of n in the range n = 0.8 -1.0 (Figure 62).

Table 28 shows the results of measurements of the activation energy and the order of the decomposition reaction of lithium peroxide. The average activation energy for the range 0 < α < 0.8 was 201 ± 10 kJ/mol.

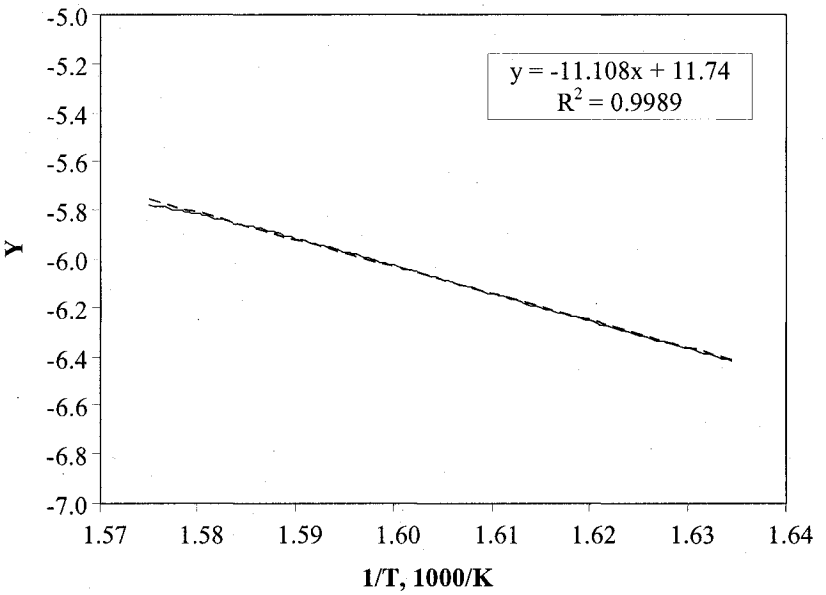

Figure 61: The plot of Y vs. 1/T for Sample 3 for the range: $0 < \alpha < 0.8$ using n = 1.

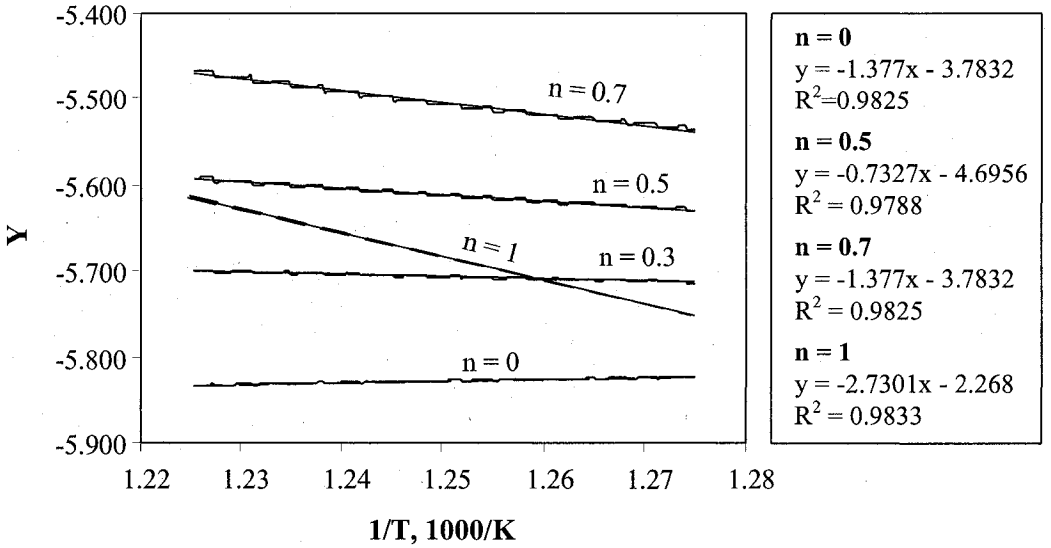

Figure 62: The plot of Y vs. 1/T for Sample 3 for the range: $0.8 < \alpha < 1$.

Table 28: The results of measurement of the activation energy and the order of decomposition of lithium peroxide

Run	Range of α	Activation energy (kJ/mol)	order of reaction
1	0 - 0.8	191.2	1
2	0 - 0.8	195.5	1
3	0 - 0.8	212.4	1
4	0 - 0.8	204.5	1

Effect of particle size on the decomposition of lithium peroxide

Figure 63 shows the TGA curves for the decomposition of lithium peroxide for two particle sizes, 56 and 212 μm, heated at 10 °C/min in argon.

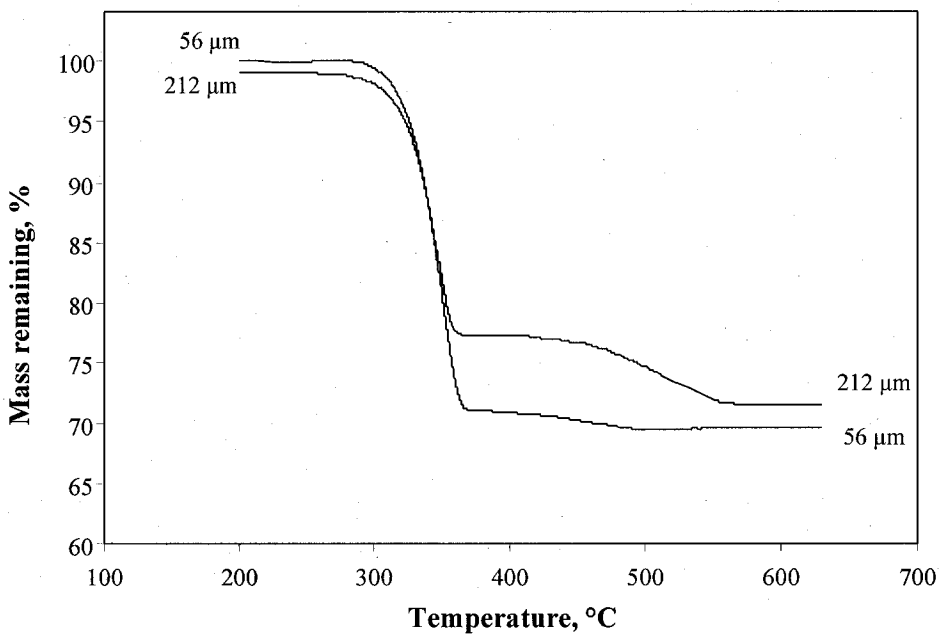

Figure 63: TG curves for lithium peroxide with the particle sizes of 56 and 212 μm at heated 10 °C/min in argon.

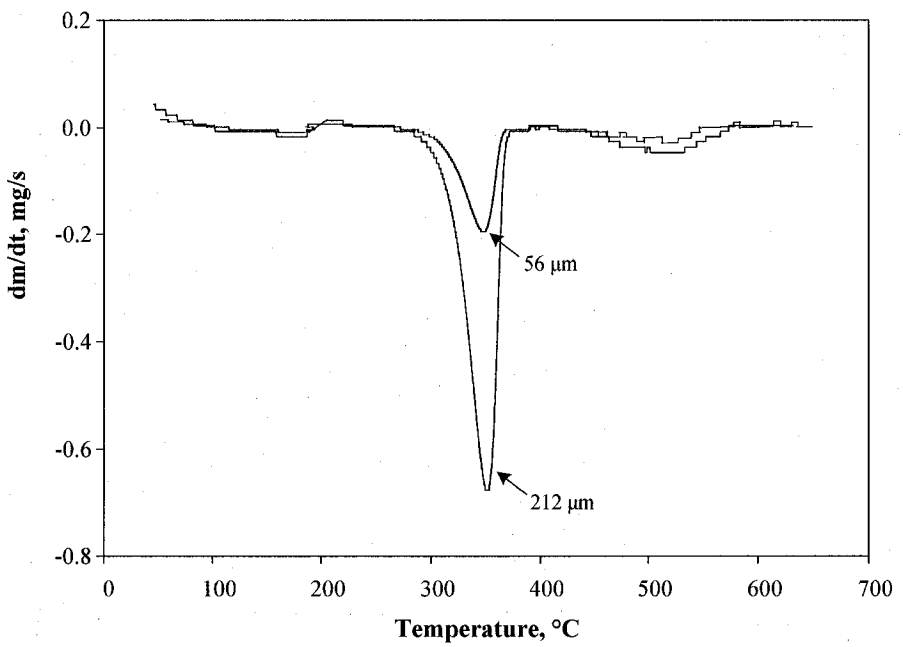

Figure 64: DTG curves for lithium peroxide with particle sizes of 56 and 212 μm at 10 °C/min in argon.

Figure 64 shows the DTG plot of lithium peroxide decomposition for particle sizes 56 and 212 μm heated at 10 °C/min in argon. It can be seen that the onset and the temperature at the maximum rate were similar. As the particle size increased, the residue of material after completion of decomposition decreased.

The same procedure was performed, as explained above, to measure the activation energy of lithium peroxide decomposition with different particle sizes. As shown in Table 29, the change of particle size had little effect on the activation energy of lithium peroxide decomposition.

Table 29: Activation energy for lithium peroxide with particle sizes 56 and 212 μm.

Sample Size	Range of α	Activation energy (kJ/mol)	order of reaction
+ 56 μm	0.28 - 0.78	198 ± 7	1
+ 212 μm	0 - 0.90	203 ± 8	1

10. DISCUSSION

The results of the experiments presented in Chapter 9 are discussed in this chapter and related to the findings of the literature survey.

10.1 Reactivity of lithium peroxide and lithium oxide

10.1.1 Reactivity of lithium peroxide

Effect of moisture: According to the literature survey [30, 31], lithium oxide is known to be a compound that reacts with the CO_2 and H_2O in ambient air. The products of reaction are lithium hydroxide and lithium carbonate. However, lithium peroxide is believed to be less reactive with CO_2 and H_2O in air [38, 39], even though the reaction of CO_2 with Li_2O_2 is thermodynamically favorable as shown below (Reaction 61) [19].

$$Li_2O_2 + CO_{2\,(g)} \rightarrow Li_2CO_3 + \tfrac{1}{2}\,O_{2\,(g)} \qquad \Delta G^\circ_{298} = -166.4\ \text{kJ/mol} \quad (61)$$

The passivity of lithium peroxide under ambient conditions was hypothesized to be due to a lack of elevated temperatures and a catalyst. Here, the experimental results showed that lithium peroxide does indeed react with ambient air (Figure 18). The product of the reaction of lithium peroxide with CO_2 and H_2O in air was Li_2CO_3. It was found that during this reaction, LiOH was formed initially. The LiOH then converted to Li_2CO_3. The formation of LiOH started rapidly. The LiOH eventually exhibited a constant rate of formation, which was a balance between its formation from Li_2O_2 and its consumption by changing to Li_2CO_3. This indicates that once LiOH was formed, due to Li_2O_2 reaction with H_2O, it was quickly converted to Li_2CO_3 by reaction with CO_2 diffusing into the original LiOH particle along with H_2O. The thickness of the LiOH layer depended on the relative diffusivities of H_2O and CO_2 in the *ash layer* (lithium carbonate). The greater molar mass and size of the CO_2 suggests that it would have a lower diffusivity. In fact, the

diffusivity of H_2O and CO_2 through air at 20 °C and 1 atm are 0.246 and 0.243 cm^2sec^{-1}, respectively [80].

Figure 65 shows a hypothetical schematic of the steps for lithium peroxide conversion to LiOH and Li_2CO_3 assuming that the particle was initially spherical. As time progressed, the Li_2CO_3 content in outer layer of the particles increased. This layer of Li_2CO_3 then impeded the further diffusion of water vapor (moisture) into the particle and its reaction with Li_2O_2. Consequently, the further reaction of lithium peroxide was greatly slowed.

The figure also illustrates that the area designated as LiOH, after its formation, did not shrink. The progressive reaction of Li_2O_2 with moisture indicated that the layer of LiOH formed did not contribute to the resistance to mass transfer.

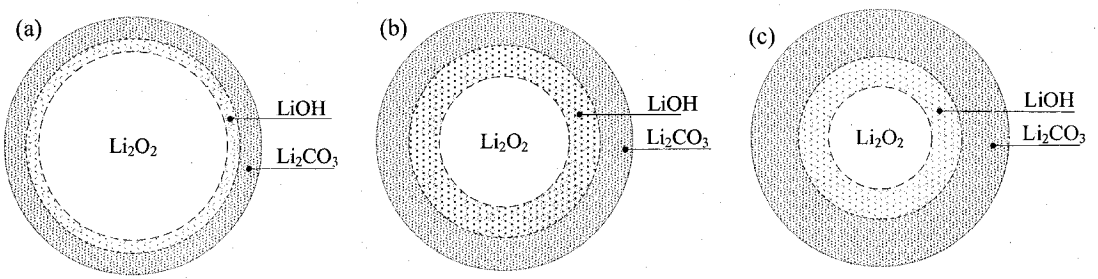

Figure 65: Schematic of lithium peroxide decomposition as a function of time, roughly to scale; a) 30 hr, b) 97 hr and c) 264 hr.

A consequence of this reaction mechanism was that a decrease in humidity of the air would result in a decrease in the reactivity of lithium peroxide (Figure 20). In other words at lower humidity, the conversion of lithium peroxide to lithium hydroxide should decrease. Indeed, in air with a relative humidity of 5 %, lithium peroxide was seen not to react. As the relative humidity of the air increased to 22 %, the reaction of lithium peroxide was seen to increase.

It was found that the trends of lithium peroxide decomposition as well as mass loss were the same for the 22 % relative humidity tests as for the 57 % relative humidity tests and approached the plateau. The formation of lithium carbonate was confirmed by XRD in the 22% relative humidity tests (Figure 24). These findings confirmed that the moisture content of air had the greatest influence on the presence of LiOH rather than the conversion of LiOH to Li_2CO_3.

From the present work, it can be concluded that the literature's claim [39] that moisture in air plays a catalytic role is incorrect. Rather H_2O is essential for conversion and for promoting the reaction of Li_2O_2 to LiOH. In the absence of moisture, the reaction of Li_2O_2 with CO_2 is slow. A fast formation of LiOH by reaction with moisture from the atmosphere proceeds according to Reaction 62 (Table 15).

$$2LiOH + CO_{2\,(g)} \rightarrow Li_2CO_3 + H_2O \qquad \Delta G°_{298} = -91.8 \text{ kJ/mol} \quad (62)$$

Effect of particle size: Tests of the effect of particle size showed that as the size of particle decreased, the lithium peroxide was more reactive (Figure 22). The extent of the difference between the reactivity of the lithium peroxide with particle sizes of 56 and 212 μm was particularly evident. By increasing the specific area of lithium peroxide particles, more sites for the occurrence of the reaction between lithium peroxide and air moisture were available. Therefore as shown in Figure 22, the lithium hydroxide and accordingly lithium carbonate were formed at a faster rate for the smaller particle sizes. Conversely, this resulted in a greater fraction of lithium peroxide remaining in the larger particles.

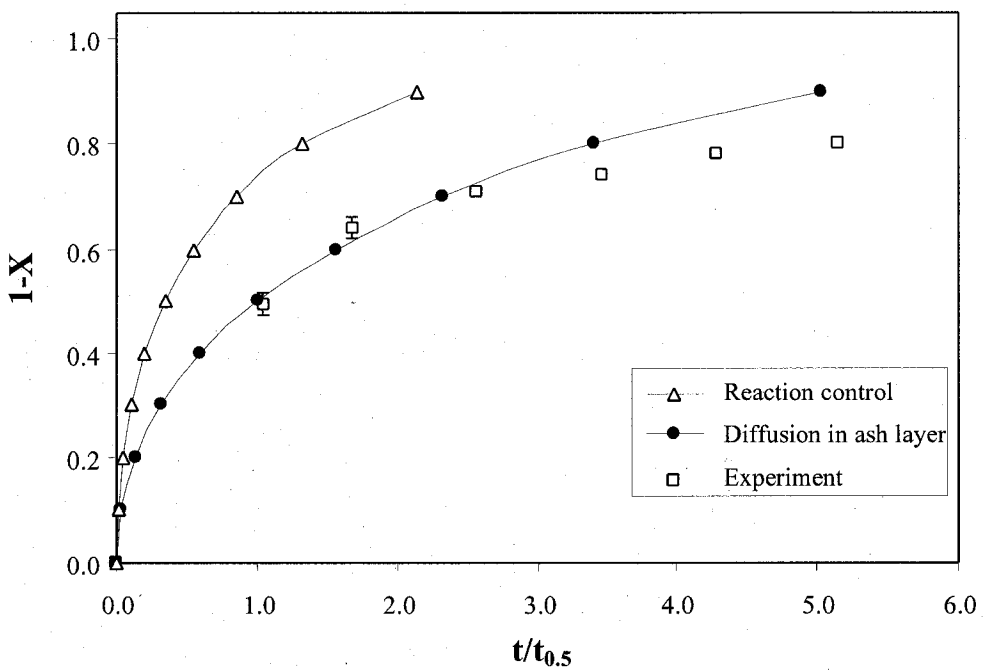

Figure 66: Comparison of Li_2O_2 conversion to the predicated values. See Appendix VI.

By examining, the kinetic data in terms of a shrinking core model and using the reduced time method (see Appendix VI), it was found that the rate of control of the conversion of lithium peroxide agreed with control by diffusion through the ash layer (Figure 66).

Figure 66 shows that the rate of reaction was not controlled by the chemical reaction or diffusion in the gas layer. It was then hypothesized that the decomposition of lithium peroxide might involve either forming water or release of oxygen molecules. Therefore, the variance from the predicted plot of control due to diffusion in the ash layer may be due to oxygen evolution or back-reaction of the products as per the possible reactions below:

$$Li_2O_{2\,(s)} + H_2O_{(g)} \rightarrow 2\,LiOH + \tfrac{1}{2}\,O_{2\,(g)} \qquad (63)$$

$$LiOH + H_2O_{(g)} \rightarrow LiOH.H_2O \qquad (64)$$

$$LiOH.H_2O + CO_{2\,(g)} \rightarrow Li_2CO_3 + H_2O \qquad (65)$$

Moreover upon decomposition, lithium peroxide can form free radicals because of dissociation of the O–O bond (Reaction 66). The formation of the radicals can be initiated by either thermal dissociation or by the presence of catalysts such as metal ions [5]:

$$LiOOLi + H_2O_{(g)} \rightarrow 2\,LiOH + O\bullet \qquad (66)$$

The mechanism of radical formation is relatively complex and depends on the presence of catalysts and indeed the availability of water in the system. However, the oxygen radical is generally unstable and forms oxygen molecules or reacts with other compounds, i.e.:

$$O\bullet + H_2O \rightarrow H_2O_2 \qquad (67)$$

Reaction 68 is a hypothetical reaction describing the back reaction of $LiOH.H_2O$ with hydrogen peroxide:

$$2\,LiOH.H_2O + H_2O_2 \rightarrow Li_2O_{2\,(s)} + 4\,H_2O \qquad (68)$$

10.1.2 Reactivity of lithium oxide

The present study showed that lithium oxide was also very reactive in atmospheric conditions (Figure 23), but in comparison to Li_2O_2, less LiOH was formed. The small formation of LiOH was accompanied by the fast formation of Li_2CO_3, suggesting the latter formed without intermediary LiOH formation which was seen in the case of lithium peroxide degradation in ambient air. The apparent creation of a fast forming, diffusion-inhibiting lithium carbonate ash layer, consequently reduced the reactivity of lithium oxide in comparison to lithium peroxide. As the humidity of air was decreased, lithium oxide was seen to be less reactive although lithium carbonate still formed at a steady rate (Figure 25).

By again considering the kinetic data in terms of a shrinking core model and using the reduced time method, it was found that the rate of control of the conversion of lithium oxide also agreed well with control by diffusion through the ash layer (Figure 67).

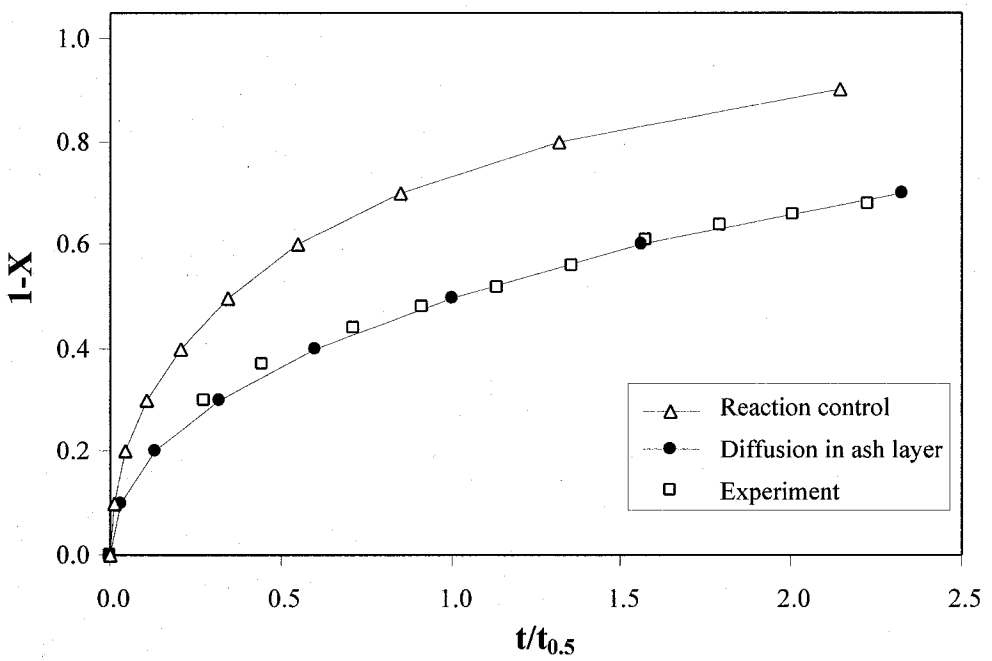

Figure 67: Comparison of Li_2O conversion to the prediction. See Appendix VI

It was seen that the Li_2O_2 had a higher conversion rate as compared to Li_2O (Figure 26), whereas lithium peroxide reached a plateau, lithium oxide continued steadily to convert to

LiOH and Li_2CO_3. This difference in behavior can be attributed to the difference in the structure of the products formed.

The XRD results showed that Li_2CO_3 was the only compound that formed by carbonation of lithium peroxide or lithium hydroxide. Other compounds, such as hydrated lithium carbonate, were not formed. In addition, the known crystal system for lithium carbonate is monoclinic [2] and the structure of lithium carbonate produced from either lithium peroxide or lithium oxide was identified as monoclinic. Therefore, the possibility of forming the different crystal structure of Li_2CO_3 from Li_2O_2 or Li_2O[xxii] was rejected. However, SEM pictures (Figure 27) showed that the appearance of the Li_2CO_3 formed from Li_2O_2 and from Li_2O were different. It can be seen that on the surface of lithium peroxide particles after exposure to air atmosphere, the lithium carbonate had a dense and to some extent, amorphous structure. On the other hand, the structure of lithium carbonate formed from lithium oxide showed a crystalline structure. The difference in the physical form of products on the surface of the particles was considered to be the major reason for the different kinetic behavior between lithium peroxide and lithium oxide.

10.2 Solubility of lithium compounds in alcohols

As presented in Section 0, the values of the solubility parameters and the relative permittivities of the alcohols can predict the dissolution of salts in alcohols. An alcohol with a higher solubility parameter and hence a lower relative permittivity dissolves more salts. As expected, methanol had highest solubility for lithium compounds followed by ethanol and 1-propanol on this basis. The logarithmic solubility of $LiOH.H_2O$ in alcohols was found to be linearly proportional to reciprocal of relative permittivities of alcohols (Figure 68).

Furthermore, due to the linear relationship between relative permittivity and solubility parameter, the logarithmic solubility of $LiOH.H_2O$ in alcohols was linearly proportional to the solubility parameters of the alcohols (Figure 69).

[xxii] Li_2O_2, Li_2O and LiOH have the crystal systems of tetragonal, cubic and tetragonal, respectively.

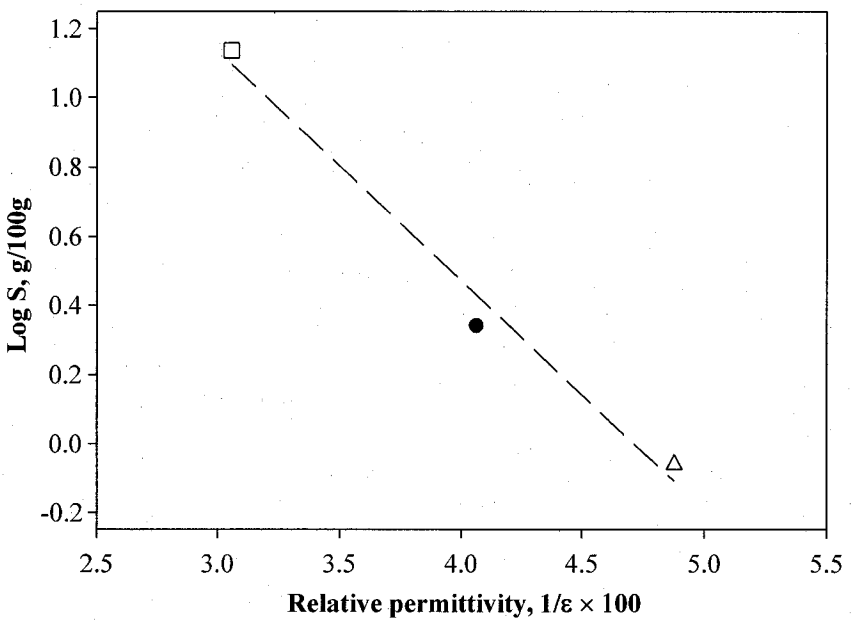

Figure 68: The relation between the measured solubility of $LiOH.H_2O$ in alcohols vs. relative permittivity of alcohols; methanol □, ethanol●, and 1-propanol △.

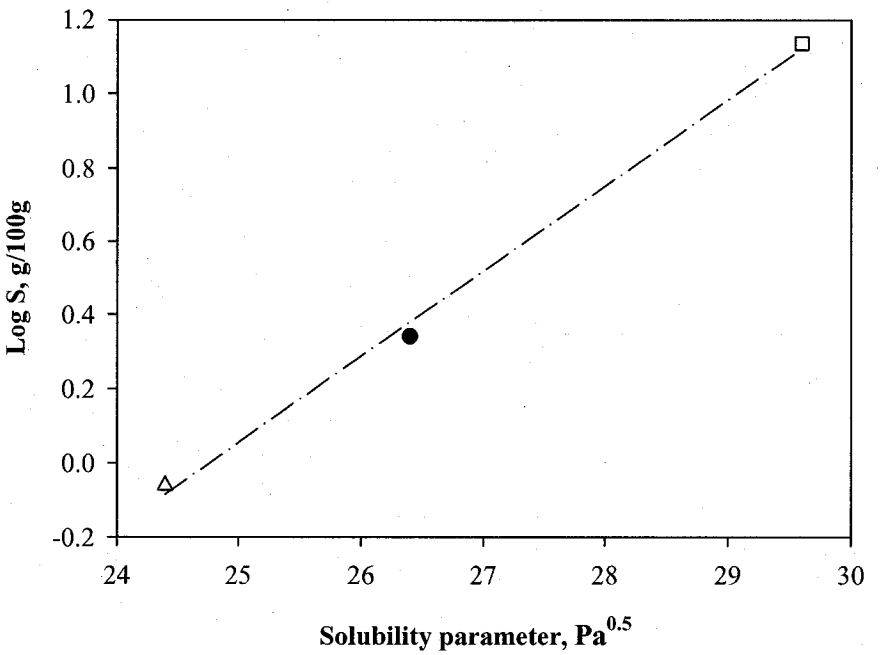

Figure 69: The relation between the measured solubility of $LiOH.H_2O$ in alcohols vs. solubility parameter of alcohols; methanol □, ethanol●, and 1-propanol △.

During the dissolution of $LiOH.H_2O$ in methanol, a temperature rise was observed indicating that the solvation was exothermic. The solvation can be attributed to the replacement of the water molecule in the monohydrate $LiOH.H_2O$ by a methanol

molecule. XRD results confirmed that the residue (after dissolving it in methanol, heating the solution until it evaporated and drying the residue) was just LiOH.

At higher temperatures, the solubility of $LiOH.H_2O$ in methanol was lower (Figure 30). This agreed with the finding that the dissolution was exothermic, as the higher temperature hindered the exothermic solvation of $LiOH.H_2O$ in methanol. The decrease in the relative permittivity of methanol at elevated temperature [69] may also contribute to the decrease in the solubility of $LiOH.H_2O$ in methanol with increasing temperature. Equation 69 presents a correlation of the present results for the solubility of $LiOH.H_2O$ in methanol as a function of temperature.

$$S = 32.98 - 0.067\,T \qquad (69)$$

Here S is the solubility (g $LiOH.H_2O$/100 g CH_3OH) and T is the temperature (K) in the range $10 < T < 60$ °C.

The higher molar solubility of $LiOH.H_2O$ in comparison to LiOH was due to the presence of water from the $LiOH.H_2O$. It is well known that water and methanol are completely miscible in each other. Moreover, by addition of water to methanol, the solubility of alkali salts in methanol is increased [81, 82]. Therefore, the higher solubility of $LiOH.H_2O$ in methanol can be correlated to the higher solubility of mixture of water-methanol for lithium hydroxide (LiOH).

Under ambient atmosphere at 20 °C, lithium hydroxide monohydrate dissolved in methanol rapidly (Figure 28). After 1 hr, methanol was saturated with $LiOH.H_2O$ and was seen to be no longer dissolving in methanol indicating that the solvation of $LiOH.H_2O$ in methanol was reached equilibrium. The solvation of $LiOH.H_2O$ in methanol also resulted in a change of the pH of the solution. The decay of pH as a function of time indicated that LiOH was gradually surrounded by methanol molecules.

As explained in Section 7.5, aprotic solvents are incapable of dissociating to give protons and it was expected that methanol partially self-dissociated or dissociated the $LiOH.H_2O$ to form ions. Since the pH of pure methanol is equal to 7.8, a high pH, 12.6-12.8 can be

explained by distinguishing the two different forms of $LiOH.H_2O$ in solution. First, a majority of $LiOH.H_2O$ was alkolized by methanol molecules, which might not have increased the pH of the methanol. Second, lithium hydroxide monohydrate was partially ionized either by water or by methanol and resulted in the increase in the pH of solution.

One of the major criteria for the selection of the alcohol for the present application was to have a high solubility for $LiOH.H_2O$ and at the same time a low solubility for Li_2CO_3 and Li_2O_2. Therefore, methanol with a ratio of $Li_2O_2/LiOH.H_2O$ equal 0.11 (0.22 and 0.26 for ethanol and 1-propanol, respectively) would be preferred over the other alcohols for application in an industrial transformation and separation process. A higher solubility of $LiOH.H_2O$ in methanol provides a higher ratio of reactant/solvent in comparison to other alcohol, which is technically favorable in industrial scale. Moreover, a better separation of reactant from product, here $LiOH.H_2O$ and Li_2O_2, can be happened when methanol is used.

10.3 Reaction stoichiometry and thermodynamics of the conversion of lithium hydroxide monohydrate to lithium peroxide

The experimental results discussed in this section deal with the reaction of hydrogen peroxide with lithium hydroxide monohydrate dissolved in alcohols.

At the outset of the experimental program, the reaction between lithium hydroxide monohydrate and hydrogen peroxide was considered to be:

$$\mathbf{R_1}\ LiOH.H_2O + \mathbf{R_2}\ H_2O_2\ (35\ \%wt) \rightarrow \mathbf{P_1}\ Li_2O_2 + \mathbf{P_2}\ H_2O \qquad (70)$$

where R and P were the amounts (in terms of moles or masses) of the reactants and the products, respectively.

However, the experimental studies found that the system was much more complicated. In fact, some of the alcohol and some of the water, either from the reactant or produced by the conversion by the H_2O_2 solution, precipitated with part the solid product. Using methanol as the example, the reaction model became:

$$\mathbf{R_1}\ LiOH.H_2O + \mathbf{R_2}\ H_2O_2.\mathbf{t}H_2O + \mathbf{R_3}\ CH_3OH \rightarrow \mathbf{P_1}\ [Li_2O_2{\cdot}\mathbf{x}H_2O_2{\cdot}\mathbf{y}H_2O{\cdot}\mathbf{z}CH_3OH]_{\text{precipitate}\downarrow} + [\mathbf{P_2}\ CH_3OH + \mathbf{P_3}\ H_2O]_{\text{raffinate}} \quad (71)$$

It should be noted that the expression above is a general expression for the reaction system. It is no longer expressed in the form of a conventional chemical reaction because it is showing some of the same substance on both sides of the reaction. The reason for using this form of the expression is that it conveys the idea of the need for excess amounts of substances in the process.

The right hand side is a representation of the mix of products present at equilibrium. In the analysis that follows, the difference between the number of moles of a substance on the right and left-hand sides is used in the equilibrium analysis and represents the amounts of substances participating in the reactions.

The experimental results showed that the reaction was incomplete and so it became necessary to represent the product as follows in order to to include all the substances present in significant quantities at the end of reaction:

$$\mathbf{R_1}\ LiOH.H_2O + \mathbf{R_2}\ H_2O_2.\mathbf{t}H_2O + \mathbf{R_3}\ CH_3OH \rightarrow \mathbf{P_1}\ [Li_2O_2{\cdot}\mathbf{x}H_2O_2{\cdot}\mathbf{y}H_2O{\cdot}\mathbf{z}CH_3OH]_{\text{precipitate}\downarrow} + [\mathbf{P_2}\ CH_3OH + \mathbf{P_3}\ H_2O + \mathbf{P_4}\ H_2O_2 + \mathbf{P_5}\ LiOH.H_2O]_{\text{raffinate}} \quad (72)$$

It should be mentioned that in Reaction 72, the possible evolution of oxygen gas (due to hydrogen peroxide dissociation) has been ignored.

The balance of this section looks to establish values of the variables, R, P x, y and z. It also extends the analysis of the thermodynamics of the solution as far as possible with the present data.

It should be noted that the following analysis has not been previously attempted and is considered original. It should also be noted that the present system is more complicated than other systems commonly considered in that the solvent phase is a mixture of three substances, the proportions of which are influenced by the amount of solute salt, itself being present in a number of forms, the proportions of which are influenced by the composition of the solvent phase.

10.3.1 Reactions involving the use of 35 wt% hydrogen peroxide ($H_2O_2 \cdot 3.5H_2O$)

Assuming the net reaction of lithium hydroxide monohydrate with hydrogen peroxide in methanol to yield a lithium peroxide compound is represented by Reaction 73, the required amount of hydrogen peroxide would be half the moles of lithium hydroxide monohydrate reacted, i.e.:

$$LiOH.H_2O_{(s)} + \tfrac{1}{2} H_2O_{2\,(aq)} \rightarrow \tfrac{1}{2} Li_2O_{2\,(s)} + 2\, H_2O_{(aq)} \qquad (73)$$

It was found that in order to produce one mole of lithium peroxide, the required amount of $H_2O_2 \cdot 3.5H_2O$ was 2.8 times the stoichiometric amount in molar terms and that the optimum molar ratio of H_2O_2:$LiOH.H_2O$ (R_2/R_1) was equal to 1.3 (Figure 31). The reasons for the consumption of hydrogen peroxide being higher than the stoichiometric amount are as follows:

1. Hydrogen peroxide, like water, is miscible to a large extent in alcohol [56]. As the content of methanol in the system increased, the activity of hydrogen peroxide decreased and resulted in a higher amount of $H_2O_2 \cdot 3.5H_2O$ at equilibrium.
2. Under alkali conditions, the decomposition rate of hydrogen peroxide increased [58]. As mentioned in Section 9.2.1.1, the pH of a mixture with the concentration of 12.5 g $LiOH.H_2O$ / 100 g CH_3OH was 12.4 indicating that the system was alkali. Therefore, hydrogen peroxide decomposition was promoted and the required amount of hydrogen peroxide for the conversion reaction was concomitantly increased.
3. As the temperature of the solution containing the hydrogen peroxide was increased to 25 °C, 5 °C higher than ambient temperature, the decomposition rate of hydrogen peroxide was doubled [56]. The conversion of $LiOH.H_2O$ by hydrogen peroxide to yield Li_2O_2 was exothermic and the consequent heat released caused the hydrogen peroxide to dissociate, i.e., H_2O_2 consumption increased.

Despite the excess addition of $H_2O_2.3.5H_2O$, the conversion of $LiOH.H_2O$ to Li_2O_2 did not reach 100%. This was due to the dissolution of either the product or the unreacted

$LiOH.H_2O$ (or LiOH) in the methanol in such a way that the lithium peroxide that was produced was dissolved in the methanol rather than being precipitated to yield lithium peroxide. Therefore, there were always a few percent of lithium peroxide or lithium hydroxide remaining in the solution.

Figure 31 shows that as the ratio of H_2O_2:$LiOH.H_2O$ increased from 1.5 to 1.7, although the efficiency decreased the product was still pure, i.e., there was no LiOH found in the dried product.

Generally, in a system containing alcohol and water, as the concentration of water increases, the solubility of alkali salts in the mixture increases [83]. In this regard, the decrease in efficiency can be explained by the excess addition of H_2O_2, and consequently an addition of H_2O as part of the hydrogen peroxide solution, that resulted in an increase in the solubility of the product in the raffinate. At ratios of 1.7 to 2, the decrease in yield continued.

The XRD results showed that at ratios above 1.7, the product was contaminated with LiOH. The presence of LiOH was due to the excess H_2O_2 (and H_2O) and an increase in the activity of water that lead to the product dissociating.

As seen in Figure 33, the changes of ORP and pH were very small. This indicated that, similar to the aqueous system, the conversion of $LiOH.H_2O$ to Li_2O_2 using H_2O_2 involved the peroxide group transfer. Therefore, an oxidation or reduction reaction did not occur and the formation of lithium peroxide can be explained by the mechanism of "peroxide group transfer". In a solution containing $H_2O_2.3.5H_2O$, one atom of hydrogen from the hydrogen peroxide was substituted by a lithium cation, Li^+ as follows:

$$2\ LiOH.H_2O + 2\ H_2O_2{\cdot}3.5H_2O \rightarrow Li_2O_2{\cdot}H_2O_2{\cdot}3H_2O + 8\ H_2O \qquad (74)$$

As seen in Figure 33, once hydrogen peroxide was added to the solution containing $LiOH.H_2O$ and methanol, the pH changed rapidly at first. The initial addition of H_2O_2 (35 %wt) was consumed rapidly to convert the ionized $LiOH.H_2O$ cation, Li^+, to Li_2O_2. The pH of solution then remained fixed at about 7.8 to 7.9 and finally returned to the pH of pure methanol, 7.8.

The formation of $Li_2O_2 \cdot H_2O_2 \cdot 3H_2O$ then continued by reaction of the added H_2O_2 (35 %wt) with $LiOH.H_2O$ (or LiOH). The constant pH of solution was indicative of the reaction of hydrogen peroxide with the alkolized $LiOH.H_2O$ (by methanol). This meant that the $LiOH.H_2O$ in the solution containing methanol and water was present in the forms of the ionized and unionized species. Indeed as expected, the proportion of the ionized $LiOH.H_2O$ was very low in comparison to the unionized component.

As stated in Section 9.2, the solubility of Li_2O_2 in pure methanol was measured as 1.52 g/100 g CH_3OH. Assuming lithium peroxide was directly formed through the reaction of $LiOH.H_2O$ with $H_2O_2 \cdot 3.5H_2O$, then methanol could dissolve 11.1 wt% ($1.52 \times 100/13.6 = 11.1$) of the lithium peroxide produced. Despite the presence of water increasing the solubility of the solution for the solutes, the high efficiency of the precipitation of $Li_2O_2 \cdot H_2O_2 \cdot 3H_2O$, about 95 %, showed that complete precipitation of $Li_2O_2 \cdot H_2O_2 \cdot 3H_2O$ in methanol meant that it had a lower solubility than Li_2O_2. This can be explained by the formation of a compound with a larger molar mass, and probably with less polarity; the two factors leading to the lower solubility.

10.3.2 The precipitation of $Li_2O_2 \cdot H_2O_2 \cdot 3H_2O$ in methanol

The process of the precipitation of lithium hydroperoxidate trihydrate, $Li_2O_2 \cdot H_2O_2 \cdot 3H_2O$, in methanol involved the attachment of methanol molecules to the product as follows:

$$Li_2O_2 \cdot H_2O_2 \cdot 3H_2O + 8CH_3OH \rightarrow Li_2O_2 \cdot H_2O_2 \cdot 3H_2O \cdot 8CH_3OH \qquad (75)$$

In other words, this compound formed by the direct combination of two separate molecular entities, $Li_2O_2 \cdot H_2O_2 \cdot 3H_2O$ and CH_3OH, in such a way that no loss of atoms occurred.

As explained in Sections 7.2 and 0, the relative permittivities of methanol, ethanol, 1-propanol are lower than water, namely 32.7, 24.6, 20.5 and 78.4, respectively. Recalling that the relative permittivity of a solvent represents the extent of polarity of a solvent and the ability of the solvent to separate its charges and orient its dipoles, only solvents with sufficiently high relative permittivity will be capable of reducing the strong electrostatic

attraction between oppositely charged ions to such an extent that ion pairs can dissociate into free solvated ions. Therefore, polar compounds like $Li_2O_2 \cdot H_2O_2 \cdot 3H_2O$ would be less soluble in methanol than in comparison to water.

One of the key considerations for the complete precipitation of salts by forming insoluble adducts with alcohols is to provide a solution with low water activity, i.e., the ions are soluble in water, and any change in decrease of the water activity will influence the solubility of the dissolved solute. Reaction 76 below, suggests that as a result of the addition of alcohol to an aqueous system, the activity of free water is decreased and the hydrolysis of the solute is reversed by the replacement of the water molecules by the alcohol molecules, i.e.:

$$M[H_2O]^{Z+}_{m\ (aq)} + ROH \rightarrow M[H_2O]^{Z+}_{(m-1)\ (aq)} + ROH\ldots H\text{-}O\text{-}H \qquad (76)$$

The alcohol disrupts the water structure by breaking the water-water hydrogen bonds and by replacing them with alcohol-water hydrogen bonds [84]. Since the present system contained predominantly methanol molecules, no hydrogen-hydrogen bonding between water molecules formed and consequently the $Li_2O_2 \cdot H_2O_2 \cdot 3H_2O \cdot 8CH_3OH$ that was formed was almost completely insoluble in methanol.

10.3.3 The effect of the kind of alcohol

The tests using ethanol and 1-propanol found that neither of them was an appropriate substitution for methanol. The efficiency of Li_2O_2 produced at the maximum yield did not exceed 64% or 82% for ethanol or 1-propanol, respectively. Similar to methanol, both alcohols required an excess of hydrogen peroxide to convert $LiOH.H_2O$ to Li_2O_2. Ethanol tests approached the maximum efficiency at a ratio of H_2O_2:$LiOH.H_2O$ equal to 1.3, whereas, with 1-propanol required more H_2O_2, i.e., the required ratio was 1.47.

Furthermore, unlike in methanol, the precipitates were contaminated by LiOH at all ratios of H_2O_2:$LiOH.H_2O$, in ethanol and 1-propanol. Because of the low solubility of LiOH in ethanol and 1-propanol ($LiOH.H_2O$ in the alcohols easily lost its water molecule and was present in the system as LiOH), LiOH was precipitated along with the product.

As mentioned in Section 0, the analysis of the precipitates showed that they were comprised of $Li_2O_2{\cdot}H_2O_2{\cdot}3H_2O{\cdot}6CH_3CH_2OH$ and $Li_2O_2{\cdot}H_2O_2{\cdot}3H_2O{\cdot}11CH_3CH_2CH_2OH$ in ethanol and 1-propanol, respectively. This indicates that the formation of lithium hydroperoxidate trihydrate, $Li_2O_2{\cdot}H_2O_2{\cdot}3H_2O$, was a phenomenon common to the alcohols studied.

It was seen that when methanol was used, the composition of the precipitate was $Li_2O_2{\cdot}H_2O_2{\cdot}3H_2O{\cdot}8CH_3OH$ indicating that the water molecules were not dislodged by methanol. As indicated in Section 0, the relative permittivity of methanol is higher than for ethanol and 1-propanol. Therefore, with a decrease in relative permittivity, the dissociation of the $Li_2O_2{\cdot}H_2O_2{\cdot}3H_2O$ was more difficult with the result that it remained undissociated.

In general and depending on the kind of alcohol and its concentration, all or part of the water molecules attached to a dissolved salt were detached and replaced by alcohol molecules. However, here it was found that the alcohols used were not able to dislodge all the water molecules from lithium hydroperoxidate trihydrate, $Li_2O_2{\cdot}H_2O_2{\cdot}3H_2O$ meaning that the interaction between water and lithium hydroperoxidate, $Li_2O_2{\cdot}H_2O_2$, was stronger than between alcohol and the ligand of $Li_2O_2.H_2O$.

In practice, the number of alcohol molecules attached to the ions of a solute depends on the solvation number of the cation dissolved in the alcohol. The solvation numbers of the lithium cation in methanol, ethanol and 1-propanol are 8, 6 and 8, respectively [72]. As mentioned before, when LiOH is dissolved in methanol, it is mostly molecular and only part of the $LiOH.H_2O$ is ionized. It is thought that the presence of water in the system, in this instance from the $LiOH.H_2O$ and from the $H_2O_2{\cdot}3.5H_2O$, is the cause of the ionization.

The number of alcohol molecules attached to the precipitate when using methanol and ethanol was identical to the solvation number of lithium cation in these alcohols, whereas for 1-propanol, the number of propanol molecules was 11. This suggests that there was not a simple relationship because the number of 1-propanol molecules attached was not in agreement with the solvation numbers of lithium cations in 1-propanol. An explanation of a possible correlation between the number of alcohol molecules attached to the precipitate

in methanol and ethanol with the solvation number of lithium cations in each of these alcohols would require a further investigation and was considered beyond the scope of the present investigation.

10.3.4 Reactions involving the use of 50 wt% hydrogen peroxide ($H_2O_2.1.9H_2O$)

The tests using H_2O_2 (50 %wt) found that the molar amount of hydrogen peroxide required to produce lithium peroxide was 2 times more than the stoichiometric value (Figure 34). The efficiencies of Li_2O_2 production using H_2O_2 50 %wt in comparison to H_2O_2 35 %wt, at the same ratio, 1:1 = H_2O_2:$LiOH.H_2O$, were 95.9% and 93.6%, respectively. The average increase in the efficiency due to using H_2O_2 50 %wt, was 1.8%. The higher efficiency of Li_2O_2 produced using H_2O_2 (50 %wt) was due to the lower water content from the hydrogen peroxide solution.

Moreover, using H_2O_2 50 %wt resulted in a change in the precipitate composition. The product of the conversion reaction using H_2O_2 50 %wt ($H_2O_2 \cdot 1.9H_2O$) was lithium hydroperoxidate dihydrate $Li_2O_2 \cdot H_2O_2 \cdot 2H_2O$. Similarly, the literature indicates that in an aqueous system, over the concentration range of H_2O_2 from 40 to 58 wt%, this is the expected product [85]. The formation of this compound showed that the concentration of the added hydrogen peroxide, i.e., hydrogen peroxide activity, is a major factor in the precipitate composition.

10.3.5 Effect of using LiOH with 35 wt% hydrogen peroxide

In the tests using LiOH instead of $LiOH.H_2O$, the efficiency was slightly increased as the ratio of H_2O_2:$LiOH.H_2O$ was increased from 0.5 to 0.7 (Figure 37). At higher ratios, the efficiency was similar to those obtained for $LiOH.H_2O$. This increase indicated that the lower water content in the system, a reduction equal to 22 wt%, resulted in a higher H_2O_2 activity. As the water content was increased for H_2O_2:$LiOH.H_2O$ ratios above 0.7, the solubility of the product in the methanol increased. Consequently, the efficiency of the conversion reaction approached values equal to those obtained with $LiOH.H_2O$.

10.3.6 Effect of temperature on conversion

In conversion tests where temperature was a variable, it was found that as the temperature increased, the efficiency of Li_2O_2 produced was decreased (Figure 38). The decline in efficiency as the temperature increased was attributed to (i) an increase in hydrogen peroxide decomposition, (ii) a lowering of the tendency for the exothermic reaction of conversion to occur, (iii) a promoting of the decomposition of the precipitate and (iv) a decrease in the solubility of LiOH in methanol.

As mentioned, the rate of hydrogen peroxide decomposition increased as the temperature of the solution increased. It was found that the rate doubled with an increase of 5 °C of the solution from ambient conditions. Therefore, for the fixed addition of $LiOH.H_2O$, an elevated temperature of solution required more hydrogen peroxide for the conversion reaction. In addition, the reaction of $LiOH.H_2O$ with H_2O_2 was exothermic, thus, at elevated temperature the conversion reaction was offset toward the reactants thereby causing lower efficiency.

The XRD results of the product showed that it was contaminated with LiOH as temperature increased. This can be explained as follows. As the temperature increased, the precipitate, $Li_2O_2{\cdot}H_2O_2{\cdot}3H_2O{\cdot}8CH_3OH$, was decomposed to LiOH. Since at higher temperature the solubility of LiOH in methanol decreased, the product was contaminated by LiOH precipitation.

10.3.7 Using excess additions of $LiOH.H_2O$

The results of conversion using the solutions with a fixed ratio (H_2O_2:$LiOH.H_2O$ equal to 1:1) showed that as the amount of $LiOH.H_2O$ added to the methanol increased, the efficiency of Li_2O_2 production decreased (Figure 40). The decrease in the efficiency was attributed to LiOH contamination of the precipitate. Up to an addition of 21.6 g $LiOH.H_2O$ to 100 g CH_3OH, the product was pure Li_2O_2. Above this concentration, contamination with LiOH occurred.

As previously explained, the conversion reaction did not occur completely; some unreacted LiOH always remained in the solution or was precipitated with the product. As the concentration of $LiOH.H_2O$ increased, more of the unreacted LiOH was present in the solution. In addition, the short times of conversion of about 15 min, did not allow the unreacted LiOH to dissolve in the methanol, and therefore, it precipitated with the product.

10.4 Prediction of the products of reaction between $LiOH.H_2O$ and H_2O_2

10.4.1 Mass and mole constraints in the present experiments

It was assumed that the products of reaction between lithium hydroxide, hydrogen peroxide in aqueous solution and an alcohol, using methanol as an example, can be represented by Equation 77 below. The equilibrium constant (also the so-called "solubility product") can be expressed as:

$$K = [K_{sp}] = [\, a_{CH_3OH}^{(P_2-R_3)} \cdot a_{H_2O}^{(P_3-tR_2)} \cdot a_{H_2O_2}^{(P_4-R_2)} \cdot a_{LiOH.H_2O}^{(P_5-R_1)} \,] \qquad (77)$$

Clearly, the challenge was to determine the values of R_1 to R_3 and of P_1 to P_5. Such determination from the present experiments was complicated by the fact that, for each of the components in the product raffinate, its activity can be represented by the product of an activity coefficient and a molar concentration, thus:

$$K = [K_{sp}] = [\, \gamma_{CH_3OH}^{(P_2-R_3)} \chi_{CH_3OH}^{(P_2-R_3)} \cdot \gamma_{H_2O_2}^{(P_3-tR_2)} \chi_{H_2O_2}^{(P_3-tR_2)} \cdot \gamma_{H_2O}^{(P_4-R_2)} \chi_{H_2O}^{(P_4-R_2)} \cdot \gamma_{LiOH.H_2O}^{(P_5-R_1)} \chi_{LiOH.H_2O}^{(P_5-R_1)} \,] \qquad (78)$$

The task at hand was then to examine the experimental data and to thermodynamically relate the component activities, or express the thermodynamic properties in ways that simplify the analysis. By this means, the number of unknowns would not be reduced, but the constraints could be related to values for the unknowns.

It should be noted that the set of values for the unknowns mentioned above would normally be called a solution. Thus, it could be said that we are "finding a solution for each of the solutions". The reader is cautioned to carefully note each use of the word solution in the following discussion.

A complete solution (thermodynamic and mathematical) for the present system would involve first identifying and then solving the necessary equations that would fully define the system for each alcohol.

By assuming that the water and methanol behave ideally, it was possible to ignore their activity coefficients in the solution represented by the right-hand side of Equation 78 and further extend the mathematical solution.

10.4.2 Values of the unknowns from mass constraints calculated from the experimental results

1. Lithium mass balance: Stoichiometrically, in order to produce one mole of lithium peroxide, two moles lithium hydroxide monohydrate was required. From Section 9.3.1 and 9.3.3, the relationship between the moles of lithium peroxide produced, P_1, and the moles of hydrogen peroxide, R_2/R_1 moles of H_2O_2 per mole of $LiOH.H_2O$ reacted is described by the following equations:

$$P_1 = -0.589 \times (R_2/R_1)^2 + 1.535 \times (R_2/R_1) \qquad (H_2O_2\ 35\ \%wt) \qquad (79)$$

$$P_1 = -0.687 \times (R_2/R_1)^2 + 1.669 \times (R_2/R_1) \qquad (H_2O_2\ 50\ \%wt) \qquad (80)$$

   The Equations of 70 and 80 were extracted from the curve fit equations Figure 31and Figure 34, respectively. When hydrogen peroxide 35 %wt was used, the maximum efficiency of the lithium peroxide production was only 0.95. In addition, the chemical analysis showed that about 0.05 mole per mole of lithium in the reactant material, $LiOH.H_2O$, was present in the raffinate as LiOH. Therefore, P_5^* can be taken as $0.05P_1$.

2. Methanol mass constraint: The mass of methanol was predetermined by using a solution whose concentration was near the solubility of $LiOH.H_2O$ in methanol, i.e., 13.5 g $LiOH.H_2O$/100 g CH_3OH. Therefore, for two moles of $LiOH.H_2O$ (R_1) as the feed material, about 20 moles of CH_3OH (R_3) were required, i.e., (R_1/R_3) was equal to 1/10.

3. Hydrogen peroxide consumption: The required amount of hydrogen peroxide, R_2, was determined by using variable masses of H_2O_2 (35 %wt) with fixed masses of $LiOH.H_2O$ and CH_3OH. The mass formula of the commercial H_2O_2 (35 %wt) and H_2O_2 (50 %wt) used in this work was changed to a molar formula for convenience. As such, the value of t defines the moles of water in the hydrogen peroxide solution in Equation 81:

$$t = \frac{M_h \times (100 - w_h)}{M_w \times w_h} = \frac{34.02 \times (100 - w_h)}{18.02 \times w_h} \quad (81)$$

where M_h is the hydrogen peroxide molecular weight, M_w is the water molecular weight and w_h is the weight percent H_2O_2. Thus, t was found to be to 3.506 and 1.89 for 35 wt% and 50 wt% hydrogen peroxide, respectively.

As indicated in Section 9.3.1, in order to produce 0.95 mole of lithium peroxide, 1.3 mole of $H_2O_2 \cdot 3.5H_2O$ was required. Therefore, R_2 equals at least $1.2R_1$ (0.95×1.3).

However, the precipitate involved hydrogen peroxide in such a way that one mole of the reacted hydrogen peroxide was transformed to lithium peroxide and one mole was attached to lithium peroxide and precipitated. Thus, in Reaction 72, R_2 equals $(1.2 + 1)R_1$.

4. Composition of the precipitate: It was found that lithium peroxide was not formed directly. Indeed, the reaction of hydrogen peroxide with the lithium hydroxide monohydrate initially formed lithium hydroperoxidate n-hydrate. Due to the presence of alcohol in the system, the precipitate that was produced also contained the methanol adducts. The compound is represented here with three variables: the moles of the hydrogen peroxide, x, the water, y, and the methanol, z.

The exponent of the water activity in Equation 77 for the precipitate, y, was dependent on the concentration of the reacted hydrogen peroxide. When either $H_2O_2.3.5H_2O$ (35 %wt) or $H_2O_2.1.89H_2O_2$ (50 %wt) was used, the numbers of the water activity in Equation 77, y, was 3 or 2, respectively, i.e.:

$$y = 0.62 \times t + 0.83 \quad (82)$$

In addition, the number of alcohol molecules attached to $Li_2O_2 \cdot H_2O_2 \cdot 3H_2O$ was determined by the analysis of the precipitate. The number of alcohol molecules was found to be equal to 8, 6 and 11 when methanol, ethanol and 1-propanol were used, respectively.

5. Composition of the raffinate: The raffinate was found to contain H_2O_2, H_2O, CH_3OH and $LiOH.H_2O$. The composition of raffinate was determined by chemical analysis of the solution. Due to the reaction of $LiOH.H_2O$ with H_2O_2, H_2O_2 was decomposed and for one mole of the reacted hydrogen peroxide, two moles water were formed:

$$2\ LiOH + H_2O_2 \rightarrow Li_2O_2 + 2\ H_2O \quad (83)$$

In addition, it was found that when the ratio of H_2O_2:$LiOH.H_2O$ exceeded 2, the content of hydrogen peroxide in the raffinate increased accordingly. Therefore, if R_2 is 2, P_4 would be 0 and if R_2 is 2.2, P_4 would be 0.2.

10.4.3 Mass balance equations

The following summarizes the equations that were used to solve the present mass balance for the reaction of $LiOH.H_2O$ with $H_2O_2 \cdot nH_2O$ and CH_3OH to yield Li_2O_2:

i) $R_1 = 2$

ii) $R_2 = 2.6$ $|H_2O_2 \cdot 3.5H_2O$

$R_2 = 2.1$ $|H_2O_2 \cdot 1.89H_2O$

iii) $t = 3.5$ $|H_2O_2 \cdot 3.5H_2O$

$t = 1.89$ $|H_2O_2 \cdot 1.89H_2O$

iv) $R_3 = 20$

v) $P_1 = -0.589 \times (R_2/R_1)^2 + 1.535 \times (R_2/R_1)$ |Methanol and $H_2O_2 \cdot 3.5H_2O$

$$P_1 = -0.687 \times (R_2/R_1)^2 + 1.669 \times (R_2/R_1) \text{ |Methanol and } H_2O_2 \cdot 1.89H_2O$$

$$P_1 = -0.539 \times (R_2/R_1)^2 + 1.17 \times (R_2/R_1) \text{ |Ethanol and } H_2O_2 \cdot 3.5H_2O$$

$$P_1 = -0.038 \times (R_2/R_1)^3 + 0.904 \times (R_2/R_1)^2 \text{ |Propanol and } H_2O_2 \cdot 3.5H_2O$$

vi) $x = 1$

vii) $y = 0.62 \times t + 0.83$

viii) $z = 8$ |Methanol ($z = 6$|Ethanol, $z = 11$|Propanol)

ix) $P_2 = R_3 - z \times P_1$

x) $P_3 = R_1 + R_2 + t \times R_2 - y \times P_1 - R_4 - R_5$

xi) $P_4 = R_2 - R_2 \times P_1$

xii) $P_5 = R_1 - R_1 \times P_1$

In order to demonstrate the relationships between the precipitate and raffinate, the contents of each component in the two phases were normalized to exclude the content of methanol (or alcohol) in each phase. Thus, it was possible to plot the relationships between the two phases; the precipitate and the raffinate, in a ternary phase diagram for the system: Li_2O-H_2O-O. In case of plotting methanol along with other three components of Li_2O, H_2O and O, a triangular pyramid can be hypothesized.

It should be mentioned that the area studied was limited by the constraints imposed by the mass balance equations presented above. For instance, at amounts of hydrogen peroxide 35 wt% (R_2) above 2.5 mole per mole of $LiOH.H_2O$, the precipitate with the composition of $Li_2O_2 \cdot H_2O_2 \cdot 3H_2O \cdot 8CH_3OH$ was found to be no longer stable.

Figure 70 shows the relationship between the composition of the precipitate and the raffinate using the equations above for hydrogen peroxide 35 %wt. Note that the composition of the precipitate was $Li_2O_2 \cdot H_2O_2 \cdot 3H_2O \cdot 8CH_3OH$. The corresponding composition of the raffinate in equilibrium with the precipitate was plotted against the change for hydrogen peroxide. By connecting the compositions of raffinate (shown by

symbols) as function of hydrogen peroxide content, the composition of raffinate can be plotted a solid line staring from $LiOH.H_2O$ then reaching pure H_2O.

The boundary of $LiOH.H_2O$-H_2O suggests that, first; the relationship between $LiOH.H_2O$, H_2O_2 and the product was not ideal, second, the composition of the raffinate in equilibrium with the precipitate changes as function of hydrogen peroxide concentration in reactant. The maximum amount of lithium peroxide produced occurred when the concentration of hydrogen peroxide in the raffinate was zero. As more hydrogen peroxide was added, $LiOH.H_2O$ appeared in the raffinate. With further increase of the hydrogen peroxide, the precipitate with the composition of $Li_2O_2 \cdot H_2O_2 \cdot 3H_2O \cdot 8CH_3OH$ was no longer stable and decomposed.

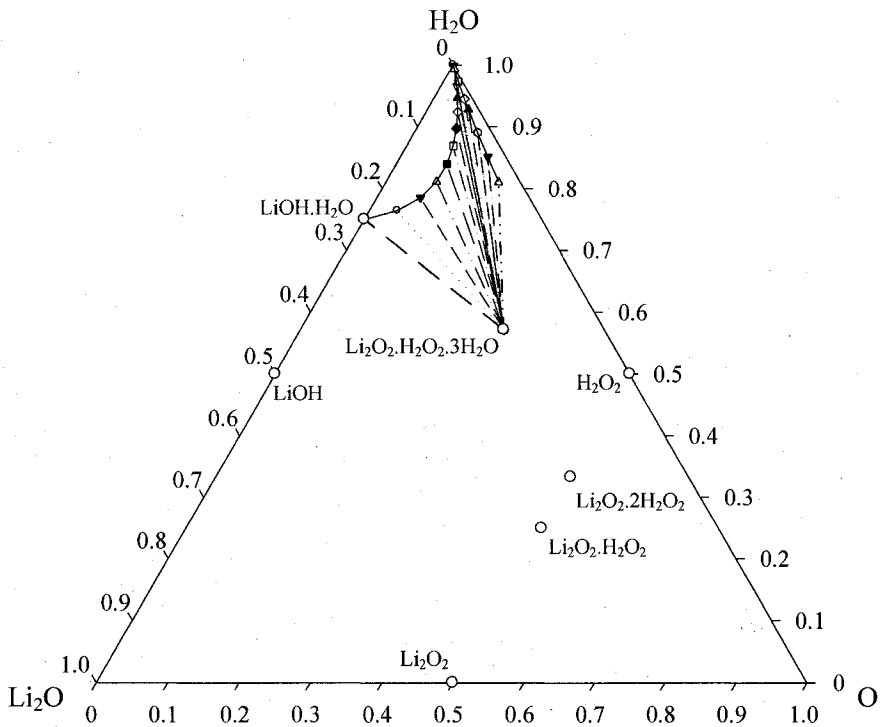

Figure 70: Equilibrium between the precipitate and the raffinate in the system Li_2O-H_2O-O at 20 °C using $H_2O_2 \cdot 3.5H_2O$ (H_2O_2 35 %wt). Data are in mole fraction.

Figure 71 shows the equilibrium between the precipitate and the raffinate using the equations above and increments in added amounts of hydrogen peroxide 50 %wt. As explained, when hydrogen peroxide 50 %wt was used, the composition of the precipitate was $Li_2O_2 \cdot H_2O_2 \cdot 2H_2O \cdot 8CH_3OH$.

Figure 71 illustrates a comparison between the raffinate composition, which contains $LiOH.H_2O$, H_2O_2 and H_2O. It can be seen that the stability region changed as the concentration of hydrogen peroxide was changed. Although the amount of water in the reactants was decreased by using hydrogen peroxide 50 wt%, the water content in the product raffinate was approximately the same. The reason was that the precipitate had lower water content when hydrogen peroxide 50 wt% was used.

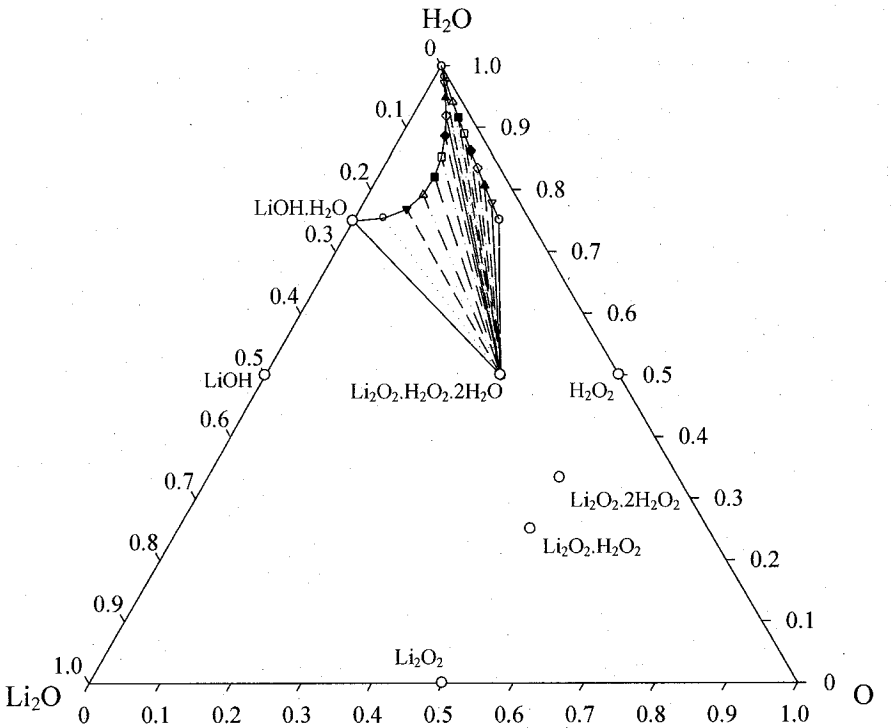

Figure 71: Equilibrium between the precipitate and the raffinate in the system Li_2O-H_2O-O at 20 °C using $H_2O_2 \cdot 1.89H_2O$ (H_2O_2 50 %wt). Data are in mole fraction.

Figure 72 shows a comparison between changes of the composition of the raffinate for the use of hydrogen peroxide 35 wt% and 50 wt%.

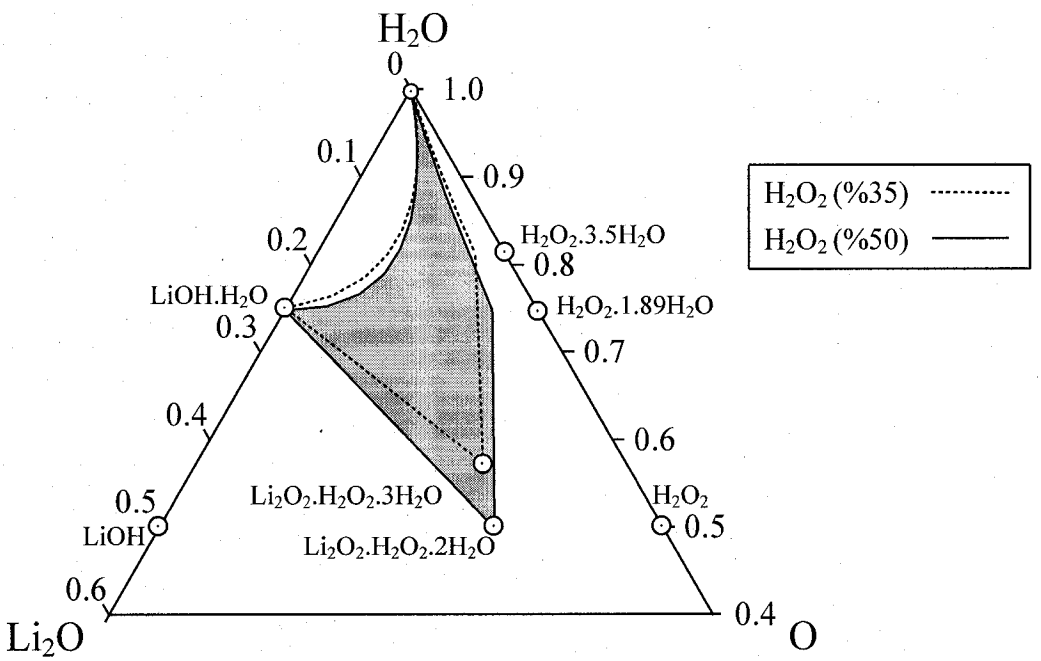

Figure 72: The composition of the raffinate in the system Li_2O-H_2O-O at 20 °C using H_2O_2 35 wt% ..... and H_2O_2 50 wt% _____. Data are in mole fraction.

Putting all the values together with the proposed reaction, the overall reaction for the conversion of $LiOH.H_2O$ using H_2O_2 (35 %wt) can be represented by Reaction 84:

$$2\ LiOH.H_2O + 20\ CH_3OH + 2.2\ (H_2O_2{\cdot}3.5\ H_2O) \rightarrow 0.95\ [Li_2O_2{\cdot}H_2O_2{\cdot}3H_2O{\cdot}8CH_3OH]_{prec.} + [12.4\ CH_3OH + 8.65\ H_2O + 0.3\ H_2O_2 + 0.1\ LiOH.H_2O]_{raffinate} \quad (84)$$

When using $H_2O_2{\cdot}1.9H_2O$, the overall reaction was:

$$2\ LiOH.H_2O + 20\ CH_3OH + 2.1\ (H_2O_2{\cdot}1.9\ H_2O) \rightarrow 0.97\ [Li_2O_2{\cdot}H_2O_2{\cdot}2H_2O{\cdot}8CH_3OH]_{prec.} + [12.24\ CH_3OH + 5.91\ H_2O + 0.16\ H_2O_2 + 0.06\ LiOH.H_2O]_{raffinate} \quad (85)$$

Figure 73 shows the solutions of the sets of equations for each of the alcohols studied. It can be seen that in agreement with the experimental results, the composition of the raffinate changed as the kind of alcohol varied. For ethanol and 1-propanol, the precipitate was always in equilibrium with a large amounts of $LiOH.H_2O$ dissolved in the raffinate. As presented in Section 8.4.4, the efficiency of the lithium peroxide produced in ethanol and 1-propanol never increased beyond 70 %. As it can be seen from Figure 73, for

ethanol and propanol, the lithium hydroxide always presented in the raffinate over the total concentration of hydrogen peroxide.

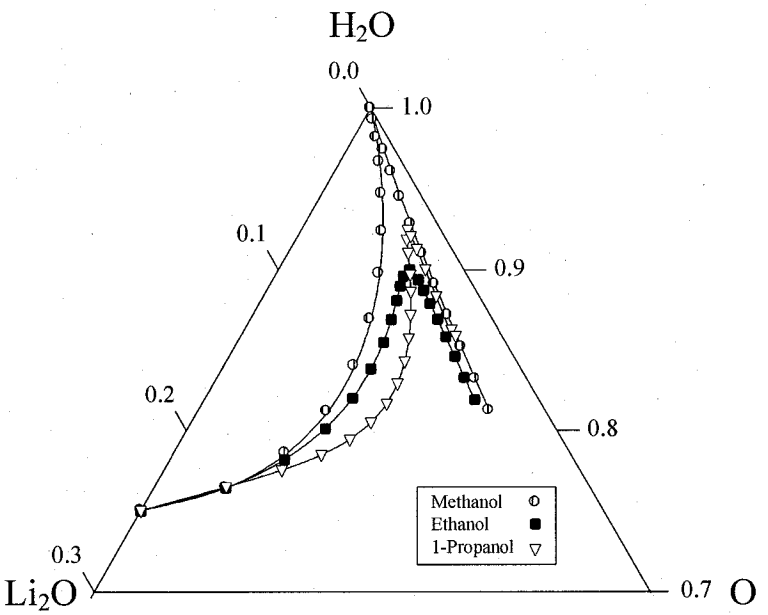

Figure 73: Composition of the raffinate in the system Li_2O-H_2O-O different alcohol at 20 °C using $H_2O_2 \cdot 3.5H_2O$ (H_2O_2 35 %wt). Data are in mole fraction.

10.4.4 Measurement of the activity coefficients in non-ideal conditions

The following section presents an outline for a proposed approach for determining the activity coefficients of species in a complex solution.

According to the literature survey, no model has been found which can predict or explain a system that contains two salts and three solvents (aqueous-electrolyte-alcohol), i.e., the present pentanary Li_2O_2-LiOH-CH_3OH-H_2O_2-H_2O system. However, some works have presented a thermodynamic study of the ternary systems. [86-88].

An explanation of the behavior of cations or anions in a mixed aqueous-organic system is believed to be very complicated due to the influence of many parameters on the solubility of cations or anions in the equilibrium between solid-liquid, gas-liquid and liquid-liquid. In addition, hydrolysis in this system, i.e., solvation of ions (alkolysis), and precipitation by the organic solvent can occur. Moreover, it is essential to know whether the salt(s) is(are) ionized or remain non-ionized in each solvent, e.g., does lithium hydroxide

monohydrate dissociate to a large extent in water to form cations and anions, whereas in methanol is it largely solvated by methanol molecules without ionization.

Some of these reactions (interactions) can be measured or predicted in a simple system, i.e., one solvent and one salt. However, in a system like the present one which contains two salts ($LiOH.H_2O$ and Li_2O_2) and three solvents (CH_3OH, H_2O and H_2O_2), the prediction of the compounds which are precipitated or remain soluble is impossible at this time. The determination of ion-ion interaction parameters in mixed solvents would require experimental measurements for mixtures containing the two solvents.

Another challenge arises either from a lack of thermodynamic data or from a lack of knowledge about the kind of compounds formed. For example, this study found that the composition of the precipitate was $Li_2O_2 \cdot H_2O_2 \cdot 3H_2O \cdot 8CH_3OH$. As the number of components in the system increases, the thermodynamical properties can be predicted only if some assumptions are made. In order to alleviate the complexity of the system, the analysis may be simplified by not taking into account the hydration or solvation of the anions due to their larger size in comparison to that of the cations. Indeed the interactions between anions and solvent (polar or nonpolar) involve stronger ion-dipole forces, with the result that the bonds between anions-solvent are not as dissociated as compared to that of the cations [86].

The activity coefficients of water, hydrogen peroxide and methanol in the raffinate solution are likely to depend strongly on the salt concentration and not be ideal as assumed.

Furthermore, regardless of the solvent, taking the standard state for the ionic species, Li, as a hypothetical ideal dilute solution in water at the system temperature and pressure, that is:

$$\gamma_{Li} \rightarrow 1, \text{ at } \chi_{Li} \rightarrow 0 \text{ and } \chi_{H_2O} \rightarrow 1 \qquad (86)$$

assumes that the solution contains the following molecular and ionic species: free water (H_2O) and alcohol molecules (CH_3OH), free cations (Li^+) and anions (OH^-), hydrated cations ($Li(H_2O)_4^+$) and solvated cations ($Li(CH_3OH)_8^+$).

The chemical reactions occurring in the solution would then be represented as follows:

$$Li^+ + 4H_2O = Li(H_2O)_4^+ \quad (87)$$

$$Li^+ + 8CH_3OH = Li(CH_3OH)_8^+ \quad (88)$$

$$2Li^+ + H_2O_2 + 3H_2O = Li_2O_2 \cdot H_2O_2(H_2O)_3^+ \quad (89)$$

The corresponding equilibrium constants would be given by:

$$K_w = \frac{a_{Li(H_2O)_4^+}}{a_{Li^+}(a_{H_2O})^4} \quad (90)$$

$$K_s = \frac{a_{Li(CH_3OH)_8^+}}{a_{Li^+}(a_{CH_3OH})^8} \quad (91)$$

$$K_h = \frac{a_{Li_2O_2 \cdot H_2O_2 \cdot (H_2O)_3^+}}{a_{Li^+} a_{H_2O_2} (a_{H_2O})^3} \quad (92)$$

where K_w, K_s and K_h are the equilibrium constants, a_{Li^+} represents the activity of the species, Li^+.

Equations 90 to 92 along with the material balance equations allow one to calculate the concentrations of various species in the raffinate solution of a given overall composition, provided the equilibrium constants K_w, K_s and K_h, the hydration and the solvation numbers w, s and h, and expressions for calculating the activity coefficients are available.

The standard state for water and alcohol is most commonly taken as the pure liquid at the system temperature and pressure. Activity coefficients for components can be obtained from the dependency of their excess partial Gibbs energy on the composition. Excess partial Gibbs energy is assumed to derive from three terms, one of which results from short-range (SR) interactions (i.e., physical forces, solvation phenomena between solvent ions), and the other two resulting from long-range (LR) ion-ion electrostatic interactions. Thus the excess Gibbs energy can be expressed as:

$$g^{E} = g^{E}_{PDH} + g^{E}_{Born} + g^{E}_{UNIQAC} \quad (93)$$

The long-range contributions are represented by the Pitzer–Debye–Hückel expression (g^{E}_{PDH}) and the Born contribution (g^{E}_{Born}) which account for the change of the Gibbs energy associated with transferring the ionic species from a mixed-solvent reference state to an aqueous reference state. The short-range contribution (g^{E}_{UNIQAC}) is represented by the local composition UNIQUAC (universal quasichemcial theory) expression which represents the interactions between vapor–liquid equilibrium, solid–liquid equilibrium, liquid–liquid equilibrium.

The UNIQUAC equation is applicable to a wide variety of non-electrolyte liquid solutions containing nonpolar or polar fluids such as alcohols and water [86].

Non-ideality of the equilibrium mixture of the various species (water, alcohol, "free", hydrated and solvated ions) can be described using the UNIQUAC model and the extended form of the Debye–Hückel equation as proposed by Pitzer [88]. Special attention needs to be paid to self-consistency in the derivation of the activity coefficients equations taking into account the dependence of the solution properties (solution dielectric constant, density, and average molar mass of mixed solvent) on the solvent composition.

The activity coefficient of an electrolyte in solution is the combination of long-range interaction effects, γ_i^{PDH} and γ_i^{Born}, and short range interaction effect, $\gamma_i^{UNIQUAC}$, among the ions present and the solvent molecules [89]:

$$\ln \gamma_i = \ln \gamma_i^{PDH} + \ln \gamma_i^{Born} + \ln \gamma_i^{UNIQUAC} \quad (94)$$

γ_i^{PDH} is a function of electronic charge, temperature, ionic charge, mole fraction, of mixture and density of the mixture, γ_i^{Born} which is a function of the dielectric constant of volume fraction of the solution and $\gamma_i^{UNIQUAC}$ which is a function of the interaction parameters and the surface area of the solvents.

To determine γ_i^{PDH} for a system containing one solvent and one salt, four adjustable parameters are necessary. In practice, UNIQUAC parameters are related to the binary interaction energies at play between the water and the methanol and the hydrogen peroxide and the methanol in the raffinate [88]. At low salt concentrations, the long-range contribution is important, but as salt concentration rises, that contribution becomes increasingly small compared to the others. At intermediate and high salt concentrations, the chemical contribution is usually much more important than the physical contribution [90].

In order to predict the concentrations of cations and anions in a complex system like this work, the preliminary steps would start with determining the behaviors of components in the binary systems such as $LiOH.H_2O$-CH_3OH or Li_2O_2-CH_3OH. In each of these binary systems, the unknown parameters and the corresponding techniques for determining them are different, i.e., while the determination of the osmotic pressure in an organic-salt system is likely a common procedure, on the other hand, in an aqueous system, the measurement of solubility of salts can be used.

It can be concluded that in order to predict the solubility of components *apriori*, the approach for selection of the appropriate model and consequently the experimental method requires more investigation of the interactions among the nonaqueous-salt-aqueous system.

10.5 Decomposition of the precipitate

It was found that drying the precipitate under an unprotected atmosphere produced lithium peroxide containing impurities of lithium carbonate and lithium oxide. To determine the steps when the formation of lithium oxide or lithium carbonate are started required slow drying of the lithium peroxide at ambient temperature. The drying of the precipitate under atmospheric conditions was seen to occur via the following steps. First, methanol was quickly removed from $Li_2O_2 \cdot H_2O_2 \cdot 3H_2O \cdot 8CH_3OH$ forming $Li_2O_2 \cdot H_2O_2 \cdot 3H_2O$. During this step, neither Li_2CO_3 nor $LiOH$ was formed. This may have been due to the presence of the methanol attached to the $Li_2O_2 \cdot H_2O_2 \cdot 3H_2O$ molecules. Second, the simultaneous removal

of water and hydrogen peroxide from $Li_2O_2 \cdot H_2O_2 \cdot 3H_2O$ and its subsequent dissociation to LiOH occurred. During this step, Li_2CO_3 formed indicating that LiOH was converted to Li_2CO_3 by reaction with the ambient CO_2. Third, after the removal of water and hydrogen peroxide from $Li_2O_2 \cdot H_2O_2 \cdot 3H_2O$, the LiOH content in the precipitate gradually diminished.

The TGA analyses provided only limited information regarding the decomposition of the precipitate, $Li_2O_2 \cdot H_2O_2 \cdot 3H_2O \cdot 8CH_3OH$, because there was co-evolution of two or three compounds. In other words, the mass loss did not provide a trace of its decomposition. However, the TGA result did indicate that the total decomposition of the precipitate was finished at 184 °C. In addition, the DTA result indicated an endothermic reaction onset at 103 °C.

The study of the isothermal decomposition of the precipitate at 90 °C confirmed that the compounds attached to Li_2O_2 were sequentially removed. As expected, similar to drying at ambient temperature, methanol molecules were initially removed and during this removal the composition of $Li_2O_2 \cdot H_2O_2 \cdot 3H_2O$ remained intact. After the removal of attached methanol, the decomposition continued with the co-evolution of H_2O and H_2O_2 in a way that the compound lithium hydroperoxidate, $Li_2O_2 \cdot H_2O_2$, was not formed. This indicated that there are strong bonds between the H_2O and the H_2O_2 of $Li_2O_2 \cdot H_2O_2 \cdot 3H_2O$. These strong bonds could explain why methanol could not detach the water molecules from $Li_2O_2 \cdot H_2O_2 \cdot 3H_2O$ once it was formed.

The slowest rate of the decomposition belonged to the step of H_2O_2 removal from Li_2O_2. Even at temperature of 175 °C, for which the methanol and water removal occurred in the one step, the H_2O_2 removal proceeded slowly.

The vales of the parameters in the Arrhenius equation for the decomposition of $Li_2O_2 \cdot H_2O_2 \cdot 3H_2O \cdot 8CH_3OH$ were calculated from the results in Section 9.4.3 as Equation 95:

$$K = A\exp(\frac{-E}{RT}) = 6.6\times10^{12}\exp(\frac{-141080}{RT}) \qquad (95)$$

Here A is the pre-exponential factor, E is activation energy (kJ/mol), T is temperature (K) and R is the gas constant. Similarly the values of the parameters in the Arrhenius equation for the decomposition of $Li_2O_2 \cdot H_2O_2 \cdot 3H_2O$ were calculated as given in Equation 96.

$$K = A\exp(\frac{-E}{RT}) = 167\exp(\frac{-43855}{RT}) \qquad (96)$$

The higher activation energy for the decomposition reaction of $Li_2O_2 \cdot H_2O_2 \cdot 3H_2O$, 43.8 kJ/mol suggests that the H_2O_2 and H_2O have strong bonds with Li_2O_2. This also indicates that the bonds between H_2O and H_2O_2 in the $Li_2O_2 \cdot H_2O_2 \cdot 3H_2O$ can be covalent, and that the water in $Li_2O_2 \cdot H_2O_2 \cdot 3H_2O$ is not an adduct molecule similar to the CH_3OH.

10.6 Lithium oxide formation

The analysis of the DTA results for lithium oxide formation from lithium peroxide found that they were consistent with the TGA results for lithium peroxide decomposition. A strong endothermic onset was observed at 324 °C that corresponded to the loss of active oxygen[xxiii]. After this endothermic reaction, no more thermal effects were observed. Other than the endothermic reactions at onsets 258 °C and 324 °C, the other thermal effects which were reported by Rode [41], such as an exothermic reaction onset at 225 °C (α to β transformation of Li_2O_2) and at 495 to 510 °C (crystallization of lithium oxide) were not observed. Rode's findings can be attributed to the presence of impurities such as LiOH and Li_2CO_3 as solid solutions of LiOH-Li_2O_2 and Li_2CO_3-Li_2O_2.

The isothermal decomposition of Li_2O_2, Section 10.6, showed that lithium peroxide was very reactive at elevated temperatures in ambient atmosphere and partially converted to LiOH. Even in a nitrogen atmosphere, which contained only a very small amount, about 0.1-0.2 v/v% H_2O vapor, lithium peroxide was still reactive and the final product contained about 0.15 mole fraction LiOH (Figure 50). In order to determine the source LiOH formation, pure Li_2O was heated in a nitrogen atmosphere at 400 °C. This test found

[xxiii] As explained, in Section 5.2, the active oxygen is referred to a single molecule of oxygen with covalent bond with other oxygen atoms having the oxidation state of –1.

that lithium oxide was stable at this condition and the formation of LiOH during heating Li_2O_2 was due to the reaction of Li_2O_2 with H_2O from atmosphere (Figure 54). Because of the high reactivity of Li_2O_2 at elevated temperatures, a controlled atmosphere having very little or no water vapor, or preferably vacuum, would be required in a commercial operation to transform Li_2O_2 to Li_2O.

The analysis of the TGA results for Li_2O_2 decomposition found that the reaction was completed in two steps (Figure 56). The mass loss for all samples in the first step of decomposition, in which the major active oxygen loss occurred, started at the same temperature. The second step of decomposition involved a wide range of observed mass losses varying with each sample. The reasons for the occurrence of two-step decomposition can be explained as two different mechanisms:

First, rapid decomposition of lithium peroxide occurred and the majority of the active oxygen was lost. The decomposition reaction was hindered by the gradual slow diffusion of the oxygen gas absorbed on, or trapped within, the lithium oxide layer. This is similar to the decomposition of SrO_2 described in reference [91].

Second, lithium peroxide was partially decomposed and Li_2O was formed. The layer of Li_2O that formed hindered the further conversion and acted as a barrier to heat transfer to the core. In addition and following the formation of Li_2O, the heat transfer to the core was impeded by the crystallization of the amorphous lithium oxide. Such processes have been suggested in the decomposition of BaO_2 to BaO where following heat absorption, the recrystallization of BaO occurs [92]. A schematic of the decomposition process considering the two alternative mechanisms (a→b→d and a→c→d) is presented in Figure 74.

The results of heating Li_2O_2 in an Ar atmosphere at 400 °C (the experiments described in Section 8.6.1) indicated that Li_2O_2 was quickly converted to Li_2O and no un-reacted Li_2O_2 was found in the samples. In addition, the analysis of the DTA results confirmed that after an endothermic reaction with an onset at 324 °C, which correlates to the decomposition of Li_2O_2, no more endothermic reactions (which would represent a further conversion of

Li_2O_2) occurred. Therefore, the first mechanism, which involves the two-step decomposition, would better describe lithium peroxide decomposition.

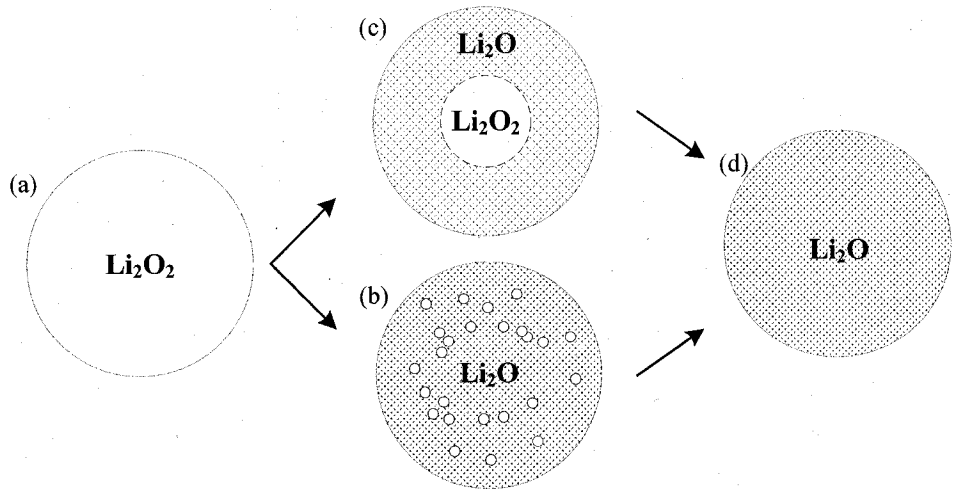

Figure 74: Schematic of the decomposition of Li_2O_2, a) pure Li_2O_2, b) decomposition with trapped O_2 gas, c) partial decomposition with unreacted Li_2O_2 in the core, and d) 100% decomposition.

10.7 Kinetics of lithium peroxide decomposition

The non-isothermal decomposition of Li_2O_2 was found to obey first-order kinetics at temperatures below 350 °C. Although the kinetics deviated from first-order behavior above 350 °C, this was explained in terms of diffusion resistance of the Li_2O ash layer. The calculated values of the activation energy for lithium peroxide decomposition did not depend strongly on the value of n in the range of fractional decomposition, α, from 0.8 to 1.0 (Figure 62). Since the mechanism of decomposition of Li_2O_2 becomes complex beyond α greater than 0.8 because of starting of evolving of atomic oxygen, the analysis of the kinetic data was restricted to the range of α from 0 to 0.8. The average of activation energy for the range of $0 < \alpha < 0.8$ was calculated as 201 ± 9.5 kJ/mol.

Among the numerous TGA experiments performed, Sample 4 was the only sample that exhibited a change in the slope of the curve. Generally this kind of behavior is referred to as an occurrence of overlap reactions and/or the formation of a solid solution compound (Figure 57) [93]. Tsentsiper [44] reported the formation of Li_2O_2-Li_2O solid solution at 50% conversion of lithium peroxide. As mentioned, in the experiment of the isothermal

decomposition of lithium peroxide at 400 °C in Ar, no unreacted lithium peroxide was found. In addition, it was found that lithium peroxide was very reactive under ambient conditions and in particular at elevated temperatures where it converted to LiOH. Therefore, the behavior of Sample 4, which can be seen as being similar to Tsentsiper's findings, was attributed to the contamination of Li_2O_2 by Li_2CO_3 and LiOH rather than the formation of the compound of $Li_2O_2.Li_2O$. The contamination occurred due to reaction of Li_2O_2 with CO_2 and H_2O in the air before or during the experiment.

It was found that the particle size of lithium peroxide influenced the activation energy of its decomposition. As shown in Table 29, the activation energies of lithium peroxide decomposition for particle sizes of 212 μm and 56 μm were 203.1 ± 7.6 and 98.2 ± 6.5 kJ/mol, respectively. This demonstrated that for the smaller particle sizes, the decomposition of lithium peroxide became easier. However, the non-isothermal analysis of lithium peroxide using samples with different particle sizes did not provide an explanation of the effect of the particle size. Indeed, even in the experiments using the same particle size, consistent behavior was not observed. Therefore, although an increase in the particle size of the sample might increase the activation energy, the differences in the measured activation energy of two particle sizes examined cannot be attributed only to the effect of particle size.

11. Conclusions and Findings

1. The experiments examining the reactivity of Li_2O_2 and Li_2O in ambient air found that lithium peroxide is more reactive than lithium oxide. Both compounds were increasingly carbonated as the humidity of the air increased at a fixed time of exposure.

   In the absence of moisture in the atmosphere, the reaction of Li_2O_2 with CO_2 was immeasurably slow. In the presence of humidity, the Li_2O_2 or the Li_2O initially formed LiOH. The lithium hydroxide then quickly converted to Li_2CO_3 by reaction with CO_2. The structure of Li_2CO_3 formed from Li_2O_2 was dense and amorphous but that formed from Li_2O was crystalline. The rate of the conversion of lithium peroxide and lithium oxide to Li_2CO_3 was found to be controlled by diffusion through the ash layer.

2. The measurement of the solubility of lithium compounds in alcohols found that methanol had highest solubility for lithium compounds. Methanol having the higher relative permittivity had more solubility for lithium hydroxide monohydrate than ethanol and 1-propanol. The high solubility of $LiOH.H_2O$ in methanol (13.6 g $LiOH.H_2O$ per 100 ml CH_3OH) and at the same time the low solubility of Li_2CO_3 and Li_2O_2 in methanol, indicated that methanol was the best option as a precipitation reagent for production of lithium peroxide among the alcohols tested.

   At the higher temperatures, the solubility of methanol for $LiOH.H_2O$ was decreased due to the exothermic nature of the dissolution reaction.

3. The conversion of $LiOH.H_2O$ to Li_2O_2 using H_2O_2 in an alcohol medium was due to the transfer of peroxide groups. The precipitation of Li_2O_2 was found to be exothermic and it involved the replacement of the water molecules adsorbed on the

dissolved lithium peroxide formed by reaction of the lithium hydroxide with the hydrogen peroxide by alcohol molecules.

4. Neither oxidation nor reduction reactions occurred during precipitation. The reaction was exothermic and the efficiency of the Li_2O_2 production decreased as the temperature increased.

5. The maximum production of lithium peroxide was 96.9% with the use of an excess amount H_2O_2 (35 %wt) equal 2.6 times the stoichiometric amount by mass. This was equivalent to a molar ratio of H_2O_2:$LiOH.H_2O$ equal 1.3.

6. The composition of the precipitate of the conversion reaction using H_2O_2 (35 %wt) was lithium hydroperoxidate trihydrate attached to an adduct of eight methanol molecules, i.e.: $Li_2O_2 \cdot H_2O_2 \cdot 3H_2O \cdot 8CH_3OH$.

   Using LiOH instead of $LiOH.H_2O$ and H_2O_2 (50 %wt) instead of H_2O_2 (35 %wt), increased the efficiency of Li_2O_2 production. By increasing the H_2O_2 concentration to 50 %wt, the composition of the precipitate changed to $Li_2O_2 \cdot H_2O_2 \cdot 2H_2O \cdot 8CH_3OH$. The contaminant decrease in the water activity in the system explained this result.

   The composition of the precipitates using ethanol and 1-propanol were $Li_2O_2 \cdot H_2O_2 \cdot 3H_2O \cdot 6CH_3CH_2OH$ and $Li_2O_2 \cdot H_2O_2 \cdot 3H_2O \cdot 11CH_3CH_2CH_2OH$, respectively.

7. The isolation of pure Li_2O_2 via the isothermal decomposition of the precipitate started with the gradual removal of methanol molecules. The decomposition then proceeded with co-evolution of H_2O and H_2O_2 from the resulting $Li_2O_2 \cdot H_2O_2 \cdot H_2O$. The removal of H_2O_2 from the final Li_2O_2 was the slowest step of the precipitate decomposition. The activation energies of the decomposition of $Li_2O_2 \cdot H_2O_2 \cdot 3H_2O \cdot 8CH_3OH$ and $Li_2O_2 \cdot H_2O_2 \cdot 3H_2O$, were 141 ± 5 and 48 ± 1kJ/mol, respectively at temperatures in the range from 125 to 175 °C.

8. The isothermal decomposition of Li_2O_2 in ambient atmosphere found that lithium peroxide was very reactive and partially converted to LiOH. In all TGA tests in argon,

the decomposition of lithium peroxide was completed in two steps. The suggested mechanism is the rapid decomposition of the lithium peroxide to lose the majority of the oxygen atoms, followed by the gradual slow diffusion of oxygen gas absorbed on, or trapped within, the lithium oxide.

9. The non-isothermal decomposition of Li_2O_2 to Li_2O obeyed first-order kinetics, although the kinetics deviated from first-order behavior above 350 °C. The deviation was explained in terms of diffusion resistance the product layer composed of Li_2O. Values of the activation energy of Li_2O_2 decomposition did not depend strongly on the degree of reaction in the range of the fractional decomposition, α, from 0.8 to 1.0. The average of the activation energy for the range of $0 < \alpha < 0.8$ was calculated as 201 ± 9 kJ/mol over the temperature range from 300 to 350 °C. The activation energy of lithium peroxide decomposition decreased as the particle size of sample decreased.

12. Contribution to Original Knowledge

1. It was the first time that the reactivity of lithium hydroxide and lithium peroxide in air was studied qualitatively and quantitatively. This study considered the effects of relative humidity and particle size. It was also an original study of the mechanism of the carbonation reaction.

2. It was the first time that the solubility of $LiOH.H_2O$, $LiOH$, Li_2O_2 and Li_2CO_3 in methanol, ethanol, 1-propanol and 1-propanol were measured. The effect of the temperature and the mixing time on the solubility of $LiOH.H_2O$ in methanol was determined.

3. The method for production of highly purity lithium peroxide using an alcohol medium and hydrogen peroxide was developed. It was the first time that lithium hydroxide monohydrate was used as feed in alcohol medium to produce lithium peroxide. The factors that led to improved efficiency were studied including the effects of hydrogen peroxide concentration, kind of alcohol, temperature, feed material and time of mixing.

4. It was the first time that the composition of the precipitates by reaction of lithium hydroperoxidate trihydrate with methanol, ethanol and 1-propanol were determined. It was also the first time that the isothermal decomposition of the precipitate, $Li_2O_2{\cdot}H_2O_2{\cdot}3H_2O{\cdot}8CH_3OH$, was studied. The activation energies of the decomposition of $Li_2O_2{\cdot}H_2O_2{\cdot}3H_2O{\cdot}8CH_3OH$ and $Li_2O_2{\cdot}H_2O_2{\cdot}3H_2O$ were measured for the first time.

5. The activation energy for lithium peroxide decomposition to high purity lithium peroxide was measured for the first time and the effect of particle size on activation energy was identified for the first time.

13. Future Work

1. When lithium peroxide and lithium oxide were exposed to air, they were initially converted to LiOH by reaction with H_2O followed by formation of Li_2CO_3 by reaction with CO_2. These two steps then continued concurrently. Experiments on pure LiOH, similar to the experiments in Section 8.2, would provide information about the mechanism of the reaction of lithium hydroxide with CO_2.

2. The structures of lithium carbonate formed by lithium peroxide and lithium oxide reacting with CO_2 were different. Further investigation to determine the reasons of the formation different structures of Li_2CO_3 would be useful.

3. In the proposed process of lithium peroxide production, the raffinate contained methanol and water. In order to recycle the methanol, the development of a method, such as partial distillation, for separation of methanol from water needs to be explored.

4. A combination of TGA tests and measurements of the oxygen evolved during the heating of Li_2O_2 might provide more details about the decomposition of Li_2O_2 to Li_2O. Further improvements in production of high purity lithium oxide could be obtained by applying vacuum and this warrants examination.

APPENDIX I: CALCULATION OF 95 % INTERVAL CONFIDENCE

Confidence limits for the mean are an interval estimate for the mean. Interval estimates are often desirable because the estimate of the mean varies form sample to sample. Instead of single estimate for the mean, a confidence interval generates a lower and upper limit for the mean. The interval estimate gives an indication of how much uncertainty there is in the estimate of the true mean. The narrower the interval, the more precise is the estimate.

Confidence limits are expressed in terms of a confidence coefficient. Although the choice of confidence coefficient is somewhat arbitrary, in practice 90%, 95%, and 99% intervals are often used, 95% being the most commonly used

The value for the 95% confidence interval was calculated according to Equation 97. The endpoints of the interval are given by [94, 95]:

$$s_{95\%} = \bar{x} \pm t(v,z)\frac{s}{\sqrt{n}} \qquad (97)$$

In Equation 1, $\bar{x}$ is the mean, s sample standard deviation, n number of samples and $t(v,z)$ is the t statistic for $v = n$-1 degrees of freedom and z = 1.96 standard normal percentile equivalent. The $t(v,z)$ returns the t-value of the t-distribution as a function of the probability and the degrees of freedom[xxiv]. In other words, v is probability associated with the t-distribution and z is the number of degrees of freedom with which to characterize the distribution.

---

xxiv In EXCEL software the function of TINV(probability,degrees_freedom) can be used to obtain t-value.

APPENDIX II: ACIDIMETRIC TITRATION FOR LITHIUM ANALYSIS

The assay of lithium in the samples was determined by acidimetric titration with hydrochloric acid, HCl. Since hydrochloric acid is highly hygroscopic, before titration of lithium, standardization of HCl was essential. Standard solutions of sodium hydroxide, NaOH, were used to standardize HCl as the titrant.

For titration, a potentiometric set-endpoint titrator manufactured by SCHOTT TitroLine[xxv] was used. The sample was hydrolyzed by distilled water to convert all forms of lithium compounds to lithium hydroxide. In particular, the lithium compounds such as Li_2O_2, Li_2O and lithium methoxide, $LiCH_3O$, are easily hydrolyzed by water and converted to LiOH.

Lithium hydroxide was then titrated with known normality HCl to a Phenolphthalein endpoint. The sample was pulled into a syringe. The syringe was sealed with a stopper and was weighed. Then, the sample in the syringe was carefully added to a beaker. The syringe was resealed and re-weighed to get the sample weight. Each time 5 ± 0.1 mL of sample was analyzed.

The weight percent of lithium was calculated according to Equation 98.

$$\text{Wt\% Li} = \frac{(\text{mL of HCl added})(N \text{ of HCl})(0.6941)}{(\text{Weight of sample in g})} \qquad (98)$$

To get the accurate results, attention was paid to prepare the titrant with the appropriate normality corresponding to the expected lithium concentration in solution samples. For each sample three titrations were performed. The standard deviation of a standard solution with the known lithium content by this method was ± 0.05 weight percent.

[xxv] TitroLine is a trademark for potentiometric supplied by SCHOTT.

APPENDIX III: ANALYTICAL METHOD FOR THE MEASUREMENT OF THE ACTIVE OXYGEN CONTENT

Titration is an accurate method for determining the amount or concentration of active oxygen. Permanganate ion is a powerful oxidizing agent, especially in acidic solutions. It can be used as titrant to analyze solutions/solids containing active oxygen[96]. Since solutions of $KMnO_4$ are readily crystallized thereby changing their normality, it is imperative that the permanganate potassium solution is standardized initially[97].

1. Standardization of $KMnO_4$

Potassium permanganate, $KMnO_4$, was standardized by its reaction with sodium oxalate, $Na_2C_2O_4$. The stoichiometric relationship between them is given by the net ionic as Reaction 99.

$$5C_2O_4^{2-} + 2MnO_4^- + 16H^+ \rightarrow 2Mn^{2+} + 10CO_2 + 8H_2O \qquad (99)$$

10 g of $KMnO_4$ was dissolved in 100 mL of deionized water and followed by dilution with deionized water to 1 L. It was allowed to stand in the dark for one week and was filtered through a fine-porosity sintered-glass disk. A graduate buret was filled with $KMnO_4$ by funnel.

2 g sodium oxalate, $Na_2C_2O_4$, was transferred to a platinum dish and dried at 100 °C for one hour. Sodium oxalate was cooled in a desiccator and added to sulfuric acid 5 % (1 mL H_2SO_4 + 19 mL H_2O). The solution containing sulfuric acid and sodium oxalate was mixed slowly with a magnetic stirrer.

Potassium permanganate was added drop-wise at intervals of 3 to 6 seconds between the drops with constant stirring of the solution. Once the color of solution started becoming a faint pink, the valve of the buret was shut and the solution let stand for about 45 s until the

pink color was disappeared. The endpoint was determined when the faint pink color persisted for at least 30 s. The same procedure was carried out with blank solution of sulfuric acid (without adding $Na_2C_2O_4$).

The normality of the $KMnO_4$ solution was calculated using Equation 100:

$$N = \frac{B}{0.06701(C - D)} \qquad (100)$$

N = Normality of $KMnO_4$ solution

B = grams of Na_2CO_4 used

C = mL of $KMnO_4$ solution required for titration of solution

D = mL of $KMnO_4$ solution required for blank titration

Standard deviation for standardization of $KMnO_4$ was ±0.03%.

2. Titration for active oxygen

The reaction between potassium permanganate and hydrogen peroxide is similar to that with sodium oxalate, Reaction 101.

$$5\,H_2O_2 + 2MnO_4^- + 6H^+ \rightarrow 2Mn^{2+} + 5O_2 + 8H_2O \qquad (101)$$

To measure the active oxygen of a solution (or solid), first a 50 mL beaker was tared on the analytical balance, and the sample to be added was weighed. 25 mL sulfuric acid (15%) was transferred to the beaker. For solution samples, a glass syringe was used for transferring. For solid samples, the beaker was gently swirled until the sample was completely dissolved.

Potassium permanganate was added drop-wise at a rate of 10 mL/min with constant stirring of the solution. The endpoint was determined when the faint pink color persisted

for 30 s. A blank sample with the same matrix was titrated with the same method to correct for the matrix effect.

The weight percentage of active oxygen was calculated according to Equation 102.

$$\text{wt \% O} = \frac{(V - B) \times (N) \times (0.799) \times (\text{C})}{\text{W}} \qquad (102)$$

V = mL $KMnO_4$ solution required for titration of samples

B = mL $KMnO_4$ solution required for titration of blank

N = normality of $KMnO_4$ solution

C = $KMnO_4$ temperature correction factor

W = grams of sample used

Since the normality of $KMnO_4$ changes with temperature, a correction factor was included to adjust effect of temperature, Table 30.

Table 30: Correction factor for $KMnO_4$ normality function of temperature

Temperature, °C	Correction factor
21	1.0010
23	1.0005
25	1.0000
27	0.9989

By measuring the average of three times of a known concentration of hydrogen peroxide, it was found that the standard deviation for titration of active oxygen was ± 0.25 wt % [97].

APPENDIX IV: ANALYSIS OF METHANOL BY RAMAN SPECTROSCOPY

1. Introduction

Raman spectroscopy is a technique for identification and analysis of molecular species. Raman spectroscopy does not require any special sample preparation meaning that many studies may be performed in situ. Raman spectroscopy is based on detection of scattered light, i.e., the Raman effect. In general, when light interacts with a substance it can do so in three main ways: the light may be absorbed, transmitted or scattered. Raman spectroscopy is a result of the scattering of light [98].

The Raman scattered light carries information about the identity of the material, and its chemical and physical states. Each compound has its own unique Raman spectrum, which can be used as a fingerprint for identification.

Raman spectroscopy is similar to I.R. spectroscopy but has several distinct advantages. Using IR spectroscopy on aqueous samples, results in a large proportion of the vibrational spectrum being masked by the intense water signals. With Raman spectroscopic techniques, analysis of aqueous samples can be performed with ease as Raman signals from the water molecule are relatively weak.

The energy shifts correspond to the vibration energy levels of the molecule. The Raman shift is reported, as the wavenumber (cm^{-1}) difference in frequency between the exciting and scattering frequencies. The wavenumber is a unit of reciprocal wavelength (measured in cm^{-1}), commonly used in spectroscopy. It represents energy, i.e., one wavenumber is equal to 1.99×10^{-27} J.

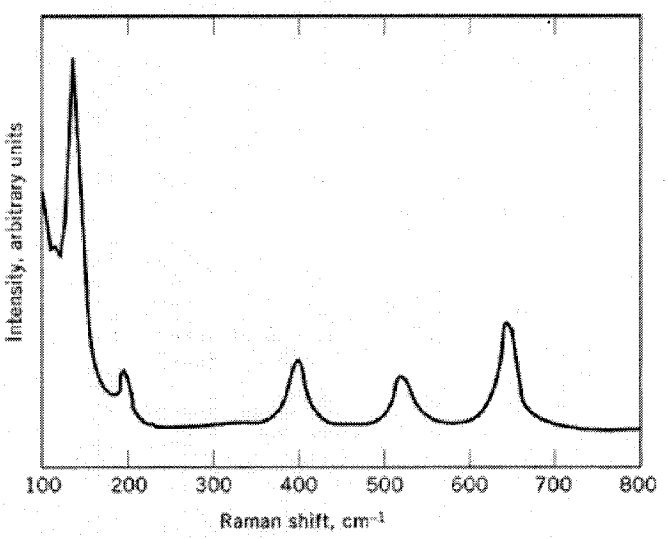

Figure 75: Raman spectrum of TiO_2, in a glass bottle, 532-nm excitation, the principal TiO_2 bands are at 143, 195, 392, 514, and 633 cm^{-1}, respectively [98].

Lasers are the ideal excitation source for Raman spectroscopy as they emit intense, highly collimated, monochromatic light. Raman spectroscopy can employ a wide range of lasers; offering excitation wavelengths ranging from the near-IR to the deep ultraviolet.

2. Instrument

An InVia Raman microscope RENISHAW® at the Department of Mining, Metals and Materials Engineering, McGill University, was used. The laser source was Ar^+ gas with excitation wavelength (λ) of equal to 514 nm.

3. Procedure

In order to measure the concentration of methanol in the solutions, the two reciprocal wavelengths of 2941.64 and 2833.21 cm^{-1} of pure methanol were selected as the reference. They had relative intensity of 0.017 and 0.029, respectively [99, 100].

As shown in Figure 76, at a wavenumber of 2833.21 cm^{-1}, pure methanol had a relative intensity of 0.017, while for effluent at the same wavenumber, the intensity was 0.011. If

the concentration of pure methanol was considered in weight present, it was calculated that the concentration of methanol in raffinate is 64.7 wt % (0.011×100/0.017).

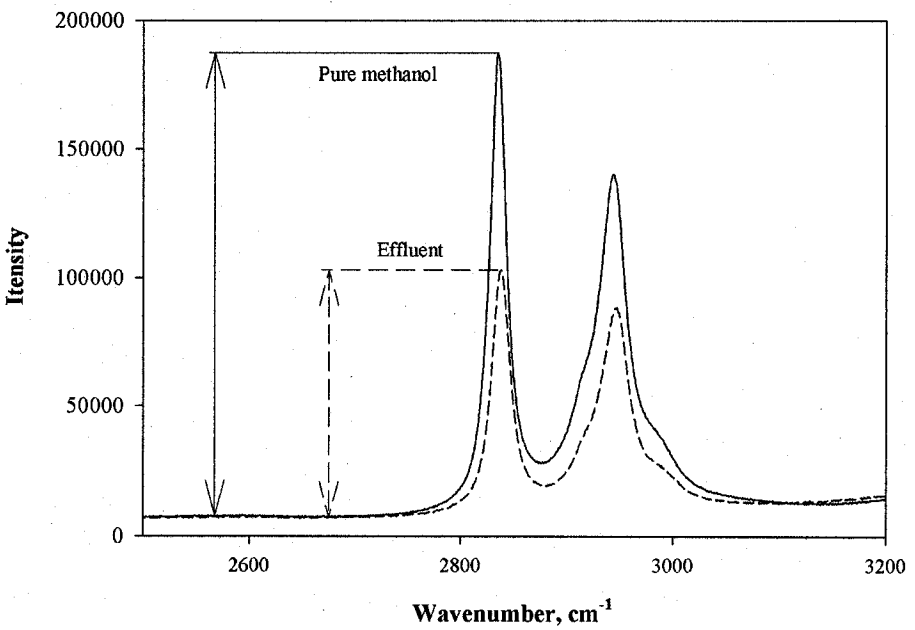

Figure 76: Spectrum of pure methanol and raffinate.

Figure 78shows the spectrum of the empty container. The intensity of the background due to the reflection of the container glass was measured and deducted from the spectra of pure methanol and other samples.

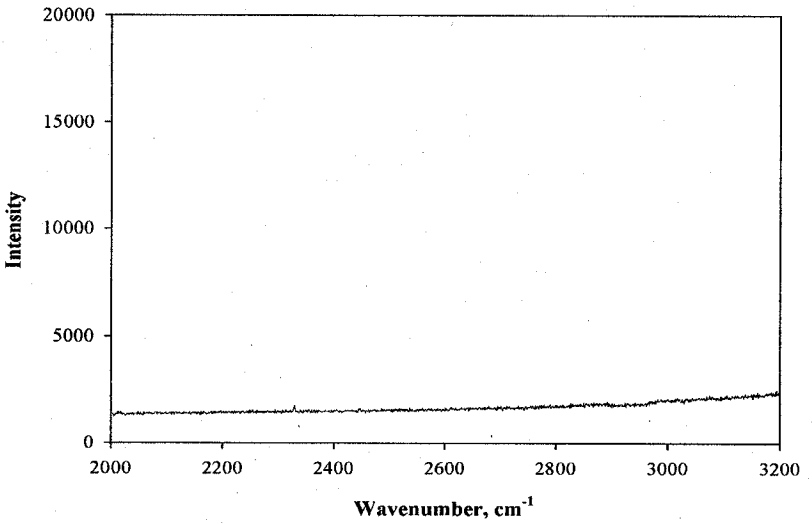

Figure 77: Raman spectrum of empty container

In addition, to make sure the spectrum of methanol does not overlap with other components, specifically at wavenumber of 2833.21 cm^{-1}, Raman spectroscopy was performed for H_2O_2, the mixture of methanol with H_2O_2 and lithium hydroxide and the empty glass container. As shown in Figure 78, there was no interference between methanol and H_2O_2.

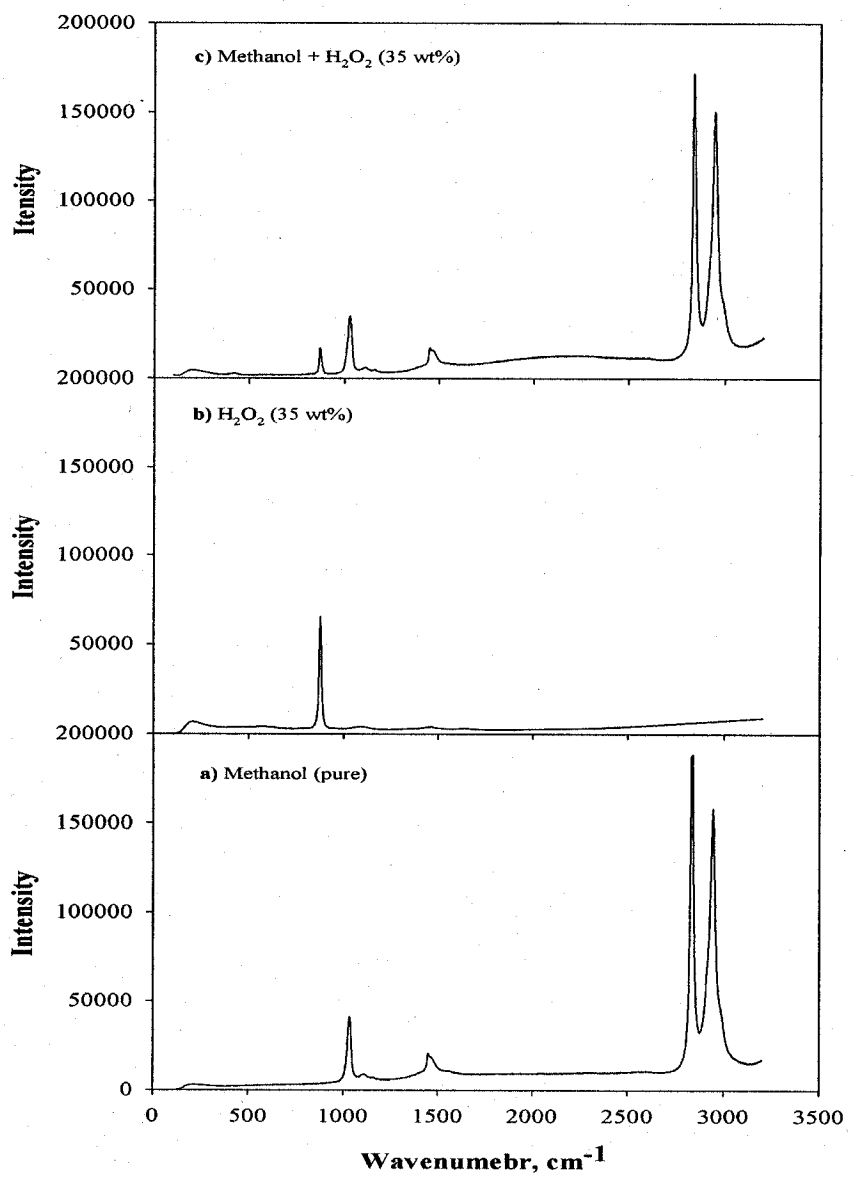

Figure 78: Raman Spectroscopy of a) pure methanol, b) H_2O_2 (35 wt %) and c) mixture of methanol and H_2O_2 (35 wt %)

APPENDIX V: DETERMINATION OF KINETIC PARAMETERS FROM THERMOGRAVIMETRIC DATA

In a general reaction of the form:

$$aA_{(s)} \rightarrow bB_{(s)} + cC_{(g)} \tag{103}$$

the rate of disappearance of A when the system is controlled by the chemical reaction kinetics may be expressed by Equation 104 [43, 79].

$$\frac{d\alpha}{dt} = k(1-\alpha)^n \tag{104}$$

where α is fraction of A decomposed at time t ($\alpha = \frac{m_{Ai} - m_{At}}{m_{Ai} - m_{Af}}$), n is order of reaction, and k is rate constant given by Equation 105:

$$k = Ae^{-E/RT} \tag{105}$$

where A is frequency factor, and E is activation energy of the reaction.

For a linear heating rate of β deg/min:

$$\beta = \frac{dT}{dt} \tag{106}$$

By combining Equations 104, 105 and 106, rearranging and integration, it can be shown:

$$\int_0^{\alpha} \frac{d\alpha}{(1-\alpha)^n} = \frac{A}{\beta}\int_0^{T} e^{-E/RT} dT \tag{107}$$

The right-hand side of Equation 107 has no exact integral, but by making the substitution $u=E/RT$ and using the relation:

$$\int_{u}^{\infty} e^{-u}u^{-b}\,\mathrm{d}u \cong u^{1-b}e^{-u}\sum_{n=0}^{\infty}\frac{(-1)^n(b)_n}{u^{n+1}} \tag{108}$$

Equation 107 becomes:

$$\frac{1-(1-\alpha)^{1-n}}{1-n} = \frac{ART^2}{\beta E}\left[1-\frac{2RT}{E}\right]e^{-E/RT} \tag{109}$$

Taking the log of Equation 109 yields Equation 110 applicable for all values of n, except $n = 1$.

$$\log_{10}\left[\frac{1-(1-\alpha)^{1-n}}{T^2(1-n)}\right] = \log_{10}\frac{AR}{\beta E}\left[1-\frac{2RT}{E}\right]-\frac{E}{2.3RT} \tag{110}$$

For the value of n = 1, after taking log of Equation 109 yields Equation 111:

$$\log_{10}\left[-\log_{10}\frac{(1-\alpha)}{T^2}\right] = \log_{10}\frac{AR}{\beta E}\left[1-\frac{2RT}{E}\right]-\frac{E}{2.3RT} \tag{111}$$

Thus a plot of either $\log_{10}\left[\frac{1-(1-\alpha)^{1-n}}{T^2(1-n)}\right]$ against $\frac{1}{T}$ or, when $n = 1$, $\log_{10}\left[-\log_{10}\frac{(1-\alpha)}{T^2}\right]$ against $\frac{1}{T}$, should result in a straight line of slope $-\frac{E}{2.3R}$ for the correct value of n. This follows from the fact that it may be shown that for most values of E and for the temperature range over which reactions generally occur, the expression $\log_{10}\frac{AR}{\beta E}\left[1-\frac{2RT}{E}\right]$ is roughly constant.

The equations may he applied by a simple graphical technique. Since there is theoretical justification for orders of reaction of 0, 1/2, 2/3, and 1 in solid state kinetics it is possible to substitute these values into Equation 110, or 111 (when $n = 1$), to obtain the appropriate plots.

APPENDIX VI: METHOD OF REDUCED TIME PLOTS FOR VALIDATION OF CONVERSION KINETIC OF LITHIUM PEROXIDE AND LITHIUM OXIDE

Lithium peroxide and lithium oxide were involved in a gas–solid reaction with the ambient air atmosphere. The unreacted core model, also known as the shrinking core model, can be used to describe topological reactions such as the present reaction of Li_2O_2 and Li_2O with air. In these reactions, it was assumed that the reaction zone was restricted to a thin front advancing from the outer surface into the particle [101]. Equations 112, 113 and 114 describe the three regimes of control of the kinetics of topological reactions.

$$\frac{t}{\tau} = 1\text{-}3(1\text{-}X)^{2/3} + 2(1\text{-}X) \tag{112}$$

$$\frac{t}{\tau} = X \tag{113}$$

$$\frac{t}{\tau} = 1\text{-}(1\text{-}X)^{1/3} \tag{114}$$

t is the time of reaction, X, the conversion of reactant, and τ is the time required to completely convert an unreacted particle into product.

Equation of 112 describes the situation when diffusion in the ash layer controls the rate of transformation. Equation 113 describes it for control due to diffusion in the gas layer and Equation 114 when the chemical reaction controls the system. However, these models predict that the complete conversion, X = 1, occurs at $t = \tau$. In practice, it is difficult to approach this boundary condition. Moreover, the models often do not properly describe the actual kinetic behavior the diffusion-layer control regime.

In order to avoid this problem, the method of "reduced time plots" was used [102]. To check which model best described the data obtained from tests; all results were plotted on the same graph. For isothermal data, plotting the value of X against $t/t_{0.5}$ often gave a single line having the characteristic shape for shrinking core processes, where $t_{0.5}$ is the time for 50% reaction. Table 31 shows the values of X versus $t/t_{0.5}$ for the various regimes described in the above equations.

Table 31: Values of X and $t/t_{0.5}$ calculated for three regimes.

X	Diffusion in ash layer	Diffusion in gas layer	Chemical reaction
0.0	0.00	0.00	0.00
0.1	0.03	0.20	0.01
0.2	0.13	0.40	0.04
0.3	0.32	0.60	0.11
0.4	0.60	0.80	0.20
0.5	1.00	1.00	0.35
0.6	1.56	1.20	0.55
0.7	2.32	1.40	0.85
0.8	3.40	1.60	1.31
0.9	5.03	1.80	2.14
1.0	9.09	2.00	9.09

Figure 79 shows plots of the values in Table 31. By plotting the mol-fraction of the unreacted Li_2O_2 or Li_2O versus $t/t_{0.5}$ from the experimental results, it is possible to evaluate which model best fitted the measured conversion. After selection of the proper model, the rate of reaction was estimated.

If the diffusion in the gas layer controlled the rate of the conversion to Li_2O_2 (or Li_2O), the rate of conversion would be influenced by the flow of gas around the samples and their size. If the resistance to diffusion through the ash layer controls the rate of reaction, the particle size, the thickness of ash and availability of unreacted surface would affect the

rate of reaction. When of the rate of the reaction is controlled by chemical reaction, the reaction would be temperature sensitive.

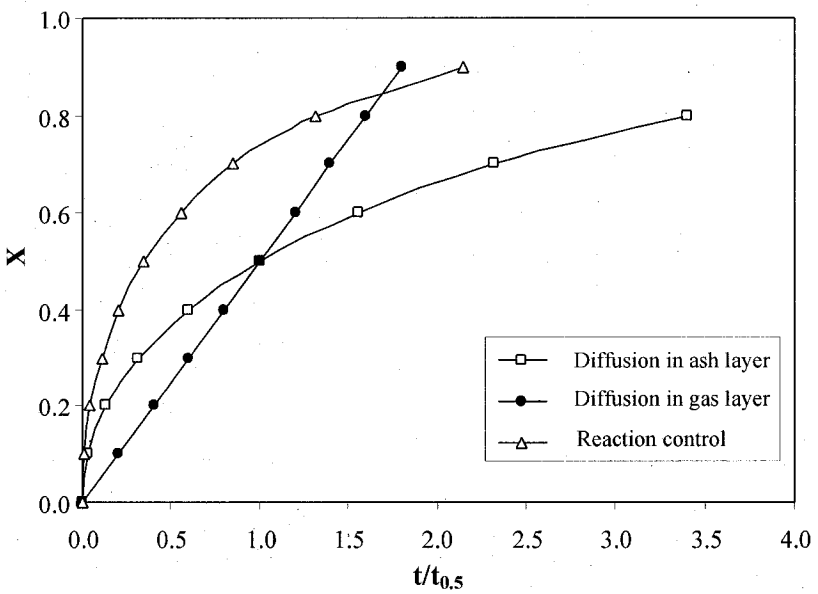

Figure 79: Plots of X against $t/t_{0.5}$ for diffusion in ash layer, diffusion in gas layer and reaction control regimes

APPENDIX VII: USING LITHIUM CARBONATE AS STARTING MATERIAL

1. Introduction

Lithium carbonate, Li_2CO_3, was evaluated as a replacement for $LiOH.H_2O$. This idea was of interest because technical grade Li_2CO_3 is less expensive than $LiOH.H_2O$[xxvi]. Moreover, in comparison to $LiOH.H_2O$, lithium carbonate is a stable compound, i.e., there is no change in its composition while exposed to air. Nothing was found in the literature dealing with this using of Li_2CO_3 [10]. In order to determine the feasibility of the conversion Li_2CO_3 to Li_2O_2, the following experiments were performed.

2. Experimental methodology

The reagents used were lithium carbonate (+99%, Zigma-Aldrich) and hydrogen peroxide (Alfa-Aesar) 35 wt%. Since lithium carbonate had no solubility in methanol or other alcohols, the experiment was performed in an aqueous solution instead of the methanol medium. First, an aqueous solution of Li_2CO_3 with a concentration of 12.5 g/100 g H_2O was prepared at 20 °C. The total amount of Li_2CO_3 was dissolved in the water without any precipitation. Incremental masses of H_2O_2 (35 wt %), from 28 to a total of 64 g, were added to the aqueous solution followed by mixing.

No precipitation or any change in the solution was observed. Then, the solution was heated to evaporate the water and H_2O_2. Drying was continued in a vacuum oven at 90 °C and 0.01 atm for 1 h. The composition of the residue was determined by XRD. As seen from XRD result shown in Figure 80, even at the higher concentration of 56 g H_2O_2, no

---

[xxvi] In March 2005, the price of Li_2CO_3 and $LiOH.H_2O$ were 2.5 and 3.4 $/kg, respectively [1].

Li_2O_2 was formed. It was concluded that because of the presence of a large amount of water in system, reaction did not occur.

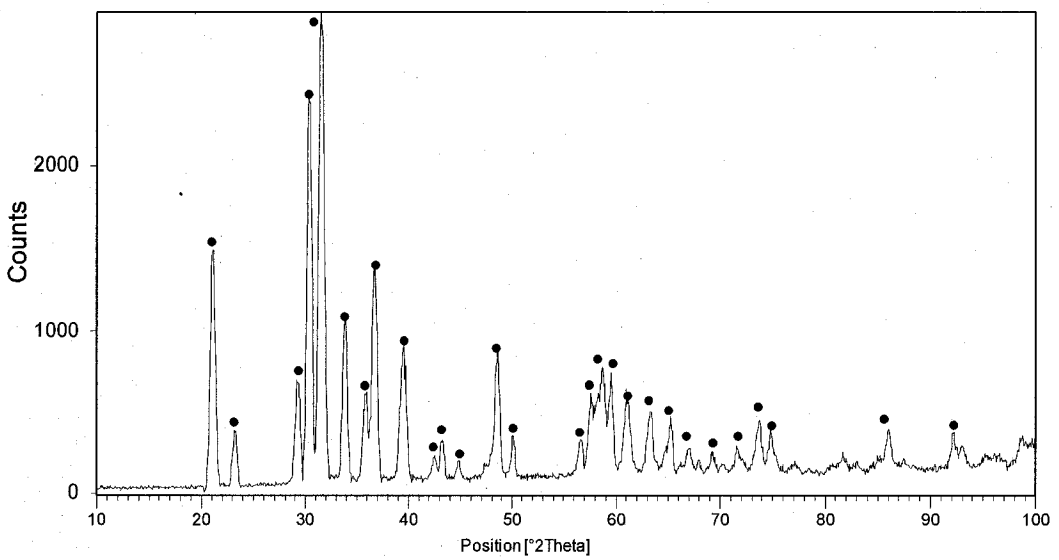

Figure 80: XRD result of 56 g H_2O_2 (35 %wt)addition to a solution with a concentration of 12.5 g Li_2CO_3/100 g H_2O, Li_2CO_3●

In other experiment, it was decided to test a system without water. Only Li_2CO_3 and H_2O_2 (35 % wt) were used. In this test, a fixed mass of Li_2CO_3 had incremental masses of hydrogen peroxide added to it. The molar ratio of H_2O_2 (35 % wt) to Li_2CO_3 started at 2 and was increased to 10 by the additions. Stoichiometrically, 1.3 mol of H_2O_2 (35 % wt) would be required to convert one mole of Li_2CO_3 to one mole of Li_2O_2.

The XRD result of product for the ratio of H_2O_2:Li_2CO_3 = 8 is presented in Figure 81. It indicates that the product compromises mainly Li_2CO_3 a small amount of Li_2O_2.

The amount of Li_2O_2 produced was measured by analyzing of the active oxygen of product. As shown in Figure 82, the maximum efficiency of Li_2O_2 production was 11.8 ± 2 %. This experiment showed that the production of Li_2O_2 from Li_2CO_3 exhibited very low efficiency.

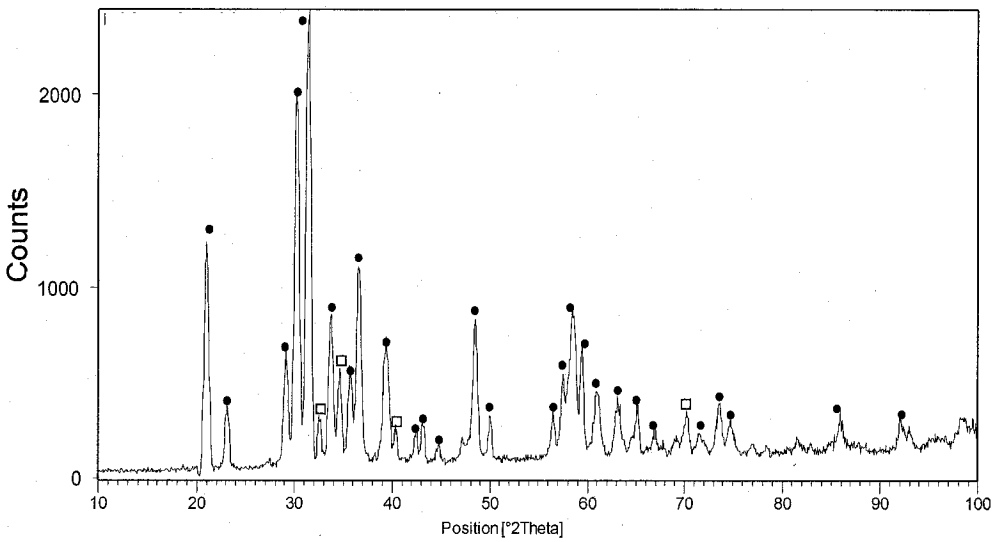

Figure 81: XRD result of Li_2CO_3 addition to H_2O_2, Li_2O_2 □ and Li_2CO_3 ●

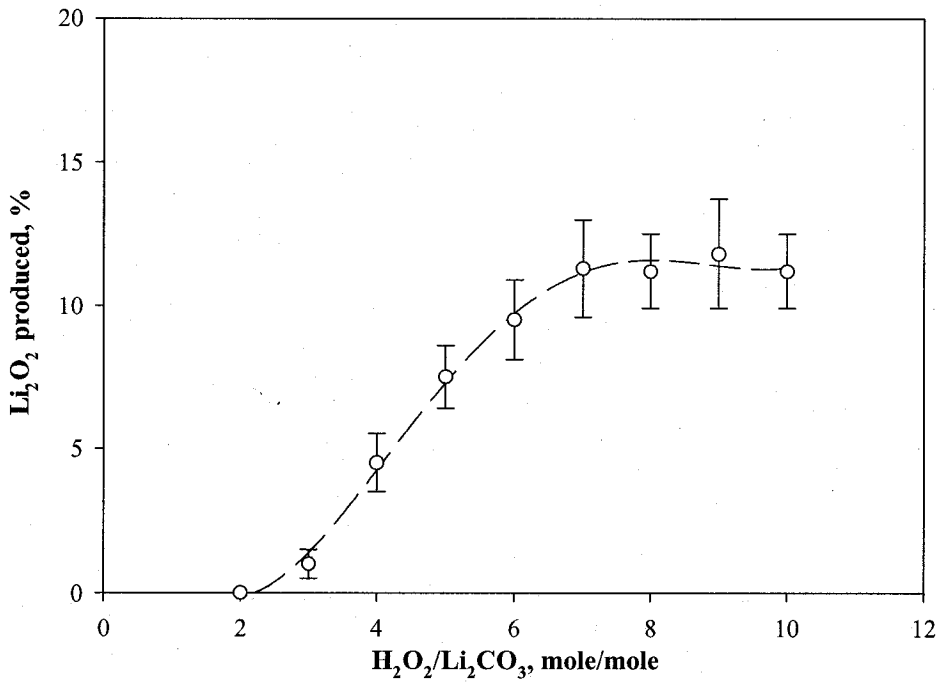

Figure 82: The conversion of Li_2CO_3 to Li_2O_2 as a function of H_2O_2 (35 %wt).

Besides the low efficiency of the conversion reaction, the other problem raised was the separation of Li_2O_2 from Li_2CO_3. Because, both Li_2O_2 and Li_2CO_3 are likely insoluble in any alcohol, the use of alcohol for separation would not be an option. On the other, both

Li_2O_2 and Li_2CO_3 are in a large extent soluble in water; therefore, a technique by which these two compounds can be separated would need a more investigation.

Overall, it was concluded that using hydrogen peroxide for the conversion of Li_2CO_3 to Li_2O_2 is not promising.

APPENDIX VIII: STRUCTURAL DATA AND PDF CARD REFERENCES FOR XRD ANALYSIS OF SAMPLES

X-ray diffraction (XRD) is used to investigate the structural characteristics of materials. XRD is a quantitative and qualitative technique which is used for the characterization of crystalline materials and their crystal structures. The diffraction pattern contains a range of peaks of different relative intensities at specific angles of diffraction, which is unique to a specific crystal structure. Crystal phases can be identified from these diffraction patterns. The following table presents the information of XRD references were used for analyzing for the sample studied in work.

Table 32: XRD references were used for analyzing for the sample

PDF index name	Chemical formula	Ref. code	Crystal system	Reference
Lithium hydroxide hydrate	$LiOH.H_2O$	25-0486	Monoclinic	*Natl. Bur. Stand. (U.S.) Monogr. 25, 11, 92, (1974)*
Lithium hydroxide hydrate	$LiOH.H_2O$	24-0619	Monoclinic	*Alcock, Acta Crystallogr., sec B, 27, 1682 (1971)*
Lithium hydroxide hydrate	$LiOH.H_2O$	74-1820	Monoclinic	*Rabaud. H., Gay. R., Bull. Soc. Fr. Mineral. Cristallogr., 80, 166 (1957)*
Lithium hydroxide	LiOH	32-0564	Tetragonal	*Natl. Bur. Stand. (U.S.) Monogr. 25, 17, 46, (1980)*
Lithium hydroxide	LiOH	76-0911	Tetragonal	*Daschs. H., Z. Kristallogr., Kristallogeom., Kristallphys., Kristallchem., 112, 60 (1959)*
Lithium Carbonate	Li_2CO_3	22-1141	Monoclinic	*Natl. Bur. Stand. (U.S.) Monogr. 25, 8, 42, (1970)*
Lithium Carbonate	Li_2CO_3	72-1216	Monoclinic	Effenberger, H., Zemann, J., *Z. Kristallogr.*, 150, 133, (1979)
Lithium oxide	Li_2O_2	09-0355	Hexagonal	Foppl. Z. Anorg. Allg. Chem., 291, 12(1957)
Lithium oxide	Li_2O_2	73-1640	Hexagonal	Feher, F., von Wilucki, I., Dost, G., Chem. Ber., 86, 1429 (1953)
Lithium oxide	Li_2O_2	74-0115	Hexagonal	Foppl. Z. Anorg. Allg. Chem., 291, 12(1957)
Lithium oxide	Li_2O	12-0254	Cubic	Natl. Bur. Stand. (U.S.) Monogr 25, 1, 25 (1962)

REFERENCES

[1] B. Bertsch-Frank, "Inorganic Peroxo Compounds" in *Ullmann's Insyclopedia of Chemical Engineering*. Weinheim, Wiley-VCH, 2005.

[2] C.W. Kamienski, D.P. McDonald, M.W. Stark, and J.R. Papcun, "Lithium and Lithium Compounds" in *Kirk-Othmer Encyclopedia of Chemical Technology*, John Wiley & Sons, Inc, 2005.

[3] A.J. Cohen, *Inorganic Syntheses*, Vol. 5, Ch. 1A, McGraw Hill, 1957.

[4] U. Wietelmann, "Lithium and lithium Compounds" in *Ullmann's Encyclopedia of Industrial Chemistry*, Wiley-VCH Verlag GmbH & Co., 2002.

[5] K.M. Abraham, *Lithium: Current Applications in Science, Medicine and Technology*, New York, J. Wiley & Sons, 1985.

[6] D. Linden and T.B. Reddy, *Handbook of Batteries*, 3 ed., New York, McGraw-Hill, 2002.

[7] R. Bauer and U. Wietelmann, "Lithium" in *Handbook of Extractive Metallurgy*, Vol. IV, F. Habashi, Ed., Weinheim, Wiley-VCH Verlag GmbH & Co., 1997.

[8] K. Heitner, "*Lithium-Metal Polymer Battery*", A.E.V. Batteries, U.S. Department of Energy, 2003, http://www.eere.energy.gov/vehiclesandfuels/pdfs/success/lithmetalbatt3_23_01.pdf

[9] Chemetall-GmbH, "*Applications*", 2005, http://www.chemetalllithium.com

[10] FMC, "*Markets-Energy*", 2005, http://www.fmclithium.com

[11] J.A. Ober, "*Lithium*", U.S.G. Survey, U.S. Department of the Interior, 2006, http://minerals.usgs.gov/minerals/pubs/commodity/lithium/lithimcs06.pdf

[12] G.E. Foltz, *Lithium and Lithium Compounds*, Inorganic Chemicals Handbook, Vol. 2, New York, Marcel Dekker, Inc., 1993.

[13] C.A. Hampel, *Lithium Electrowinning*, Encyclopedia of Electrochemistry, Vol. 1, 1972.

[14] G.J. Kipouros and D.R. Sadoway, "Toward New Technologies for the Production of Lithium", *JOM*, 1998, 50(5), pp. 24-26.

[15] P. Mahi, A.A.J. Smeet, D.J. Fray, and J.A. Charles, "Lithium-Metal of Future", *JOM*, 1986, 38(11), pp. 20-26.

[16] R. Harris, "Lithium Production and Refining" McGill University, National Sciences and Engineering Research Council of Canada CRD Proposal, 17 March 2004.

[17] W. Morris and L.M. Pidgeon, "The Vapor Pressure of Lithium in the Reduction of Oxide by Silicon", *Can. J Chem.*, 1958, 36(6), pp. 910-914.

[18] W.J. Kroll and A.W. Schlechton, "Laboratory Preparation of Lithium Metal by Vacuum Metallurgy", *Trans. Am. Inst. Mining Met. Engrs*, 1947, 14, pp. 266-74.

[19] A. Roine, "*HSC Chemistry 5.11*", Outukumpu Research Oy, Pori, 2002.

[20] R.A. Stauffer, "Vacuum process for preparation of lithium metal from spodumene", *Trans. Am. Inst. Mining Met. Engrs.*, 1949, 182, pp. 275-85.

[21] A.A.J. Smeets and D.J. Fray, "Extraction of Lithium by Vacuum Thermal reduction with Aluminum and Silicon", *Transactions of IMM: Section C*, 1991(100), pp. C42-C55.

[22] C.W. Bale, A.D. Pelton, P. Chartrand, S.A. Degterov, R.B. Mahfoud, J. Melançon, G. Eriksson, K. Hack, and S. Petersen, "*FACTSage: Thermo Chemical Software and Databases 5.2* ", Montreal, 2005.

[23] D.J. Salmon, "High purity lithium oxide process", US Patent 4,732,751, 22 March 1988.

[24] J.A. Anno and H.H. Boeing, "Method of Producing Porous Lithium Oxide", US Patent 4,221,775, 9 Sep 1980.

[25] M.S. Ortman and E.M. Larsen, "Preparation, Characterization, and Melting Point of High-Purity Lithium Oxide", *American Ceramic Society*, 1983, 66(9), pp. 645-8.

[26] G.K. Johnson, R.T. Grow, and W.N. Hubbard, "The Enthalpy of Formation of Lithium Oxide", *Journal of Chemical Thermodynamics*, 1975, 7, pp. 781-786.

[27] R.O. Bach and W. Boardman, "Preparation of Anhydrous Lithium Peroxide", US Patent 3,185,546, 25 May 1965.

[28] J.M. Kiat, G. Boemare, B. Rieu, and D. Aymes, "Structural Evolution of LiOH: Evidence of a Solid-Solid Transformation toward Li_2O Close to the Melting Temperature", *Solid State Communications*, 1998, 108, pp. 241-245.

[29] J.D. Wheenberger, "Properties of Pure Nickel after Long Term Exposure to LiOH and Vacuum at 775 K ", *Journal of Material Engineering*, 1991, 13(4), pp. 257-271.

[30] D.A. Boryta and A.J. Maas, "Factors Influencing Rate of Carbon Dioxide Reaction with Lithium Hydroxide", *Ind. Eng. Chem. Process Des. Develop.*, 1971, 10(4), pp. 489-494.

[31] J. De Palblo, J. Andersson, and M. Azoulay, "Kinetic Investigation of the Sorption of Water by Lithium Hydroxide", *Thermochemica Acta*, 1987, 113, pp. 87-94.

[32] E. Wiberg, *Inorganic Chemistry*, Academic Press, 2001.

[33] A.D. McNaught and A. Wilkinson, *Compendium of Chemical Terminology*, IUPAC, Vol., Blackwell Science, 1997.

[34] N. Steiner and W. Eul, "Peroxides and Peroxide Compounds" in *Kirk-Othmer Encyclopedia of Chemical Technology.*, John Wiley & Sons, Inc, 2001.

[35] I.I. Vol'nov, *Peroxides, Superoxides, and Ozonides of Alkali and Alkaline Earth Metals*, New York, Plenum Press, 1966.

[36] L.G. Cota and P. De la Mora, "On the structure of lithium peroxide, Li_2O_2", *Acta Crystallographica*, 2005, B61, pp. 133–136.

[37] S.Z. Makarov and T.A. Dobrynina, "Systems Containing Hydrogen Peroxide at High Concentration. Communication 9. the Ternary System $LiOH-H_2O_2-H_2O$", *Bulletin of the Academy of Sciences of the USSR*, 1955, pp. 365-71.

[38] A. Capotosto and A.W. Petrocelli, "*Use of Lithium Peroxide for Atmosphere Regeneration",* G. General Dynamics Corp., US Government Research and Development Report, 1969, 69(2),

[39] M.M. Markowitz, D.A. Boryta, and H. Stewart, "Concurrent carbon dioxide absorption and oxygen evolution by lithium peroxide", *J. Inorg. Nuclear Chem.*, 1964, 26(11), pp. 2028-33.

[40] W. Hesse, M. Jansen, and W. Schnick, "Recent Results in Solid State Chemistry of Ionic Ozonides, Hyperoxides, and Peroxides", *Progress in Solid State Chemistry*, 1989, 19(1), pp. 47-110.

[41] T.V. Rode and T.A. Dobrynina, "Thermal Analysis of Lithium Peroxide", *Russian Academy of Sciences Doklady*, 1953, 91, pp. 125-7.

[42] M.M. Pavlyuchenko and T.I. Popova, "Kinetics of Thermal Decomposition of Lithium Peroxide", *Institute of Bioorganic Chemistry*, 1965, pp. 80-5.

[43] T. Tanifuji and S. Nasu, "Heat Capacity and Thermal Decomposition of Li_2O_2", *Journal of Nuclear Materials*, 1979, 87, pp. 189-195.

[44] A.B. Tsentsiper and Z.I. Kuznetsova, "Thermal Decomposition of Lithium Peroxide", *Bulletin of the Russian Academy of Sciences, Division of Chemical Science*, 1965, 10, pp. 1902-4.

[45] A.J. Cohen, "Observation on Several Compounds of Lithium and Oxygen", *J. Am. Chem. Soc*, 1952, 74(15), pp. 3762-64.

[46] W.N. Smith, "Method for Preparing Lithium Peroxide", US Patent 3,446,588, 27 May 1969.

[47] R.O. Bach and W.W. Boardman, "Lithium peroxide ", *Chemical Engineering News*, 1962, 40.

[48] S.F. Lincoln, D.T. Richens, and A.G. Sykes, "Metal Aqua Ions" in *Comprehensive Coordination Chemistry*, Vol. 1, J.A. McCleverty and T.J. Meyer, Eds., Oxford, Elsevier Pergamon, 2003.

[49] A.E. Smith, "A Study the Variation with pH of the Solubility and Stability of Some Metal Ions at Low Concentration in Aqueous Solution", *Analyst*, 1973, 98 (1164), pp. 209-12.

[50] S.Z. Makarov and T.A. Dobrynina, "Investigation of Systems Containing Concentrated Hydrogen Peroxide, Characteristics of the Solid Phase Systems $LiOH-H_2O_2-H_2O$", *Bulletin of the Academy of Sciences of the USSR*, 1956, pp. 283-7.

[51] H. Strater, "Method of Making Lithium Peroxide in Methanol", US Patent 2,962,358, 29 November 1960.

[52] E.L. Klebba, "Safe Preparation of Pure alkali Metal Peroxides", US Patent 3,212,850, 10 Oct 1965.

[53] Y.A. Ferapontov, S.I. Simanenkov, N.F. Gladyshev, and B.V. Putin, "Development of Wasteless Technology of Lithium Peroxide Preparation", *Chemical Technology*, 2004, 4, pp. 2-4.

[54] N.F. Gladyshev, B.V. Putin, S.I. Simanenkov, and Y.A. Ferapontov, "Preparation of lithium peroxide from hydroxide by oxidation in ethanol solution", RU 2001-101825, 2002.

[55] G. Goor, J. Glenneberg, and S. Jacobi, "Hydrogen Peroxide": Wiley-VCH GmbH & Co., 2000.

[56] W.C. Schumb, C.N. Satterfield, and R.L. Wentworth, *Hydrogen Peroxide*, American Chemical Society, 1955.

[57] K. Pandiarajan, *Hydrogen Peroxide*, Synthetic Reagent, Vol. 6, Ellis Horwood, 1985.

[58] N.M. Beylerian and M.Z. Asaturyan, "On the Mechanism of Hydrogen Peroxide Decomposition in Alkaline Medium ", *Oxidation Communications*, 2004, 27(2).

[59] C. Reichardt, *Solvents and Solvent Effects in Organic Chemistry*, Willey-VCH, 2003.

[60] K. Izutsu, *Electrochemistry in Nonaqueous Solutions*, Wiley-VCH Verlag GmbH & Co, 2002.

[61] J.A. Monick, *Alcohols: Their Chemistry, Properties and Manufacture*, New York, Reinhold Book Corportion, 1968.

[62] J. Falbe, H. Bahrmann, and W. Lipps, "Alcohols " in *Ullmann's Encyclopedia of Industrial Chemistry*, Wiley-VCH Verlag GmbH & Co., 2002.

[63] E. Fiedler, G. Grossmann, D.B. Kersebohm, G. Weiss, and C. Witte, "Methanol" in *Ullmann's Encyclopedia of Industrial Chemistry*, Wiley-VCH Verlag GmbH & Co., 2002.

[64] N. Kosaric, Z. Duvnjak, and A. Farkas, "Ethanol" in *Ullmann's Encyclopedia of Industrial Chemistry*, Wiley-VCH Verlag GmbH & Co., 2002.

[65] A.J. Papa, "Propanols" in *Ullmann's Encyclopedia of Industrial Chemistry*, Wiley-VCH Verlag GmbH & Co, 2002.

[66] J.A. Riddick, W.B. Bunger, and T.K. Sakano, *Organic Solvents, Physical Properties and Methods of Purification*, 4 ed., New York, Wiley & Sons, 1986.

[67] J.R. Chipperfield, *Non-aqueous Solvents*, Oxford Chemistry Primers, Vol., Oxford, Oxford University Press, 1999.

[68] T. Takamatsu, "The Solubility Study of Ion-pairs in Organic Solvents", *Bulletin of the Chemical Society of Japan*, 1974, 47(11), pp. 2647-9.

[69] R.G. Bates and R.A. Robinson, "Acid-Base Behaviour in Methanol-Water Solvents" in *Chemical Physics of Ionic Solutions*, B.E. Conway and R.G. Barradas, Eds., New york, John Wiley & Sons Inc., 1966, pp. 211-235.

[70] J. Jander and C. Lafrenz, *Ionizing Solvents*, Chemical Topics for Students, Vol., John Wiley & Sons Ltd., 1970.

[71] G.W. Tindall, "Mobile-Phase Buffers, Part I- The Interpretation of pH in Partially Aqueous Mobile Phases ", in *LCGC North America*, vol. 20, 2002, pp. 1028-1032.

[72] J.F. Hinton and E.S. Amis, "Solvation Numbers of Ions", *Chemical Reviews*, 1971, 71 (6), pp. 627-674.

[73] R.C. Mehrotra and A. Singh, *Recent Trends in Metal Alkoxide Chemistry*, Progress in Inorganic Chemistry, Vol. 46, John Wiley & Sons, Inc., 1997.

[74] G. Wilkinson, R.D. Gillard, and J.A. McCleverty, *Comprehensive Coordination Chemistry*, Comprehensive Coordination Chemistry, Vol. 2, Pergamon Press, 1987.

[75] G. Goor, J. Glenneberg, and S. Jacobi, *Hydrogen Peroxide*, Industrial Inorganic Chemicals and Products, Vol., Weinheim, Wiley-VCH Verlag GmbH & Co., 2005.

[76] C.W. Jones, *Applications of Hydrogen Peroxide and Derivatives*, Cambridge, The Royal Society of Chemistry, 1999.

[77] *ASTM E1148-02: Standard Test Method for Measurements of Aqueous Solubility*, ASTM Standards, Vol. 11.06, American Society for Testing and Materials, 1999.

[78] S.P. Pinho and E.A. Macedo, "Solubility of NaCl, NaBr, and KCl in Water, Methanol, Ethanol, and Their Mixed Solvents ", *Journal of Chemical and Engineering Data*, 2005, 50(1), pp. 29 -32.

[79] A.W. Coats and J.P. Redfern, "Kinetic Parameters from Thermogravimetric Data", *Nature*, 1964, 201(4914), pp. 68-69.

[80] R.B. Bird, W.E. Stewart, and E.N. Lightfoot, *Transport Phenomena*, John Wiley & Sons, New York, 1960.

[81] V.A. Stenger, "Solubility of Various Alkali Metal and Alkaline Earth Metal Compounds in Methanol", *J. Chem. Eng. Data*, 1996, 41, pp. 1111-3.

[82] M.E. Taboada, D.M. Véliz, H.R. Galleguillos, and T.A. Graber, "Solubility, Density, Viscosity, Electrical Conductivity, and Refractive Index of Saturated Solutions of Lithium Hydroxide in Water + Ethanol ", *Journal of Chemical and Engineering Data*, 2005, 50(1), pp. 187 -190.

[83] A. Cartón, F. Sobrón, S. Bolado, and J. Tabarés, "Composition and Density of Saturated Solutions of Lithium Sulfate+Water+Methanol", *Journal of Chemical Engineering Data*, 1994, 39, pp. 733-734.

[84] A. Wakisaka, S. Komatsu, and Y. Usui, "Solute-Solvent and Solvent-Solvent Interactions Evaluated through Clusters Isolated from Solutions; Preferential Solvation in Water-Alcohols Mixtures ", *Journal of Molecular Liquids*, 2001, 90, pp. 175-184.

[85] W.F. Linke, *Solubilities: A Compilation of Solubility Data from the Periodical Literature*, Volume II, Washington, D.C., American Chemical Society, 1965.

[86] A. Balaban, G. Kuranov, and N. Smirnova, "Phase Equilibria Modeling in Aqueous Systems Containing 2-Propanol and Calcium Chloride or/and Magnesium Chloride", *Fluid Phase Equilibria*, 2002, Fluid Phase Equilibria 194–197 (2002) 717–728, pp. 717–728.

[87] I. Kikic, M. Fermegilia, and P. Rasmussen, "UNIFAC Prediction of Vapor-Liquid Equilibrium Mixed Solvent-Salt systems ", *Chemical Engineering Science*, 1991, 46(11), pp. 2775-2780.

[88] J.M. Prausnitz, R.N. Lichtenthaler, and E. de Azevedo, *Molecular Thermodynamics of Fluid-Phase Equilibria*, Englewood Cliffs, N.J., Prentice-Hall Inc., 1986.

[89] K. Nasirzadeh and A. Salabat, "The Modified Three-Characteristic-Parameters Correlation Model for Nonaqueous Electrolyte Solutions", *Journal of Molecular Liquids*, 2004, 113, pp. 9-11.

[90] H. Zerres and J.M. Prausnitz, "Thermodynamics of Phase Equilibria in Aqueous-Organic Systems with Salt", *Journal of American Institute of Chemical Engineering*, 1994, 40(4), pp. 676-691.

[91] M.J. Tribelhorn and M.E. Brown, "Thermal Decomposition of Barium and Strontium Peroxides", *Thermochimica Acta*, 1995, 255, pp. 143-154.

[92] M.A. Fahim and J.D. FORD, "Energy Storage Using the BaO_2-BaO Reaction Cycle", *The Chemical Engineering Journal*, 1983, 27, pp. 21 - 28.

[93] P.J. Haines, *Thermal Methods of Analysis Principles, Applications and Problems*, Blackie Academic & Professional, 1995.

[94] *ASTM D 6091-97: Standard Practice for 99 %/95 % Interlaboratory Detection Estimate (IDE) for Analytical Methods with Negligible Calibrtaion Error*, ASTM Standards, Vol. 11.01, American Society for Testing and Materials, 1997.

[95] I. Gertsbakh, *Measurement Theory for Engineers*, Berlin, Springer, 2003.

[96] *ASTM D 2180-89: Standard Test Method for Active Oxygen in Bleaching Compounds*, ASTM Standards, Vol. 15.04, American Society for Testing and Materials, 1999.

[97] *ASTM E 200-97: Standard Practice for Preparation, Standardization, and Storage of Standard and Reagent Solutions for Chemical Analysis*, ASTM Standards, Vol. E15.03, American Society for Testing and Materials, 1999.

[98] J.R. Ferraro, K. Nakamoto, and C.W. Brown, *Introductory Raman Spectroscopy*, second ed., San Diego, Academic Press, 2003.

[99] T.J. Vickers and C.K. Mann, "Quantitative Analysis by Raman Spectroscopy ", *Chemical Analysis*, 1991, 114, pp. 121-137.

[100] J.H. Giles, D.A. Gilmore, and M.B. Denton, "Quantitative Analysis Using Raman Spectroscopy without Spectral Standardization", *Journal of Raman Spectroscopy*, 1999, 30, pp. 767-771.

[101] O. Levenspiel, *Chemical Reaction Engineering*, New York, John Wiley & Sons, Inc., 1972.

[102] J.H. Sharp, G.W. Brindley, and B.N.N. Achar, "Numerical Data for Some Commonly Used Solid State Reaction Equations ", *Journal of American Ceramic Society*, 1966, 49, pp. 379-388.